NASA Technical Memorandum 1998-206892, Volume 2

SeaWiFS Postlaunch Technical Report Series

Stanford B. Hooker, Editor

NASA Goddard Space Flight Center
Greenbelt, Maryland

Elaine R. Firestone, Senior Technical Editor

SAIC General Sciences Corporation
Beltsville, Maryland

Volume 2, AMT-5 Cruise Report

James Aiken, Denise G. Cummings, Stuart W. Gibb, Nigel W. Rees, Rachel Woodd-Walker, E. Malcolm S. Woodward, and James Woolfenden

Plymouth Marine Laboratory
Plymouth, United Kingdom

Stanford B. Hooker

NASA Goddard Space Flight Center
Greenbelt, Maryland

Jean-François Berthon

Joint Research Centre
Ispra, Italy

Cyril D. Dempsey

Satlantic, Inc.
Halifax, Canada

David J. Suggett

Southampton Oceanographic Centre
Southampton, United Kingdom

Peter Wood

University of Strathclyde
Glasgow, Scotland

Craig Donlon

University of Colorado Center for Astrodynamics Research
Boulder, Colorado

Natalia González-Benítez, Ignacio Huskin, and Mario Quevedo

University of Oviedo
Oviedo, Spain

Rosa Barciela-Fernandez

University of Vigo
Vigo, Spain

Colomban de Vargas

Universite de Geneve
Chene-Boorgeries, Switzerland

Connor McKee

University of East Anglia
Norwich, United Kingdom

Preface

This report, prepared by Dr. Jim Aiken, Chief Scientist of PML's AMT programme is an outstanding expression of the technical and scientific achievements made in the course of the AMT-5 cruise, 14 September–17 October 1997, which has contributed strategic bio-optical and sea-truthing information to SeaWiFS. AMT has also provided a cost-effective basin scale platform of opportunity to develop wide-ranging initiatives on biogeochemical provinces, biogas production and exchange, plankton and pigment biogeography, and broad nutrient geochemistry for the upper layers of the North and South Atlantic Ocean.

AMT will remain a springboard for data gathering and, increasingly, for process oriented research in CCMS' new core strategic programmes due to start in 1999.

I would like to congratulate Dr. Jim Aiken, associated colleagues, and all the collaborators from NASA, JRC, Italy, SOC and UK universities (UEA, Plymouth), who have contributed through their participation in AMT-5. I look forward to the seminal papers describing the exciting discoveries and achievements in the AMT programme.

Plymouth, United Kingdom — R.F.C. Mantoura
August 1998 Director, PML

The AMT program is a joint experiment with the British and is an unique opportunity to periodically sample the variety of oceanic bio-optical and atmospheric aerosol provinces of the North and South Atlantic Oceans. In fact, the transect traverses nearly 110° of latitude. The first cruise, AMT-1 (Robins et al. 1996), was documented in the *SeaWiFS Technical Report Series* (Prelaunch). To participate in these 5–6 week deployments requires a major effort for all those involved, especially those who deploy from foreign locations, as the SeaWiFS Project staff can testify. Despite the difficulties associated with frequent and prolonged travel, shipping, communications, and extended work at sea, AMT is providing a wealth of new data of exceptional quality for validation and algorithm development. Also, AMT is proving to be an invaluable test bed for refining measurement techniques and equipment designs. I want to thank our British colleagues, particularly the British Antarctic Survey and the Plymouth Marine Laboratory, for inviting the SeaWiFS Project to participate in the program.

Greenbelt, Maryland — C.R. McClain
August 1998 SeaWiFS Project Manager

Abstract

This report documents the scientific activities on board the Royal Research Ship (RRS) *James Clark Ross* (JCR) during the fifth Atlantic Meridional Transect (AMT-5), 14 September to 17 October 1997. There are three objectives of the AMT Program. The first is to derive an improved understanding of the links between biogeochemical processes, biogenic gas exchange, air–sea interactions, and the effects on, and responses of, oceanic ecosystems to climate change. The second is to investigate the functional roles of biological particles and processes that influence ocean color in ecosystem dynamics. The Program relates directly to algorithm development and the validation of remotely-sensed observations of ocean color. Because the Sea-viewing Wide Field-of-view Sensor (SeaWiFS) instrument achieved operational status during the cruise (on 18 September), AMT-5 was designated the SeaWiFS Atlantic Characterization Experiment (SeaACE) and was the only major research cruise involved in the validation of SeaWiFS data during the first 100 days of operations. This third objective involved the near-real time reporting of *in situ* light and pigment observations to the SeaWiFS Project, so the performance of the satellite sensor could be determined.

1. INTRODUCTION

The Atlantic Meridional Transect (AMT) Program exploits the passage of the Royal Research Ship (RRS) *James Clark Ross* (JCR) latitudinally through the Atlantic Ocean between the United Kingdom (UK) and the Falkland Islands (approximately 52°N to 52°S) in support of British Antarctic Survey (BAS) research activities in the Antarctic and its environs.† In September, the JCR sails southward, sampling the boreal fall and the austral spring; the following April it returns to the UK, sampling the austral fall and the boreal spring. The cruise track crosses a range of ecosystems and biophysical regimes, within which conditions vary from subpolar to tropical, and from eutrophic shelf seas and upwelling systems to oligotrophic mid-ocean gyres. The JCR is an ideal platform for measuring physical, biological, and bio-optical properties and processes through these diverse ecosystems of the North and South Atlantic Oceans.

The AMT Program goals are to:

1. Test and refine hypotheses on the responses of oceanic ecosystems and the coupled marine atmosphere to anthropogenically-forced environmental change;
2. Develop a holistic research strategy, integrating *in situ* measurements, remote sensing, and modeling;
3. Provide calibration and validation of new satellite sensors of ocean color, sea surface temperature and height, and solar radiation;
4. Improve the knowledge of marine biogeochemical processes, ecosystem dynamics, food-webs and fisheries, and characterize biogeochemical provinces;
5. Develop coupled physical–biological models of production and ecosystem dynamics; and
6. Quantify oceanic responses to changes in abundance of radiatively- and chemically-active trace gases.

† This publication constitutes an official Plymouth Marine Laboratory (PML) cruise report, and its contents have been approved by the Director, R.F.C. Mantoura.

It has been an inherent goal of the AMT Program to examine the hypothesis of biogeochemical provinces and determine their characteristic properties. Traditionally, oceanographers have partitioned the oceans on the basis of physical and biological characteristics: for the former, topography, geostrophic flows, wind driven circulation, gyres, fronts, upwelling zones and patterns of seasonal stratification; for the latter, biological productivity, as well as phytoplankton and zooplankton assemblages and community structure. Taken together, this biophysical partitioning provides the descriptors of regional ecosystems or biogeochemical provinces, each with discrete boundaries and each having distinct flora and fauna. The concept of biogeochemical provinces has been promoted particularly as a means of evaluating patterns of basin-scale productivity from remotely-sensed measurements of ocean color, making use of province-specific physical and biological parameterizations (climatological values of the key variables).

There have been four prior AMT cruises: AMT-1 Sep.–Oct. 1995; AMT-2 Apr.–May 1996; AMT-3 Sep.–Oct. 1996, and AMT-4 Apr.–May 1997. AMT-5, coinciding with the start of the operational phase of the Sea-viewing Wide Field-of-view Sensor (SeaWiFS) instrument (18 September 1997), started in Grimsby (UK) on 14 September 1997 and ended in Stanley (Falkland Islands) on 17 October 1997. In between, there was a fueling stop in Portsmouth (15–16 September) and a ship's trials period off Madeira (23–25 September). AMT-5 was designated the SeaWiFS Atlantic Characterization Experiment (SeaACE) as the only major research cruise involved in the calibration and validation of SeaWiFS data during the first 100 days of operations. The specific objectives of SeaACE were to:

1. Derive and report downwelling irradiance, (E_d), upwelled radiance (L_u), and the diffuse attenuation

coefficient, (K_d), at the SeaWiFS instrument wavelengths;

2. Report measured phytoplankton pigments, by high performance liquid chromatography (HPLC) and fluorometry, in particular, chlorophyll *a* and phaeopigments (where measured) for validating the SeaWiFS level-2 product; and
3. Compare measured and retrieved values of pigments and the diffuse attenuation coefficient at 490 nm, $K(490)$, for validation of the algorithms.

In addition to providing validation data for SeaWiFS (McClain et al. 1998), the AMT-5 cruise contributed to validation activities of the Topography Experiment (TOPEX) satellite and the Radiometric Observations of the Sea surface and Atmosphere (ROSSA) project.

1.1 Cruise Strategy

The inital strategy for AMT-1 and AMT-2, involved having only two extra passage days for scientific activities, and was based on one sampling station per day. Each station lasted less than one hour, and was complimented by surface underway measurements using water from the non-toxic supply, and was supplemented by one or two Undulating Oceanographic Recorder (UOR) tows into and out of the station. By AMT-3, additional ship time had been increased to six days, so two daily stations were possible: the primary (late morning) station provided water for productivity and other biological sampling along with a complete set of optical measurements; the secondary (early afternoon) station was restricted to optical instruments that could be deployed rapidly (free-fall profilers that could be deployed by hand). At the outset, the strategy for AMT-5 was to plan for two optical stations per day, subject to other constraints.

The primary station commenced at approximately 1100 (ship's time) to coincide with the SeaWiFS overpass. The principal objective was to acquire optical measurements at the SeaWiFS wavelengths and concurrent data on phytoplankton pigments and species, zooplankton, hydrographic properties, and water for primary productivity, biogases, and nutrients. The main instruments deployed were as follows:

1. Sea-Bird Electronics (SBE) 911plus CTD (conductivity, temperature, and depth) sensor deployments from the dedicated midships gantry, with fluorometer, transmissometer, and photosynthetically available radiation (PAR) instruments, plus a 12×30 l bottle water sampler for phytoplankton pigments, productivity, etc., from 12 depths to 250–600 m;
2. SeaWiFS Optical Profiling System (SeaOPS) casts from the (stern) starboard crane for the measurement of $E_d(z,\lambda)$, $L_u(z,\lambda)$, CT, plus chlorophyll fluorescence (F);
3. SeaWiFS Free-Falling Advanced Light Level Sensors (SeaFALLS) casts from the stern for the measurement of $E_d(z,\lambda)$, $L_u(z,\lambda)$, CT, plus F; and
4. Repeated zooplankton net deployments from the forward crane.

The SBE CTD, SeaOPS, and SeaFALLS (along with their solar irradiance reference sensors) were provided by the SeaWiFS Project; the former was a new instrument; the latter two had been deployed on previous AMT cruises, but SeaOPS was equipped with more sensors than had been used in the past.

The high quality of the ship's crew (Appendix A) allowed for the safe deployment of all four main instrument systems simultaneously; this was the primary reason why station time could be kept to the shortest time possible without negatively impacting data collection opportunities. For AMT-5, the CTD and SeaOPS were deployed simultaneously and at similar descent rates, approximately $0.25\,\mathrm{m\,s^{-1}}$. At the maximum depth for the optics cast, usually the 1% light level, the CTD system was profiled at a safe speed to the maximum depth of 250–600 m. The two instrument systems were not synchronized for the up casts. The zooplankton nets and SeaFALLS were profiled independently, but the latter was deployed simultaneously with the SeaOPS down and up casts.

Since the SBE CTD (equipped with 12×30 l water bottles) gave sufficient water that only one 45 min cast was needed per station, contingency time for other activities was available. Extra casts were needed on three occasions when bottles failed to close correctly at the deep chlorophyll maximum (DCM) and on the last three days when the rich spring bloom waters of the Sub-Antarctic Convergence Zone (SACZ) were sampled simultaneously with the afternoon optical casts. The second station in the afternoon was always timed to exploit the most favorable sky conditions. In general, this worked well, and many of the afternoon stations were in excellent cloud-free conditions; on only a few occasions were conditions so unfavorable that the afternoon station was cancelled.

When conditions were at their most favorable during the morning or afternoon station, full advantage was taken, and up to two hours were spent on optical casts, which resulted in some of the best optical measurements of any AMT cruise. In the southern-most end of the Brazil Current, but still north of the confluence with the Falkland Current, the waters were consistently low in chlorophyll, so no afternoon stations were scheduled to save time for the more interesting waters farther south. A total of 49 stations was executed (46 full stations, 1 test station, and 2 trial deployments) during which data were acquired from 32 CTD casts (31 SeaWiFS and 1 BAS to 2,000 m), 64 SeaOPS casts, 152 SeaFALLS casts, and 52 Low-Cost NASA Environmental Sampling System (LoCNESS, another optical free-fall profiler) casts. This inventory of measurements, summarized in Table 1, made AMT-5 the

Table 1. A summary of the station work executed during AMT-5. The HPLC column gives the surface chlorophyll *a* pigment concentration ($mg\,m^{-3}$). The time entries are in Greenwich Mean Time (GMT).

Date	SDY	Sta.	Time	Longitude	Latitude	CTD	SeaOPS	SeaFALLS	LoCNESS	HPLC
15 Sep.	258	0	0730	−0.717	50.617		0			
16 Sep.	259	1	1422	−1.652	50.460	1	1			0.790
17 Sep.	260	2	1605	−8.457	48.670	2				0.336
18 Sep.	261	3	1008	−13.205	47.983	3	2			0.341
19 Sep.	262	4	1013	−18.482	47.173	4	3			0.285
20 Sep.	263	5	1010	−19.963	42.842	5	4			0.140
	263	6	1430	−19.962	42.433			1–3		0.121
21 Sep.	264	7	1010	−20.012	38.717	6	5	4–7		0.111
22 Sep.	265	8	0644	−19.530	35.448	BAS				0.085
	265	9	0907	−19.523	35.445	7	6	8–9		0.071
	265	10	1430	−19.145	35.043			10–11		0.065
25 Sep.	268	T1	1347	−17.227	32.310	8	7– 8	12–14		0.063
26 Sep.	269	11	1103	−20.968	29.047	9	9	15–20		0.073
	269	12	1400	−20.985	28.633			21–23		0.055
27 Sep.	270	13	1106	−20.998	24.135	10	10–11	24–28		0.161
	270	14	1400	−21.010	23.725			29–31		
28 Sep.	271	15	1103	−20.528	19.720	11	12–13	32–37		0.631
	271	16	1600	−20.418	19.050			38–39		0.838
29 Sep.	272	T2	1106	−20.010	15.492		14	40–41		
30 Sep.	273	17	1104	−20.870	10.922	12	15	42–43		0.230
	273	18	1600	−21.177	10.212			44–45		0.228
1 Oct.	274	19	1102	−22.472	7.027	13	16–17	46–48		0.141
2 Oct.	275	20	1106	−24.163	2.817	14	18–21	49		0.164
	275	21	1640	−24.463	2.077		22	50–53		0.095
3 Oct.	276	22	1039	−25.663	−0.778	15	23–24	54–59		0.116
	276	23	1610	−25.897	−1.358			60–62		0.081
4 Oct.	277	24	1140	−27.368	−4.787	16	25–27	63–72		0.137
	277	25	1600	−27.598	−5.308			73–76		0.079
5 Oct.	278	26	1137	−29.115	−8.967	17	28	77–79		0.057
	278	27	1700	−29.382	−9.613			80–81		0.058
6 Oct.	279	28	1135	−30.705	−12.877	18	29–33	82–85		0.066
7 Oct.	280	29	1135	−32.363	−16.685	19	34			0.048
	280	30	1500	−32.547	−17.147		35	86–89		0.053
8 Oct.	281	31	1145	−34.225	−20.662	20	36–40	90–100		0.056
	281	32	1635	−34.557	−21.082			101–102		0.061
9 Oct.	282	33	1145	−37.285	−23.903	21	41			0.103
10 Oct.	283	34	1135	−40.977	−27.690	22	42			0.300
11 Oct.	284	35	1200	−44.867	−31.620	23	43		0	0.209
12 Oct.	285	36	1243	−48.860	−35.477	24	44	103–107	1–5	0.354
	285	37	1755	−49.450	−36.090			107–111	6–9	0.243
13 Oct.	286	38	1200	−51.923	−38.835	25	45	112–119	10–14	1.400
	286	39	1600	−52.147	−39.198			120–122	15–18	1.023
14 Oct.	287	40	1240	−54.455	−42.238	26	46–50	123–130	19–26	0.814
	287	41	1640	−54.877	−42.822	27	51–53	131–132	27–28	1.212
15 Oct.	288	42	1214	−56.700	−46.045	28	54–56	133–144	29–40	0.857
	288	43	1709	−56.753	−46.540	29		145	41	0.663
16 Oct.	289	44	1243	−57.660	−49.795	30	57–58	146–149	42–45	0.937
	289	45	1615	−58.235	−49.797	31	59–61	150–152	46–52	0.556
17 Oct.	290	46	1120	−57.703	−51.665		62–64			0.539

most productive for bio-optical data so far in the AMT Program.

2. CRUISE TRACK

The AMT-5 cruise started in Grimsby on 14 September 1997 and had a refueling stop in Portsmouth on 15–16 September. After Portsmouth, the vessel followed the usual AMT cruise track westward to 20°W,47°N, with a short diversion on 17 September to answer and assist in a man-overboard distress call. After 20°W,47°N, the vessel followed a southerly course until the enforced suspension of scientific research for a ship's trials period off Madeira from 23–25 September. When the the research program resumed, the vessel continued the southerly course along the 20°W meridian, through the edge of the West African upwelling to 13°N, after which, the vessel altered course to the south–southwest for a way point approximately 200 nautical miles east of Montevideo, Uruguay. From this point, the course was almost due south to the Falkland Islands. The JCR arrived in Stanley during the morning of 17 October and the expedition was terminated. A plot of the complete ship's track is shown in Fig. 1 and a summary of the Scientific Bridge Log is given in Appendix B.

Plymouth Marine Laboratory (PML) scientists and the other members of the scientific party, including colleagues from the United States, Canada, Spain, Italy, and Switzerland, travelled to Grimsby on, or by, Wednesday 10 September. The scientific equipment from various scientific institutes was unloaded Thursday morning and by the end of the first day, most had been installed and the decks were quite clear. This unexpectedly good situation, was undoubtedly a result of the efforts of the many *old hands* on board and the practice established from four previous AMT cruises. With minor exceptions, most instrument systems were operational by Friday. The final scientific preparations were completed prior to departure from Grimsby at 0400 GMT Sunday morning (14 September).

The nontoxic water supply was turned on and the underway sampling commenced at 0700 GMT on 14 September, sequential day of the year (SDY) 257. There was no station sampling on Sunday, but with good progress through the southern North Sea, the Straits of Dover, and the eastern English Channel, there was sufficient time to conduct a *shake-down* or test station (designated Station 0) just east of Portsmouth at 0730 GMT on Monday morning. Station 0 produced almost zero data, because the starboard crane for the SeaOPS rig spurted hydraulic oil over the deck and the CTD termination electrically shorted. Eventually, there was a successful SeaOPS profile, using the 10 t midships crane, but the CTD, although repaired, remained untested. On a positive note, it was valuable to trap these faults early, with ample time to make repairs. Optical data from Station 0, were analyzed, quality assured, and reported to the SeaWiFS Project as a calibration data set (to test the agreed upon reporting formats and procedures).

After loading aviation fuel for the BAS Antarctic bases on Monday afternoon and Tuesday morning, giving time for urgent repairs and modifications, the JCR departed Portsmouth at 1100 GMT 16 September; seawater systems and sensors were turned on at 1330 GMT and underway sampling commenced (every 2 hours) for pigments, nutrients, zooplankton, etc. Station 1 was conducted as planned at 1400 GMT southwest of the Isle of Wight in 40 m water. The following instruments were deployed:

1. SeaOPS using the 10 t crane (a completely successful operation);
2. SBE CTD with one bottle at 2, 5, 10, 15, and 20 m, and six bottles at 25 m (a successful CTD profile resulted, but all of the water bottles leaked);
3. Bongo zooplankton nets from the forward crane (the samples were collected successfully); and
4. The UOR, fitted with a fast repetition rate fluorometer (FRRF), was launched and towed at 4 kts for 10 min to test the sensors and logging systems (which was only partially successful, because the FRRF did not activate).

The optical data were analyzed, quality assured, and reported to the SeaWiFS Project as another test calibration data set. Water from all depths was filtered for phytoplankton pigments, notably three depths within the first optical depth (2, 5, and 10 m).

With repairs to the water bottles completed (the tension for the *power chord* closing mechanisms was set incorrectly by the manufacturer), the scientific party was geared up for a complete station Wednesday morning. Unfortunately, a man-overboard distress call from a Russian sailing ship deflected the JCR from station sampling to a search and rescue mission. The JCR arrived at the site in just over 3 h (average speed 16 kts) and searched for over 3 h with the scientific party acting as lookouts. With the rescue effort called off by 1600 GMT, there was time to deploy the repaired CTD (Station 2) for water samples to 100 m, SeaFALLS to check trim and descent rate, and two zooplankton nets; all were completed successfully. No optical data were reported to the SeaWiFS Project, but water samples were analyzed for phytoplankton pigments.

A deterioration in the weather, force 6 with large swell, was the problem to contend with for Station 3 (1100 GMT) on Thursday 18 September (SDY 261), but the deployment of the CTD, SeaOPS, and zooplankton nets went ahead without any major problems; SeaFALLS was not deployed because of the rough seas and poor illumination conditions. The new CTD worked well with only minor water leakage, although, two separate endcaps sheared off during normal usage. The UOR with the FRRF was deployed at the end of the station and was towed for about 2 h to test the system. The FRRF data looked good, but there was some doubt about the data from the CT sensors. The first SeaWiFS image was received from the PML Remote Sensing Group (RSG) for 16 September. The image showed a good

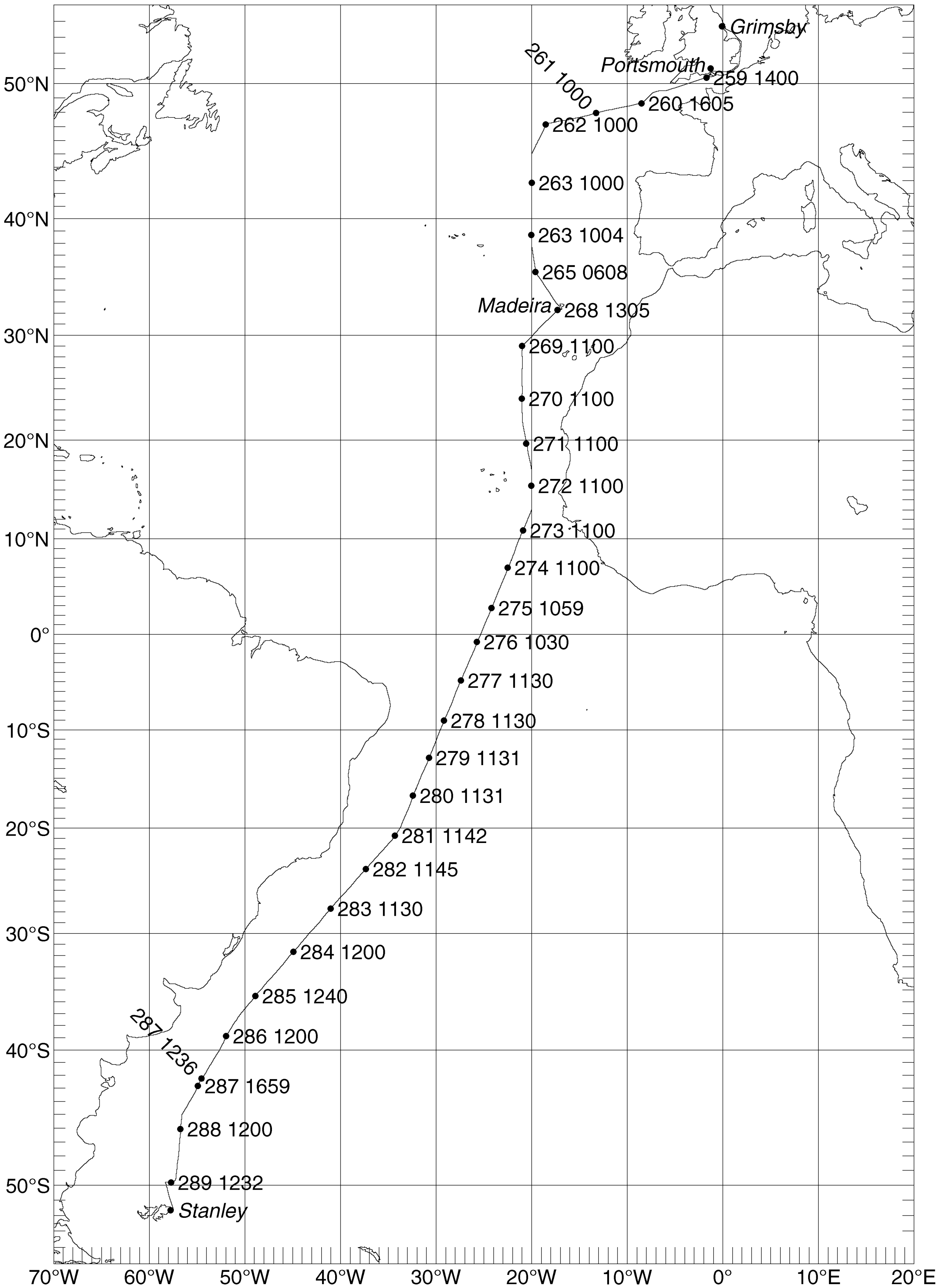

Fig. 1. The AMT-5 cruise track.

view of the English Channel, including the area around the Isle of Wight, the location of the station for that day.

The poor weather continued through Station 4, 1000 GMT Friday 19 September, which made the execution of the main station difficult, but everything went ahead without major mishap. Two water bottles failed to *fire* at the depths triggered, although, subsequent investigation showed no cause for the failure. The CTD cast was to a depth of 250 m and lasted 45 min. SeaFALLS was not deployed due to the rough conditions, and the SeaOPS cast lasted only 35 min. The net casts for zooplankton became the longest activity on station which lasted about 1 h. The UOR was towed away from the station for 3 h and FRRF data were recorded. At the end of the tow, SeaFALLS was deployed to test and modify the trim and monitor the descent speed. Optics data for the first three casts, along with pigment data for the first three stations, were reported to the SeaWiFS Project, clearing the backlogs from the first few days and indicating that the data processing of optical data was fully operational. On board quality assurance of measured versus retrieved $K_d(\lambda)$ data were in good agreement, confirming the veracity of both K_d and L_u data to a certain extent.

Station 5 (Saturday 20 September) was the first station in fair seas and light winds, although clouds obscured the sun. Only SeaOPS was deployed during the morning optical station. Problems persisted with the CTD water sampler and four bottles did not fire at their triggered depths. On redeployment, the same four bottles malfunctioned; the suspicion was that excessive tension was to blame (although the tension was measured and found to be within specification) and a new arrangement for the bottle lanyards was prepared as a solution. The UOR was towed out of the station and recovered at 1400 GMT before the afternoon station; good FRRF data were acquired for the third day. Station 6 was restricted to the deployment of SeaFALLS and was the first station in sunshine (with some high cirrus).

Continuing south along the 20°W line, Station 7 (20 September) proceeded as planned with the set routines of CTD, SeaOPS, nets, and SeaFALLS at 1100 GMT. An increasing number of bottle misfires meant that the CTD had to be redeployed to get water from the key depths missed around the chlorophyll maximum; fortunately, with plenty of time in hand for the leg to Madeira, there were no constraints on having a second CTD cast. The UOR was towed away from the morning station and recovered just before the afternoon SeaFALLS station (Station 8). Entering the Canary Islands, Azores, Gibraltar Observations (CANIGO) region, the first nighttime nets were taken at 2100 GMT.

The final station before Madeira (Station 9) was at the CANIGO target position of 36°N. The BAS CTD was deployed to 2,000 m (some of the sensors on the SBE CTD had a depth limitation of 600 m); throughout the 2-hour deployment, multiple net hauls were executed. The SBE CTD and SeaOPS casts went ahead at 1000 GMT which were immediately followed by SeaFALLS deployments. Regrettably, one CTD bottle at the DCM did not fire, necessitating a second CTD cast. There was a second series of rapid SeaFALLS casts later on (Station 10). Since the exclusive economic zone (EEZ) off Madeira was nearby, there was no UOR tow after the station; the ship made full speed for the rendezvous and the dynamic positioning trials.

Two days were spent in the vicinity of Madeira, during which time, any data backlog was processed, and further tests were made on the CTD (some under guidance from SBE by fax). A new sampling strategy was established, whereby of the top six bottles (numbers 7–12 which were nearly always reliable), two would be fired at the DCM and four would be spread through the surface layer; the bottom six, with the two most unreliable bottles (numbers 2 and 6), would be fired below these in the thermocline (the other two unreliable bottles, numbers 3 and 5, were in this bottom six). If the top six bottles fired reliably, a second CTD cast would not be needed. Unfortunately, the bottle spares ordered from the manufacturer when the endcaps sheared off did not reach Madeira before the JCR left Madeira.

Departure from Madeira was delayed to mid-day on Thursday 27 September (SDY 270), 18 hours later than planned, so no regular station work was permitted. Some time was taken for equipment tests, however: the CTD was fired at the surface and at depth to confirm the unreliable bottle numbers. In addition, SeaOPS and SeaFALLS were tested for trim modifications.

Friday 28 September (Station 11) established the pattern for the next few days, with the routine of previous AMT cruises getting set. With the clocks advanced by 2 h, stations started at 1000 ship's time (1100 GMT) with a deep CTD to 600 m (still in the CANIGO region), a SeaOPS cast to 100 m, several SeaFALLS deployments to 150 m, and net casts to 200 m. With only one CTD cast (10 bottles fired reliably), the station was completed in about 1 h. At 1300 ship's time, there was a second SeaFALLS station in good sky conditions, giving the best optics data of the cruise so far. Still in the CANIGO region, there was a night zooplankton net cast at 2200.

An almost identical pattern was followed for Stations 13 (1100 GMT) and 14 (1600 GMT) on 27 September, and Stations 15 (1100 GMT) and 16 (1600 GMT) on 28 September, with excellent optical data being collected during clear sky conditions. All other activities went as planned, with CTD deployments to 600 m being the new set pattern. On Monday 29 September, the ship was in the EEZs between the Cape Verde Islands and Senegal, so no station was executed (no CTD); there were some test deployments of the SeaFALLS profiler which was exhibiting some problems with the auxiliary CT sensors. Another excellent day of clear sky conditions followed on 30 September (Station 17 at 1100 GMT and Station 18 at 1600 GMT) with a matching CTD cast.

Approaching the equator, the weather turned cloudy and overcast with occasional rain squalls, making the optical work difficult at times and less relevant to SeaWiFS validation objectives. Nevertheless, some acceptable casts were accomplished in between the clouds on 1 October (Station 19) and the complete overcast stations were used to intercompare radiometers (Stations 20 and 21 on 2 October). Over these 2 days, the CTD and water sampler worked perfectly (all 12 bottles fired), and the measurement of the pigments and accessory parameters proceeded unhindered.

South of the equator, blue skies with a few fluffy clouds predominated; the conditions were excellent for SeaWiFS validation. Stations 22 and 23 on 3 October (SDY 276), interrupted only by the *crossing the line ceremony*, and Stations 24 and 25 on 4 October provided excellent conditions and lots of casts: at the main morning station (Station 24), there were 3 SeaOPS casts and 10 SeaFALLS casts, which were followed by 3 SeaFALLS casts during the afternoon (Station 25). The large number of casts will allow for an investigation into the broader issues of intra- and inter-pixel variability of optical properties over distances of 1–2 km.

The following two days were hampered by more than the average amount of cloud cover. Two stations were completed on 5 October (Stations 26 and 27), but only one on 6 October (Station 28), with good illumination conditions for at least part of each station. Standard CTD casts to 600 m were completed satisfactorily on each day, with all 12 water bottles firing and closing reliably.

Conditions were overcast for the morning station on 7 October (Station 29), so there was only one SeaOPS cast coincident with the CTD and zooplankton net casts; in the poor illumination conditions, SeaFALLS was not deployed. The UOR was towed from the station and recovered at 1500 GMT prior to the next station. In contrast, the afternoon station (Station 30) was completely cloud free, so there was a second SeaOPS cast to 150 m and four SeaFALLS casts to 200 m; all were rated as probably the best of the cruise to date.

Even better sky conditions were encountered during Station 31 (1130 GMT) on the morning of 8 October (SDY 281), which was completely cloud-free. During this station, 5 SeaOPS casts and 11 SeaFALLS casts were executed; the resulting data set was probably the best optical data ever collected on an AMT cruise. The extra time for optics casts gave ample time for numerous zooplankton net casts and the CTD to be deployed to 600 m. Once again the UOR with FRRF was towed away from the station until midafternoon and produced good data. Cloudy conditions dominated the afternoon casts of SeaFALLS (Station 32), but useful data were acquired.

SeaWiFS images transmitted to the ship showed the spring bloom was well advanced on the Patagonian Shelf. To make good speed as the JCR proceeded south in the Brazil Current towards the productive zones of the Patagonian Shelf, stations were restricted to only one in the morning with a duration of less than 1 hour. Cloudy conditions hampered the SeaOPS casts (Station 33 on 9 October and Station 34 on 10 October), but the CTD and net casts were completed with no problems on both days.

During Station 35 on 11 October (SDY 284), the CTD wire jammed (off a sheaf) when the CTD was at about 180 m. Unfortunately, the CTD cast had to be aborted and no water samples were obtained. The problem was rectified fairly quickly (100 min), but 200 m of cable had to be discarded and the CTD cable reterminated. Meanwhile, the other activities (SeaOPS and net casts) proceeded uninterrupted.

Station 36 on 12 October proceeded smoothly with the CTD, zooplankton nets, SeaOPS, SeaFALLS, and LocNESS all deployed. With the ship back at regular speed, the UOR with FRRF was towed from the morning station to the early afternoon station. A SeaFALLS and LocNESS intercomparison was the feature of the afternoon station (Station 37), which was unfortunately dominated by cloud cover; for both of these stations, there was a significant rise in chlorophyll concentration to over $0.35\,\mathrm{mg\,m^{-3}}$ as the confluence was approached. Late night zooplankton net casts were also executed.

Station 38 on 13 October (SDY 286) was the first in the high chlorophyll waters of the confluence, where the chlorophyll concentration reached $1.4\,\mathrm{mg\,m^{-3}}$ at the surface for the morning station. The heterogeneity of the region was illustrated by the variation in structure of temperature and chlorophyll derived from successive, closely-spaced vertical profiles with SeaFALLS and LoCNESS—five profiles in a row, within 40 min of one another, were all significantly different, some by a large amount. It was the same for the afternoon station (Station 39) when, like the morning, cloud-free skies provided excellent conditions for optical measurements. The UOR was towed again between stations, giving another series of data with the FRRF in waters of high activity for photosynthesis and primary productivity in the spring bloom.

The following day (October 14) proved to be more of the same, with high chlorophyll concentrations and very dynamic physical conditions. The rapid deployment of expendable bathythermograph (XBT) probes through the confluence tracked 6 eddies clustered around a warm core ring, validating the structure in TOPEX imagery for the previous few days (which had been relayed to the vessel from a laboratory on shore). The highly complex vertical structures were reproduced in the phytoplankton taxa and pigment assays. Mostly cloud-free skies gave a large number of good optical profiles with SeaOPS, SeaFALLS, and LocNESS for both the morning and afternoon stations (Stations 40 and 41, respectively). The CTD was deployed to a depth of 600 m for both stations.

For the third day in a row (15 October), the stations were in high chlorophyll water and, for at least part of each period, there was cloud-free, sunny skies providing very good optical conditions and excellent data. Once again, the CTD was deployed in the morning (Station 42) and afternoon (Station 43).

By Stations 44 and 45, the transect had crossed the Falkland Current, although the water on the continental shelf (300 m) at 5.8°C was probably still influenced by it. Chlorophyll concentrations, although lower than recent days, were still moderate at approximately $1\,\mathrm{mg\,m^{-3}}$. Good conditions prevailed for the optical casts and some of the best data ever obtained south of Montevideo was collected. The UOR was again towed between morning and afternoon stations and the CTD was deployed at both locations. Even more remarkable, for the final station just off Stanley on 17 October (SDY 290), blue skies allowed for a final cast of SeaOPS at 57.500°W,51.667°S (the most southerly station executed in the AMT Program) in high chlorophyll water. Unfortunately, the sun was rather low in altitude at 0900 ship's time, which did not make for the best optical conditions. The CTD was not deployed and the scientific work was terminated after the station.

3. RESEARCH REPORTS

In this section, the individual research reports from the scientific groups participating in the AMT-5 cruise are presented.

3.1 Physical Oceanography

The primary physical oceanographic measurements during AMT-5 were of water properties and velocities; the former were measured by CTD and XBT casts, and the latter by an acoustic doppler current profiler (ADCP).

3.1.1 Water Properties

The CTD measurements were made by profiling a SBE 911plus when the ship was stationary. This usually involved daily stations in the late morning at 1000 or 1100 ship's time. Also fitted to the CTD, were secondary temperature and conductivity sensors, a WETstar miniature fluorometer (Wet Labs, Inc.), a Cstar transmissometer (Wet Labs, Inc.), and a spherical PAR sensor (Biospherical Instruments, Inc.). With these dual CT sensors, the SBE 911plus instrument is self-checking and nominally self-calibrating. The average difference between the primary and secondary sensors was seen to be 0.001°C in temperature (T) and 0.005 in salinity (S). Salinity values were compared with 70 salinity bottle samples, taken from the top and deepest water bottles from each CTD cast, showing differences typically of less than 0.002.

The CTD package included a rosette water bottle sampling system fitted with 12×30 l polyvinylchloride (PVC) bottles. For most of the cruise, there was one station late morning each day; there were afternoon CTD casts for the last three days (SDY 287–289) in the high chlorophyll regions at the southern end of the transect. The initial CTD casts were troubled by mechanical (and perhaps electrical) problems, which resulted in a number of bottles failing to close properly. The mechanical shortcomings were overcome by adjusting the tensioning in the bottle closing mechanisms (power chords) and altering the lanyard connections to the release latches. An intermittent electrical problem resulted in 1–4 of the release latches failing to fire on each of the first 10 casts. Extensive testing and communication with the manufacturer failed to isolate the problem; however, after cast 10, all latches fired consistently. From casts 5–7 there was insufficient water sampled at the chlorophyll maximum because the bottles failed to close, so a second cast was required. A summary of the CTD log is presented in Appendix C.

For casts 1–8 and cast 31, the CTD was profiled to a depth of 250 m, while for casts 9–30, the CTD was profiled to a depth of 600 m. Data was recorded at 24 Hz via a SBE deck unit onto both a Dell PC and the shipboard computer level-C data logger using BAS Research Vessel Services (RVS) software. Station 23 was aborted at 200 m when the coaxial CTD cable frayed on the winch; no bottles were fired. The CTD was reterminated prior to cast 24. There was one deep CTD cast with a (BAS) Neil Brown Mk IIIB CTD to 2,000 m at 19.5233°W,35.4450°N, within the CANIGO area. A contour plot of the salinity to 200 m is shown in Fig. 2, the fluorometer to 200 m in Fig. 3, and the water transmission at 660 nm, in Fig. 4.

During the cruise, a total of 70 Sippican T–5 XBTs and 66 Sparton T–7 XBTs were deployed (Appendix D). Temperature profiles were obtained down to a depth of 1,830 m for the T–5 probes with the ship slowed to 8 kts, and 760 m for the T–7 probes with no restriction on speed. Typically, the T–7 deployments were at 0700, 1300, 1900, and 2400 ship's time each day. This strategy was altered for regions of special interest (e.g., frontal crossings), at which time T–5 probes were deployed at 50 km intervals. The regions targeted for analysis were:

- 38°N to 35°N, analysis of which showed evidence of the spreading Mediterranean Water centered at a depth of 1,000 m (Fig. 5);
- 10°N to 3°S, which resolved the currents in the equatorial zone (Fig. 6 and Section 3.2); and
- 38°S and 45°S at the confluence of the Brazil Current and Falkland Current systems (Fig. 7).

Occasionally, T–7 XBTs were deployed at the daily station for intercalibration with the CTD. The preliminary analysis of the temperature of the CTD and XBT, shows a consistent structure, but, in general, the XBT values were approximately 0.5°C higher than the CTD. Contour plots of the temperature structure (surface to 750 m) for the Northern and Southern Hemispheres are shown in Figs. 8 and 9, respectively. No calibration correction has been applied to the XBT data shown in the contour plots.

Near-surface T-S values were obtained from an SBE thermosalinograph (TSG) using water pumped in from a

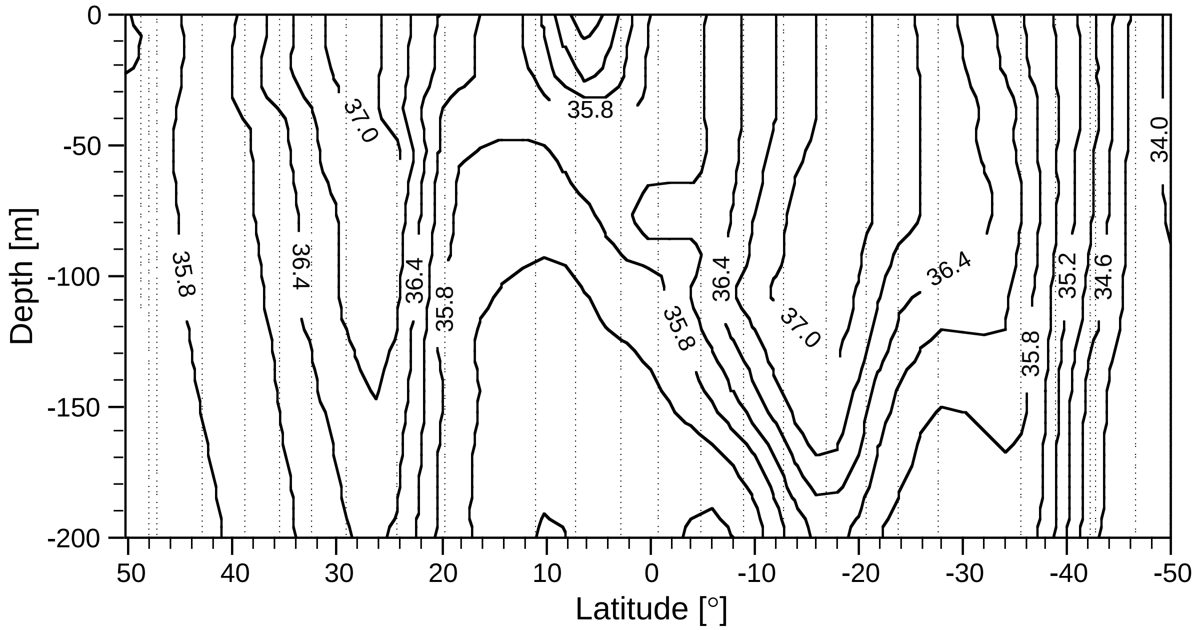

Fig. 2. A contoured vertical section of salinity from CTD casts (the dotted lines are the individual CTD stations).

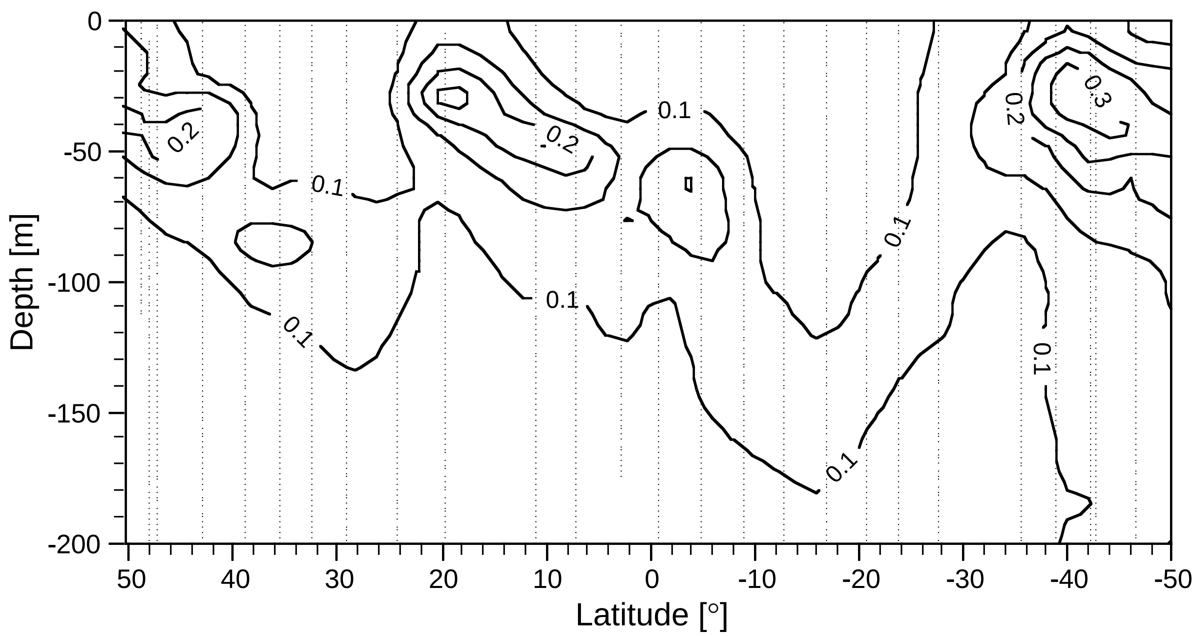

Fig. 3. A contoured vertical section of chlorophyll fluorescence from station casts (in volts).

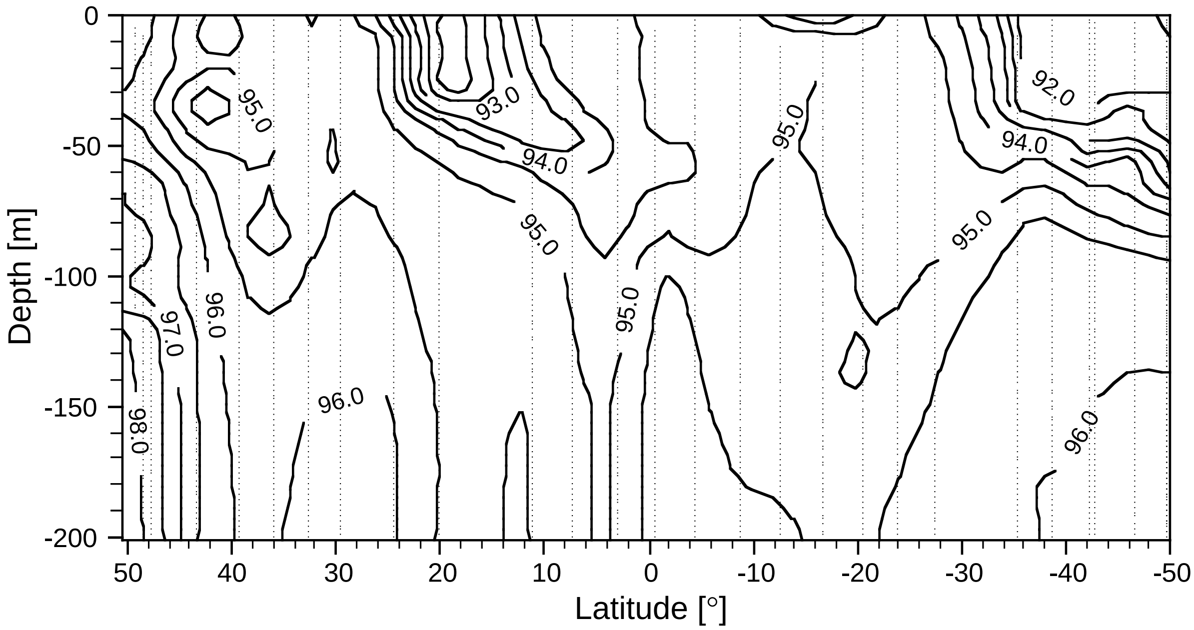

Fig. 4. A contoured vertical section of transmittance (%) from station profiles.

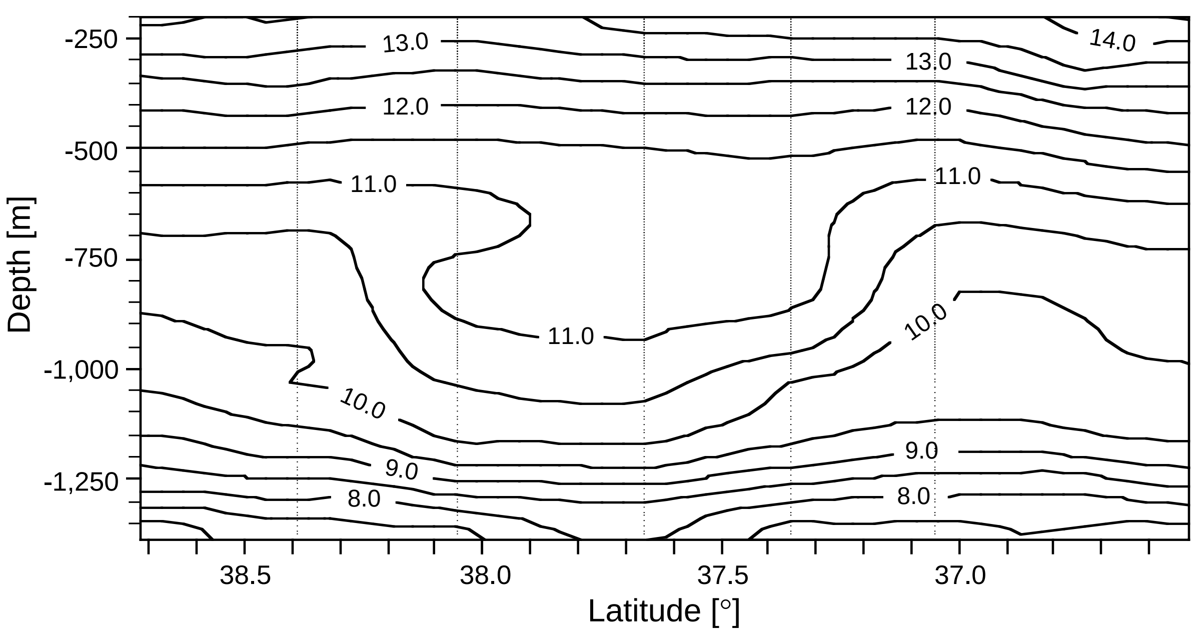

Fig. 5. A contoured XBT section (°C) showing Mediterranean Water at 1,000 m (the dotted lines are the individual XBT casts)

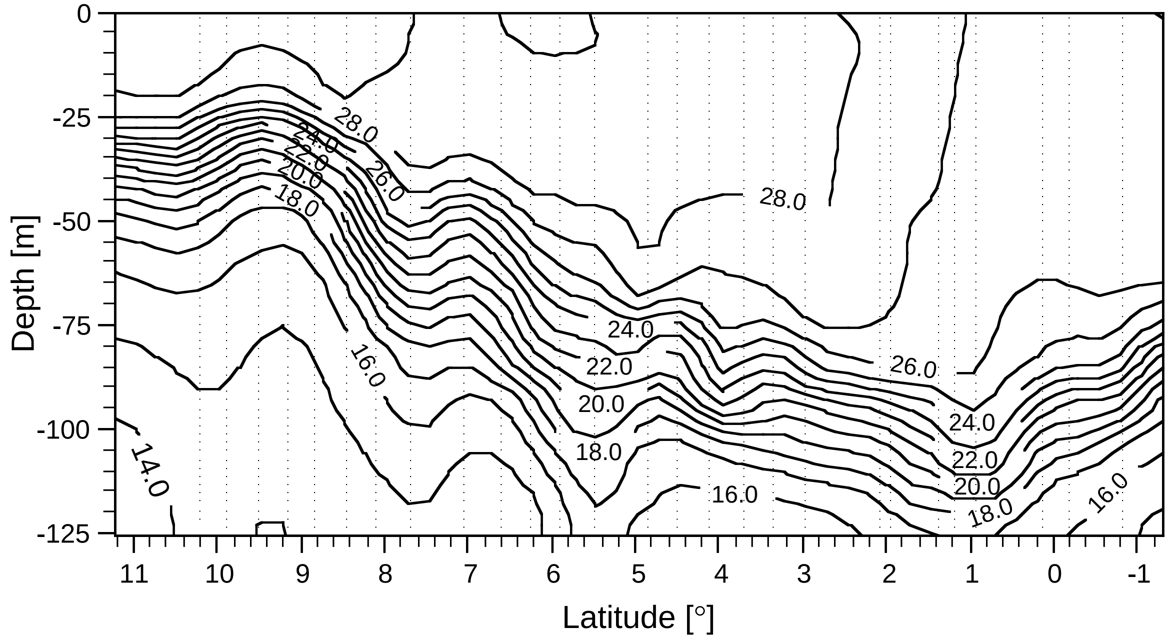

Fig. 6. A contoured XBT section (°C) through the equatorial region.

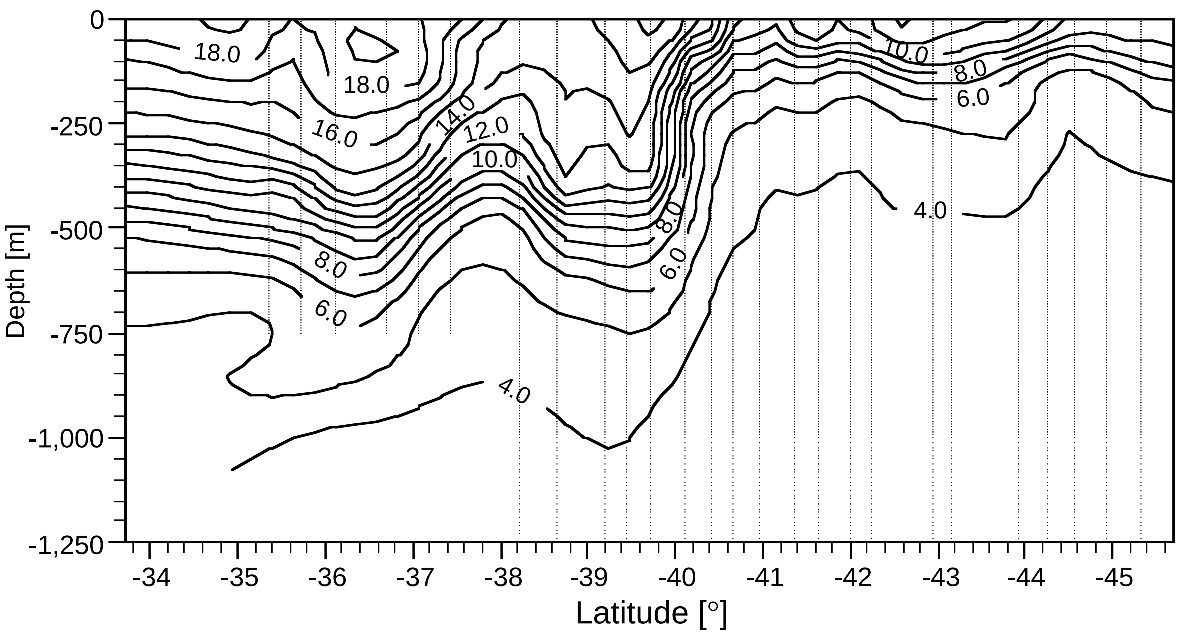

Fig. 7. A contoured XBT section (°C) through the confluence region.

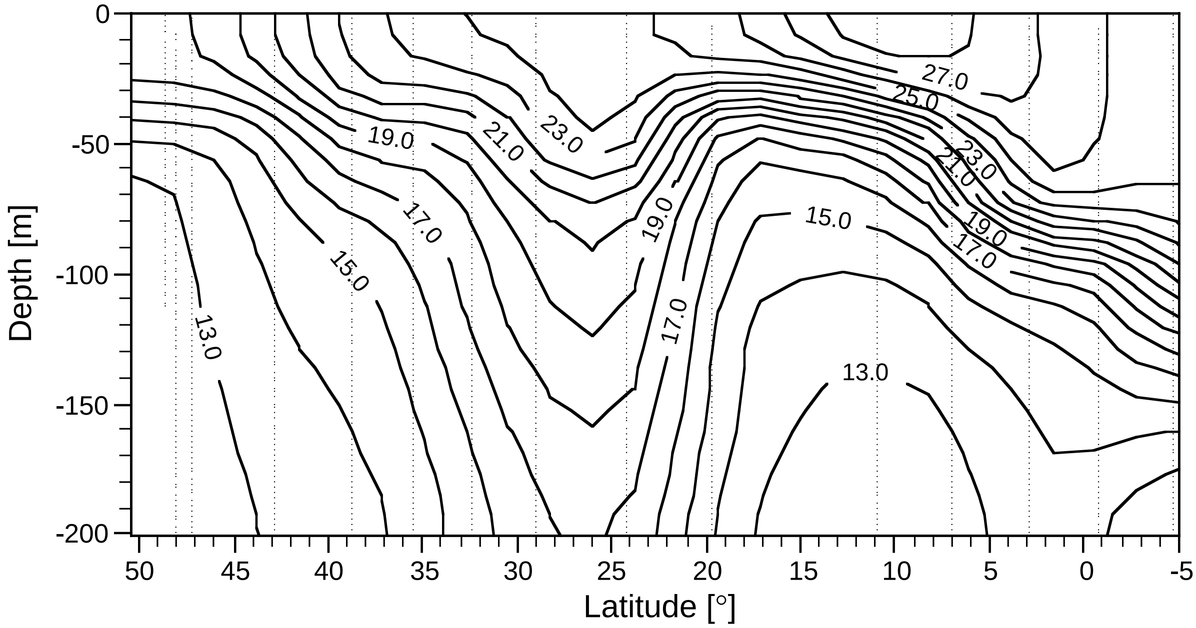

Fig. 8. A contoured XBT section (°C) of the Northern Hemisphere.

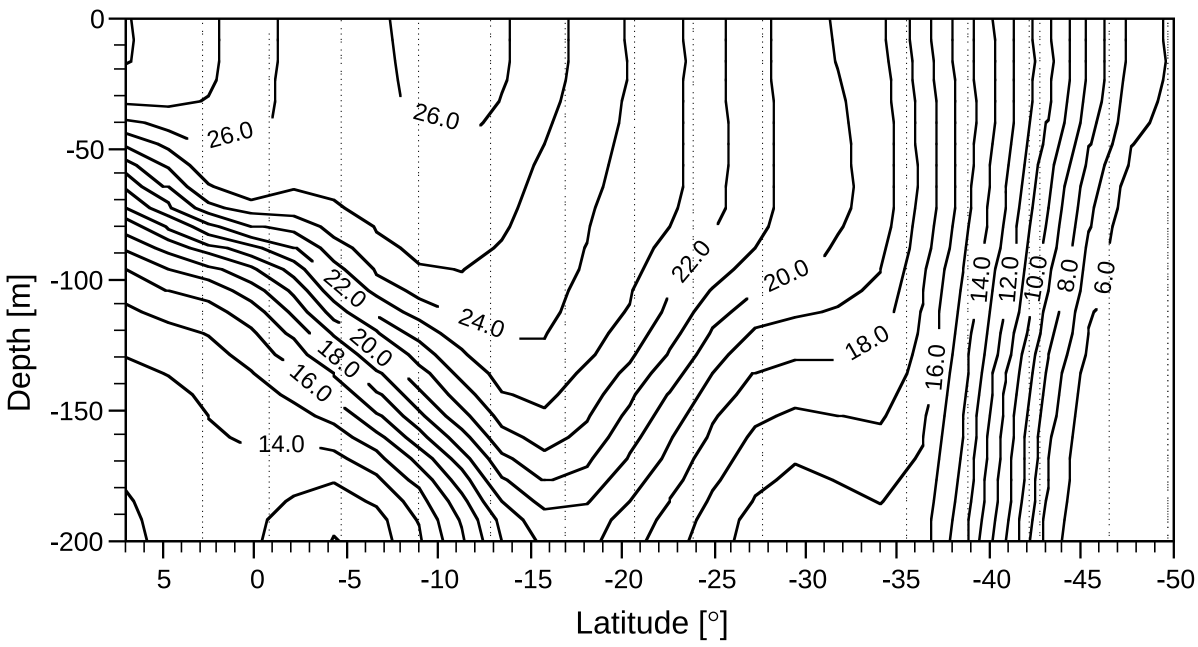

Fig. 9. A contoured XBT section (°C) of the Southern Hemisphere.

hull-mounted tube 7 m below the surface. A measurement was made every 5 s, which was logged into the ship's computer system.

3.1.2 Water Velocities

The JCR has a hull-mounted 150 kHz Research Designs Instruments ADCP unit. The transducer is enclosed in an oil-filled sea chest recessed into the hull to protect it from ice. This chest is enclosed by a 33 mm thick window of low density polyethylene and filled with silicone oil. The ADCP unit uses a Doppler shift of the signals reflected from four, pulsed acoustic beams radiating out and downwards to derive subsurface currents. The method relies on particulate material in the water to scatter the acoustic signals. The acoustic frequency employed is optimal for scattering from particles of the dimensions of zooplankton.

Data were collected at 2 min intervals in 64 8 m bins. The ADCP data obtained during AMT-5 were logged and archived for subsequent processing. Distinct patterns of zooplankton migration were observed on a diel time scale as the zooplankton migrated to depth during the day and returned to the surface waters (within the ADCP range) by night. The combination of the special housing of the ADCP with high ship speed and very low particle concentrations during the day resulted in signal returns that were undetectable for large parts of the transect within the oligotrophic gyres.

3.2 TOPEX

It is particularly difficult to directly validate satellite altimetric measurements over the oceans due to the ever changing topography of the sea surface. In many areas, ocean topography maps often appear to be composed of many chaotic features, whereas in other regions, definite strong and coherent features are apparent. During AMT-5, a concerted effort was made to validate sea surface height (SSH) anomaly maps derived from the TOPEX altimeters using *in situ* measurements derived from XBT, CTD, and underway T-S measurements. TOPEX maps of SSH anomaly were used to identify the major features of the AMT-5 transect, which were then used to devise an appropriate *in situ* sampling strategy to resolve the major features seen in the imagery.

The Atlantic equatorial current system displays an east-to-west, and west-to-east banded structure which dominates the surface flow and hydrography of the region. The North Equatorial Current (NEC) is a region of broad uniform westward flow north of 10°N. The easterly flowing North Equatorial Counter Current NECC, is highly seasonal and weakest in February when the trade winds in the Northern Hemisphere are strongest. The South Equatorial Current (SEC) is a broad and uniform westward flow, and extends from approximately 3°N to at least 15°S. The strongest equatorial current is the westward flowing Equatorial Under Current (EUC) centered on the equator at a depth of 100 m. At a depth of 200 m north and south of the equator, there are the narrow and swift North Equatorial Undercurrent (NEUC) and South Equatorial Undercurrent (SEUC), respectively.

The discharge from the Amazon River is carried northwestward and then eastward by the NECC, whereupon it combines with the excess in precipitation over evaporation found in this region. It is limited to a depth of approximately 100 m at about 25°C (Emery and Dewar 1982) and a salinity less 35.0 (Müller-Karger et al. 1988).

The NECC is prevented from flowing north by the east–west orientation of the African coastline; however, some of it does escape north and combines with the NEUC to drive a cyclonic gyre centered at 22°W,10°N. Because of the observed doming of the thermocline in the summer, the gyre is known as the Guinea Dome. The associated circulation reaches to depths of 150 m and exists throughout the year, although, it weakens in winter.

3.2.1 Along-Track SSH

The TOPEX satellite was launched in August 1992 and carries the most precise radar altimeters available to date. Two altimeters (C-band and Ku-band) are operated in tandem to facilitate the corrections required to compensate for the delay of the radar pulse caused by variations in ionospheric structure. Further corrections for the effect of tropospheric signal attenuation are undertaken using data derived from an on board microwave radiometer which determines the integrated water vapor content of the atmosphere. Extremely precise orbit tracking and position systems including a laser retroreflector array (for orbit tracking and height determination), a Doppler orbitography and radio-positioning system, plus an experimental global positioning system (GPS), allow the TOPEX satellite orbit to be maintained to within ±500 m. Operating in a 10-day repeat cycle, the TOPEX altimeters provide near-complete coverage of the world ocean between 66°N and 66°S having an equatorial track spacing of approximately 300 km. The precise orbit determination and novel atmospheric correction strategy adopted by the TOPEX mission, when referenced to the most current geoidal model, means that estimated SSH anomaly data have an accuracy of better than 5 cm.

The region of the Atlantic equatorial current system was selected to validate along-track SSH anomaly data derived from the TOPEX altimeter. TOPEX along-track data were spatially interpolated to produce two-day analysis maps at the University of Colorado Center for Astrodynamics Research (CCAR). These data were then supplied to the JCR in near-real time via electronic mail (e-mail) communications.

A combination of *in situ* profiling and underway instruments were used to resolve the vertical and horizontal structure of the region. Temperature profiles were obtained down to a depth of 1,830 m using T–5 XBTs. The deployment of the T–5s began as the vessel crossed over the Guinea Dome at approximately 20°W,10°N, continuing at 50 km intervals until the equator. In total, 25 XBTs were deployed through the region. Near-surface *T-S* values were obtained from the TSG. A measurement was made every 5 s, which was logged on the ship's main computer system. The density of the surface waters was derived from the near-surface *T-S* values. CTD profiles were made with the SBE 911plus when the ship was stationary, which was deployed at three stations marked in Fig. 10 at 20.87°W,10.92°N, 22.47°W,7.03°N, and 24.16°W,2.82°N to a depth of 600 m.

Figure 10 shows the TOPEX and second Earth Resources Satellite (ERS-2) analysis derived on 28 September 1997 for the region 12°N to 1°S. The AMT-5 cruise track has been overlaid onto this image together with the position of CTD Stations 12, 13, and 14 (heavy circles) and the XBT profiles (squares) completed within the region shown by the image. The TOPEX data reveals an east–west band of positive SSH anomaly greater than 10 cm in the latitude range of 9–4°N. CTD Stations 12 and 14 straddle the positive anomaly to the north and south, respectively, and CTD Station 13 was made in the central region. Complemented by two-hourly XBT casts and underway sampling, these stations were considered adequate for the validation of the SSH anomaly feature seen in Fig. 10.

Figure 6 shows the XBT section derived from 25 XBT casts between the latitudes of 12°N and 1°S along the transect shown in Fig. 10. Within this figure, all of the major equatorial current features are resolved, including the Guinea Dome at 9°N, the NECC bounded by the 28°C isotherm between 8–3°N extending to a shallow depth of 40 m, the EUC shown by a deepening of the thermocline and a separation of the isotherms at 4–1°N, and the SEC together with the equatorial upwelling seen at 1°N.

The NECC and associated currents are best resolved by salinity and density differences rather than by the temperature structure alone. CTD Stations 12, 13, and 14 are shown in Fig. 11. The salinity casts are shown in Fig. 11a and clearly reveal the NECC as a strong surface feature having a marked halocline at a depth of 30 m (Station 13). Station 12 reveals the NEC as a subsurface salinity maximum at a depth of 30 m, whereas Station 14 shows the characteristic deepening of the mixed layer and salinity maximum of the EUC at a depth of 50–100 m. Figure 11b shows the associated temperature cast data and reveals the NECC as a shallow (30 m) warm layer.

As the NECC has a component of less dense water originating from the Amazon outflow, the surface density has been computed from underway temperature and salinity data from 7 m in depth, which is presented in Fig. 12. Here, the NECC is seen between 8.5–4.5°N with a low density core located between 6–7°N. These data are in excellent agreement with the position of the NECC, seen as positive SSH anomaly data shown in Fig. 10, and clearly demonstrate the ability of the TOPEX altimeter to locate major geostrophic current features.

3.2.2 Conclusions

TOPEX along-track SSH anomaly data have been interpolated to produce two-day analysis maps which were supplied to the AMT-5 team in near-real time by the CCAR via e-mail communications. These images highlight the two-dimensional oceanographic surface structures which describe the context of the physio-chemical and biological ocean–atmosphere data sets recorded during the AMT-5 experiment. In particular, these data have been useful for determining the large-scale geostrophic current systems in the tropical regions where ocean color and thermal imagery are difficult to obtain due to the large amounts of cloud cover characteristic of these regions. Throughout the AMT-5 experiment, XBT profiles and CTD casts were made, which were used to validate the TOPEX sea surface height anomaly maps.

Imagery supplied on 28 September 1997 clearly highlighted the NECC as the most dominant feature of the AMT-5 transect between 0–12°N and was chosen as a target area for TOPEX validation. *In situ* data sets, including XBT and CTD casts at regular intervals, as well as continuous underway sampling, were used to produce *T-S* sections and surface density measurements along the AMT-5 cruise track between 10°N to 1°S. These data clearly reveal the NECC characterized by warm less-saline waters. SSH anomaly maps derived from TOPEX for the same region clearly show the NECC as a positive SSH anomaly, and the position of the NECC suggested by the TOPEX data agrees exceptionally well with the *in situ* data.

Satellite altimeter data provide an unprecedented view of the ocean surface providing information on the dynamics of geostrophic current systems through differences of ocean surface topography manifested in images of SSH anomaly. Vertical sections of the *T-S* structure of the North Atlantic equatorial current system between 12°N and 1°S identify the features seen in TOPEX SSH anomaly data as the NECC.

3.3 ROSSA

In order to understand the regulation of heat, momentum, and gas transfer, improved modeling of the processes defining the structure and state of the air–sea interface is required, which in turn, requires comprehensive *in situ* validation data sets. The current understanding of these processes remains poor, because of the limited availability of existing *in situ* data sets; however, data sets of this nature are required as a forcing function to atmospheric and climate models. In the case of coupled ocean–atmosphere models, understanding and quantification of the processes occurring at the air–sea interface are critical, because it is through this thin layer that all ocean–atmosphere heat, gas, and momentum exchange occurs. Many satellite instruments have complementary spectral wavebands and viewing geometries which provide both regional and global

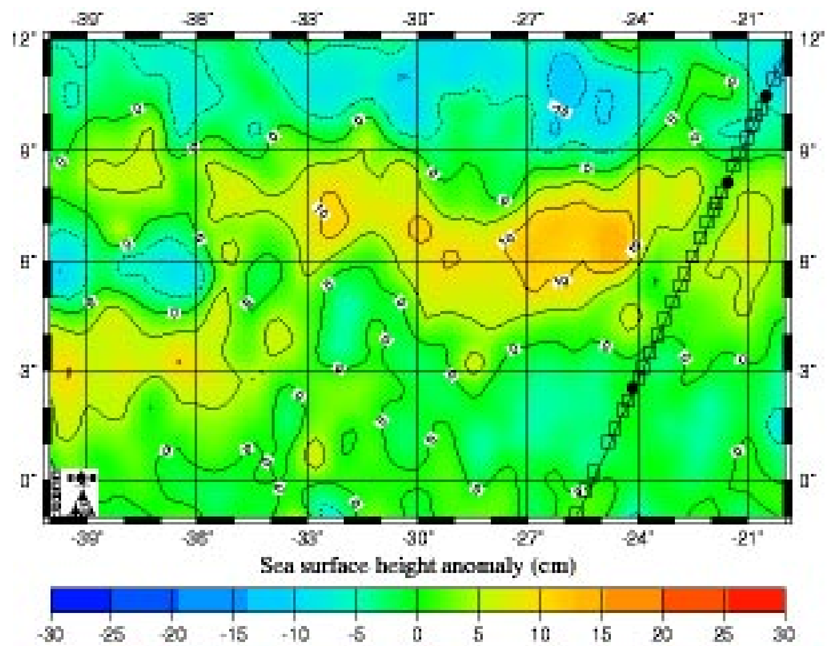

Fig. 10. TOPEX/ERS-2 SSH analysis supplied to the JCR for 28 September 1997. Solid circles show CTD stations and open squares show the position of XBT casts along the AMT-5 transect.

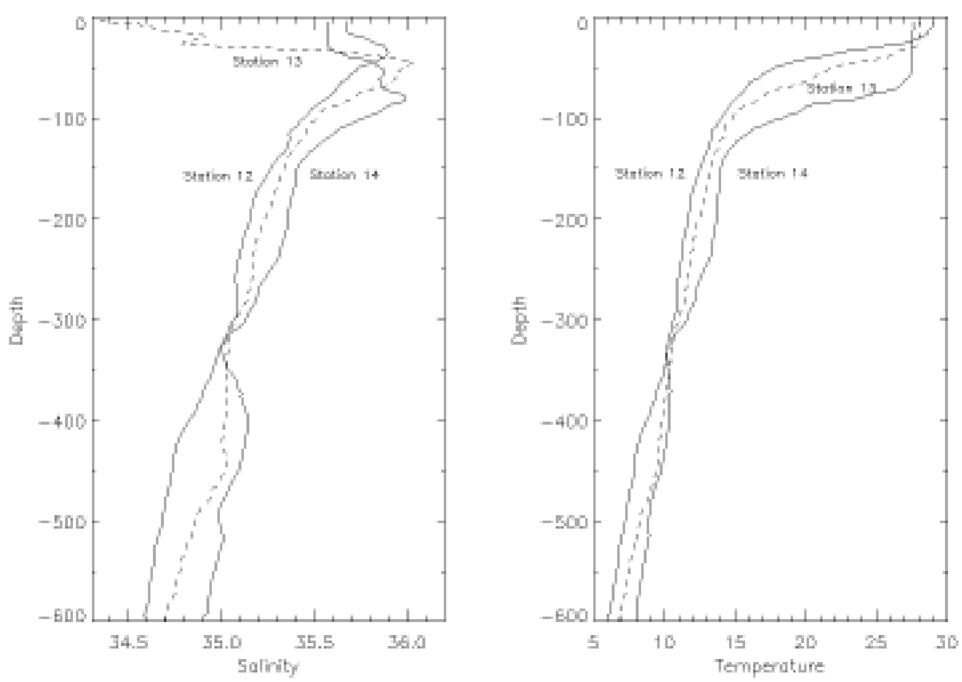

Fig. 11. Salinity casts made at Stations 12, 13, and 14 along the AMT-5 transect (left panel) and the corresponding temperature casts (right panel).

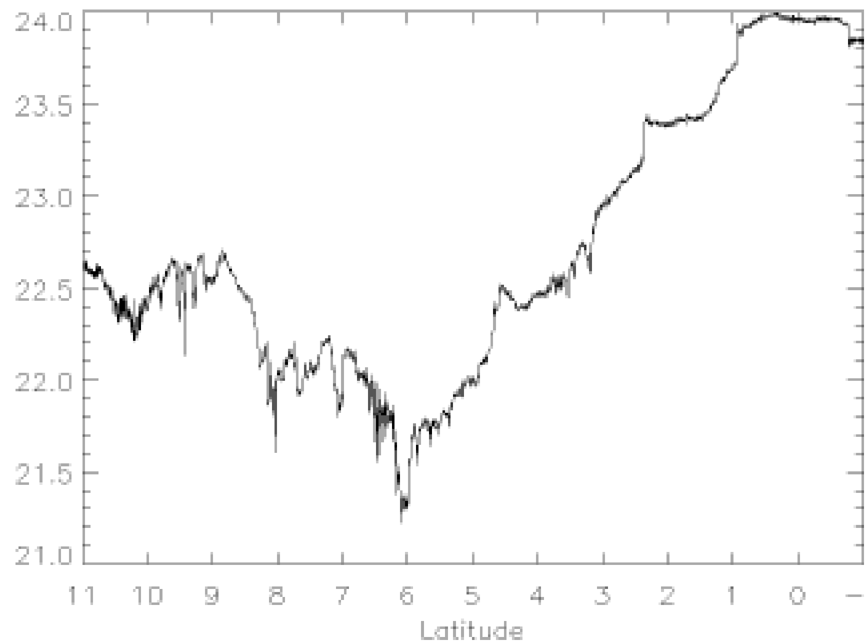

Fig. 12. Underway density computed from the 7 m temperature and salinity data along the AMT-5 cruise track.

coverage. Observations of the integrated atmospheric water vapor content or estimates of the surface wind speed, surface roughness, air temperature, cloud cover, and dynamic structure of the ocean are all possible.

The objective of the ROSSA activity within the AMT Program is to increase the understanding of the air-sea interface by obtaining detailed *in situ* oceanographic and meteorological observations of both the interface itself plus the general structure of the deeper ocean and upper atmosphere which define the behavior of the physio-chemical and biological processes occurring at the air-sea interface. These data are collected for use with contemporaneous and spatially coincident satellite observations from the National Oceanic and Atmospheric Administration (NOAA) Advanced Very High Resolution Radiometer (AVHRR), ERS-2 Along-Track Scanning Radiometer (ATSR), the eighth Geostationary Operational Environmental Satellite (GOES-8), the Meteorological Satellite (METEOSAT) infrared radiometer, the TOPEX radar altimeter, and the Special Sensor for Microwave/Imaging (SSM/I) microwave radiometer. When used synergistically, this combination of satellite and *in situ* observation allows for a more complete description of the sea surface and atmosphere to be obtained. Of particular importance is the need to develop techniques to derive estimates of the heat flux across the air–sea interface from satellite data alone, and to understand the physio-biochemical processes which have a surface interface expression (e.g., biological slick material) by combining *in situ* and satellite data. The AMT program is ideally suited to this task.

3.3.1 SOSSTR

This is the second ROSSA experiment to be executed within the AMT Program. ROSSA has a number of objectives.

1. Measure the sea surface *skin* temperature (SSST) of the air–sea interface, atmospheric humidity, longwave downwelling infrared, shortwave solar radiation, and bulk sea surface temperature measurements (BSST) for the investigation of heat and gas exchange between the ocean and atmosphere.
2. Provide the mean atmospheric conditions of the AMT-5 experiment, from upper air profiles of temperature and humidity, which are required to validate the atmospheric transmission models and algorithms used by satellite sensors (in both the infrared, microwave, and visible spectral wavebands), which account for the atmospheric attenuation of water-leaving signals.
3. Provide a precision BSST measurement of the upper 0.5 m of the sea surface.
4. Validate (and calibrate) SSST measurements derived from the GOES-8, NOAA AVHRR, ERS-2 ATSR, and METEOSAT satellite infrared radiometers.
5. Validate new technology for the measurement of the SSST deviation with the aim of deploying semi-autonomous infrared radiometer systems on ships of opportunity.

6. Validate TOPEX altimeter measurements using a combination of XBT and CTD casts together with underway T-S sampling.

A new single-channel, broadband (8–12 μm) infrared radiometer system has been specifically developed through a joint effort of the CCAR and the Southampton Oceanography Centre (SOC), which aims to provide an autonomous system for accurately determining (0.1 K) the SSST. AMT-5 is the first deployment of this system which will be used in a more widespread ship of opportunity sampling program based at the University of Colorado.

The ship of opportunity sea surface temperature radiometer (SOSSTR) consists of two TASCO THI-500L infrared radiometer heads (PRL 500L) mounted in a weatherproof enclosure together with a calibration subsystem, data logging, and communication package. The SOSSTR system uses a two-point continuous calibration obtained by viewing one of two precision blackbody cavities maintained at different temperatures. The blackbody units are attached to an armature which rotates 360° in approximately 12 minutes, thereby providing a complete end-to-end calibration cycle for both radiometer heads. The internal temperature of the instrument is monitored by three separate platinum resistance temperature (PRT) sensors located at different points within the instrument enclosure.

The radiometer output signals, together with instrument thermometry and housekeeping data, are sampled at 16 bits via a Campbell Scientific AM416 multiplexer to a CR10x data logger. Data are logged in real time to a workstation located in the Underway Instrumentation and Control (UIC) room via a dedicated RAD SRM6A/F short-haul modem link run through the ship's scientific wiring. The CR10x uses onboard 2 Mbyte random access memory (RAM) which acts as a *ring buffer* in case of communication problems between the UIC and the instrument. This provides over 5 h of onboard data storage should a communication problem occur. The configuration described above provides large flexibility in terms of real-time data access and instrument control, which can all be achieved using the workstation connection.

The SOSSTR instrument was installed on the forward mast of the JCR to view the sea surface at an angle of 38° from nadir and the sky at the complementary vertical angle using a small laser unit. After initial setup and laboratory calibration of the radiometers and PRT sensors using an SIS T416 digital reversing thermometer and a blackbody unit, the instrument was thoroughly tested on the Grimsby-to-Portsmouth leg. Several problems were encountered including communication, operation, and instrument thermal stability issues. These were traced to a faulty Earth connection and the system was operated continuously for the remainder of the AMT-5 cruise. Additional optical alignment experiments were undertaken *in situ* off Madeira based on discrepancies in the analyzed data, but no adjustment to the optical train was required. The instrument proved to be robust against inclement weather conditions, including heavy tropical rainfall events and up to force 8 sea conditions.

Viasala RS-80 radiosonde packages measuring atmospheric temperature, pressure, and relative humidity were deployed every day. These data were logged to a Viasala PP-11 PTU preprocessor deck unit and finally to a personal computer (PC). Processing software to generate geophysical variables from the raw data were written during the cruise in the Interactive Data Language (IDL). Figure 13a shows the positions of all the radiosonde releases completed during the AMT-5 cruise, and Fig. 13b shows a sample of the processed vertical profiles of potential temperature and specific humidity obtained on SDY 280.

The batch of RS-80 sondes supplied by BAS from the UK meteorological office were more consistent this year, and only one sonde was rejected because of faulty sensors. It is recommended that a future installation of the receiving antenna be located at a higher part of the ship, ideally on the main mast, due to reception difficulties in certain conditions. For example, when the sonde flew to starboard, significant reception deterioration was encountered due to shielding by the ship's superstructure. All data were reported in near-real time to the UK meteorological office as part of the ship's meteorological program.

3.3.2 Radiation Measurements

An Eppley longwave (5.0–50.0 μm) pyrgeometer and shortwave pyranometer (0.3–3.0 μum) were installed in the JCR foremast *bird table* using custom gimbal mounts. Because of the difficulty of installing and removing a larger mount bracket, which was attached to the top of the bird table during AMT-3, the instruments were directly attached to the side of the mast. Data were logged to a Campbell Scientific CR10x data logger installed at the foremast first stage. Because of data logger problems, these data were available for only the Madeira-to-Stanley leg. Calibration of the pyranometer was a straightforward application of predetermined calibration coefficients; however, in the case of the pyrgeometer measurements, recent evidence suggested that solar heating of both the instrument case and of the filtered hemisphere directly contribute to the measured signal as errors. A correction for these effects will be derived after the Eppley pyranometer has been calibrated at the SOC Institute of Oceanographic Sciences (IOS) pyrgeometer calibration facility.

A second Kipp and Zonen CM-10 pyranometer, owned by BAS and logged by the Oceanlogger system, was installed in the first stage island of the JCR foremast. The instrument was not mounted on gimbals and suffered from shading by the foremast. This effect is difficult to correct for, since signal bias depends not only on the direct shading of the mast but also on any reflection that may occur from the white paint of the mast structure. A full analysis of the differences between the BAS and CCAR Eppley radiometers will be undertaken in the future to correct the BAS pyranometer data.

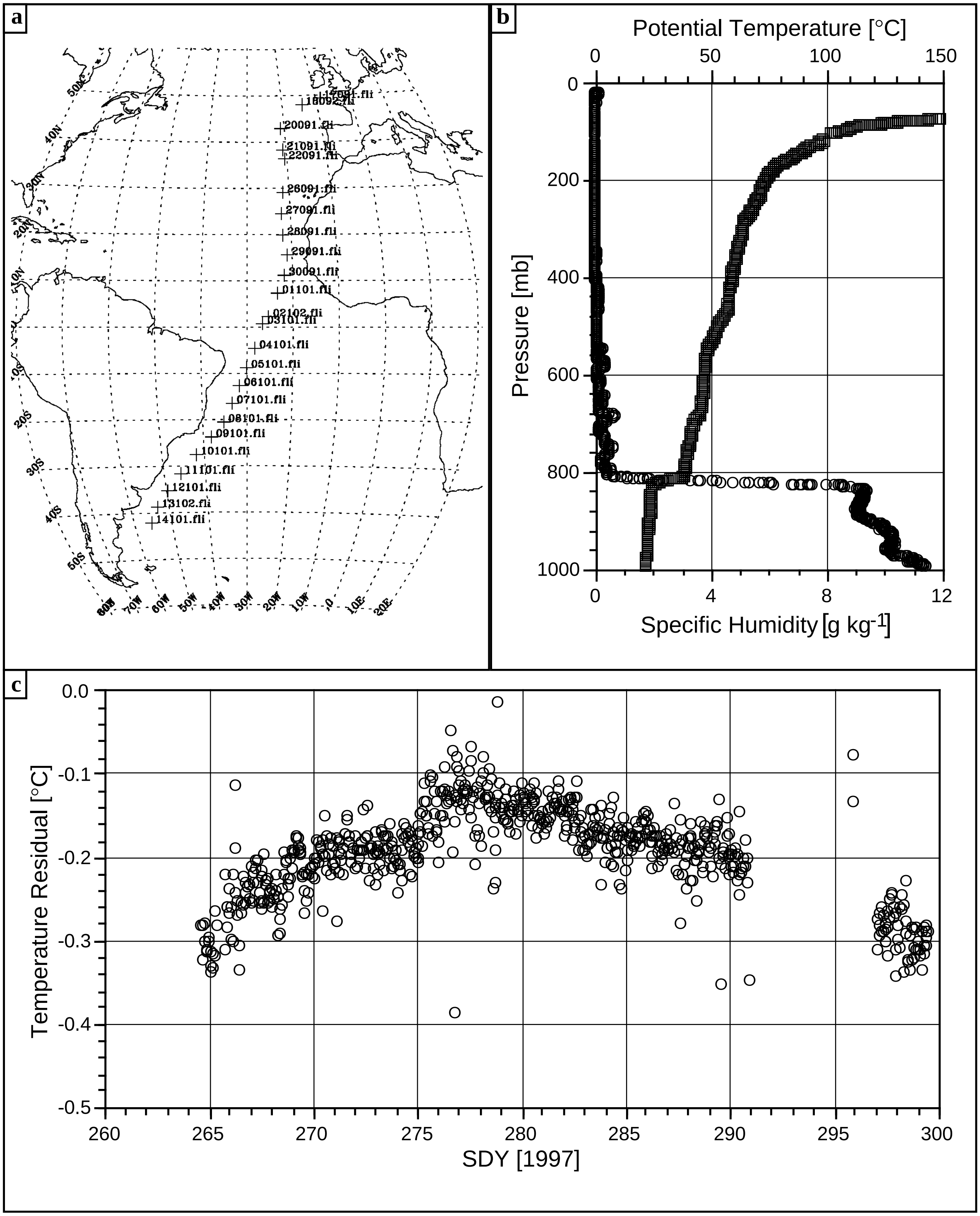

Fig. 13. SOSSTR summaries for AMT-5: **a)** the positions of all the radiosonde releases, **b)** potential temperature (squares) and specific humidity (circles) as a function of pressure, and **c)** the temperature difference (residual) between the SST and the hull mounted temperature probe.

Near-surface BSST measurements have been obtained from an IOS trailing thermistor sensor deployed from the port side of the JCR. The thermistor cable is attached to a heavy 12 mm steel cable having a counterweight attached to its length at approximately 2 m from the tether point. The tether was from a 3 m scaffold pole deployed on the port side of the ship. This configuration resulted in superior streaming of the sensor at a depth of approximately 0.05–0.1 m. Data was logged continuously to the Oceanlogger system (channel SP3) for the entire AMT-5 cruise via a Rhopoint frequency module after signal conditioning. BSST data derived from this sensor were accurate to 0.02 K after the following polynomial coefficients were applied to the logged frequency data: PDM009 calibration run number SP21897A (08–19–1997) $C_0 = 65.39008$, $C_1 = -0.108196$, $C_2 = 1.258201 \times 10^{-4}$, and $C_3 = -9.341802 \times 10^{-8}$.

Significant temperature differences in excess of 1 K were found when the trailing thermistor data were compared with the scientific BSST data. These were due to the vertical stratification of the water column and highlight the need for this type of independent temperature sensor, especially for air–sea exchange studies.

In order to check the accuracy of the ship's BSST (7 m temperature), periodic *bucket* casts were made throughout the cruise. The *in situ* sensor on the JCR is difficult to calibrate because of its installation location. The 5 m CTD temperatures can be used, although, the ship is no longer moving through the water during CTD deployments. The primary aim of the science PRT is to apply a correction to the more accurate and precise TSG located within the ship, which derives a more precise BSST having a warm bias due to water flowing through the ship's internal pipes and pumping system. As shown in Fig. 13c, the simple correction shows a distinct nonlinearity with the BSST itself. Bucket SST observations made on a daily basis show that the science PRT is accurate to within the tolerances of the bucket determination (± 0.1 K). The quadratic coefficients required to correct the T-S data for ship warming are as follows: $C_0 = 0.410645$, $C_1 = 0.991333$, and $C_2 = -2.38419 \times 10^{-5}$.

3.3.3 Meteorological Observations

Since the BAS Viasala HMP-30 humidity sensor (osmotic type) was unavailable, a World Ocean Circulation Experiment (WOCE) standard IOS psychrometer unit was installed ino the JCR foremast in a clean air stream. The unit used an electric fan to aspirate a wet and dry PRT sensor located in a robust sun shield. These data were logged via Rhopoint modules to the Oceanlogger system (channels SP1 and SP2) for the entire AMT-5 transect. Wet and dry bulb air temperatures (accurate to better than 0.02 K) were obtained by applying the following calibration coefficients to these data streams: psychrometer IO2001 wet-bulb calibration run number TW22397A (08–19–1997) $C_0 = -10.17774$, $C_1 = 3.778868 \times 10^{-2}$, $C_2 = 2.720534 \times 10^{-6}$, and $C_3 = -3.03224 \times 10^{-10}$; and psychrometer IO2001 dry-bulb calibration run TD00897A (08–19–1997) $C_0 = -10.18599$, $C_1 = 3.809756 \times 10^{-2}$, $C_2 = 2.238674 \times 10^{-6}$, and $C_3 = -1.021467 \times 10^{-10}$.

During the cruise, the bridge officers kept an hourly log of the general atmospheric conditions including cloud type and amount, swell direction and magnitude, and sea state. This is available on request as an American Standard Code for Information Interchange (ASCII) text file.

3.3.4 Satellite Data Sets

Several satellite data sets, including GOES-8, NOAA AVHRR ERS-2 ATSR, SSM/I and the METEOSAT sensors, are available to the AMT-5 cruise participants (on request).

3.4 In-Water Optics

As with many of the other types of measurements collected during AMT-5, optical data were collected underway and on station. The UOR and a hand-held sun photometer provided the majority of the former; whereas, the latter were provided principally by three different multispectral profiling systems: SeaOPS, SeaFALLS, and LoCNESS (Appendix E). SeaOPS was deployed using a winch and crane, whereas, SeaFALLS and LoCNESS are tethered systems that were deployed by hand. The crane used with SeaOPS had about a 10 m reach over the side of the ship, and the tethered systems were at least 30 m away before any data were collected. All of the in-water profiling instruments collected $E_d(z, \lambda)$ and $L_u(z, \lambda)$ data.

Underway and station surface (solar) irradiance data were provided by an in-air irradiance sensor, $E_s(0^+, \lambda)$, that was mounted on the port trawl post mast, as part of SeaOPS; the SeaWiFS Square Underwater Reference Frame (SeaSURF), which is composed of an in-water irradiance sensor, $E_d(0^-, \lambda)$, suspended below a tethered, square floating frame; the SeaWiFS Buoyant Optical Surface Sensor (SeaBOSS), which is composed of an in-air irradiance sensor, $E_s(0^+, \lambda)$, fitted inside a buoyant collar, so it can be deployed on a mast or as a tethered buoy; and a PAR sensor (with a deck cell) which was integrated into the CTD system.

The redundancy in optical instruments deployed on AMT cruises is a direct consequence of the weaknesses and strengths associated with winch and crane deployment systems versus tethered or free-fall systems. Optical instruments deployed with crane and winch systems potentially suffer from more disadvantages than advantages:

1. Cranes have a limited reach, so ship shadow can be a problem.
2. The ship is not decoupled from the ocean surface, so roll and pitch can cause measurement problems (particularly for irradiance sensors).

3. Winches and cranes are sophisticated electromechanical systems, so there is a continuing vulnerability associated with breakdowns, this is especially so with the hydraulic subsystems.
4. Winches and cranes require relatively lengthy preparation time for operations to begin and end, which means a quick cast during optimal sky conditions is difficult to achieve.
5. The instruments are not lowered into the water until they are far from the side of the ship, so there is very little chance of them being damaged by wave action.
6. Many winches have relatively low descent and ascent rates, so the cycle rate for a complete cast is relatively long. (A long cycle rate means cloud contamination during a cast is very likely. This means the cast must be temporarily stopped to allow the cloud to pass, which in turn adds to the time required.)

Tethered (or free-fall) systems, in comparison, have more strengths than weaknesses:

A. The reference(s) and profiler are deployed away from the ship clear of any ship-induced perturbations to the light field.

B. The profiler is not subject to wave action, but it must be properly trimmed to ensure minimal tilts during descent.

C. A free-floating reference is not decoupled from surface motion, but engineering solutions and deployment practices can be adopted to reduce this effect.

D. There is a direct cable connection between the instruments and the data acquisition units, so there is no complicated (hydraulic) machinery or electrical (slip ring) connection which can require long repair times in the event of a failure.

E. The cable is usually a lighter weight material than steel (e.g., Kevlar®†), and is more easily damaged in comparison to the standard hydrowire used with winch systems.

F. The instruments are usually hand lowered close to the side of the ship, so they are vulnerable to damage by wave action.

G. Deployment and recovery can be accomplished with only two scientists (and no crew), so a rapid cycle rate can be achieved.

The latter is particularly important, because it means casts can be executed in between cloud passage and more casts can be done in a particular unit of time. It also means station scheduling can be kept informal with the ship being stopped only when the illumination conditions are optimal.

Since station time is limited during AMT cruises, it is not always apparent immediately before a station which system will produce the best data. Part of the difficulty arises from the competing requirements of all of the instrumentation that is deployed at each station and the vessel maneuvers (to counter wind, wave, and current effects) which are required to maintain station. Profilers require the vessel to stay clear of the instruments which usually means some forward motion is needed. Unfortunately, forward motion is not always an option, since the other instruments can be negatively affected by this movement. If conditions permitted, the daily station included simultaneous SeaOPS and SeaFALLS (and at times LoCNESS) casts, and when conditions prevented simultaneous casts, SeaOPS was deployed first, and the tethered instruments were deployed soon after.

All of the radiometers used with the UOR, SeaOPS, and SeaFALLS, including any spares, were manufactured by Satlantic, Inc.† (Halifax, Canada). This commonality in equipment was not by accident; the AMT optical scientists decided this was the easiest way to ensure redundacy and intercalibration. The UOR and SeaOPS use 7-channel ocean color radiance series 200 (OCR-200) sensors, as well as 7-channel ocean color irradiance series 200 (OCI-200) sensors. The OCI-200 and OCR-200 radiometers use 16-bit analog-to-digital (A/D) convertors and are capable of detecting light over a four decade range. SeaFALLS, SeaSURF, and SeaBOSS are all equipped with 13-channel OCI and OCR series 1000 radiometers, which employ 24-bit A/D converters, and are capable of detecting light over a seven decade range.

A spare OCR-200 (S/N 035) and OCI-200 (S/N 029) were taken on AMT-5 to provide redundancy for the UOR and SeaOPS. All of the series 200 radiometers made measurements in the same seven spectral bands (approximately 412, 443, 490, 509, 555, 665, and 683 nm), which were selected to support SeaWiFS calibration and validation activities (McClain et al. 1992); in comparison, the series 1000 radiometers cover the SeaWiFS bands plus other parts of the spectrum in greater detail.

Towards the end of the cruise, SeaOPS was reinstrumented with spare components. The original SeaOPS light sensors and data acquisition unit were used to build LoCNESS which is very similar to SeaFALLS in looks and functions. Daily monitoring of the calibration of the UOR, SeaOPS (and LoCNESS), SeaFALLS, SeaBOSS, and SeaSURF radiometers was provided by the SeaWiFS Quality Monitor (SQM), which was used on AMT-3 (Hooker and Aiken 1998) and AMT-4.

† Kevlar is a registered trademark of E.I. du Pont de Nemours and Company, Wilmington, Delaware.

† Identification of commercial products and equipment to adequately specify or document the experimental problem does not imply recommendation or endorsement, nor does it imply that the equipment identified is necessarily the best available for the purpose.

3.4.1 SeaOPS

SeaOPS is composed of an above-water and in-water set of sensors comprising several subsystems. The in-water optical sensors are a downward-looking radiance sensor which measures upwelling radiance, L_u, and an upward-looking irradiance sensor which measures downwelling irradiance, E_d; the former is a Satlantic OCR-200 sensor (S/N 021), and the latter an OCI-200 sensor (S/N 029). There is also a WetLABS minifluorometer and a CT probe. All of the sensors send their analog signals to an underwater data unit, a Satlantic DATA-100 (S/N 004), which converts the analog signals to RS-485 serial communications. The above-water unit, a Satlantic Multichannel Visible Detector System (MVDS), measures the incident solar irradiance just above the sea surface, $E_s(0^+)$. The MVDS unit (S/N 009), is composed of an OCI-200 irradiance sensor (S/N 030) packaged with a separate A/D module that converts the analog output of the OCI-200 radiometer to RS-485 serial communications. For AMT-5, the two units were mounted on top of a pole that was sited on top of the port stern gantry masts. The pole is long enough to ensure none of the ship's superstructure shadows the irradiance sensor under most illumination conditions.

The RS-485 signals from the MVDS and the DATA-100 are combined in a Satlantic deck box, the PRO-DCU (S/N 023), and are converted to RS-232 communications for computer logging. The deck box also provides the (computer controlled) direct current (DC) power for all the sensors and is designed to avoid instrument damage due to improper power-up sequences over varying cable lengths. For AMT-5, the MVDS cable length was approximately 25 m whereas the DATA-100 cable length was about 280 m (250 m on the winch and 30 m from the winch to the deck box).

A custom-built profiling rig was used to carry SeaOPS. This rig was the same one used during the previous AMT cruises (Robins et al. 1996). The positioning of the equipment on the rig was developed with a geometry that ensured all radiance sensors did not view any part of the support. The narrow geometry of the rig was designed to provide a minimal optical cross section. The field of view of the irradiance sensors was only influenced by the 7 mm wire and careful attention was paid to the balance of the rig, even though SeaOPS has tilt and roll sensors. The rig was trimmed with lead weights in air, accounting for the in-water weights of the sensors; after final assembly of the rig, visual checks for correct trim were carried out *in situ*.

The profiling rig was deployed from a midships crane with a reach of about 10 m over the starboard side of the ship. The typical lowering and raising speed of the winch was approximately 20–25 $\mathrm{cm\,s^{-1}}$. For most stations, the sun was kept on the starboard side except during adverse weather conditions. In addition, sea- and sky-state pictures were taken using a charge-coupled device (CCD) digital camera during almost all of the optical stations. The digital photographs were usually taken at the bottom of the SeaOPS down cast.

Data was logged on a Macintosh PowerPC 7300/200 using software developed at the University of Miami Rosenstiel School for Marine and Atmospheric Science (RSMAS) and the National Aeronautics and Space Administration (NASA) Goddard Space Flight Center (GSFC). The software, called Combined Operations (C-OPS), is written in LabVIEW and is used to control both the in-air and in-water SeaOPS data streams. The primary task of C-OPS is to integrate the RS-232 outputs from the deck box that handles the power and telemetry to the underwater optical instruments and to control the logging and display of these data streams as a function of the data collection activity being undertaken: dark data (caps on the radiometers), upcast, downcast, constant depth soak, along track, etc. All of the telemetry channels are displayed in real time and the operator can select from a variety of plotting options to visualize the data being collected.

C-OPS file naming is handled automatically, so all an operator has to do is select what data streams are to be recorded and then set the execution mode of the data collection activity. Each tab-delimited file has a single header, identifying what is recorded in each column, and all data records are time stamped. The files are written in ASCII and are easily viewed with a simple text editor or ingested into a commercial off-the-shelf (COTS) spreadsheet software package.

3.4.2 SeaFALLS

SeaFALLS deployments typically involve three instruments all manufactured by Satlantic: the profiler itself, which is based on a SeaWiFS Profiling Multichannel Radiometer (SPMR); SeaSURF, which is an in-water irradiance sensor based on a SeaWiFS Multichannel Surface Reference (SMSR); and SeaBOSS, which is an in-air version of the SMSR. SeaFALLS mesures E_d (OCI-1000 S/N 023) and L_u (OCR-1000 S/N 016) as it falls through the water column, SeaSURF measures $E_d(0^-)$ (OCI-1000 S/N 045), and SeaBOSS measures $E_s(0^+)$ (OCI-1000 S/N 046). Like SeaOPS, SeaFALLS is fitted with a WetLABS minifluorometer and a CT probe.

SeaFALLS receives its power and sends its data via an umbilical cable while the in-water reference floats away from the ship (Waters et al. 1990). The references also receive power and send data over a tethered cable: SeaBOSS, can be mounted on a mast or deployed as a drifting buoy, whereas, SeaSURF is floated away from the boat using a buoyant frame. The ability to get the light instruments far away from the ship minimizes any ship-induced disturbances to the *in situ* light field (Mueller and Austin 1995). Since the profiler and both references can be deployed quickly with only two people, the ship can be stopped when light conditions are optimal. More importantly, the profiler descends at approximately 1 $\mathrm{m\,s^{-1}}$ so a relatively deep cast can be acquired very quickly (about 3 minutes for a 150 m cast), which means casts can be timed to coincide with clouds moving clear of the sun.

Data telemetry for SeaFALLS is very similar to SeaOPS. A PRO-DCU deck unit (S/N 008) supplies the power for both the profiler and the in-water reference independently. The output voltage is automatically adjusted for the cable length being used. An internal computer shuts down the system under fault conditions while indicating the type of fault. RS-485 telemetry at 19.2 Kbaud is converted in the deck box to RS-232 for input into a microcomputer. A separate PRO-DCU deck unit (S/N 020) supplies the power and telemetry conversion for SeaBOSS. The SeaFALLS data was logged on a Macintosh PowerPC 7300/200 using a software package developed by RSMAS and GSFC. This package, called C-FALLS, functions very similarly to C-OPS. The primary difference is C-FALLS has an option for recording the data in a binary format which is compatible with the Satlantic analysis software package called PROSOFT.

SeaFALLS (and LoCNESS) were deployed from the stern of the vessel, and whenever possible, the ship maintained a headway speed of approximately 0.5 kts. The profiling instrument was carefully lowered into the water and slowly released at the surface until it had drifted clear of any possible shadowing effect. In some wave and current conditions, a short burst from the stern thruster was needed to create enough *prop wash* to push the profiler (and surface reference) away from the stern (this short burst was not forceful enough to move the ship significantly and thereby negatively effect the other instruments that were deployed on wires).

When the profiler reached the desired distance from the stern (30 m minimum), it was ready for deployment. Continued effort was made for preventing the telemetry cable from ever coming under tension; even brief periods of tension on the cable can adversely affect the vertical orientation (tilt) and velocity of the profiler. To ensure this did not occur, the operator always left several coils of cable at the surface. Care was taken not to leave too much free cable in the water, because the cable could move under the ship and become entangled in the propeller or stern thruster intake. To ensure a tangle-free and continuous feed of cable into the water, all of the profiler cable (approximately 300 m) was laid out on deck prior to each case in such a manner as to minimize any entanglements.

The SeaSURF and SeaBOSS references are each attached to a 100 m telemetry cable and deployed from the stern of the vessel on the starboard side (although the latter was usually mounted on a pole on the starboard gantry mast). SeaFALLS is deployed at the same time on the port side. The surface reference is then held at approximately 15 m behind the vessel until SeaFALLS is in the correct position for deployment. When the drop command is given, both instruments are released in unison. The reference cable is paid out freely so that minimal tension is placed on the cable which in turn minimizes reference tilt. When SeaFALLS has reached the point of maximum descent (usually the 1% light level), both instruments are pulled back to their original positions, and are ready to be re-deployed. The same care must be taken with the surface reference cable, i.e., making sure too much cable is not released and that any slack is taken in.

Several experiments were conducted with SeaBOSS to determine how best to cheaply and effectively float an in-air sensor away from the ship while keeping it dry and minimizing tilts. Normally, SeaBOSS is fitted with a foam floatation collar instead of a floatation frame (like SeaSURF). After several trials, an in-water reference floation frame was added to SeaBOSS with bungee isolation chords fitted between the frame and the body of the irradiance housing. The instrument was then deployed in the same fashion as the in-water reference. The only extra detail to remember is that the SeaBOSS iradiance sensor must remain dry, so extra care must be taken when the instrument is lowered into the water.

3.4.3 LoCNESS

LoCNESS is not a new instrument per se, but instead, is built up from the SeaOPS components: the DATA-100 (S/N 004) and the two light sensors, OCR-200 (S/N 021) and OCI-200 (S/N 029). Once assembled, LoCNESS is a free-falling unit that looks and functions very similar to SeaFALLS (Fig. 14), and it is deployed in the same fashion. The data acquisition for LoCNESS is the same one used for SeaOPS. The only difference in the software is the orientation selector within the control panel must be changed from the horizontal to the vertical orientation. SeaOPS has two pairs of internal tilt sensors, one pair for when it is oriented horizontally and one pair for when it is oriented vertically; the software switch ensures that the correct set of sensors are being displayed and logged.

The principal advantage of LoCNESS is its cost and flexibility; it can be assembled from relatively low cost components (in comparison to SeaFALLS) and it can be quickly reconfigured, because the radiometers used are not integral to the design. For example, rather than measure E_d and L_u, a spare OCI-200 can be used in place of the OCR-200 radiometer and LoCNESS can measure E_d and E_u. Of course in comparison to SeaFALLS, there is a commensurate loss in sensitivity, so one of the AMT-5 cruise objectives was to evaluate the capabilities of LoCNESS in comparison to SeaFALLS. This was done by making simultaneous deployments of the two with one another. During most deployments of LoCNESS, data was also collected from SeaSURF, SeaBOSS, and the SeaOPS MVDS irradiance sensor.

3.4.4 SQM

The validation of ocean color satellite sensors requires a quantification of the uncertainties associated with *in situ*

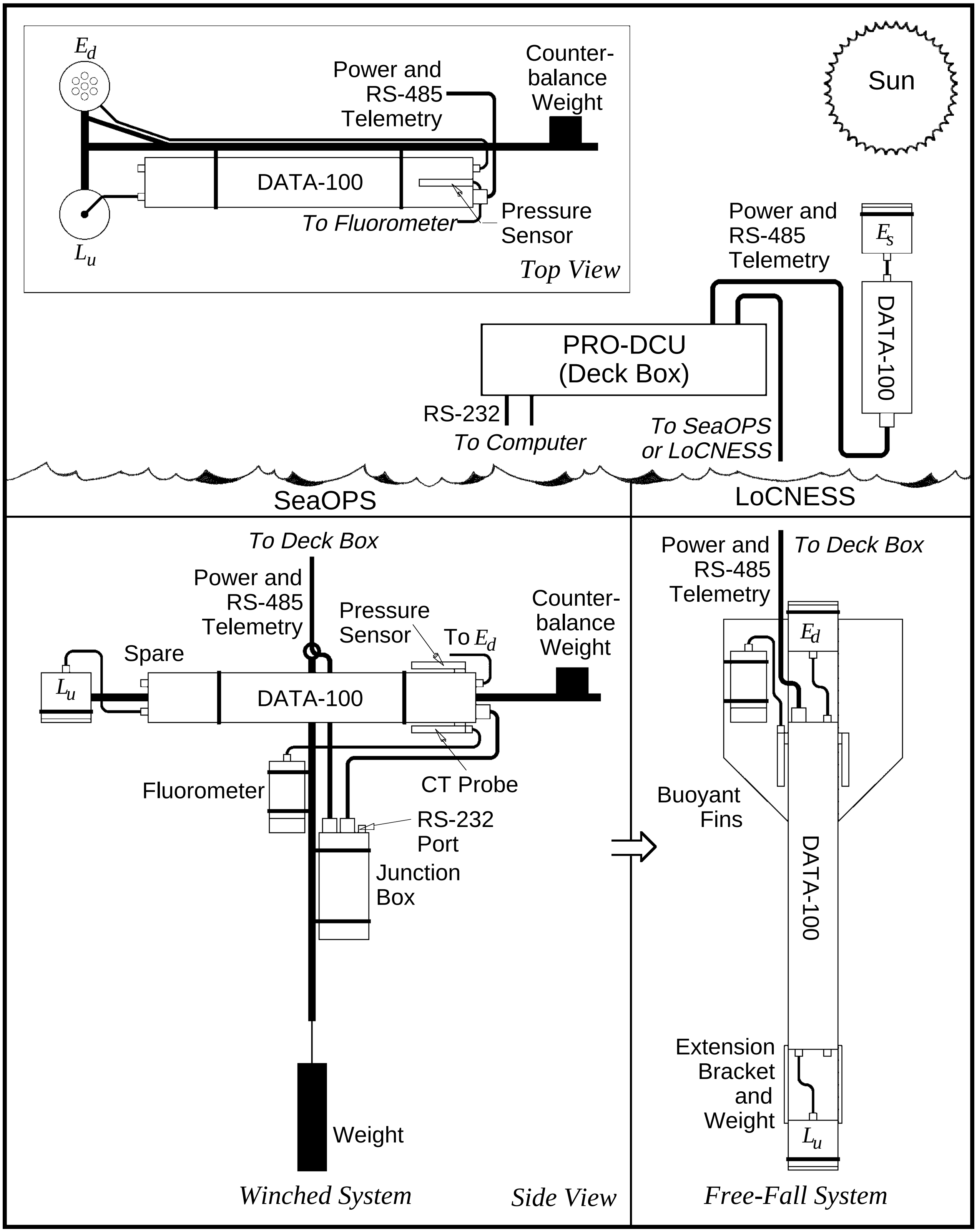

Fig. 14. The conversion of SeaOPS into LoCNESS.

radiometric measurements. Presently, there is no convenient way to check or monitor the calibration of a field radiometer while it is being deployed. Consequently, individual investigators have relied either on the manufacturer's calibration data or on pre- and post-cruise calibrations of their instruments. The severe environmental changes encountered by a radiometer during shipment or a long cruise, however, calls into question whether either one of these practices is satisfactory, which in turn raises the concern of the data quality achieved during field deployments.

In response to a demand for an onboard calibration capability, the SeaWiFS Project and the National Institute of Standards and Technology (NIST) jointly designed and constructed a prototype of a portable light source to illuminate various radiometers during oceanographic cruises. This device, called the SQM, produces a diffuse and uniform light field and is designed to be flush-mounted to radiance or irradiance sensors with a spectral range from 380–900 nm (Johnson et al. 1998). The deviation in uniformity of this source is less that 2% over a circular area 15 cm in diameter. To account for changes in the illuminance of the SQM, three temperature-controlled photodiodes measure the exit aperture light level: one has a responsivity in the blue part of the spectrum, another in the red part of the spectrum, and the third has a broad-band response.

The SQM has two banks of subminiature halogen lamps with eight lamps in each bank. For AMT-5, both banks were populated with Gilway model 187 (4.2 V and 1.05 A) lamps. The power supply for the lamps is via two highly regulated Xantrex model HPD 60-5 power supplies. Both power supplies are controlled over a general purpose interface bus (GPIB). The output current values from the power supplies are monitored by measuring the voltages across two precision 1 Ω shunt resistors with a multiplexed Keithley 2000 digital voltmeter (DVM). The DVM voltages are acquired over the GPIB, and the program controlling the power supplies and acquiring the signals converts the resistance values to current and adjusts the output of the power supplies to ensure a constant current supply to the lamps.

Data logging for the SQM involves two computer systems: one for the device under test (DUT) and one for the SQM. Three of the DUTs used during AMT-5 were fiducials, that is, dummy radiometers with different reflective surfaces: a white one, a black one, and a black one with a glass face (made of the same glass used in the Satlantic radiometers). The purpose of the fiducials is to be able to collect data with them before and after actual radiometers as another way of tracking the short- and long-term characteristics of the SQM light chamber as determined by the internal photodiodes.

Whenever the DUT was a field radiometer, a computer system was needed to acquire and log the data from the radiometer. For AMT-5, the UOR and SeaOPS radiometers were logged using the C-OPS software running on a Macintosh PowerBook 3400c computer, and the SeaFALLS radiometers were logged on the same computer using C-FALLS.

The SQM control software is written in LabVIEW and is hosted on a Macintosh PowerBook 5300ce computer. The SQM computer controls the Xantrex power supplies and acquires five other signals from the Keithley DVM: three photodiode voltages from inside the SQM and two voltages across the two shunts. The latter are converted into currents, since the resistance of the shunts is known. All of this information is time stamped and logged into a tab-delimited ASCII file.

3.5 Surface Optics

A shipborne, broadband (350–800 nm) spectrograph was built to make measurements of remote sensing reflectance, R_{rs}, from which other in-water parameters can be derived. The system is composed of three main parts: a sensing head, a computer control deck box, and a power unit. The total distance between the user and the sensing head was 20 m. The instrument made sequential measurements of incident irradiance and upwelled radiance with an acquisition time of 0.1 s per spectra. It had a spectral resolution of 4 nm and a radiance field of view of 1°. Both sensors were spectrally calibrated at PML using a 1 kW standard lamp. The radiance measurements were made at the Brewster angle, 53° from vertical for seawater, at which reflected light is horizontally plane polarized. A linear polarizer in the vertical orientation placed in front of the radiance optics removed surface reflected light.

The pitch and roll of the ship and the presence of waves meant ideal conditions were rarely realized, so a set of measurements were taken with the polarizer in the horizontal orientation. From this, an estimate of the directly reflected light spectrum was obtained which was then normalized and scaled using the value of the polarizer vertical measurement at 750 nm. This was subtracted from the horizontal signal to give an estimate of the water-leaving radiance. The AMT-5 cruise provided the first opportunity to compare the instrument across a wide range of bio-optical provinces with other optical systems, such as SeaOPS and SeaFALLS, and to make measurements coincident with SeaWiFS overpasses.

Intermittent failures at high temperatures and humidity were overcome by covering the sensing head body with a white cloth and moving the computer deck box from outside to inside the ship. HPLC pigment data were available to compare with chlorophyll concentrations derived with an algorithm which uses the R_{rs} values at 443 nm and 555 nm. Figure 15a shows the values of $K_d(490)$ derived from an algorithm of Moore et al. (1997) which compare closely to those measured directly by SeaOPS. Figure 15b shows the predicted values of chlorophyll concentration against the measured values (top 20 m averaged).

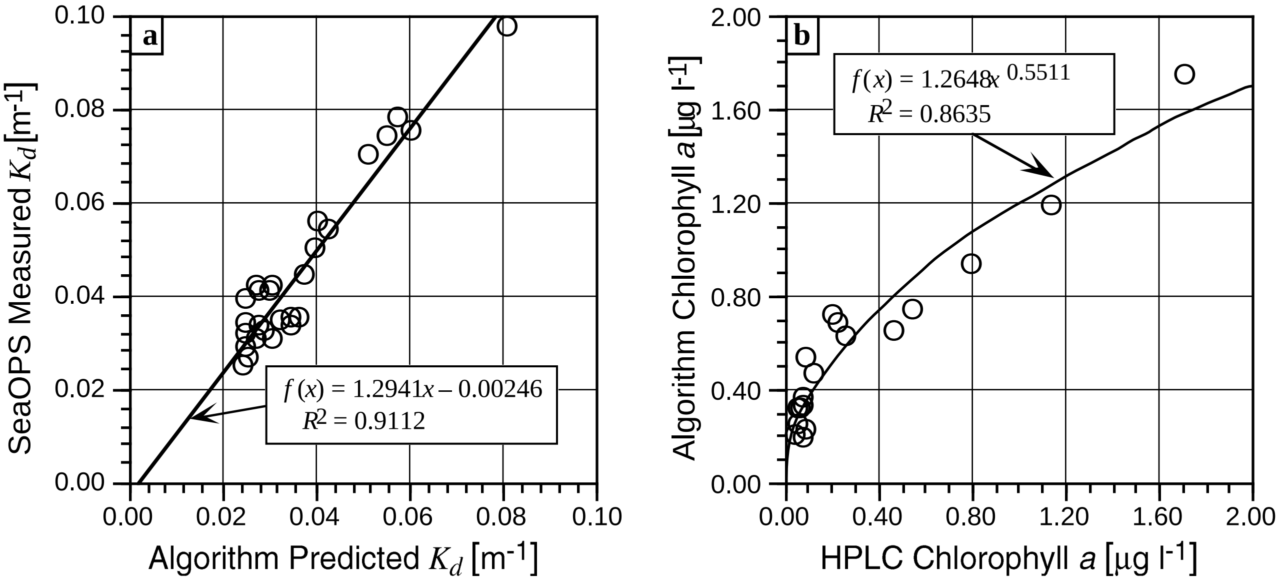

Fig. 15. Analysis products relevant to surface optics analysis: **a)** Algorithm was derived from the morning stations data and used to predict the measured chlorophyll from the afternoon stations, and **b)** K_d derived from an algorithm using above surface reflectance compared with *in situ* measurement from SeaOPS.

3.6 Sun Photometer

The aerosol optical thickness (AOT) is needed for the vicarious calibration of the radiometric signal recorded at an ocean color satellite. The calibration compares the satellite data with the results of an atmospheric radiative transfer model. Knowing the atmospheric optical properties, the *in situ* measured water-leaving radiances are propagated through the atmosphere to the space sensor. Among the components involved, the aerosol component is the most variable in space and time, and requires an *in situ* estimation.

The main difficulty of the atmospheric correction procedure lies in the retrieval of the AOT and its spectral properties. *In situ* measurements of the AOT are used to evaluate the accuracy of such procedures and validate their operational use. Sun photometry measurements performed during SeaACE provided *in situ* estimates of the AOT at SeaWiFS wavelengths. The development of atmospheric correction algorithms, as evoked above, requires previous knowledge on the spectral attenuation properties of the aerosols (as expressed by the Ångström exponent and coefficient, for example) and on their spatial variability: extensive measurements along AMT-5 transect also contributed to the elaboration of a climatology of the different aerosol types and their properties over this area.

3.6.1 Measurement Protocols

Direct sun irradiance was measured using a hand-held sun photometer CIMEL CE317. It allowed measurements at three wavelengths in the visible (centered at 442, 550, and 671 nm), and two in the near-infrared (centered at 783 and 868 nm), having their equivalents in the SeaWiFS waveband set. The instrument was also equipped with a sixth channel at 936 nm. As water vapor absorption is very weak at the SeaWiFS wavelengths, no use was made here of this supplementary wavelength for water vapor absorption correction purposes.

Measurements were performed by manually pointing the collimator at the sun and moving it across the solar disk; the *peak hold* function allowed the retention of the measured maximal value. This operation was repeated sequentially for each wavelength. In addition, GMT time and internal temperature recordings were made at the end of each measurement sequence, which lasts about one minute. Taking into account the sequential logging of data, the specific acquisition time for each channel was extrapolated from the GMT time recording. The estimated error on the resulting absolute time was less than 10 s. This error was only relevant in situations of very low sun elevation, i.e., when the sunlight path across the atmosphere varied in a non-negligible way during a measurement sequence. The dark signal (taken by masking the collimator) was recorded regularly, especially in situations of high external temperature in tropical and equatorial regions. A dark signal different from 0 digital counts was never observed.

Before the AMT-5 cruise, the instrument was calibrated (using the Langley method) at sea level (near Ispra, Italy) to derive the total optical thickness from the digital counts registered by the instrument for the six sampled wavelengths. These calibration coefficients were used for the data presented herein. Some improvements, in particular a higher accuracy in the retrieved AOT values, would be expected from a calibration done at a high altitude (above 3,000 m). Nevertheless, the measurements for the AMT-5 cruise, made on very clear days and relatively extended air mass range, showed similar calibration coefficient values (within 0.1–0.7%), except for the blue channel for which values were about 1.5% lower. A sensitivity analysis showed that a 1% error on the calibration coefficients would lead to a maximum misestimation globally of about 0.01 in the retrieved absolute value of the AOT.

In general, during the day and underway, measurements were taken as soon as conditions of clear sun were encountered. As far as possible, double or triple consecutive measurement sequences were taken in order to assess any short time scale variability of the atmospheric conditions.

In situations of clear sky all day long, measurements were made at a frequency of 10–30 min, depending on the sun elevation. During optics station and SeaWiFS overpasses (generally close to one another) the frequency was, if possible, increased (every 5–10 min), particularly in situations of unstable illumination (broken clouds passing rapidly, high cirrus, etc.). Obviously, no unique strategy could be adopted as readings depended on clear sky conditions. Some measurements were deliberately taken in situations of high thin cirrus masking the sun (they are not documented in this document).

Appendix F is a table of the measurements recorded during the cruise and retained for the present study, together with their correspondence with optics stations. A written log containing comments on the quality of the associated atmospheric conditions was maintained for each measurement sequence. An *a posteriori* cleaning of the data set has been based on these comments. Additional variables needed for the data processing, as ship geographic position and atmospheric pressure, were downloaded from the ship log data streams.

3.6.2 Data Processing

When solar radiation enters the Earth's atmosphere a part of the incident energy is attenuated through scattering and absorption processes. For a wavelength λ_i, the solar irradiance E measured at an observation point (here the sea level) can be expressed as a function of the extraterrestrial solar irradiance E_0 as:

$$E(\lambda_i) = E_0(\lambda_i)e^{-\tau(\lambda_i)m}, \tag{1}$$

where τ is the atmospheric total optical thickness and m the relative air mass. Air mass was computed according to Karsten (1966):

$$m = \left[\cos\left(\frac{\theta}{57.296}\right) + 0.15(93.885 - \theta) - 1.253\right]^{-1}, \tag{2}$$

where θ is the sun zenith angle (a function of latitude and solar time).

By knowing E_0 (the aim of the Langley calibration was to determine the E_0 value in digital counts measured by the instrument) and measuring E (the present measurements in digital counts), τ can then be derived. In the absence of absorption by water vapor and uniformly mixed gases, τ can be decomposed into the sum of the optical thickness specific of each major optical components of the atmosphere (at the wavelengths of interest):

$$\tau = \tau_R + \tau_O + \tau_A, \tag{3}$$

where the R subscript stands for the Rayleigh component (molecules of the air), O for the ozone, and A for the aerosols, respectively. When τ_R and τ_O is known or computed, τ_A can consecutively be obtained. τ_R has been computed here according to Fröhlich and Shaw (1980) revised by Young (1980) and introducing the altitude dependence (Marggraf and Griggs 1969):

$$\tau_R(\lambda_i) = \frac{P}{P_0} 0.00864\,\lambda_i^{-\delta} e^{-0.1188H - 0.00116H^2}, \tag{4}$$

where P is the atmospheric pressure at the observation point and P_0 is the standard atmospheric pressure at sea level, $\delta = 3.916 + 0.074\lambda_i + 0.050\lambda_i^{-1}$, and H is the altitude (in kilometers) of the observation point. τ_O has been derived from a climatology of the atmospheric ozone concentration C_O (Robinson 1966) and the spectral absorption coefficient for ozone a_O^* (Leckner 1978 and Vigroux 1953),

$$\tau_O(\lambda_i) = C_O a_O^*(\lambda_i). \tag{5}$$

The wavelength dependency of the aerosol optical thickness, τ_A, is commonly expressed by the Ångström law (Ångström 1961) as,

$$\tau_A(\lambda_i) = \beta\lambda_i^{-\alpha}, \tag{6}$$

where α and β are the Ångström exponent and coefficients, respectively.

They have been computed here by a least squares fit of the estimated $\tau_A(\lambda_i)$ versus λ in the wavelength intervals 440–870, 440–670, and 670–870 nm as a matter of comparison, the spectral behavior of τ_A being generally different from the visible part to the near-infrared part of the spectrum. For a set of α and β values, τ_A can then be computed at each SeaWiFS wavelengths.

In situations of low aerosol optical thickness, a maximum has been systematically observed at 783 nm, of relatively constant amplitude equal to about 0.01 (in situations where $\tau_A(783)$ is higher than about 0.1 this effect is masked). Such a particular spectral behavior cannot be explained by any physical properties of aerosols and must be interpreted as an artifactual effect. The two following hypotheses for its explanation have been successively rejected:

i) A non-negligible source of attenuation, like water vapor or uniformly mixed gases, was omitted in the decomposition of the total optical thickness into separate components (2). However, computations performed with the 5S code (Tanré et al. 1990) for uniformly mixed gases and with Iqbal (1983) for 1 cm of water vapor showed that the sum of the optical thickness of both components is negligible at that wavelength (about 0.0015 in the extreme case).

ii) Calibration coefficients have been badly estimated for that specific wavelength. In such a case, the amplitude of the observed peak should show a dependence with the intensity of the aerosol optical thickness at 783 nm itself or with the air mass. Actually, this is not the case.

An instrumental problem (such as a nonperfect monochromatic transmission of the filter) may be a cause for this observation. The correction procedure used here is as follows: a constant value of 0.009 was subtracted from the measured $\tau_A(783)$. This value was obtained by averaging the observed difference between the measured AOT at 783 nm, $\tilde{\tau}_A(783)$, and the estimated one, $\hat{\tau}_A(783)$, using the Ångström law parameters computed for the pair [$\tau_A(671)$,$\tau_A(868)$]. The corresponding standard deviation around the mean was equal to 0.003.

3.6.3 Preliminary Results

Figure 16 shows the AOT (τ_A) at SeaWiFS nominal wavelengths along the cruise transect computed for each individual measurement using the Ångström law (6) and the two coefficients (α, β) estimated for 412, 443, 490, and 510 nm (panels a–d) and 555, 670, 765, and 865 nm (panels e–h).

High values (between 0.30 and 0.55 at 443 nm) of the AOT were observed in the Southern Hemisphere around the equator (0–10°S) for hazy sky situations (Fig. 16). In the Northern Hemisphere, high values of 0.15–0.25 at 412 nm were observed around 20°N in the area possibly influenced by Saharan dust (note the corresponding low values, around 0.5, of the Ångström exponent for the 442–671 nm interval, Fig. 17). The lowest aerosol atmospheric loads were observed south of 50°S near the Falkland Islands. There was non-negligible variability (at small scale) of the τ_A values shown by the measurements performed on a restricted distance (one measurement day), e.g., $\tau_A(443)$ varies between 0.40–0.55 around 10°S (Fig. 16).

Although they are globally correlated, the Ångström exponents computed for the visible range (442–671 nm) are generally higher than those computed for the near-infrared range (671–868 nm), (Fig. 17). Although the calibration coefficients used for the aerosol optical thickness estimates have not been obtained in ideal conditions, the data presented here can be considered reliable. They may be subject to small readjustments, mainly for situations where the aerosol content was low, when more accurate coefficients are obtained from a high altitude calibration experiment.

3.7 UOR Optics and the FRRF

A UOR 800 series (Nu-Shuttle) was towed most days throughout the transect, except when the vessel was making high speed passage at 15 kts. The undulator carried an FRRF (Chelsea Instruments) which logged data into an internal flash memory card and additional sensors for temperature (PRT), and conductivity (SBE), plus downwelling irradiance and upwelling radiance (Satlantic OCI-200 and OCR-200). The signals from these devices, plus the analog signals from the FRRF, were logged by a PML data logger (S/N JA8 or S/N JA10). The UOR was deployed once per day, after the morning station and recovered just before the afternoon station.

The UOR was towed on 250–270 m of cable at 11–12 kts with a programmed depth range of 3–55 m undulating over a cycle of 288 s; the 1 Hz logging rate gave a depth resolution of approximately 0.2 m. This depth range was optimal for the irradiance and radiance measurements and near optimal for the FRR fluorometry in most waters. There were a number of equipment failures (data loggers re-setting) which led to the loss of some data. After early problems with the FRRF, including a broken connector on one unit, the instrument performed reliably and data were acquired in a wide variety of waters of different productivities (Appendix H). None of the data were analyzed at sea.

Several FRRF experiments were carried out on deck by submersing the instrument in a tank filled from the ship's nontoxic supply. Filters that simulated the light at different depths were placed over the tank sequentially so as to measure the phytoplankton photosynthetic characteristics at different light intensities. The FRRF was used in waters that were close to or below its lower limit of capability of 0.1 mg l^{-1} found in the oligotrophic gyres. After experimenting with various protocols, data analysis suggested that by increasing the gain and the number of repetitions or sequences, the signal-to-noise ratio could be improved. In the more productive parts of the Southern Ocean, the gain setting was reduced to prevent the saturation of the signals. These data will help define the operational protocols to exploit the performance of the instrument efficiently, for the wide range of ecosystems encountered on AMT cruises.

Expendable optical, temperature, and depth probes (XOTD) were deployed after every morning station before the UOR deployments. The XOTD system recorded data on scattering and temperature to over 400 m (Appendix G).

3.8 Seawater Filtration

Seawater was drawn from the nontoxic seawater supply every 2 h and filtered for subsequent analysis for phytoplankton pigments. All water was collected into clean

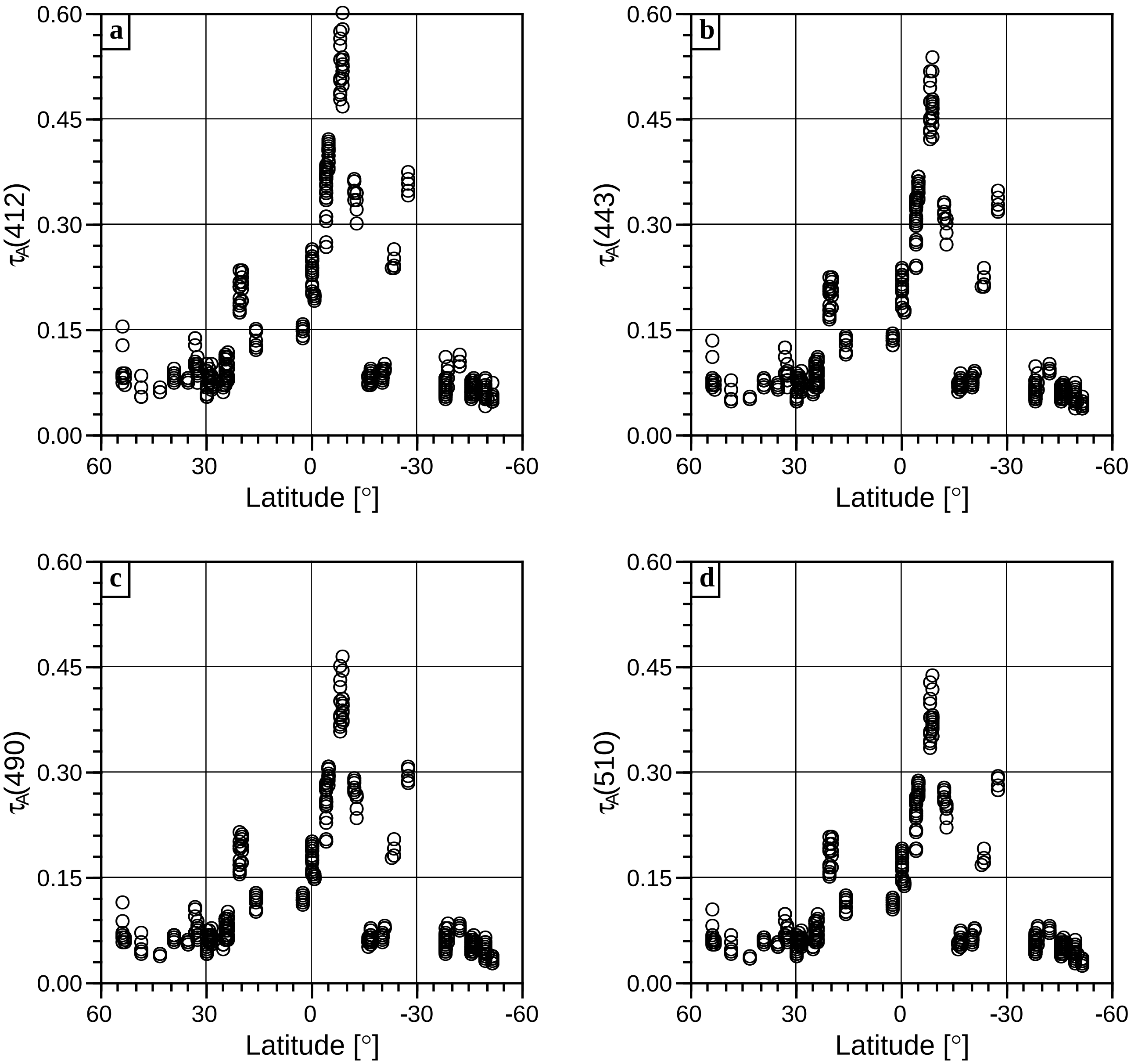

Fig. 16. AOT along-track values for **a)** 412, **b)** 443, **c)** 490, and **d)** 510 nm.

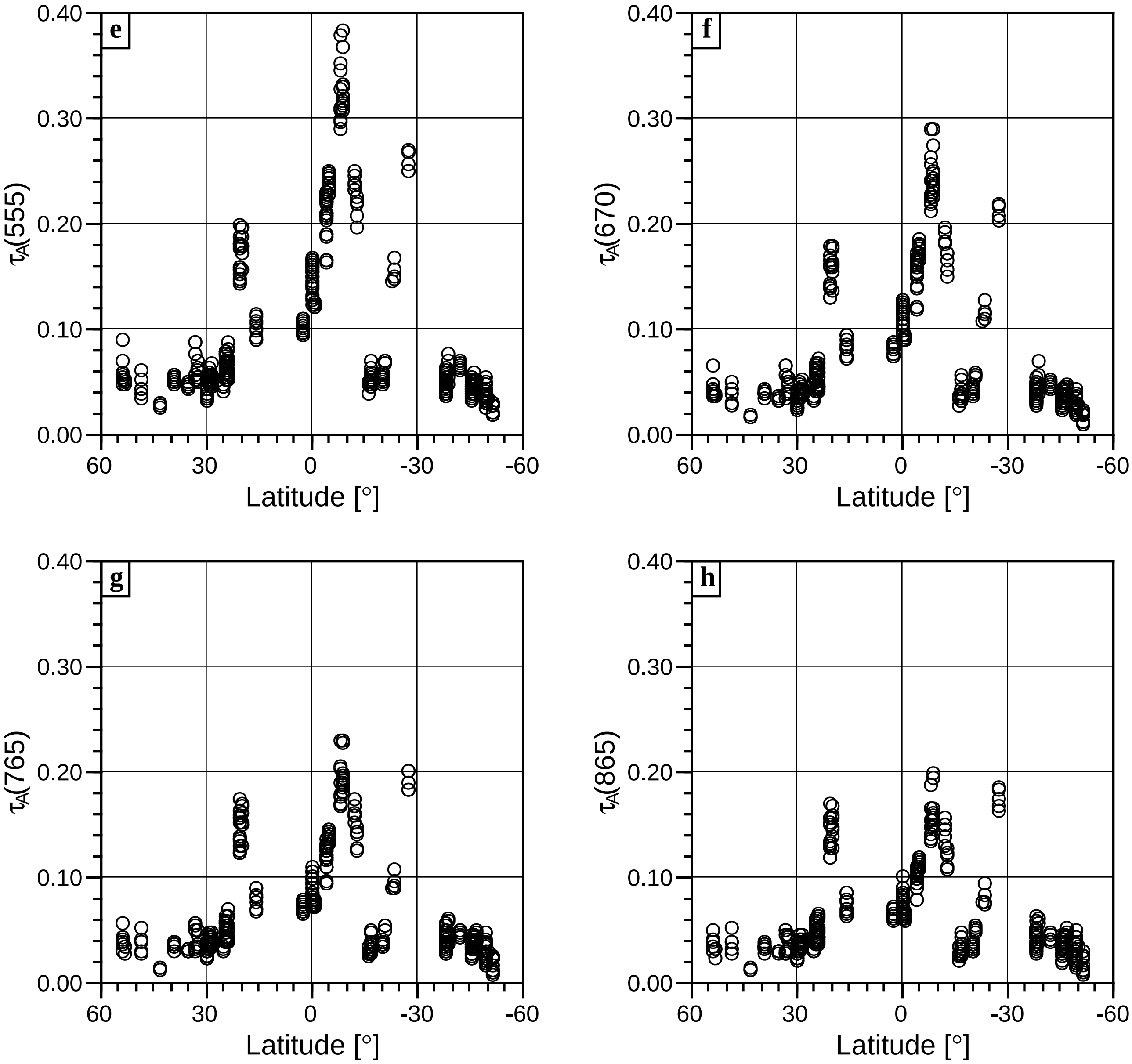

Fig. 16. (cont.) AOT along-track values for **e)** 555, **f)** 670, **g)** 765, and **h)** 865 nm. Note the change in amplitude in the *y*-axis values (especially with respect to Figs. 16a–16d.

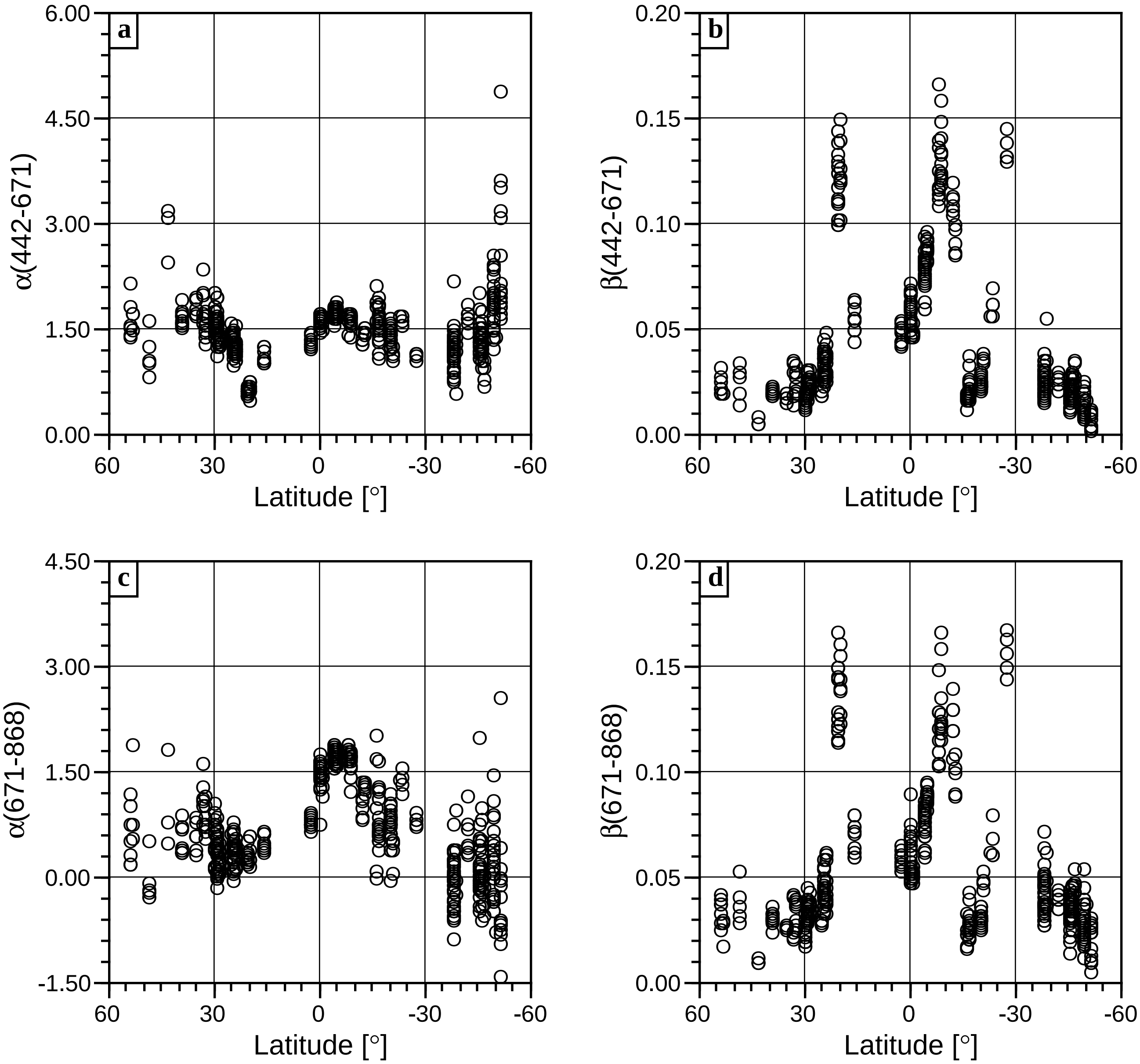

Fig. 17. Along-track values for **a)** α (442–550–671 nm), **b)** β (442–550–671 nm), **c)** α (671–783–868 nm), and **d)** β (671–783–868 nm).

10 l containers before being split into smaller 2.15 l bottles for filtration. The overall volume of water that was filtered for each sample was dependent on the time taken for samples to pass through the filter, i.e., a function of the concentration of particulates within each sample. All volumes of water, in addition to values of surface salinity, temperature, fluorescence, time (GMT), latitude, and longitude observed at the time of collection for each sample are given in Appendix I.

The seawater samples were filtered through Whatman GF/F filters. These individual filters were placed into cryovials using forceps. Several replicates for each sample were taken in order to separately analyze chlorophyll *a* and accessory pigments by fluorometric and HPLC techniques, respectively. All replicates were immediately stored at −80°C until subsequent analyses. One set of replicates from each sample was transferred into liquid nitrogen after accumulation in the −80°C for 1–2 d. This set of replicates was shipped back to the UK, Italy, and the USA for later HPLC analysis.

Seawater was drawn from each CTD that was deployed. Water was collected from 10–12 depths corresponding to each CTD fluorometer profile signature, and subsequently processed for phytoplankton pigments as described above. The volume of water that could be filtered was often dependent on the amount available; hence, all quantities are displayed in Appendix I for all CTD stations.

Seawater from each depth was collected for future analysis of picoplankton. Two 1 ml samples were drawn from each water bottle using a bubble pipette and placed into a corresponding cryovial. To each vial, 30 μl of 25% glutaraldehyde was added. Samples were then incubated for 10 min before being frozen in the −80°C freezer.

3.9 Phytoplankton Pigment Distributions

Chlorophylls and carotenoids, the key light harvesting pigments in phytoplankton, are central to the introduction of energy into oceanic ecosystems and, thus, mediate the biogeochemical cycles of carbon, nitrogen, and oxygen. In the oceans, the photosynthetic pigments, particularly chlorophyll *a*, have long been recognized as unique molecular markers of phytoplankton biomass.

Although the distribution of chlorophyll *a* has traditionally been studied using spectrophotometry and fluorometry (Holm-Hansen et al. 1965), both methods suffer from inaccuracies associated with spectral interferences from chlorophyll *b*, carotenoids, and from chlorophyll *a* degradation products (for example, chlorophyllides, phaeophytins, and phaeophorbides) which may occur during senescence, grazing, sedimentation, and resuspension of phytoplankton (Mantoura et al. 1997). The application of HPLC provides a more accurate estimate of chlorophyll *a* and the rapid separation and quantification of up to 50 additional chloropigments and carotenoids in marine plankton (Wright et al. 1991 and Jeffrey et al. 1997).

Many pigments have strong chemotaxonomic associations which may be exploited to map the oceanographic distribution and taxonomic composition of the phytoplankton community. For example, 19′-hexanoyloxyfucoxanthin is used as a biomarker of prymnesiophytes (Bjornland and Liaaen-Jensen 1989), while fucoxanthin has been used as a marker for diatoms (Barlow et al. 1993). More recently, the discovery of divinyl chlorophyll *a* and chlorophyll *b* (Chisholm et al. 1988), which are highly specific marker pigments of prochlorophytes, has improved the understanding of picophytoplankton (size 0.2–2 μm) in subtropical and tropical oligotrophic oceanic waters, which are likely to account for a significant component of primary production in the world ocean (Partensky et al. 1993).

Characterizing the spatial and temporal variability of phytoplankton abundance and composition is a crucial step in understanding and quantifying the fluxes and processes involved in oceanic biogeochemical cycling. With the advent of remote sensing, ocean temperature and color can now be monitored from space (Aiken et al. 1992) allowing algal biomass and, hence, aspects of biogeochemical cycling to be studied on a global scale.

3.9.1 HPLC Methodology

The objectives of the HPLC analysis activity were to map the distribution of phytoplankton pigments along the AMT cruise transect in vertical profiles and in surface waters using HPLC with high sensitivity diode array detection, and to use these data to:

1. Map, along the AMT transect, the chemotaxonomic distribution of phytoplankton;
2. Provide ground truth data for the development of SeaWiFS remote sensing algorithms and provide an accurate pigment database for the calibration of fluorescence and optical sensors;
3. Determine regional absorbance characteristics and basin-scale variations in phytoplankton biomass and community structure to partition the North and South Atlantic Ocean into well-characterized ocean-break ographic provinces; and
4. Assess the taxon-specific production of simultaneously determined biogenic gases and, thus, provide an evaluation of the utilization of phytoplankton pigments as proxy markers for these climatically important species.

Seawater samples were collected from the CTD water bottles (10 depths) and from the nontoxic supply at 2 h intervals. Phytoplankton were harvested by filtering 1–6 l samples through 25 mm GF/F filters using positive-pressure filtration, and the pigment extracted from the filters into 90% acetone with the aid of ultrasonication. Extracts were centrifuged and filtered through Teflon syringe filters to remove debris. Extracts were then analyzed for chlorophyll using a Turner Designs 10-AU fluorometer and for a range of chlorophyll, carotenoids, and phaeopigments by reverse phase HPLC.

Extracts were held at 2°C in an autosampler unit, and vortex mixed with ammonium acetate buffer (1:1 v/v) before injection. Pigments were separated on a C-8 column using a binary mobile phase system with linear gradient (methanol/1.0 M ammonium acetate; 100% methanol; Barlow et al. 1998). Pigments and phaeopigments were detected by absorbance at 440 nm and 667 nm, respectively, using diode array detection. Pigment identity was secured by co-elution with authentic pigments (VKI, Denmark) and confirmed through spectral correlation with standard UV-visible spectra (300–750 nm). Pigments were quantified with respect to a canthaxanthin internal standard via relative response factors, while phaeopigments were quantified using response ratios. As well as the resolution of key chemotaxonomic chlorophyll and carotenoid pigments, baseline separation of monovinyl and divinyl chlorophyll *a*, and lutein and zeaxanthin, and partial separation of monovinyl and divinyl chlorophyll *b* was achieved in a total analysis time of less than 30 m.

Replicate seawater samples were filtered through GF/F filters for the determination of fluorometric chlorophyll. Chlorophyll was extracted from the filters into 90% acetone and quantified using a fully calibrated Turner Designs 10-AU fluorometer using the method of Welschmeyer (1994).

3.9.2 HPLC Achievements

Samples were collected, processed, and analyzed on board from all CTD stations and from underway samples collected at 2 h intervals. Data were processed and made available to the scientific party and transferred to SeaWiFS Project on a daily basis. Figure 18 demonstrates the relationship between fluorometrically determined chlorophyll *a* and HPLC total chlorophyll *a*.

Depth profiles, at two contrasting stations, are illustrated in Fig. 19; this figure shows the distribution of chlorophyll *a* (biomass), divinyl chlorophyll *a* (prochlorophytes), hex-fucoxanthin (prymnesiophytes), fucoxanthin (diatoms), and zeaxanthin (cyanobacteria).

3.10 Productivity

Over the course of the AMT-5 cruise track, which covered a wide range of marine ecosystems, primary production was estimated by incorporating radioactive ^{14}C by phytoplankton during photosynthesis. Primary production is constrained by physiological, ecological, and environmental factors, such as nutrients or light availability. To describe the size structure of the community, the primary production the biomass were fractionated into three size fractions: picoplankton (less than 2 μm), nanoplankton (2–20 μm), and net-plankton (greater than 20 μm).

The taxonomic diversity of phytoplankton assemblages is a crucial determinant of the carbon flux in any oceanic region. Diatoms possess higher growth potential compared to flagellates when nutrients are available (Furnas 1990). In addition, grazing controls of phytoplankton production are more likely to occur when algal size is small (Kiorbe 1993). Irradiance is a critical factor affecting the amount of carbon fixed into organic compounds and photosynthesis-irradiance (P-I) experiments can indicate different strategies of energy utilization by marine phytoplankton.

The objectives of the productivity experiments were to:

1. Describe the meridional distribution of size-fractionated phytoplankton abundance and taxonomic composition;
2. Determine the patterns of meridional distribution of photosynthetic rates in three different size fractions (picoplankton, nanoplankton, and net-plankton);
3. Characterize the meridional and vertical variability of the photosynthetic parameters of the microalgal assemblages and their relationship with the physical and chemical factors;
4. Determine the production of dissolved organic carbon (DOC) in the Azores area and determination of total organic carbon (TOC) along the latitudinal transect; and
5. Determine the community net production in relation to the community structure and to quantify the balance between production and respiration in the photic layer.

3.10.1 Methodology

Water samples collected from the CTD bottles at 5 or 6 depths at each station were used for all of the standing stock and rate measurements. Size-fractionated chlorophyll *a* concentration was determined fluorometrically, with a Turner Designs 10 AU Fluorometer, after sequential filtration of a 250 ml sample through 20 μm, 2 μm, and 0.2 μm polycarbonate filters and subsequent extraction in 90% acetone at −20°C overnight. The fluorometer had been set up to use the nonacidification technique of Welschmeyer (1994). Water samples from the surface and the DCM at each station were preserved with formalin and lugol's iodine for microplankton species identification and counting.

3.10.1.1 Primary Production

Vertical profiles of size-fractionated primary production were obtained from ^{14}C incubations on deck with a range of filters for 10 irradiances from 97% to 1% of the surface volume. Triplicate water samples in 70 ml polycarbonate bottles, were spiked with 10 μCi $NaH^{14}CO_3$ and incubated for 6.5–7.5 h at an irradiance close to that of their original depth, as determined by the optical profile from the PAR sensor on the CTD. At the end of the incubations, samples were filtered sequentially through 20 μm, 2 μm, and 0.2 μm polycarbonate filters. Filters were exposed to concentrated HCl fumes for 12 hours to remove

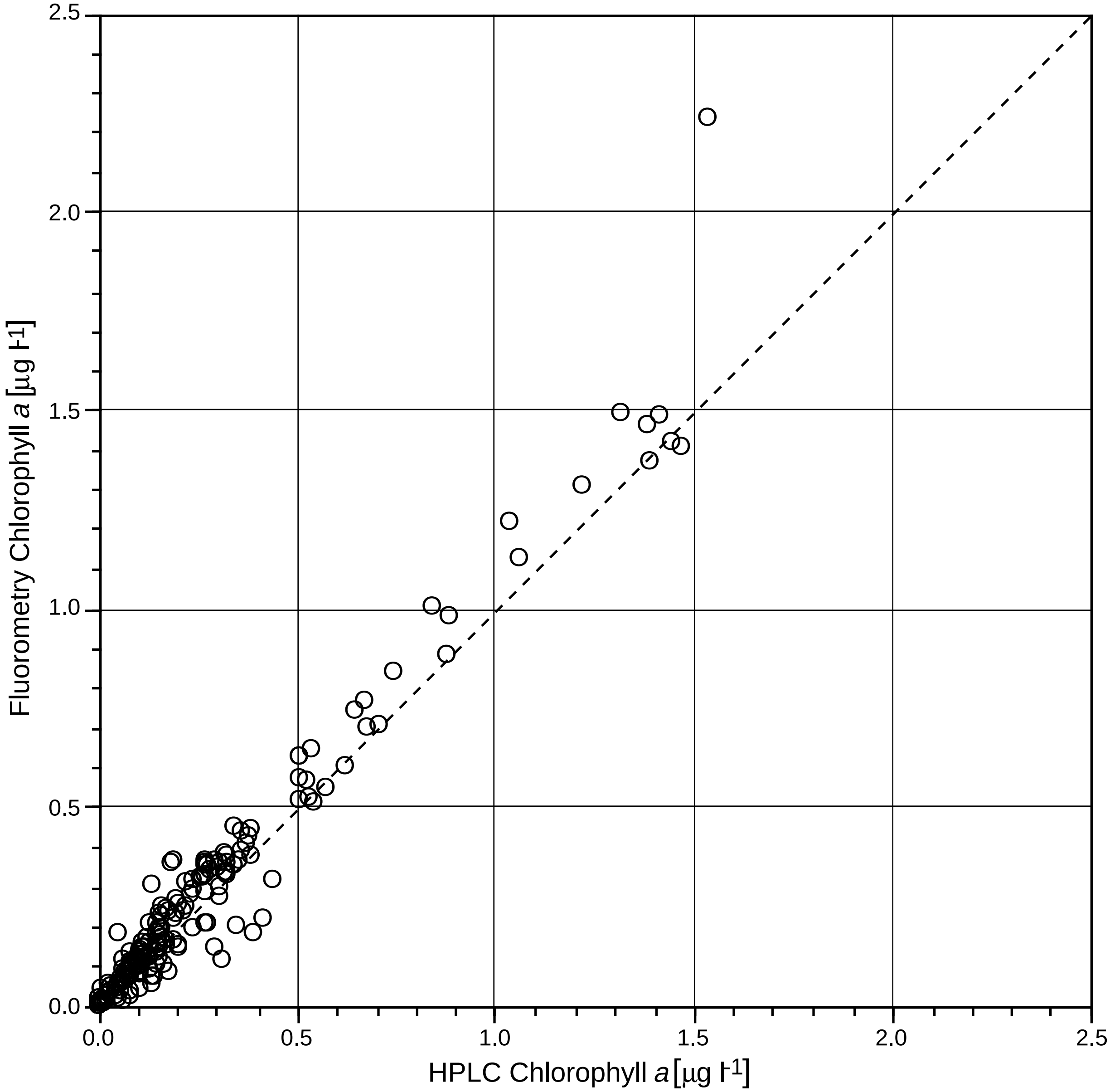

Fig. 18. The correlation of fluorometrically determined chlorophyll a and HPLC total chlorophyll a [$f(x) = 0.8809x + 0.00883$ and $R^2 = 0.9555$].

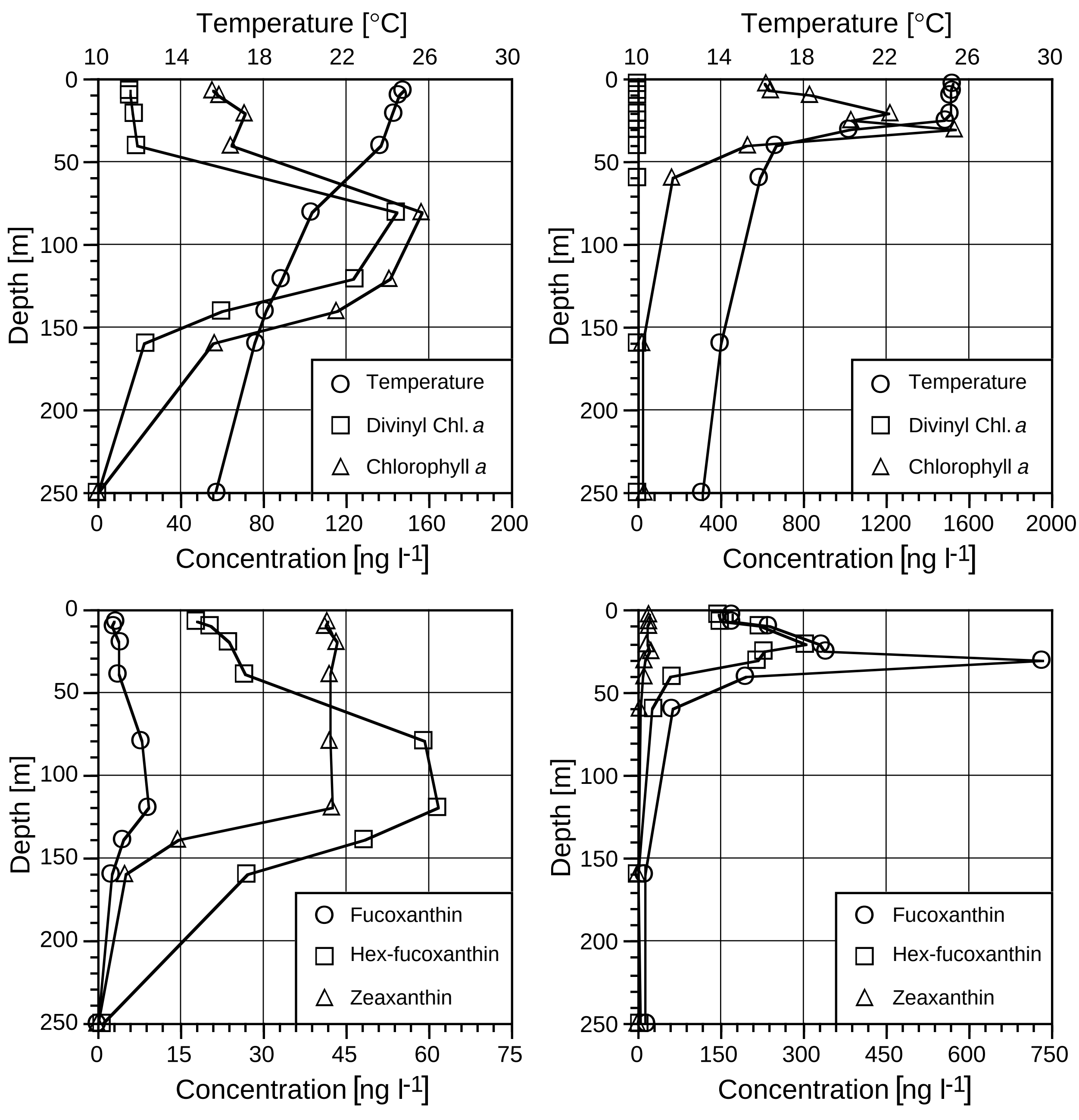

Fig. 19. Depth profiles of chlorophyll *a*, divinyl chlorophyll *a*, fucoxanthin, hex-fucoxanthin, and zeaxanthin at CTD Stations 9 (left two panels) and 11 (right two panels).

inorganic ^{14}C. The radioactivity of each fraction was determined on a Beckman liquid scintillation counter after the addition of 3.5 ml scintillation cocktail to each vial.

Photosynthesis-irradiance (P-I) experiments were carried out with bench incubators equipped with 100 W halogen lamps which provided a range of light intensities. At two depths (the surface and the DCM) for each station along the transect and at three depths (surface, DCM, and an intermediate depth) at 6 stations in the Azores area, water samples were collected for P-I experiments. The samples were cooled using the surface water supply. The incubations lasted for 2–2.5 hours, after which each sample was filtered through a 0.2 μm polycarbonate filter, decontaminated, and counted as described above.

3.10.1.2 Dissolved Organic Carbon Production

DOC production was determined at three depths on each station in the Azores area. Triplicate water samples in 30 ml glass bottles, were spiked with 75 μCi $NaH^{14}CO_3$ and incubated on deck for 2–3 h at an irradiance level close to the original level experienced by the phytoplankton cells. At the end of the incubation, 10 ml of each sample was filtered by glass microfibre filters (GF/F). The filtrate was acidified with phosphoric acid to a pH level of 2, the samples were stirred for 24 h to remove inorganic ^{14}C, and 14 ml scintillation cocktail were added to each vial. The GF/F filters were exposed for 12 hours to concentrated HCl fumes, to remove inorganic ^{14}C, and then placed in vials with 3.5 ml scintillation cocktail for the determination of radioactivity using a Beckman liquid scintillation counter.

3.10.1.3 Total Organic Carbon Production

Samples were collected for determining TOC for 10 stations within the CANIGO area, the same stations for which DOC production experiments were performed. Because of the extremely low particulate organic carbon (POC) levels in open ocean waters, the samples were not filtered on board while at sea, since contamination during filtration is one of the main sources of error in DOC measurements. Triplicate seawater samples were drawn directly into 10 ml glass ampules (ashed 450 °C, 12 hours). After acidification with phosphoric acid to a pH of 2, the ampules were heat-sealed and preserved in the dark at 4°C, the most convenient and practical method for TOC preservation for long periods. The samples will be analyzed in the next few months by the high temperature catalytic oxidation (HTCO) technique, at the laboratory of the *Instituto de Investigaciones Marinas*, in collaboration with Vigo University.

3.10.1.4 Respiration and Net Production

Along the latitudinal transect at three depths on each station (55% and 1% light depths and the DCM), water samples were taken for oxygen analysis. The incubation procedure used was the same as that employed for primary production. Three kinds of experiments, each with 6 replicates, were performed: one to measure the initial oxygen concentration, another for the oxygen respired, and a third for the phytoplankton production. The analysis used the potentiometric Winkler technique with end point detection.

3.10.2 Preliminary Results

For most of the AMT-5 transect, the total chlorophyll concentration within the surface mixed layer was less than 0.4 $mg\,m^{-3}$. In two areas, however, the total concentration was higher: greater than 1.4 $mg\,m^{-3}$ in the African upwelling, and more than 0.8 $mg\,m^{-3}$ within the latitudinal range 30.617–42.233°S. In the oligotrophic areas, where the phytoplankton abundance was low, most of the chlorophyll *a* was associated with the picoplankton size class. In contrast, the contribution of the net-plankton (greater than 20 μm) size class to total chlorophyll *a* was high in those areas with relatively high levels of microalgal abundance. The vertical distribution of chlorophyll *a* showed a maximum located in the thermocline. This DCM reflected photoadaptation of microalgae to low irradiance, producing enhanced levels of cellular chlorophyll *a*, rather than a biomass maximum.

All of the curves from the light-saturation experiments have been plotted, although, statistical fitting to the appropriate models has yet to be completed. The results presented in this report, therefore, are only to be considered as preliminary. The light saturated rate of chlorophyll *a*-specific photosynthesis varied widely throughout the cruise and with depth. Higher values were always found in the surface populations except in the bloom station (located at 48.867°W,35.483°S). Photoinhibition was present in most samples from the DCM, indicating photoadaptation to low light levels. When statistical analysis is complete, the latitudinal and vertical variability of the P-I parameters will be compared to the distribution of other variables, such as, temperature, nutrient concentration, and phytoplankton composition.

3.11 Nutrients

The objectives of the micronutrient and nanonutrient analyses were to:

1. Study the spatial and temporal variations of the micronutrients (nitrate, nitrite, phosphate, silicate, and ammonia) in the water column;
2. Deploy for the first time during the AMT Program a nanomolar ammonia analysis system; and
3. Deploy a nanomolar chemiluminescence analysis system for detecting nitrate and nitrite.

The nanomolar analyzers will enhance the understanding of nutrient regimes and may provide nutrient signatures and characteristics of the oceanic provinces that are encountered.

3.11.1 Methodology

The nutrient analyzer used during the AMT-5 cruise was a five-channel Technicon AAII, segmented flow autoanalyser. The chemical methodologies used were: nitrate (Brewer and Riley 1965), nitrite (Grasshoff 1976), phosphate (Kirkwood 1989), silicate (Kirkwood 1989), and ammonia (Mantoura and Woodward 1983). The nanomolar nitrate and nitrite detection methodology was from Garside (1982), and the nanomolar ammonia system was adapted from Jones (1991). Water samples were taken from the CTD system, and subsampled into clean Nalgene bottles (Appendix J). The analysis of the samples was completed within 3 h of sampling. Clean handling techniques were employed to avoid any contamination of the samples, particularly by ammonia. No samples were stored.

Underway continuous sampling of surface water used the nontoxic water system. The water was filtered in-line (Morris et al. 1978), before analysis of the macronutrients. For the underway nanomolar ammonia system, a discrepancy between the CTD samples and the underway analysis was detected, so the Millipore filter was removed and the water was only coarse filtered through a stainless steel mesh. The results for the CTD and underway samples from the same approximate depth of 7 m then agreed. Underway sampling was carried out where possible for the nanomolar ammonia system and where necessary. Where values reached microgram concentrations, the five-channel Technicon analyzer was deployed for the other nutrients.

All CTD samples were analyzed successfully with a negligible sample loss rate. As usual, the Technicon system showed its reliability and reproducibility in the harsh environment of marine research. The nanomolar nitrate/nitrite chemiluminescent system worked well, although, even this system was at the limits of its detection for many mixed layer samples from the oligotrophic stations south of the equator. The ammonia system performed well once a faulty peristaltic pump was replaced, giving unique measurements of ammonia concentration data from this part of the world ocean.

3.11.2 Preliminary Results

Nitrate was depleted from the surface mixed layer while still in the western approaches of the English Channel. At the 19°W,47°N station, surface nitrate was 23 nmol l^{-1}, with uniform concentrations throughout the mixed layer until the thermocline at 50 m, which also corresponded to the nutracline. At 250 m, the nitrate concentration was 10.9 μmol l^{-1}, phosphate was 0.56 and silicate was 4.41 μmol l^{-1}. The ammonia concentrations in the surface were at nanomolar concentrations from The Solent onwards. At the stations off the Bay of Biscay, the concentration was close to 30 nmol l^{-1} throughout the water column down to 250 m, with no discernible concentration maximum.

Off West Africa at 20.52°W,10.55°N the thermocline was relatively shallow at 43 m, nitrate was 26 nmol l^{-1} at the surface, decreasing to 8 nmol l^{-1} at 30 m, and then increasing sharply at the thermocline. Ammonia was elevated close to the upwelling region and was about 70–80 nmol l^{-1} in the surface waters. At 250 m, nitrate was 24 μmol l^{-1}, and silicate and phosphate was 10.6 μmol l^{-1} and 1.7 μmol l^{-1}, respectively. At the station south of the equator (27.22°W,04.47°S), the thermocline had deepened to 83 m with surface nitrate at 18 nmol l^{-1}, dropping to 9 nmol l^{-1} at samples down to the thermocline, where the nitrate increased sharply to 29 μmol l^{-1} at 250 m.

In the South Atlantic gyre, the thermocline and nutracline were at a depth of 145 m, with severe nitrate depletion observed throughout the water column. Surface nitrate at 2 m was 21 nmol l^{-1}, but deeper, it was below the sensitivity limit of the NOx Box, effectively 0–4 nmol l^{-1} and just detectable at 125 m at 7 nmol l^{-1}. At 250 m, the lowest depth, nitrate was only 5.74 μmol l^{-1}. Ammonia concentration was only 35–40 nmol l^{-1} in this region of severely nutrient depleted water. South of this station the thermocline was shallower and nitrate became detectable again. South of Montevideo, in a region of increased fluorescence, CTD 25 (51.55°W,38.50°S) had a surface nitrate concentration of 3.5 μmol l^{-1}. These high nitrate waters continued to the Falkland Islands, increasing in concentration onto the continental shelf north of the islands. The nitrite water column distribution generally showed a primary nitrite maximum at around the thermocline in the chlorophyll maximum region.

On a number of occasions, there was also an ammonia maximum in the water column, particularly in the more temperate northern waters, and this was found just shallower than the nitrite maximum. There was, however, no evidence of this maximum in the south Atlantic gyre. This feature was observed previously when nanomolar analysis systems were deployed. With the high resolution pigment data also available, it is hoped to get a better understanding of the mechanism for the formation of these maxima.

3.12 Nitrate and Ammonium Uptake

To determine the uptake rates for ammonium and nitrate, samples were taken through the water column with the CTD water bottle system for laboratory analysis (Appendix K). With the availability of the nanomolar analyzers for nitrate and ammonium ions, the natural isotope ^{15}N can be added to the water samples at 10% of the ambient concentrations, to determine uptake rates. From these uptake rates, the f-ratio (defined as nitrate uptake divided by total nitrogen uptake) can be determined, which provides an estimate of carbon export. These rate determinations will be developed in combination with temperature and nitrate algorithms and used with satellite images of SST to derive maps of the f-ratio.

Nutrients analyses were carried out as described in the nutrients section. Samples for the uptake experiment were taken at nominally the 33% light penetration depth. A 2 l sample was taken for both nitrate and ammonium, plus two duplicate samples that were incubated in the dark. The natural isotope ^{15}N was added to the samples at 10% of the ambient concentrations. The samples were incubated through a light screen of 33%, in a water incubator filled with a flow from the nontoxic water supply. The incubations were carried out for 3 hours, ideally, over the maximum light irradiance period of the day, and no longer than 5 hours. After this time, the samples were filtered through an ashed GF/F filter, dried in an oven at 50°C and stored for analysis by low-level mass spectrometry techniques (Owens and Rees 1989).

New analytical low-level detection mass spectrometry protocols developed at PML will be used to analyze the returned samples. These techniques cannot be carried out at these ambient concentrations at any other laboratory worldwide, a facility unique to PML.

3.13 Biogasses

Nitrogen, a biologically essential element in the marine environment, is found in a variety of inorganic and organic forms in oxic seawater ranging from the thermodynamically most-stable species, nitrate, to reduced compounds such as ammonia and its methyl derivatives, the methylamines (MAs): monomethylamine (MMA), dimethylamine (DMA), and trimethylamine (TMA). These are biogenic compounds widely distributed in the marine environment and intimately involved in oceanic nitrogen fertility. In seawater, they partition between their dissolved gaseous form (e.g., NH_3 (s)), which may participate in air–sea gas exchange, and the solvated cationic form (e.g., $NH_4{}^+$(s)) which typically accounts for greater than 90% of their total dissolved concentrations.

Like other reduced biogenic gases (Fig. 20), e.g., methane and dimethylsulfide (DMS), NH_3 and the MAs are end-products of the microbial turnover of labile organic matter. For example, MAs may be produced by phytoplankton via the enzymatic breakdown (Hoffman elimination) of intracellular quaternary amine osmotica, such as, choline and glycine betaine (King 1988). This process is analogous to the production of DMS from its algal precursor dimethylsulphoniopropionate (DMSP). Although substantial data are available for primary productivity throughout the world ocean, little information exists linking phytoplankton community composition with climatically important biogas production on a global scale.

By virtue of their volatility, the dissolved gases NH_3 and MAs are capable of transfer across the air–sea interface (Van Neste et al. 1987, and Quinn 1988, and Quinn et al. 1988). Although only trace atmospheric constituents and poor absorbers of thermal radiation, NH_3 and MAs are proposed to play a key role in several aspects of tropospheric chemistry and climate modification. Recent field deployments of novel instrumentation (Gibb et al. 1995 and 1998) have, for the first time, allowed for characterizing the distribution of MAs in the marine and atmospheric environments and the demonstration of the importance of the marine atmosphere in their global redistribution.

The objectives of the biogases analyses were to:

1. Map the distribution of MAs and ammonium in representative surface samples and vertical profiles along the AMT transect;
2. Determine the MA concentrations in the gaseous, aerosol, and rainwater phases of the overlying atmosphere and, hence, calculate the direction and magnitude of their air–sea exchange fluxes;
3. Correlate MA concentrations and fluxes with pigment abundance and evaluate the potential of pigments as proxy markers of these biogases; and
4. Examine the relationship between MAs and DMS (the sulphur analog to MAs), in contrasting oceanic provinces and in the overlying atmospheric phases.

3.13.1 Methodology

Total dissolved ammonia and total MAs ($NH_4{}^+{}_{(aq)tot}$ and $MAs^+{}_{(aq)tot}$; Table 3) were determined simultaneously in seawater using the flow injection gas-diffusion coupled to ion chromatography (FIGD-IC) technique (Gibb et al. 1995). In the technique, the solvated cations $NH_4{}^+{}_{(aq)tot}$ and $MAs^+{}_{(aq)tot}$ are deprotonated to their gaseous forms (NH_3(aq) and MAs(aq)) through addition of alkali (NaOH) to a pH greater than 12, and selectively transferred via diffusion across a gas-permeable Gore-Tex®† membrane into a dynamic, acidic acceptor stream (40 mmol methane sulphonic acid) in which they are enriched in their cationic forms. The addition of ethylenediaminetetraacetic acid (EDTA) was used to chelate seawater alkali Earth metals. The enriched acceptor stream was transferred directly to a Dionex DX-100 ion chromatograph. Here, $NH_4{}^+$ and MA^+ cations were separated isocratically on 3×Dionex CG-10 columns within 15 min in a methane sulphonic acid eluent (40 mmol) and quantified by chemically suppressed conductimetric detection; *sec*-butylamine was used as an internal standard. A custom computer-interfaced control unit and data capture unit were used in series to direct the solenoid valve switching sequence of the flow-injection system, the ion chromatograph operation, and collection of data (Gibb et al. 1995).

Aerosol and gas phase atmospheric samples were collected in tandem using a cyclonic filter-pack air-sampling technique (Quinn et al. 1988 and 1990), adapted for use with an automated FIGD-IC system. Aerosols were collected on untreated polyfluorotetraethylene (PTFE) prefilters (47 mm in diameter with a 1 μm poresize—from Co-

† Gore-Tex is a registered trademark of W.L. Gore and Associates, Elkton, Maryland.

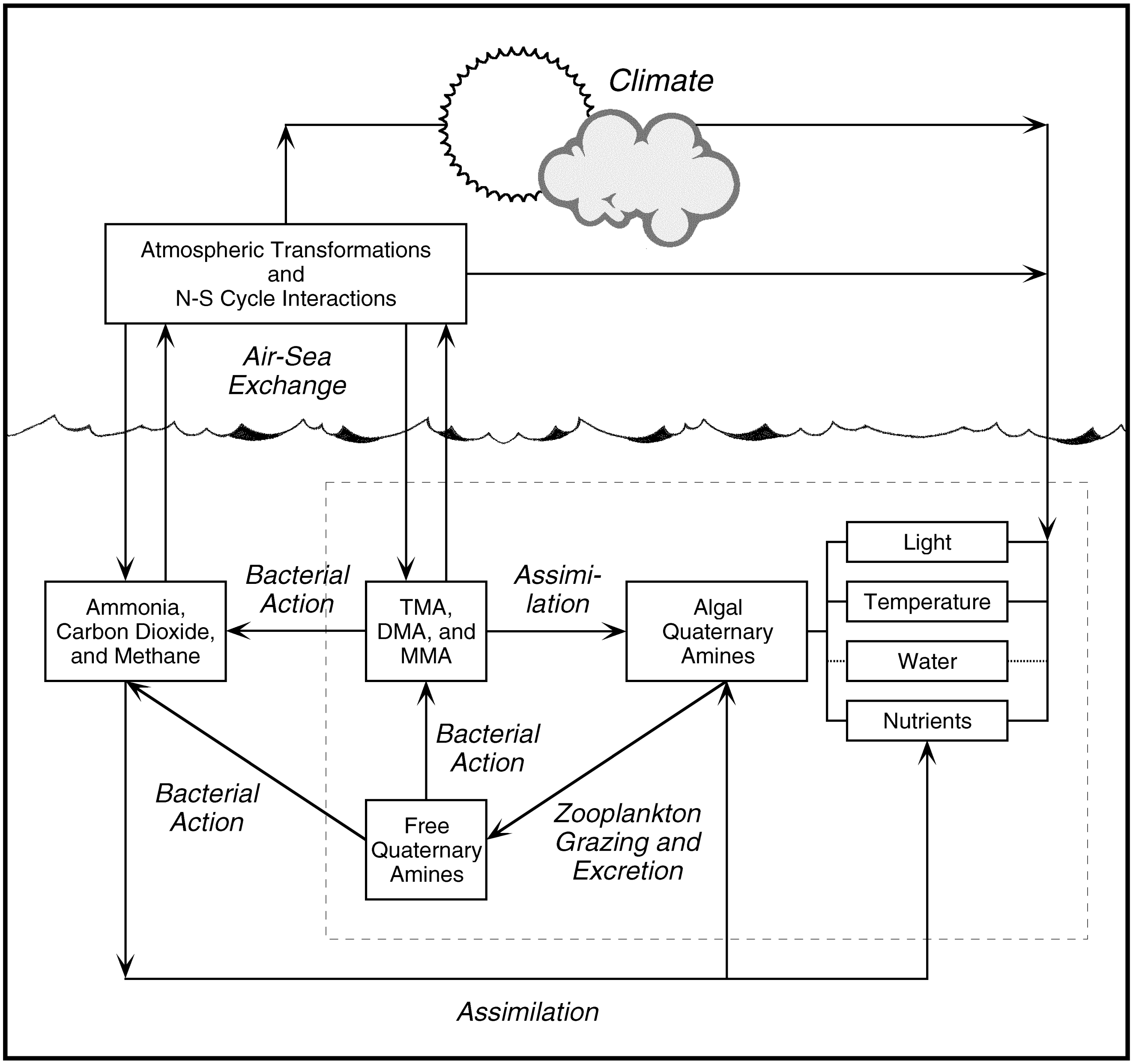

Fig. 20. A schematic showing selected aspects of the biogeochemical cycling of MAs in the marine environment.

star, UK), while gaseous species were collected downstream on pairs of oxalic acid-impregnated paper filters (47 mm diameter, Whatman 40, Whatman Scientific, UK). The cyclone separators have been shown to pass approximately 100% of particles less than 0.4 μm in diameter and 50% of those 0.9 μm in diameter, while Teflon particle filters had a reported collection efficiency of greater than 99% for particles with diameters greater than 0.035 μmol (Liu and Lee 1976). The combined system was thus effective in collecting accumulation mode aerosol, while rejecting coarse mode particles, because the intermode minimum of the bimodal distribution lies within the range of 0.5–1.0 μm (Quinn et al. 1990).

Rainwater samples were collected on an event-only basis using a series of polyethylene funnel-bottle combination collectors. Samples were analyzed unfiltered by FIGD-IC as for seawater samples. The data thus represents total deposition during the rain event.

3.14 Biogenic Sulphur Distribution

Biogenic DMS emissions from the world ocean are a significant source of sulfur to the atmosphere. The products of the atmospheric photochemical oxidation of DMS, most notably the sulfate aerosol, are believed to act as cloud condensation nucleii (CCN) which regulate the number of cloud droplets and, thus, the reflectivity (or albedo) of marine clouds. The resulting changes in global temperature caused by increased cloud cover closes a multistep feedback loop which directly links ocean biota with climate regulation (Charlson et al. 1987).

Significant DMS production is limited to a few classes of phytoplankton, primarily the *Dinophyceae* (dinoflagellates) and the *Prynmesiophyceae* (including the coccolithophores). Studies have shown other less predominant producers to be certain members of *Bacillariophyceae* (the diatoms) and *Chrysophyceae* (Keller et al. 1989). Biogenic DMS can be emitted directly from the cell or via the breakdown of DMSP, a compound thought to act as an osmolyte within phytoplankton cells (termed DMSPp). DMSP can also be directly released into seawater, most likely during zooplankton grazing or lysis, and is then called dissolved DMSP (DMSPd). The precise fate of DMSP in the water column is uncertain, but it is most likely that bacterial breakdown of DMSPd to DMS is most significant. Concentrations of DMSP in the world ocean have been sparsely studied, and the data set is even smaller than that existing for DMS.

The objectives of the biogenic sulphur distribution activity were to:

1. Determine the spatial distributions of DMS, DMSPp, and DMSPd in seawater surface transects and vertical profiles along the AMT-5 cruise track (Fig. 21);
2. Correlate DMS and DMSP distributions with those of chemotaxonomic phytoplankton pigments and, hence, to evaluate the potential of these pigments as proxy markers of DMS and DMSP;
3. Calculate air–sea exchange fluxes for DMS;
4. Examine the relationship between the distribution and fluxes of DMS and its nitrogenous analogs, the methylamines, in both the oceanic and atmospheric components of the environment; and
5. Characterize the chemical composition of marine aerosols and rainwater.

Seawater samples were taken from the nontoxic supply approximately every 2 h from 0800–2000 ship's time and daily from the CTD, typically from six depths. Samples were stored in a cool box and analyzed within 4 h of collection. Analysis for DMS was carried out on board by purging samples with nitrogen gas and cryogenically trapping in liquid nitrogen before injecting into a gas chromatograph (Varian 3300) with flame photometric detection.

Dissolved DMSPd is retained in the purged seawater, which is placed in 60 ml glass vials with 1 ml NaOH (10 M) and crimp sealed with gas-tight lids. Analysis for DMSPd will be carried out at a later date. Samples were first filtered through Millipore AP25 filters, to retain particulate DMSPp. The filters were placed in 20 ml glass vials containing 1 ml NaOH (10 M) and 19 ml purified water and then sealed with gas-tight crimp lids for subsequent laboratory analysis.

Aerosols were collected using a Graseby Anderson high volume sampler fitted with a cascade impactor. The flow rate was typically 0.8 $m^3\,min^{-1}$. Samples were normally collected over 24 h periods and only when the relative wind speed was greater than 3 $m\,s^{-1}$ and blowing from a 180° sector ahead of the ship. Filters were stored in reclosable plastic bags and frozen for subsequent laboratory analysis. Rainwater samples were collected on an event-only basis using a series of polyethylene funnel-bottle combination collectors.

3.15 Zooplankton

The objectives of the zooplankton research activity for AMT-5 were to examine spatial and temporal variation in zooplankton abundance, size and community structure, using the Optical Plankton Counter (OPC), carbon analysis, conventional taxonomic analysis, and to determine copepod feeding rates and its impact on phytoplankton primary production and chlorophyll stock.

At each daily station, three double WP-2 (200 and 100 μm mesh) vertical net casts were made. The first two casts were to 200 m and the third to 20 m. The first 200 m cast was used for gut evacuation experiments. From the second 200 m and 20 m casts, the 100 μm net sample was used for foramanifera analysis, and the 200 μm for OPC and biomass analysis. In addition, there were a number of night stations (three between 20–40°N, one close to the equator, and two in the South Atlantic). Night stations

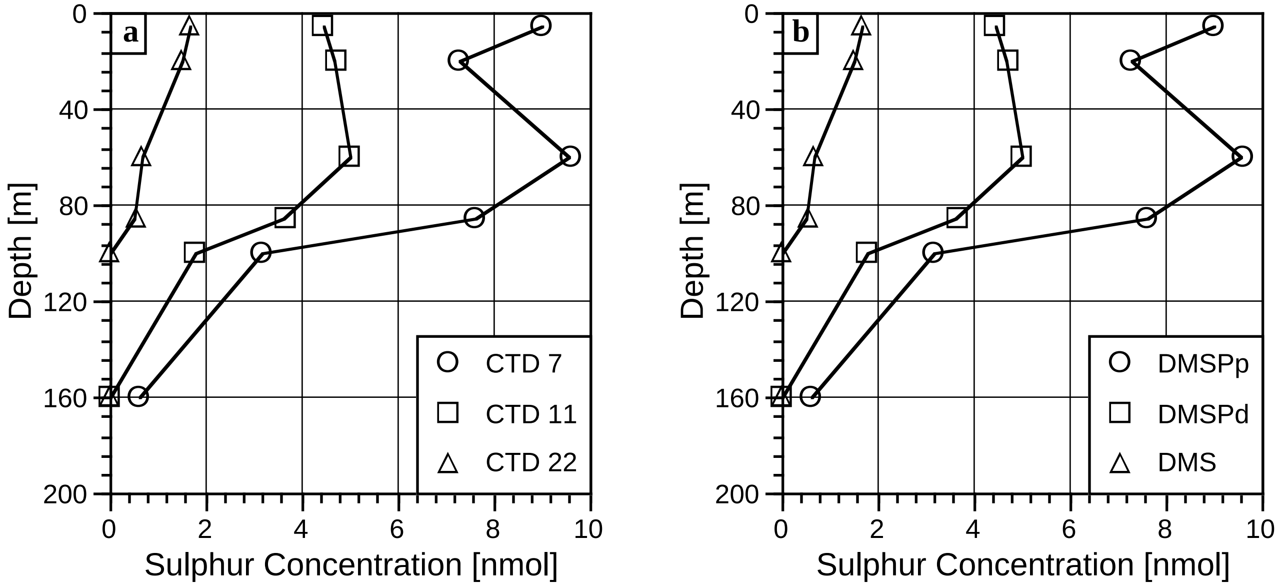

Fig. 21. DMS vertical profiles for **a)** CTD 7 (19.5233°W,35.4450°N), CTD 11 (20.5283°W,19.7200°N) in the Mauritanian upwelling, CTD 22 (40.9783°W,27.6900°S); and **b)** DMS, DMSPp, and DMSPd vertical profiles for CTD 7 (19.5233°W,35.4450°N).

consisted of a single cast of the double net (200 μm) to 200 m. One net sample was used for gut content analysis, and one for OPC and carbon analysis (the latter was split using a Folsom splitter).

3.15.1 Size-Fractionated Carbon

Half of the 200 m net (200 μm) sample was used for carbon analysis. The zooplankton were size fractionated by screening the sample through 2,000, 1,000, 500, and 200 μm sieves to create fractions of 200–500, 500–1,000, 1,000–2,000, and greater than 2,000 μm. The greater than 2,000 μm fraction was preserved. The other size fraction was made up to 500 or 1,000 ml depending on the density of zooplankton, and 50 ml aliquots of each size fraction were filtered onto pre-ashed Whatman GF/F filters (in triplicate). Filters were dried for 48 h in a 60°C oven and then compacted in aluminium foil for subsequent carbon-hydrogen-nitrogen (CHN) analysis at PML. The remainder of the sample was preserved with borax buffered formaldehyde (4%) for taxonomic identification.

3.15.2 OPC

Half of the 200 m net was passed through the OPC to give an estimate of the size structure. This sample was then collected and preserved in 4% formalin for subsequent taxonomic analysis. The 20 m net zooplankton sample was processed through the OPC in a similar manner and preserved.

The OPC was used in continuous flow-through mode during most of the cruise using the uncontaminated seawater supply. This was interrupted only briefly at local dusk and dawn to change data files, and for about 2 h each day on station to process the net samples. Its use was also prevented around Madeira, because of the ship's speed. In-line samples were collected from the OPC outflow using 200 μm mesh collection. This was preserved for subsequent analysis to validate the OPC data. A log of all zooplankton samples taken and samples for analysis are given in Appendix L.

3.15.3 Copepod Ingestion Rates

The gut fluorescence-evacuation method was used to obtain ingestion rates. At each station, one WP2 plankton net (200 μm) was deployed to 200 m. The sample was immediately screened to obtain three different size fractions (200–500, 500–1000, and more than 1,000 μm. Subsamples of each fraction were filtered and frozen for further determination of initial gut contents in each fraction. The remainder of one of the size fractions (one different fraction each day) was used for gut evacuation experiments. Copepods were kept in a cold box filled with filtered seawater from the station (7 m) and subsamples were taken every 5 min for half an hour. Extra subsamples, at 45 and 60 min, were taken if copepod abundance was enough. Subsamples were also filtered and frozen for further gut content analysis.

In some stations along the transect, particularly in the Azores area, night stations were used to compare night and day gut contents. A fixed number of herbivorous copepods were taken from the frozen filters to extract gut contents. The copepod number used was 25 for the large fraction, 50 for the medium, and 75 for the small. Between 1–3 replicates were taken each time. Chlorophyll was extracted using 5 ml of acetone (90%) in 20 ml vials for 24 hours at 4°C. Copepod gut fluorescence was determined using a Turner fluorometer before and after acidification, and expressed as chlorophyll *a* equivalents (in nanograms). Copepod gut content was plotted against time to obtain gut evacuation curves. Data were fitted to an exponential curve to calculate gut evacuation rate (slope of the curve).

3.15.4 Particulates

Samples for carbon–nitrogen analyses were obtained from two different depths: near surface (7 m) and the chlorophyll maximum, as determined by the fluorometer on the CTD. Water from the two depths was filtered through a membrane filter of 5 μm and a 200 μm gauze. The filtrate from each size fraction was filtered in triplicate onto pre-ashed Whatman GF/F filters to produce a series of replicate samples of the two size fractions (less than 5 μm and less than 200 μm). Filters were maintained for 48 h in an oven (60°C) and then compacted in pre-ashed aluminium foil for CHN analysis (Appendix M).

3.15.5 Preliminary Results

The total biovolume of zooplankton in the top 200 m, and the proportion represented by each size fraction changes markedly across the transect (Fig. 22a). In comparison to previous AMT transects at the same time of year, the AMT-5 pattern is slightly different (Fig. 22b). In the North, streamers of high productivity associated with upwelling, were crossed. The zooplankton in this area was higher than in previous years. The peak in biovolume at the southern end of the transect was smaller for the last two stations.

The underway data, shows marked diel changes. In general, the total biovolume is higher at night, and is characterized by an increase in the larger size fractions, e.g., days 274–276 (Fig. 22c).

3.16 Microzooplankton

Samples were taken to assess the latitudinal variability in composition and biomass of microzooplankton assemblages, and the potential relationship of these parameters with phytoplankton composition and environmental variables. The second objective was to carry out experiments to determine microzooplankton grazing activity at the DCM within the latitudinal range of the survey.

3.16.1 Methods

Microzooplankton samples were taken from Niskin bottles at every main daily CTD station (Appendix N). Four depths were sampled along the first part of the cruise until the beginning of CANIGO region, and six depths thereafter. The three sampling depths that were always chosen were: surface water, the DCM, and a sample beneath the DCM. The other sampling depths varied according to the available range of Niskin bottles between the surface and the DCM.

In order to obtain estimates of microzooplankton biomass, 500 ml water samples were fixed in 3% [final concentration (f.c.)] pre-added acid Lugol solution and stored dark in the cold room for subsequent analysis using the Uthermol sedimentation technique, an inverted microscope and a video-image analysis system.

Between 40–20°N, two replicates of 50 ml water samples were taken from six depths, as above, to assess the trophic status of the microzooplanktonic community. The samples were fixed in 1% (f.c.) glutaraldehyde, filtered through 0.8 μm black polycarbonate membrane filters, mounted onto slides and stored frozen (−80°C) for subsequent analysis under an epifluorescence microscope.

3.16.2 Grazing

Water incubations to determine microzooplankton grazing were carried out at alternate CTD stations following the standard dilution method (Landry 1993).

Water from the chlorophyll *a* maximum was taken from the CTD into an acid-washed polycarbonate carboy and combined with 0.2 μm filtered water to obtain four levels of natural water concentrations (20, 40, 70, and 100%). Filtered water was obtained by passing a sample through sequential 3.0, 0.6, and 0.2 μm Gelman filters. This process presumably removes all phytoplankton including prochlorophytes (Verity et al. 1996) and was always carried out immediately before use, to avoid the growth of bacteria in the filtered water. Filtered water (100 ml) from the 250 m depth Niskin bottle was added to each incubation bottle to avoid nutrient depletion and, then, growth limitation. One of the 100% level bottles was kept as a control, with no added nutrients.

Three replicate 2 l and 3 l polycarbonate bottles were slowly filled for each experimental concentration, thereby, avoiding bubbles. Silicon tubing was used for all the transfer procedures. Water was incubated on deck for 24 h, and cooled to ambient levels using underway flow, while a calibrated neutral mesh was used to simulate *in situ* light intensity.

At the beginning of the incubations, three replicates of 250 ml of natural water were filtered onto GF/F filters to assess the initial chlorophyll concentration. After incubation, chlorophyll *a* concentration was determined for each bottle (two replicates per bottle) using a Turner 10-005 R fluorometer. To control for changes in the abundance of grazers during the experiment, a 500 ml water sample from the 100% level bottle was taken at the end of the incubation period and fixed in 3% (f.c.) pre-added acid Lugol solution. The fluorometer used in the experiments and the one used for chlorophyll analysis were intercalibrated during the cruise.

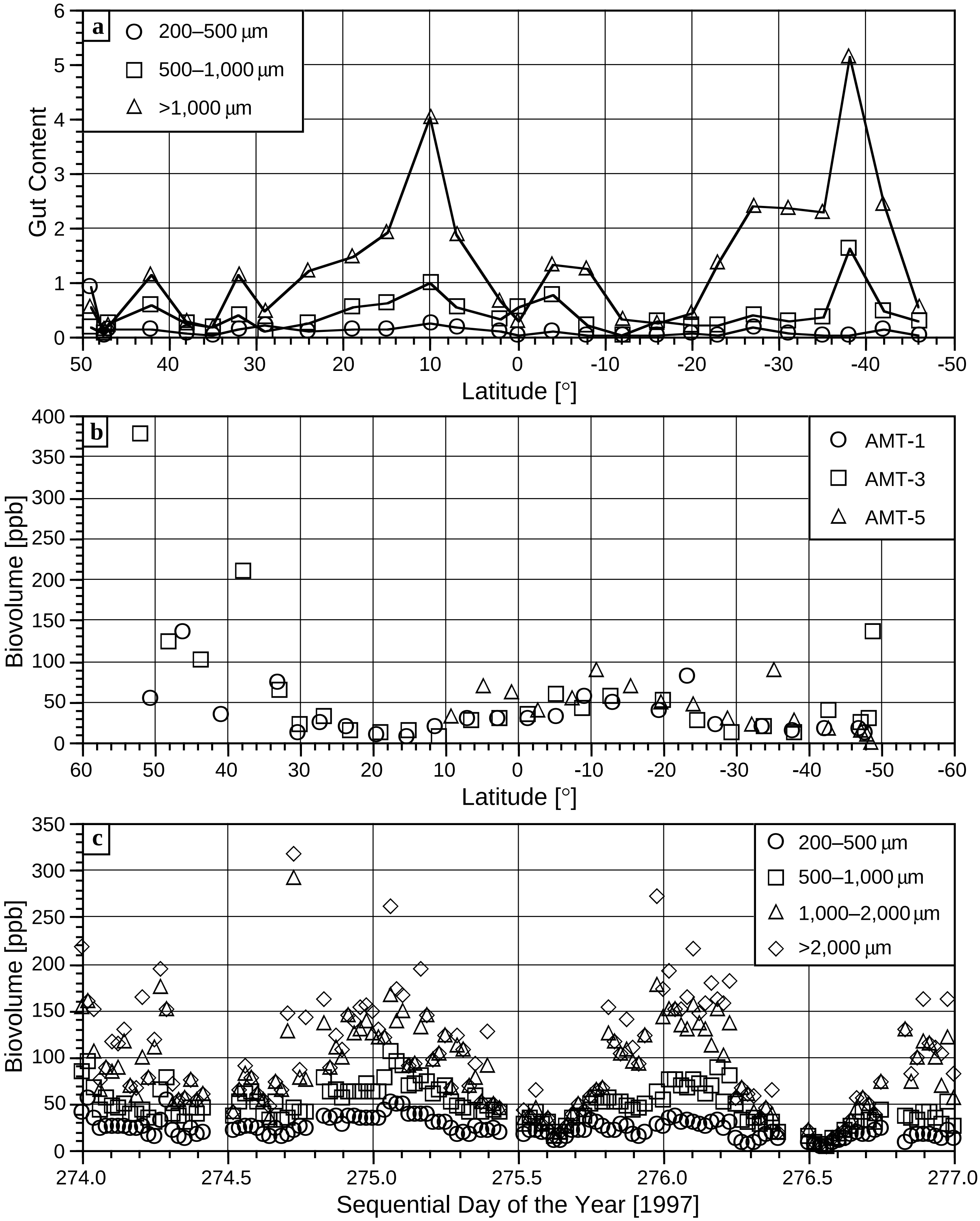

Fig. 22. Zooplankton biovolume anayses: **a)** size-fractionated biovolume along the transect (from 200 m vertical hauls); **b)** total biovolume of AMT-5 compared to AMT-1 and AMT-3; and **c)** size fractionated underway (30-minute bins).

3.17 DNA Analysis of Foraminifera

The planktonic foraminifera are a group of protists ubiquitous among the marine zooplankton. Their calcareous shells contribute approximately 70% to the oceanic carbonate sediment for the world ocean and are widely used for paleoenvironmental, stratigraphic, and evolutionary analyses. The planktonic foraminifera are the only extant group in which all species can be preserved as fossils in the geologic record.

The objectives of the deoxyribonucleic acid (DNA) analysis of foraminifera were:

1. An evolutionary study of the molecular clock to infer a general molecular phylogeny (with the ribosomal ribonucleic acid [rRNA] coding genes) of the planktonic foraminifera and to calibrate it with the fossil record, in order to calculate DNA evolutionary rates among the different lineages; and
2. A broad-scale study of the genetic variability in a planktonic group of organisms to a) characterize the latitudinal variability of DNA sequences at the species level in order to define the genetic boundaries between the populations in comparison with the physical oceanic characteristics, and b) to study the gene flows across the different water masses.

3.17.1 Methods

At each daily CTD station, between two and four net tows (100 and 200 μm mesh collected from a depth of 20 and 200 m) were made for the DNA analyses of the planktonic foraminifera. Samples were immediately distributed in petri dishes and examined with a dissecting microscope. The foraminifera were isolated and transferred to other receptacles containing filtered seawater. The samples were then sorted by species, based on their morphotypes when taxonomic identification was impossible with the optics available on board. In the latter case, some specimens were dried and stored on micropaleontological cells for further examination by scanning electronic microscopy (SEM).

DNA extractions were performed on the same day as collection, in order to avoid damage of the fragile specimens and artifacts due to degradation of cell material. The planktonic foraminifera were individually cleaned by brushing to eliminate the spines, detritus, and microorganisms at their surface. DNA extractions were performed by either 1) grinding individual or groups of specimens in 50 μl of an extraction buffer containing 100 mmol of trisamine (pH=8.5), 4 mmol of EDTA, 1% of sodium deoxycholate, 0.2% of Triton x-100, and incubated for 1 h at 60°C; or 2) by dissolving specimens in 40 μl of a guanidine-based buffer containing guanidium isothiocyanate, tris-HCl, EDTA, sodium lauryl sarkosinate, and β-mercaptoethanol. In addition, experimental tests to extract and conserve DNA from a single cell with preservation of its calcareous shell were carried out on 60 individuals. All DNA extracts were preserved at −20°C.

3.17.2 Accomplishments

A total of 631 DNA extractions on 30 specimens were achieved during AMT-5 and are presented in the log of Appendix O. Overall, 31 species belonging to 13 different genera (on 15 living) were determined and extracted. This represents two thirds of all living planktonic foraminiferal species. Representatives of all the families (*Globigerinidae, Hastigerinidae, Globorotalinidae* and *Candeinidae*) were found plus several species that have interesting evolutionary features, or unknown fossil origin. Most of the same species were found at several different stations in the transect, sometimes in different water masses (e.g., *Orbulina universa*, one of the most widely distributed species, was intensively studied at each station and will be used as a reference species for studying the plankton community genetic structure over basin scales.

Postcruise work in Geneva will consist of DNA amplification by polymerase chain reaction (PCR), cloning of the PCR products in supercompetent bacteria, and sequencing of the clones on a ABI 377 Prism automated sequencer. To start with, the gene coding for the ribosomal RNA will be targeted.

4. SeaWiFS

As stated in the goals of the AMT Program, the calibration and validation of satellite remotely-sensed ocean color data is an inherent objective, and the Program is a major contributor to the SeaWiFS validation effort (Hooker and McClain 1998). For AMT-5, which was designated Sea-ACE, this became the priority objective of the cruise, the objectives of which were as follows:

- Derive $E_d(\lambda)$, $L_u(\lambda)$, and $K_d(\lambda)$ from the SeaOPS and SeaFALLS casts at all SeaWiFS wavelengths, and report the values daily to the SeaWiFS Project; the optical data were quality assured at sea using the SQM, and the derived parameters were quality assured by statistical assessments, self-consistency checks on spectral shape, plus magnitude and empirical algorithm analyses.
- Report measured phytoplankton pigments (by at-sea HPLC and fluorometry), notably chlorophyll *a* and phaeopigments (where measured), 1 d in arrears to the SeaWiFS Project; these data were quality assured by intercomparison of the measurements by the two methods and by using an internal non-marine phytoplankton pigment as an internal standard (canthaxanthin).
- Compare measured and retrieved values (from measurements of water-leaving radiance, L_W, or R_{rs}, using a standard algorithm) of pigment concentration (chlorophyll *a* plus phaeopigments) and $K(490)$ as a quality assurance of the data and analyses techniques.

SeaOPS data were processed using the following procedures:

1. The SeaOPS and MVDS data, which by analogy with satellite data were designated raw level-0, were calibrated to engineering units (level-1a data) by the application of the relevant calibration files (after the detector dark values were subtracted).
2. The in-water and reference calibrated data sets were merged to form a combined data stream of $E_d(\lambda)$, $L_u(\lambda)$, and $E_s(\lambda)$ and auxiliary data (CTD, fluorescence, tilt, roll, etc.). The data were merged based on the time stamp data of the in-water and reference units (which should agree to within 0.1 s).
3. For quality assurance and data quality assessment, a subset of the level-1a data were plotted; scatter plots of $E_d(\lambda)$, $L_u(\lambda)$, and $E_s(\lambda)$ versus depth were produced as well as plots of profiles of temperature, fluorescence, and tilt and roll. All data were inspected for sensor reliability and screened for excessive tilt and roll values, cloud contamination, or any unfavorable experimental conditions (ship shadow, very low E_s values, etc.).
4. From the plotted data, upper and lower depth limits of data acceptability were set, which encompassed temperature and chlorophyll *a* mixed layer depths, as well as, the $E_d(\lambda)$ and $L_u(\lambda)$ linearity range within at least (approximately) two optical depths.
5. The depth range to be used for extrapolating the in-water data to the surface were chosen by visual examination of plots of the remnant data for the surface layer at each station. The upper and lower depths for extrapolations were selected after a cautious examination of the L_u profile, the E_s stability, the profiler behavior (tilt and roll) and the CTD and fluorescence profiles. The radiometric data were regressed versus depth to produce $E_d(0^-)$, K_d, $L_u(0^-)$, K_{L_u}, L_W, R_{rs} and L_{WN}.
6. At each station, the cast conducted under the best experimental conditions (i.e., best sea and sky conditions and ship orientation) was selected or, when all casts were considered good, an average value was computed.

For quality assessment, the following analyses were performed:

A. The diffuse attenuation coefficient, K, is a robust apparent optical property and, under most conditions, values of K_d and K_{L_u} should be very similar for the surface 1–2 optical depths. Significant difference between these two coefficients derived from simultaneous measurements, indicates a problem with either the measurement or the analysis of one or the other parameter. Individual data points can then be reanalyzed or rejected, if no assurance is forthcoming.

B. The comparison of the retrieved attenuation, from the measured $L_W(\lambda)$ data and a standard algorithm, and the measured attenuation from the *in situ* data, provides a validation of the L_W data, given that the measured K_d data have been prevalidated as in step 1. In this case, the SeaWiFS prelaunch algorithm for $K_d(490)$ (Mueller and Trees 1997), hereafter referred to as the MT97 algorithm, was used as the benchmark. In addition, this provided an assessment of the relative accuracy, as a fraction of the variance explained, of the algorithm considered.

C. The measured (*in situ*) chlorophyll concentration ($\tilde{C}$) versus the retrieved (remote sensing) chlorophyll concentration ($\hat{C}$) was computed using a standard algorithm. This is strictly not an assessment of the quality of any of the optical data, but rather an assessment of the accuracy of the *standard algorithm*. In this case, the SeaWiFS chlorophyll *a* operational algorithm (O'Reilly et al. 1998) has been used as the benchmark.

Figure 23a shows the plot of raw K_{L_u} versus raw K_d for all AMT-5 SeaOPS data. The figure shows a close agreement (slope equals 0.99), with a high percentage of the variance explained ($R^2 = 0.994$). Some outliers are evident, mostly at the low end, probably due to surface effects (light focusing by waves) influencing the downwelling data close to the surface. Interim versions of the regression, produced as the cruise progressed, identified some outliers, which on close examination were modified or deleted. In fact nearly all the data acquired passed this quality test and the only data omitted were those when the sky conditions were so variable that no good data could be retrieved reasonably.

Figure 23b shows the plot of the retrieved (modeled) and measured diffuse attenuation coefficients, $\hat{K}_d$ and $\tilde{K}_d$, respectively. The agreement between the two is generally good except for three stations at the high end which are underestimated by the model. Among these outliers, one is a station in the English Channel while the other two are stations in the vicinity of the Falkland Islands. Without these three (presumably Case 2) stations, the regression statistics are $\hat{K}_d(490) = 0.7903\tilde{K}_d(490) + 0.01$ with $R^2 = 0.8763$. It is important to note that the data processing scheme is optimized towards generating the L_W with the highest possible accuracy. The selection of the depth range used for extrapolating the in-water data to the surface is a crucial step. The diffuse attenuation coefficients are computed from the same depth range which might not be the most appropriate for the derivation of K_d. When considering K_{L_u} instead of K_d in this analysis, the statistical results are slightly better.

For the third quality assessment test, if the assessment is *good* (i.e., the data fits the model with a large fraction of the variance explained and with close to a 1:1 relationship, then inherently the bio-optical data used with the retrieval

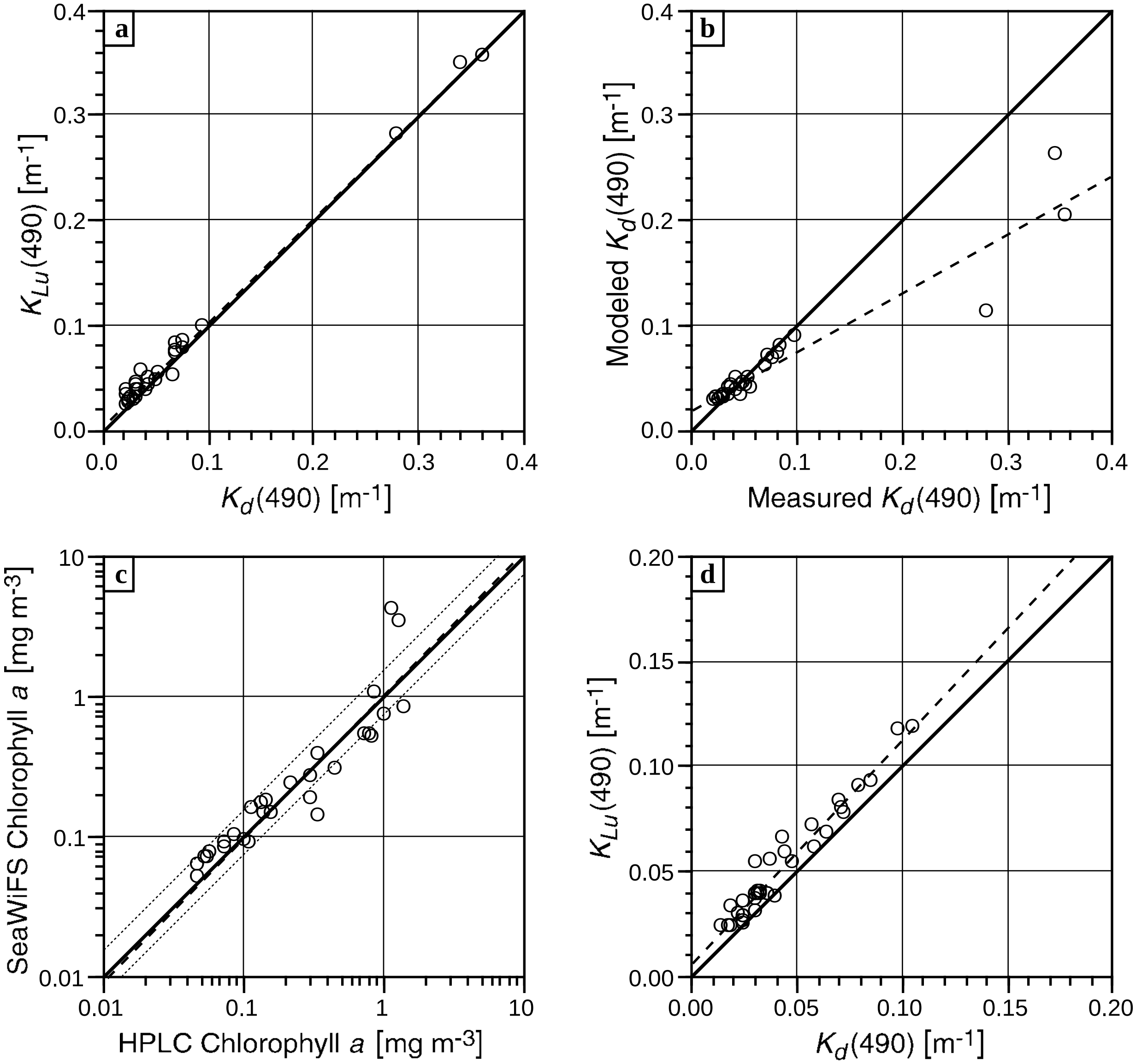

Fig. 23. Data quality assessment test results for SeaOPS and SeaFALLS data, **a**–**c** and **d**–**f**, respectively: **a)** raw K_{L_u} versus raw K_d data; **b)** modeled versus measured diffuse attenuation coefficients, $\hat{K}_d$ and $\tilde{K}_d$, respectively; **c)** *in situ* (HPLC) chlorophyll concentration versus the retrieved (remote sensing) chlorophyll concentration; and **d)** raw K_{L_u} versus raw K_d data.

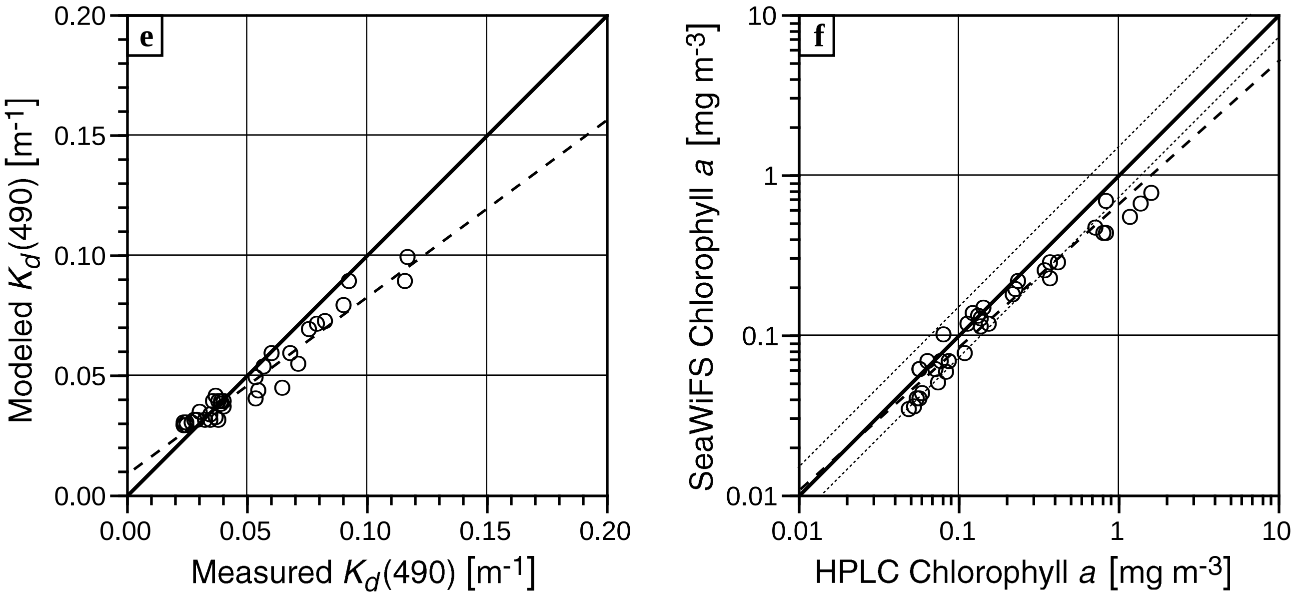

Fig. 23. (cont.) Data quality assessment test results for SeaFALLS data **e)** modeled versus measured diffuse attenuation coefficients, $\hat{K}_d$ and $\tilde{K}_d$, respectively; and **f)** *in situ* (HPLC) chlorophyll concentration versus the retrieved (remote sensing) chlorophyll concentration.

algorithm agree well with the data used to derive the algorithm, except for unlikely or anomalous circumstances. Figure 23c shows the results for the algorithm assessment (the dotted lines represent the ±35% boundaries of the 1:1 line).

SeaFALLS data are similar to SeaOPS data with two exceptions: a) there are 13 channels of E_d data and 13 channels of L_u data, and b) all of the E_d and L_u channels have auto gain switching to cover the wide dynamic range of the sensor response. In addition, the L_u sensors are 0.9 m deeper than the E_d sensors, and this must be taken into account when propogating the L_u data to the surface to derive L_W. SeaFALLS data are processed by programs that adhere to the same protocols and procedures adopted for SeaOPS, but take into account the gain switching. The processed data are quality assured using the same analysis procedures established for SeaOPS. Figures 23d–23f show the three quality assessment products for SeaFALLS.

For chlorophyll, the modeled versus measured regressions (on log transformed data) have slopes close to unity and a large fraction of the variance explained ($R^2 = 0.86$ for SeaOPS and $R^2 = 0.95$ for SeaFALLS). Again, the statistics of SeaOPS are influenced by the three stations mentioned previously. For both radiometers, most stations fit within the ±35% limits. Both instruments differ slightly as chlorophyll *a* derived from SeaOPS data are relatively distributed around the 1:1 line while chlorophylls from SeaFALLS data tend to underestimate actual concentrations.

Acknowledgments

The AMT Program combines a variety of research initiatives and receives resources and financial support from a number of diverse sources. The Centre for Coastal and Marine Studies (CCMS) funds the additional ship time added to the passage of the JCR. The PML Strategic Research Projects 1 and 4 provide scientific support, equipment, and resources. The NERC community research project PRIME funds two core AMT projects: Bio-optical Signatures and Zooplankton Characterization. The NASA SeaWiFS and MODIS Projects provide financial and logistical support, plus state-of-the-art optical, hydrographic, and calibration equipment. The EU CANIGO project participates and there are links with the EU Joint Research Centre at Ispra through various EU projects and NASA collaborations. The scientific objectives of the EU project SOMARE use the AMT project as a model. G. Zibordi is thanked for his help and advice during the preparation of the cruise and the analysis of the sun photometer data. S. Maritorena of the SeaWiFS Project provided optical data analysis results during the cruise, as well as a complete review and revision of the material presented in Section 4.

Appendices

A. RRS *James Clark Ross*
B. Scientific Bridge Log
C. CTD Station and Bottle Log
D. XBT Log
E. Optics Log
F. Scientific Bridge Log
G. XOTD Cast Log
H. FRRF Tow Log
I. Underway and Station Filtration Logs
J. Nutrient Sample Log
K. Nitrate Sample Log
L. OPC Sample Log
N. Microzooplankton Sample Log
O. DNA Analysis of Foraminifera Log
P. AMT-5 Cruise Participants

Appendix A

RRS *James Clark Ross*

A detailed description of the scientific spaces, facilities, and equipment on board the RRS *James Clark Ross* can be found in Robins et al. (1996). The 27 officers and crew members of the RRS *James Clark Ross* during AMT-5 are listed in Table A1.

Table A1. The crew list for AMT-5.

Name		*Rank*
Elliott	Christopher	Master
Harper	John, R.	Chief Officer
Paterson	Robert, C.	Second Officer
Kilroy	Robin, T.	Third Officer
Waddicor	Charles, A.	Radio Officer
Cutting	David, J.	Chief Engineer
Kerswell	William, R.	Second Engineer
Jones	Roger, S.	Third Engineer
Eadie	Steven, J.	Fourth Engineer
Wright	Simon, A.	Deck Engineer
Thomas	Norman, E.	Electrician
Olley	Kenneth, R.	Catering Officer
Brookes	Martin	Bosun
Williams	James, H.W.	Bosun Mate
Graham	Roderick	Seaman First Class
Fairbrother	Carl, D.	Seaman First Class
Macko	Westley	Seaman First Class
Cossey	Peter, A.	Seaman First Class
Davis	Raymond, A.	Seaman First Class
Smith	Sydney, F.	Motorman
Robinshaw	Mark, A.	Motorman
Fox	Roy, W.	Chef
Bailey	David, R.	Second Chef
Clancey	John, A.	Second Steward
Dixon	Tony, N.	Steward
Baldwin-White	Lawrence, B.	Steward
Hadgraft	Simon, D.	Steward

Appendix B

Scientific Bridge Log

The Scientific Bridge Log is presented in Table B1.

Appendix C

CTD Station and Bottle Log

Summaries of the CTD Station and Bottle Logs are presented in Tables C1 and C2, respectively.

Appendix D

XBT Cast Log

A summary of the XBT casts is presented in Table D1.

Appendix E

Optics Deployment Log

A summary of the SeaOPS, SeaFALLS, and LoCNESS Station Logs are presented in Tables E1, E2, and E3, respectively.

Appendix F

Sun Photometer Log

A summary of the Sun Photometer Station Log is presented in Table F1.

Appendix G

XOTD Cast Log

A summary of the XOTD Deployment Log is presented in Table G1.

Appendix H

FRRF Tow Log

A summary of the FRRF Tow Log is presented in Table H1.

Appendix I

Underway and Station Filtration Logs

A summary of the Underway and Station Filtration Logs are presented in Tables I1 and I2, respectively.

Appendix J

Nutrients Sample Log

A summary of the Nutrients Sample Log is presented in Table J1.

Appendix K

Nitrate Sample Log

A summary of the Nitrate Sample Log is presented in Table K1.

Appendix L

OPC Sample Log

A summary of the OPC Sample Log is presented in Table L1.

Appendix M

CHN Sample Log

A summary of the CHN Sample Log is presented in Table M1.

Appendix N

Microzooplankton Sample Log

A summary of the Microzooplankton Sample Log is presented in Table N1.

Appendix O

DNA Analysis of Foraminifera Log

Summaries of the DNA extractions in DOC buffer and guanidinium buffer are presented in Tables O1 and O2, respectively.

Appendix P

AMT-5 Cruise Participants

A summary of the AMT-5 cruise participants is presented in Table P1.

Table B1. A summary of the Scientific Bridge Log for AMT-5. All times are in GMT.

Date	*SDY*	*Longitude*	*Latitude*	*Time*	*Activity*
16 September	259	1° 39.2′ W	50° 25.8′ N	02:00 PM	Stopped on Station 1.
				02:16 PM	SeaOPS deployed.
				02:19 PM	CTD deployed.
				02:31 PM	Plankton nets deployed.
				02:33 PM	CTD on surface.
				02:34 PM	SeaOPS on surface.
				02:34 PM	CTD recovered.
				02:35 PM	Plankton nets recovered.
				02:45 PM	XBT launched.
				02:50 PM	UOR deployed at 4 kts.
				02:58 PM	Resume cruising speed.
17 September	260	8 27.6	48 40.1	04:05 PM	Stopped on Station 2.
				04:10 PM	Plankton nets deployed.
				04:12 PM	CTD deployed.
				04:13 PM	SeaFALLS deployed.
				04:18 PM	Plankton nets recovered.
				04:22 PM	SeaFALLS recovered.
				04:32 PM	CTD recovered.
18 September	261	12 28.4	48 6.0	06:52 AM	XBT launched.
		13 12.3	47 59.0	10:00 AM	Stopped on Station 3.
				10:02 AM	SeaOPS deployed.
				10:05 AM	CTD and plankton nets deployed.
				10:34 AM	SeaOPS recovered.
				10:38 AM	CTD recovered.
				10:39 AM	Meteorology balloon launched.
				10:51 AM	Plankton nets recovered.
				10:55 AM	XBT launched.
				10:58 AM	Speed at 4 kts for UOR deployment.
				11:06 AM	UOR deployed on 250 m line.
19 September	262	17 58.7	47 15.6	08:00 AM	XBT launched.
		18 28.8	47 10.4	10:00 AM	Stopped on Station 4.
				10:09 AM	SeaOPS deployed.
				10:12 AM	CTD and plankton nets deployed.
				10:34 AM	SeaOPS recovered.
				10:39 AM	CTD recovered.
		18 28.5	47 10.2	10:39 AM	XBT launched.
				10:43 AM	Plankton nets recovered.
				11:10 AM	Speed 4 kts.
				11:25 AM	UOR deployed.
				11:25 AM	UOR recovered.
				11:37 AM	UOR redeployed.
				02:19 PM	UOR recovered.
		18 26.5	46 24.1	02:29 PM	SeaFALLS deployed.
				02:30 PM	Trimming SeaFALLS.
				03:00 PM	SeaFALLS recovered.
		18 58.6	46 26.2	04:40 PM	XBT launched.
		19 35.5	45 30.6	09:35 PM	XBT launched.
20 September	263	20 0.2	43 29.7	06:55 AM	XBT launched.
		19 57.0	42 50.6	10:00 AM	Stopped on Station 5.
				10:04 AM	CTD and plankton nets deployed.
				10:10 AM	SeaOPS deployed.
				10:30 AM	SeaOPS recovered.
				10:35 AM	CTD recovered; XBT launched.
				10:38 AM	Plankton nets recovered.

Table B1. (cont.) A summary of the Scientific Bridge Log for AMT-5. All times are in GMT.

Date	*SDY*	*Longitude*	*Latitude*	*Time*	*Activity*
20 September	263			11:11 AM	Meteorology balloon launched.
				11:19 AM	CTD redeployed.
				11:38 AM	CTD recovered; speed increased to 4 kts.
				11:45 AM	UOR deployed; speed increased to 11 kts.
				02:13 PM	UOR recovered.
		19° 57.6′ W	42° 26.0′ N	02:27 PM	Stopped on Station 6.
				02:29 PM	SeaSURF deployed.
				02:33 PM	SeaFALLS deployed.
				02:50 PM	SeaFALLS recovered.
		20 0.3	41 57.3	05:35 PM	XBT deployed.
		20 0.3	41 4.9	10:12 PM	XBT launched.
21 September	264	20 0.1	39 21.0	06:50 AM	XBT launched.
		20 0.7	38 42.9	10:04 AM	Stopped on Station 7.
				10:06 AM	SeaOPS and CTD deployed.
				10:09 AM	Plankton nets deployed.
				10:36 AM	SeaOPS and CTD recovered.
				10:39 AM	Plankton nets recovered.
				10:48 AM	SeaSURF deployed.
				10:50 AM	SeaFALLS deployed.
				11:18 AM	SeaSURF recovered.
				11:20 AM	SeaFALLS recovered.
				11:42 AM	CTD redeployed.
				11:58 AM	CTD recovered.
				12:00 PM	Speed increased to 4 kts.
				12:18 PM	UOR deployed; speed 11 kts.
				02:12 PM	UOR recovered; XBT deployed.
		19 59.9	38 2.1	04:00 PM	XBT launched.
		19 58.4	37 40.3	05:50 PM	XBT launched.
		19 58.2	37 39.5	06:04 PM	XBT launched.
		19 54.5	37 20.2	07:45 PM	XBT launched.
		19 51.9	37 7.3	09:05 PM	Plankton nets deployed.
				09:22 PM	Plankton nets recovered.
		19 51.4	37 3.0	10:00 PM	XBT launched.
22 September	265	19 45.1	36 30.0	12:58 AM	XBT launched.
		19 31.8	35 26.9	07:08 AM	Stopped on Station 8.
				07:20 AM	Plankton nets deployed.
				07:44 AM	BAS CTD deployed.
				08:22 AM	CTD at 2,000 m.
		19 31.8	35 26.7	08:36 AM	CTD at 1,500 m.
				09:10 AM	CTD recovered.
				10:00 AM	Stopped on Station 9.
				10:06 AM	Sea-Bird CTD and SeaOPS deployed.
				10:32 AM	SeaOPS recovered.
				10:41 AM	Plankton nets recovered.
				10:45 AM	SeaSURF deployed.
				10:47 AM	SeaFALLS deployed.
				11:21 AM	SeaSURF recovered.
				11:22 AM	SeaFALLS recovered.
				11:27 AM	CTD at 85 m.
				11:35 AM	CTD recovered.
		19 29.7	35 25.0	11:55 AM	XBT launched.
				12:13 PM	Resume cruising speed.
		19 8.7	35 2.6	02:28 PM	Stopped on Station 10.
				02:29 PM	SeaSURF deployed.
				02:30 PM	SeaFALLS deployed.

Table B1. (cont.) A summary of the Scientific Bridge Log for AMT-5. All times are in GMT.

Date	*SDY*	*Longitude*	*Latitude*	*Time*	*Activity*
				02:46 PM	SeaSURF and SeaFALLS recovered.
23 September	266			10:48 AM	CTD deployed.
				10:58 AM	CTD recovered.
25 September	268	17° 14.4′ W	32° 18.7′ N	01:05 PM	Stopped on station T1.
				01:07 PM	CTD deployed for testing firing mechanism.
				01:40 PM	SeaSURF deployed.
				01:42 PM	SeaFALLS deployed.
				01:47 PM	CTD redeployed.
				02:15 PM	SeaSURF and SeaFALLS recovered.
				02:22 PM	CTD recovered.
				02:33 PM	Plankton nets recovered.
		18 33.0	31 12.7	09:42 PM	XBT launched.
26 September	269	20 32.1	29 24.8	08:34 AM	XBT deployed.
		20 58.4	29 3.1	11:00 AM	Stopped on Station 11.
				11:05 AM	CTD, SeaOPS, and plankton nets deployed.
				11:06 AM	SeaSURF deployed.
				11:10 AM	SeaFALLS deployed.
				11:42 AM	SeaOPS recovered.
		20 59.1	28 51.2	01:00 PM	XBT launched.
		20 59.1	28 38.0	02:05 PM	Stopped on Station 12.
				02:07 PM	SeaSURF deployed.
				02:08 PM	SeaFALLS deployed.
				02:35 PM	SeaSURF recovered.
				02:38 PM	SeaFALLS recovered.
		20 59.2	27 44.4	06:39 PM	XBT launched.
		21 0.0	26 46.3	11:00 PM	Plankton nets deployed.
		21 0.0	26 42.4	11:50 PM	XBT launched.
27 September	270	20 59.5	24 34.1	09:00 AM	XBT launched.
		20 59.9	24 8.1	11:00 AM	Stopped on Station 13.
				11:02 AM	CTD, SeaOPS, and plankton nets deployed.
				11:11 AM	SeaSURF and SeaFALLS deployed.
				11:48 AM	SeaOPS and CTD recovered.
				11:51 AM	SeaSURF and SeaFALLS recovered.
		21 0.5	23 51.8	01:17 PM	XBT launched.
		21 0.6	23 43.5	02:00 PM	Stopped on Station 14.
				02:05 PM	SeaSURF and SeaFALLS deployed.
				02:34 PM	SeaSURF and SeaFALLS recovered.
		20 59.9	22 50.5	06:50 PM	XBT launched.
		20 59.3	21 59.4	11:00 AM	Stopped on station.
				11:01 AM	Plankton nets deployed.
28 September	271	20 44.6	20 43.1	05:31 AM	XBT launched.
		20 40.7	20 25.4	07:10 AM	XBT launched.
		20 35.1	19 59.9	09:20 AM	XBT launched.
		20 30.0	19 43.1	11:00 AM	Stopped on Station 15.
				11:03 AM	CTD, SeaOPS, and plankton nets deployed.
				11:50 AM	CTD recovered.
				11:52 AM	SeaOPS recovered.
				12:04 PM	SeaFALLS recovered.
				12:12 PM	UOR deployed; XBT launched.
				12:22 PM	UOR on 250 m cable; cruising speed resumed.
				03:55 PM	Reducing speed for UOR recovery.
				04:05 PM	UOR recovered.
		20 25.1	19 3.0	04:08 PM	Stopped on Station 16.
				04:10 PM	SeaFALLS and SeaSURF deployed.

Table B1. (cont.) A summary of the Scientific Bridge Log for AMT-5. All times are in GMT.

Date	*SDY*	*Longitude*	*Latitude*	*Time*	*Activity*
28 September	271			04:28 PM	SeaSURF recovered.
				04:29 PM	SeaFALLS recovered.
		20° 23.2′ W	18° 52.1′ N	05:27 PM	XBT launched.
		20 14.4	18 11.0	08:53 PM	XBT launched.
		20 8.5	17 47.9	11:00 PM	Stopped on station.
				11:02 PM	Plankton nets deployed.
				11:25 PM	Plankton nets recovered.
29 September	272	20 4.5	17 24.6	01:12 AM	XBT launched.
		20 0.0	17 1.5	03:19 AM	XBT launched.
		20 0.0	16 38.7	05:16 AM	XBT launched.
		20 0.0	16 15.4	07:13 AM	XBT launched.
		20 0.6	15 29.5	11:00 AM	Stopped on Station T2.
				11:01 AM	SeaOPS and plankton nets deployed.
				11:06 AM	SeaFALLS and SeaSURF deployed.
				11:30 AM	SeaSURF recovered.
				11:31 AM	SeaFALLS recovered.
				11:32 AM	SeaOPS recovered.
		20 0.9	15 13.6	12:54 PM	XBT launched
		19 59.7	14 0.3	06:54 PM	XBT launched.
30 September	273	20 52.2	10 55.3	11:00 AM	Stopped on Station 17.
				11:02 AM	Plankton nets deployed.
				11:04 AM	CTD and SeaOPS deployed.
				11:10 AM	SeaFALLS and SeaSURF deployed.
				11:35 AM	SeaOPS recovered.
				11:44 AM	SeaFALLS and SeaSURF recovered.
				11:45 AM	Plankton nets recovered.
				11:55 AM	UOR deployed.
				03:55 PM	Reducing speed for UOR recovery.
				04:04 PM	UOR recovered.
		21 11.8	10 13.2	04:06 PM	Stopped on Station 18.
				04:16 PM	Off station seeking clear sky.
		21 10.6	10 12.7	04:30 PM	On station.
				04:33 PM	SeaFALLS and SeaSURF deployed.
				04:53 PM	SeaFALLS and SeaSURF recovered.
1 October	274	21 51.8	8 27.0	03:00 AM	XBT launched.
		22 1.6	8 3.1	05:08 AM	XBT launched.
		22 10.8	7 40.4	07:10 AM	XBT launched.
		22 16.8	7 24.1	08:44 AM	XBT launched.
		22 28.2	7 1.6	11:00 AM	Stopped on Station 19.
				11:02 AM	Plankton nets deployed.
				11:04 AM	SeaOPS and CTD deployed.
				11:06 AM	SeaFALLS and SeaSURF deployed.
				11:47 AM	SeaOPS recovered.
				11:48 AM	CTD recovered.
				11:50 AM	Plankton nets recovered.
				11:53 AM	XBT launched.
		22 37.2	6 34.8	02:19 PM	XBT launched.
		22 44.2	6 17.0	04:06 PM	UOR recovered.
		22 44.9	6 15.0	04:15 PM	XBT launched.
		22 53.7	5 54.1	06:15 PM	XBT launched.
		23 4.1	5 29.3	08:33 PM	XBT launched.
		23 19.8	4 52.2	11:55 PM	XBT launched.
2 October	275	23 29.5	4 28.8	02:00 AM	XBT launched.

Table B1. (cont.) A summary of the Scientific Bridge Log for AMT-5. All times are in GMT.

Date	*SDY*	*Longitude*	*Latitude*	*Time*	*Activity*
2 October	275	23° 39.1′ W	4° 05.0′ N	04:04 AM	XBT launched.
		23 47.6	3 43.4	06:00 AM	XBT launched.
		23 56.6	3 21.4	08:00 AM	XBT launched.
		24 7.3	2 55.4	10:05 AM	XBT launched.
		24 9.8	2 49.0	10:59 AM	Stopped on Station 20.
				11:06 AM	CTD SeaOPS and plankton nets deployed.
				11:45 AM	CTD and SeaOPS recovered.
				12:00 PM	SeaOPS redeployed.
				12:10 PM	SeaOPS recovered.
				12:15 PM	UOR deployed.
		24 13.9	2 38.0	01:15 PM	XBT launched.
				04:27 PM	Reduce speed for UOR recovery.
				04:35 PM	UOR recovered.
		24 27.8	2 4.6	04:40 PM	Stopped on Station 21.
				04:49 PM	SeaOPS and SeaSURF deployed.
				04:52 PM	SeaFALLS deployed.
				05:30 PM	SeaOPS recovered.
				05:45 PM	SeaSURF recovered.
				05:47 PM	SeaFALLS recovered.
		24 27.0	2 3.1	05:55 PM	XBT launched.
		24 30.0	1 56.0	06:40 PM	XBT launched.
		24 47.2	1 21.1	10:00 PM	XBT launched.
		24 51.2	1 11.2	11:00 PM	Plankton nets deployed.
				11:24 PM	Plankton nets recovered.
		24 51.3	1 11.0	11:30 PM	XBT launched.
3 October	276	24 58.0	0 54.4	12:48 AM	XBT launched.
		25 7.5	0 29.6	03:15 AM	XBT launched.
		25 17.0	0 7.4	05:20 AM	XBT launched.
		25° 26.0′ W	0° 13.0′ S	07:20 AM	XBT launched.
		25 39.9	0 46.4	10:30 AM	Stopped on Station 22.
				10:31 AM	Plankton nets deployed.
				10:40 AM	CTD and SeaOPS deployed.
				11:30 AM	CTD recovered.
				11:50 AM	SeaFALLS and SeaSURF recovered.
				12:10 PM	SeaOPS recovered.
				12:15 PM	SeaFALLS and SeaSURF deployed.
				12:30 PM	SeaFALLS and SeaSURF recovered.
		25 41.7	0 50.2	01:03 PM	XBT launched.
		25 53.8	1 21.5	04:10 PM	Stopped on Station 23.
				04:13 PM	SeaSURF deployed.
				04:15 PM	SeaFALLS deployed.
				04:46 PM	SeaSURF recovered.
				04:50 PM	SeaFALLS recovered.
		26 4.8	1 48.5	07:58 PM	XBT launched.
4 October	277	26 26.6	2 37.3	12:20 AM	XBT launched.
				09:20 AM	XBT launched.
		27 22.0	4 47.1	11:30 AM	Stopped on Station 24.
				11:40 AM	CTD and SeaOPS deployed.
				11:41 AM	SeaSURF deployed.
				11:45 AM	SeaFALLS deployed.
				12:30 PM	CTD recovered.
				12:33 PM	Plankton nets recovered.
				01:06 PM	SeaOPS recovered.
				01:12 PM	SeaSURF recovered.

Table B1. (cont.) A summary of the Scientific Bridge Log for AMT-5. All times are in GMT.

Date	*SDY*	*Longitude*	*Latitude*	*Time*	*Activity*
4 October	277			01:14 PM	SeaFALLS recovered.
		27° 35.9′ W	5° 18.5′ S	04:05 PM	Stopped on Station 25.
				04:07 PM	SeaFALLS and SeaSURF deployed.
				04:39 PM	SeaSURF recovered.
				04:42 PM	SeaFALLS recovered.
		27 37.5	5 22.3	05:00 PM	XBT deployed.
5 October	278	29 0.4	8 41.5	09:57 AM	XBT launched.
		29 6.9	8 58.0	11:30 AM	Stopped on Station 26.
				11:32 AM	Plankton nets deployed.
				11:38 AM	CTD and SeaOPS deployed.
				12:19 PM	SeaOPS recovered.
				12:22 PM	CTD recovered.
				12:35 PM	Nets, SeaFALLS, SeaSURF, and SeaBOSS deployed.
				01:10 PM	Plankton nets recovered.
				01:12 PM	SeaOPS recovered.
				01:18 PM	UOR deployed.
				05:07 PM	UOR recovered.
		29 22.9	9 36.8	05:10 PM	Stopped on Station 27.
				05:12 PM	SeaBOSS deployed.
				05:15 PM	SeaSURF deployed.
				05:16 PM	SeaFALLS deployed.
				05:35 PM	SeaSURF recovered.
				05:37 PM	SeaBOSS recovered.
				05:38 PM	SeaFALLS recovered.
		29 23.6	9 38.3	05:50 PM	XBT launched.
		29 39.6	10 14.7	09:03 PM	XBT launched.
6 October	279	30 42.3	11 8.2	01:50 AM	XBT launched.
		30 42.3	12 52.6	11:31 AM	Stopped on Station 28.
				11:32 AM	Plankton nets deployed.
				11:35 AM	SeaOPS and CTD deployed.
				11:45 AM	SeaFALLS, SeaSURF, and SeaBOSS deployed.
				12:06 PM	Plankton nets recovered.
				12:12 PM	CTD recovered.
				01:17 PM	Plankton nets and SeaOPS recovered.
				01:20 PM	SeaSURF recovered.
				01:26 PM	SeaFALLS and SeaBOSS recovered.
				01:29 PM	UOR deployed.
				04:29 PM	UOR recovered.
		30 57.1	13 28.5	05:12 PM	XBT launched.
		31 10.4	13 57.0	08:04 PM	XBT launched.
		31 25.6	14 28.6	11:12 PM	XBT launched.
7 October	280	31 39.3	15 1.4	02:10 AM	XBT launched.
		31 46.6	15 17.8	03:35 AM	XBT launched.
		32 11.5	16 16.0	09:02 AM	XBT launched.
		32 21.8	16 41.0	11:30 AM	Stopped on Station 29.
				11:31 AM	Plankton nets deployed.
				11:32 AM	CTD, SeaOPS, SeaFALLS, and SeaSURF deployed.
				11:37 AM	SeaBOSS deployed.
				12:10 PM	SeaOPS recovered.
				12:24 PM	CTD and plankton nets recovered.
				12:26 PM	XBT launched. UOR deployed.
				03:07 PM	UOR recovered.
		32 32.8	17 8.8	03:12 PM	Stopped on Station 30.
				03:13 PM	SeaOPS deployed.
				03:17 PM	SeaBOSS and SeaSURF deployed.

Table B1. (cont.) A summary of the Scientific Bridge Log for AMT-5. All times are in GMT.

Date	*SDY*	*Longitude*	*Latitude*	*Time*	*Activity*
7 October	280			03:20 PM	SeaFALLS deployed.
				03:53 PM	SeaOPS recovered.
				04:02 PM	References recovered.
				04:04 PM	SeaBOSS and SeaSURF recovered.
		32° 48.0′ W	17° 49.4′ S	07:56 PM	XBT launched.
		33 10.7	18 40.1	01:30 AM	XBT launched.
8 October	281	34 3.0	20 24.0	09:52 AM	XBT launched.
		34 13.5	20 39.7	11:42 AM	Stopped on Station 31.
				11:43 AM	SeaOPS and plankton nets deployed.
				11:45 AM	CTD deployed.
				12:30 PM	CTD recovered.
				01:31 PM	SeaOPS and plankton nets recovered.
				01:40 PM	SeaSURF recovered.
				02:01 PM	UOR deployed.
				04:35 PM	UOR recovered.
		34 33.4	21 4.9	04:44 PM	Stopped on Station 32.
				04:45 PM	SeaSURF deployed.
				04:46 PM	SeaFALLS deployed.
				05:04 PM	SeaSURF recovered.
				05:05 PM	SeaFALLS recovered.
		35 18.5	21 52.9	10:10 PM	XBT launched.
9 October	282	36 53.2	23 29.6	08:56 AM	XBT launched.
		37 17.1	23 54.2	11:40 AM	Stopped on Station 33.
				11:43 AM	CTD plankton nets and SeaOPS deployed.
				12:06 PM	SeaOPS recovered.
				12:21 PM	CTD recovered.
				12:23 PM	Plankton nets recovered.
		38 21.2	24 59.9	07:07 PM	XBT launched.
10 October	283	39 6.5	25 48.8	12:01 AM	Plankton nets deployed.
				12:25 AM	Plankton nets recovered.
		40 24.1	27 4.2	07:57 AM	XBT launched.
		40 58.6	27 41.4	11:30 AM	Stopped on Station 34.
				11:32 AM	Plankton nets deployed.
				11:36 AM	CTD and SeaOPS deployed.
				12:06 PM	SeaOPS recovered.
				12:14 PM	CTD recovered.
				12:15 PM	Plankton nets recovered.
		41 20.3	28 2.1	02:22 PM	XBT launched.
11 October	284	42 55.9	29 40.3	12:01 AM	Plankton nets deployed.
				12:14 AM	Plankton nets recovered.
		43 12.2	29 55.0		XBT launched.
		44 24.3	31 10.6	09:15 AM	XBT launched.
		44 52.0	31 37.2	12:00 PM	Stopped on Station 35.
				12:02 PM	Plankton nets deployed.
				12:12 PM	CTD and SeaOPS deployed.
				12:16 PM	LoCNESS deployed.
				12:26 PM	CTD wire off sheave; repair commenced.
				02:40 PM	SeaOPS recovered.
				01:30 PM	Recovery of CTD resumed.
				01:36 PM	Plankton nets recovered.
				01:43 PM	CTD recovered; no water available.
		44 54.3	31 38.1	01:55 PM	XBT launched.
		45 52.9	32 38.4	07:30 PM	XBT launched.
12 October	285	46 59.4	33 43.1	02:00 AM	XBT launched.

Table B1. (cont.) A summary of the Scientific Bridge Log for AMT-5. All times are in GMT.

Date	*SDY*	*Longitude*	*Latitude*	*Time*	*Activity*
12 October	285	48° 43.9′ W	35° 21.3′ S	11:43 AM	XBT launched.
		48 51.8	35 29.5	12:40 PM	Stopped on Station 36.
				12:41 PM	Plankton nets deployed.
				12:42 PM	CTD deployed.
				12:44 PM	SeaOPS deployed.
				12:51 PM	SeaOPS recovered; SeaFALLS and LoCNESS deployed.
				12:57 PM	Plankton nets deployed.
				01:30 PM	CTD recovered.
		49 4.1	35 43.4	03:37 PM	XBT launched.
		49 27.0	36 5.4	06:03 PM	Stopped on Station 37.
				06:05 PM	LoCNESS and SeaFALLS deployed.
				06:18 PM	LoCNESS redeployed after trimming.
				06:43 PM	XBT launched.
		50 5.7	36 42.3	10:52 PM	XBT launched.
13 October	286	50 26.7	37 2.5	01:00 AM	Stopped on station.
				01:02 AM	Plankton nets deployed.
				01:25 AM	Plankton nets recovered.
		50 27.8	37 3.6	01:39 AM	XBT launched.
		50 47.9	37 26.4	03:46 AM	XBT launched.
		51 25.5	38 13.7	08:09 AM	XBT launched.
		51 47.1	38 40.3	10:50 AM	XBT launched.
		51 54.4	38 49.9	12:00 PM	Stopped on Station 38.
				12:13 PM	Plankton nets deployed.
				12:15 PM	SeaOPS and CTD deployed.
				12:37 PM	SeaOPS recovered.
				12:50 PM	CTD and plankton nets recovered.
				12:58 PM	Plankton nets, SeaFALLS, and LoCNESS deployed.
				01:45 PM	All recovered.
				01:50 PM	UOR deployed.
				04:08 PM	UOR recovered.
		52 8.8	39 11.9	04:13 PM	Stopped on Station 39.
				04:21 PM	LoCNESS deployed.
				04:34 PM	LoCNESS redeployed after trimming.
				04:40 PM	SeaFALLS deployed.
				05:21 PM	SeaOPS recovered.
		52 6.3	39 12.3	05:28 PM	XBT launched.
		52 15.6	39 27.0	07:11 PM	XBT launched.
		52 28.3	39 44.1	08:59 PM	XBT launched.
		52 43.2	40 6.5	11:15 PM	XBT launched.
14 October	287	52 58.4	40 23.6	01:00 AM	Plankton nets deployed.
				01:16 AM	Plankton nets recovered.
		52 59.3	40 25.6	01:30 AM	XBT launched.
		53 12.7	40 41.5	03:12 AM	XBT launched.
		53 25.4	40 58.9	05:00 AM	XBT launched.
		53 45.3	41 22.3	07:28 AM	XBT launched.
		53 58.1	41 39.4	09:08 AM	XBT launched.
		54 14.9	42 1.0	11:08 AM	XBT launched.
		54 27.6	42 14.3	12:36 PM	Stopped on Station 40.
				12:44 PM	Plankton nets, CTD, and SeaOPS deployed.
				01:33 PM	CTD recovered.
				01:39 PM	SeaOPS recovered.
				01:44 PM	LoCNESS and SeaFALLS recovered.
				01:54 PM	UOR deployed.
		54 31.9	42 16.2	02:00 PM	XBT launched.

Table B1. (cont.) A summary of the Scientific Bridge Log for AMT-5. All times are in GMT.

Date	*SDY*	*Longitude*	*Latitude*	*Time*	*Activity*
14 October	287			04:43 PM	UOR recovered.
		54° 52.0′ W	42° 47.8′ S	04:59 PM	Stopped on station.
				05:03 PM	SeaOPS and CTD deployed.
				05:45 PM	CTD recovered.
				05:56 PM	LoCNESS deployed.
				06:12 PM	All recovered.
		54 58.4	42 56.8	06:56 PM	XBT launched.
		55 6.7	43 10.2	08:00 PM	XBT launched.
		55 27.0	43 37.9	10:00 PM	XBT launched.
15 October	288	55 41.0	43 55.0	12:01 AM	XBT launched.
		55 41.9	43 56.8	12:05 AM	XBT launched, second attempt.
		55 49.6	44 4.6	01:00 AM	Plankton nets deployed.
				01:14 AM	Plankton nets recovered.
		55 57.5	44 15.9	02:16 AM	XBT launched.
		56 13.5	44 35.5	04:03 AM	XBT launched.
		56 31.5	44 55.5	06:05 AM	XBT launched.
		56 37.0	45 18.0	08:02 AM	XBT launched.
		56 40.1	45 41.8	10:06 AM	XBT launched.
		56 42.1	46 2.6	12:00 PM	Stopped on Station 42.
				12:02 PM	Plankton nets deployed.
				12:13 PM	CTD deployed.
				12:20 PM	LoCNESS and SeaFALLS deployed.
				12:55 PM	CTD recovered.
				01:00 PM	SeaOPS deployed.
				01:24 PM	SeaOPS and plankton nets recovered.
				01:37 PM	SeaOPS deployed.
				02:20 PM	SeaOPS recovered.
				02:36 PM	UOR deployed.
				05:00 PM	UOR recovered.
		56 45.2	46 32.4	05:09 PM	Stopped on Station 43.
				05:12 PM	CTD deployed.
				05:25 PM	LoCNESS and SeaFALLS deployed.
				05:38 PM	LoCNESS and SeaFALLS recovered.
				05:40 PM	CTD recovered.
		56 53.9	47 42.4	11:42 PM	XBT launched.
16 October	289	56 57.9	48 7.2	12:49 AM	XBT launched.
		57 37.6	49 47.6	12:32 PM	Stopped on Station 44.
				12:33 PM	Plankton nets and SeaOPS deployed.
				12:40 PM	CTD deployed.
				12:45 PM	LoCNESS and SeaFALLS deployed.
				01:00 PM	CTD recovered.
				01:20 PM	SeaOPS recovered.
				01:26 PM	LoCNESS and SeaFALLS recovered.
				01:30 PM	Plankton nets recovered.
				01:44 PM	UOR deployed.
				03:49 PM	UOR recovered.
		58 14.1	49 47.8	03:55 PM	Stopped on Station 45.
				04:08 PM	SeaOPS deployed.
				04:15 PM	CTD deployed.
				04:17 PM	LoCNESS and SeaFALLS deployed.
				04:42 PM	CTD recovered.
				05:15 PM	SeaOPS recovered.
17 October	290	57 42.2	51 39.9	11:20 AM	Stopped on Station 46.
				11:25 AM	SeaOPS deployed.
				12:00 PM	SeaOPS recovered.

Table C1. A summary of the CTD Station Log for AMT-5. All times are in GMT.

Cast	*Date*	*SDY*	*Time*	*Longitude*	*Latitude*	*Comment*
1	16 September	259	1422	1° 39.1′ W	50° 27.6′ N	All bottles leaked badly.
2	17	260	1611	8 27.4	48 40.2	Bottles 2 and 5 did not fire.
3	18	261	1008	13 12.3	47 59.0	Bottle 5 did not fire.
4	19	262	1013	18 28.9	47 10.4	Bottles 2, 3, 5, and 6 did not fire.
5	20	263	1009	19 57.8	42 50.5	Bottles 2, 3, 5, and 6 did not fire.
5a	20	263	1116	19 57.8	42 50.5	Bottles 2, 5, and 6 did not fire.
6	21 September	264	1010	20 0.7	38 43.0	Bottles 2, 5, 6, and 9 did not fire.
6a	21	264	1144	20 0.7	38 43.0	Bottle 9 did not close.
7d	22	265	0744	19 31.9	35 26.9	BAS CTD no bottle data available.
7	22	265	0907	19 31.4	35 26.7	Bottle 6 did not fire.
7a	22	265	1028	19 31.4	35 26.7	Bottles 2, 3, 5, and 6 did not fire.
8	25	268	1344	17 13.6	32 18.6	Bottles 2 and 5 did not fire.
9	26 September	269	1103	20 58.1	29 2.8	Bottles 2 and 5 did not fire.
10	27	270	1106	20 59.9	24 8.1	Bottles 2 and 6 did not fire.
11	28	271	1102	20 31.7	19 43.2	All bottles fired.
12	30	273	1104	20 52.2	10 55.3	All bottles fired.
13	1 October	274	1102	22 28.3	7 1.6	All bottles fired.
14	2	275	1105	24 9.8	2 49.0	All bottles fired.
15	3 October	276	1039	25° 39.8′ W	0° 46.5′ S	Bottle 2 failed to close at the bottom.
16	4	277	1140	27 22.1	2 47.2	All bottles fired.
17	5	278	1136	29 6.9	8 58.0	All bottles fired.
18	6	279	1135	30 42.3	12 52.6	All bottles fired.
19	7	280	1136	32 42.3	16 52.6	All bottles fired.
20	8	281	1145	34 13.5	20 39.7	All bottles fired.
21	9 October	282	1144	37 17.2	23 54.1	All bottles fired.
22	10	283	1135	40 58.6	27 41.4	All bottles fired.
23	11	284	1210	44 52.1	31 37.2	Cast aborted due to wire failure.
24	12	285	1242	48 51.6	35 28.6	All bottles fired.
25	13	286	1215	51 55.1	38 50.1	All bottles fired.
26	14	287	1240	54 27.3	42 14.3	All bottles fired.
27	14 October	287	1701	54 52.6	42 49.3	All bottles fired.
28	15	288	1214	56 41.9	46 2.7	All bottles fired.
29	15	288	1713	56 45.2	46 32.4	All bottles fired.
30	16	289	1243	57 39.6	49 47.7	All bottles fired.
31	16	289	1615	58 14.1	49 47.8	All bottles fired.

Table C2. A summary of the CTD Bottle Log for AMT-5. The temperature from CTD sensors 1 and 2 (T_1 and T_2, respectively) are in units of degrees Celcius, the salinity from CTD sensors 1 and 2 (S_1 and S_2, respectively) are in PSU, the transmittance (T_r) is in percent light transmitted, and the fluorescence, PAR, and deck cell PAR (F, PAR, and PAR_S, respectively) are all in volts.

Cast	*Bottle*	*Depth*	T_1	S_1	T_2	S_2	T_r	F	PAR	PAR_S
1	1	24.7	17.7	35.223	17.7	35.222	0.78	0.208	0.00	1.07
	2	24.5	17.7	35.223	17.7	35.222	0.78	0.211	0.00	1.07
	3	24.7	17.7	35.223	17.7	35.222	0.78	0.195	0.00	1.08
	4	24.5	17.7	35.223	17.7	35.222	0.78	0.218	0.00	1.08
	5	24.6	17.7	35.223	17.7	35.222	0.78	0.214	0.00	1.08
	6	24.6	17.7	35.223	17.7	35.222	0.78	0.217	0.00	1.08
	7	14.7	17.7	35.223	17.7	35.222	0.79	0.217	0.45	1.17
	8	14.6	17.7	35.223	17.7	35.222	0.79	0.223	0.47	1.18
	9	14.6	17.7	35.223	17.7	35.222	0.79	0.213	0.51	1.24
	10	9.3	17.7	35.223	17.7	35.222	0.79	0.229	1.37	1.28

Table C2. (cont.) A summary of the CTD Bottle Log for AMT-5.

Cast	*Bottle*	*Depth*	T_1	S_1	T_2	S_2	T_r	F	PAR	PAR_S
1	11	4.6	17.7	35.223	17.7	35.221	0.79	0.240	2.13	1.28
	12	1.6	17.7	35.223	17.7	35.222	0.80	0.218	2.62	1.24
2	1	114.7	12.2	35.598	12.2	35.597	0.95	0.088	0.00	0.91
	2	100.2	12.2	35.598	12.2	35.596	0.96	0.090	0.00	1.05
	3	98.2	12.2	35.598	12.2	35.596	0.95	0.089	0.00	0.66
	4	80.7	12.2	35.598	12.2	35.596	0.96	0.090	0.00	1.03
	5	59.7	12.2	35.599	12.2	35.597	0.96	0.091	0.15	0.46
	6	46.1	12.6	35.598	12.6	35.594	0.97	0.113	0.48	0.59
	7	35.7	14.4	35.578	14.4	35.572	0.97	0.200	0.79	0.39
	8	35.1	14.4	35.579	14.4	35.576	0.96	0.210	0.80	0.39
	9	24.8	16.1	35.558	16.1	35.548	0.96	0.245	1.23	0.43
	10	15.2	16.7	35.567	16.7	35.565	0.96	0.178	1.56	0.40
	11	9.1	16.7	35.566	16.7	35.564	0.97	0.161	1.74	0.40
	12	5.3	16.8	35.547	16.9	35.545	0.97	0.114	1.90	0.41
3	1	252.0	11.4	35.565	11.4	35.564	0.98	0.066	0.00	1.23
	2	161.3	12.0	35.632	12.0	35.632	0.98	0.066	0.00	1.22
	3	101.9	12.5	35.695	12.5	35.693	0.98	0.067	0.00	1.06
	4	81.7	12.7	35.714	12.7	35.712	0.98	0.081	0.00	0.77
	5	80.3	12.7	35.714	12.7	35.712	0.98	0.081	0.00	0.78
	6	61.8	12.8	35.723	12.9	35.721	0.98	0.119	0.22	1.27
	7	41.8	13.6	35.713	13.7	35.708	0.96	0.271	0.73	1.26
	8	42.8	13.7	35.716	13.7	35.712	0.96	0.266	0.78	1.34
	9	32.2	16.5	35.640	16.4	35.627	0.95	0.262	1.00	1.07
	10	17.1	17.5	35.634	17.5	35.632	0.96	0.131	1.24	0.48
	11	12.2	17.5	35.635	17.5	35.633	0.96	0.130	1.53	0.53
	12	7.1	17.5	35.635	17.5	35.633	0.96	0.108	1.86	0.88
4	1	248.4	12.0	35.621	12.0	35.620	0.98	0.067	0.00	1.69
	2	161.4	12.5	35.691	12.5	35.690	0.98	0.069	0.00	0.61
	3	101.2	12.8	35.723	12.8	35.721	0.98	0.087	0.00	0.57
	4	83.0	13.0	35.734	13.0	35.731	0.98	0.107	0.00	0.49
	5	82.0	13.0	35.737	13.0	35.735	0.98	0.109	0.00	0.48
	6	67.6	13.3	35.745	13.3	35.738	0.97	0.133	0.00	0.40
	7	52.8	14.7	35.760	14.6	35.759	0.96	0.300	0.25	0.29
	8	53.8	14.6	35.764	14.6	35.761	0.96	0.294	0.21	0.28
	9	40.6	17.6	35.760	17.4	35.756	0.96	0.165	0.72	0.31
	10	22.7	17.8	35.763	17.8	35.761	0.96	0.131	1.29	0.41
	11	12.9	17.8	35.763	17.8	35.761	0.96	0.131	1.53	0.38
	12	6.5	17.8	35.763	17.8	35.761	0.96	0.131	1.73	0.33
5	1	251.3	12.7	35.719	12.7	35.717	0.96	0.067	0.00	0.97
	2	161.8	13.4	35.811	13.4	35.809	0.96	0.069	0.00	0.81
	3	99.7	14.1	35.913	14.1	35.911	0.96	0.082	0.00	0.87
	4	78.6	14.3	35.943	14.3	35.941	0.96	0.112	0.25	0.81
	5	60.3	14.5	35.953	14.5	35.951	0.95	0.153	0.67	0.82
	6	51.4	14.7	35.947	14.7	35.945	0.95	0.254	0.92	0.80
	7	40.6	16.0	35.913	16.0	35.910	0.94	0.297	1.29	0.81
	8	40.1	16.0	35.910	16.1	35.909	0.94	0.309	1.32	0.81
	9	30.9	19.1	35.864	19.1	35.863	0.95	0.089	1.57	0.82
	10	21.1	19.1	35.871	19.1	35.868	0.95	0.088	1.81	0.86
	11	11.2	19.1	35.871	19.1	35.869	0.95	0.082	2.08	0.88
	12	5.9	19.1	35.871	19.1	35.869	0.95	0.079	2.27	0.92
5a	1	160.6	13.4	35.816	13.4	35.813	0.96	0.067	0.00	0.75
	2	160.6	13.4	35.817	13.4	35.814	0.96	0.067	0.00	0.75
	3	160.6	13.4	35.816	13.4	35.814	0.96	0.067	0.00	0.75

Table C2. (cont.) A summary of the CTD Bottle Log for AMT-5.

Cast	*Bottle*	*Depth*	T_1	S_1	T_2	S_2	T_r	F	PAR	PAR_S
5a	4	100.4	14.0	35.907	14.0	35.905	0.96	0.078	0.00	0.76
	5	100.3	14.0	35.909	14.0	35.907	0.96	0.079	0.00	0.76
	6	100.0	14.0	35.912	14.1	35.911	0.96	0.080	0.00	0.76
	7	60.2	14.6	35.943	14.6	35.941	0.95	0.221	0.70	0.75
	8	60.3	14.6	35.945	14.6	35.942	0.95	0.230	0.70	0.75
	9	60.1	14.6	35.945	14.6	35.943	0.95	0.235	0.71	0.76
	10	50.6	15.0	35.949	15.0	35.947	0.94	0.284	1.00	0.76
	11	50.8	15.3	35.943	15.3	35.939	0.94	0.302	1.01	0.76
	12	50.6	15.3	35.943	15.3	35.942	0.94	0.296	1.02	0.77
6	1	252.8	12.9	35.763	12.9	35.760	0.96	0.063	0.00	1.40
	2	162.4	13.7	35.884	13.7	35.882	0.96	0.066	0.00	1.41
	3	122.4	14.3	35.948	14.3	35.945	0.96	0.087	0.00	1.47
	4	102.1	14.6	35.987	14.7	35.985	0.96	0.104	0.26	1.36
	5	92.0	14.8	36.001	14.8	35.992	0.96	0.121	0.05	0.39
	6	81.4	15.3	36.037	15.3	36.034	0.95	0.193	0.77	1.41
	7	81.5	15.3	36.037	15.3	36.034	0.95	0.192	0.77	1.41
	8	66.9	16.4	36.047	16.4	36.040	0.95	0.136	1.19	1.40
	9	41.9	18.4	36.041	18.4	36.038	0.95	0.084	1.74	1.30
	10	22.2	22.0	36.228	22.0	36.222	0.95	0.072	2.18	1.43
	11	12.3	22.1	36.242	22.1	36.239	0.95	0.070	2.37	1.43
	12	7.3	22.1	36.242	22.1	36.239	0.95	0.068	2.50	1.45
6a	1	163.0	13.8	35.896	13.8	35.894	0.96	0.068	0.00	1.84
	2	162.7	13.8	35.898	13.8	35.894	0.96	0.068	0.00	1.81
	3	163.5	13.8	35.897	13.8	35.894	0.96	0.067	0.00	1.62
	4	92.7	15.0	36.019	15.1	36.022	0.95	0.149	0.63	1.32
	5	92.5	15.1	36.036	15.1	36.034	0.95	0.166	0.55	1.12
	6	92.8	15.1	36.037	15.1	36.033	0.95	0.157	0.51	1.22
	7	82.7	15.6	36.047	15.6	36.043	0.95	0.208	0.82	1.12
	8	82.8	15.6	36.049	15.6	36.046	0.95	0.210	0.76	1.05
	9	82.7	15.6	36.052	15.6	36.049	0.95	0.212	0.69	0.94
	10	42.7	19.2	36.065	19.2	36.063	0.95	0.079	1.67	1.07
	11	42.8	19.1	36.066	19.1	36.063	0.95	0.080	1.59	0.95
	12	42.7	19.1	36.066	19.1	36.063	0.95	0.080	1.57	0.94
7	1	250.4	13.6	35.887	13.6	35.883	0.96	0.064	0.00	0.45
	2	161.4	14.7	36.040	14.7	36.037	0.96	0.069	0.00	0.52
	3	121.7	15.2	36.077	15.2	36.076	0.96	0.090	0.00	0.75
	4	101.6	15.7	36.120	15.7	36.112	0.95	0.118	0.00	0.76
	5	86.4	16.3	36.127	16.3	36.124	0.95	0.205	0.41	0.78
	6	86.3	16.3	36.126	16.3	36.123	0.94	0.209	0.42	0.79
	7	75.9	17.0	36.181	17.0	36.179	0.95	0.105	0.73	0.83
	8	60.8	18.0	36.197	18.1	36.194	0.95	0.089	1.12	0.85
	9	40.5	20.8	36.270	20.9	36.274	0.95	0.073	1.61	0.80
	10	21.1	23.3	36.506	23.3	36.496	0.95	0.067	1.88	0.79
	11	11.0	23.5	36.477	23.5	36.464	0.95	0.066	2.21	1.02
	12	6.3	23.7	36.400	23.7	36.392	0.95	0.066	2.27	1.15
7a	1	85.4	16.5	36.162	16.4	36.160	0.95	0.188	0.17	0.38
	2	86.1	16.4	36.168	16.4	36.164	0.94	0.212	0.15	0.37
	3	85.8	16.4	36.167	16.4	36.165	0.94	0.214	0.14	0.37
	4	85.9	16.4	36.164	16.4	36.162	0.94	0.213	0.13	0.36
	5	85.6	16.4	36.164	16.4	36.163	0.94	0.212	0.13	0.36
	6	85.6	16.4	36.163	16.4	36.162	0.94	0.220	0.13	0.36
	7	20.2	23.1	36.529	23.1	36.524	0.95	0.070	1.45	0.38
	8	20.3	23.2	36.529	23.2	36.526	0.95	0.070	1.46	0.38

Table C2. (cont.) A summary of the CTD Bottle Log for AMT-5.

Cast	*Bottle*	*Depth*	T_1	S_1	T_2	S_2	T_r	F	PAR	PAR_S
7a	9	20.4	23.2	36.528	23.2	36.524	0.95	0.070	1.46	0.38
	10	20.5	23.2	36.533	23.2	36.532	0.95	0.070	1.46	0.39
	11	20.4	23.1	36.537	23.1	36.532	0.95	0.070	1.47	0.39
	12	20.3	23.1	36.537	23.1	36.532	0.95	0.070	1.48	0.40
8	1	250.0	14.8	36.050	14.8	36.046	0.96	0.062	0.00	1.53
	2	160.8	16.1	36.242	16.1	36.239	0.96	0.066	0.00	1.60
	3	121.2	17.0	36.404	17.0	36.401	0.96	0.085	0.27	1.51
	4	101.6	17.5	36.520	17.5	36.517	0.96	0.104	0.53	1.18
	5	91.8	17.6	36.526	17.6	36.522	0.96	0.117	0.63	0.95
	6	76.6	17.9	36.540	17.9	36.533	0.96	0.147	0.99	0.98
	7	76.6	17.9	36.540	17.9	36.536	0.96	0.159	1.06	1.02
	8	76.8	17.9	36.540	17.9	36.536	0.95	0.152	1.08	1.04
	9	61.2	18.2	36.540	18.1	36.533	0.96	0.139	1.48	1.08
	10	42.0	20.1	36.612	20.1	36.609	0.96	0.075	1.89	1.13
	11	21.8	22.6	36.838	22.4	36.818	0.96	0.066	2.23	1.04
	12	11.5	23.9	36.915	23.9	36.912	0.96	0.065	2.50	1.29
9	1	249.9	15.7	36.231	15.7	36.228	0.96	0.071	0.00	1.41
	2	180.0	17.3	36.503	17.3	36.504	0.96	0.083	0.00	1.04
	3	160.2	17.6	36.574	17.6	36.567	0.96	0.086	0.00	1.43
	4	140.2	18.2	36.661	18.1	36.653	0.96	0.103	0.00	1.43
	5	130.5	18.5	36.704	18.5	36.702	0.96	0.117	0.19	1.44
	6	118.2	18.9	36.782	18.9	36.779	0.96	0.124	0.48	1.45
	7	118.5	18.9	36.783	18.9	36.780	0.96	0.125	0.48	1.46
	8	118.3	18.9	36.784	18.9	36.781	0.96	0.126	0.49	1.47
	9	80.3	20.4	36.810	20.3	36.806	0.96	0.098	1.41	1.47
	10	40.2	23.7	37.195	23.8	37.194	0.96	0.078	2.17	1.45
	11	20.7	24.3	37.189	24.3	37.181	0.96	0.074	2.49	1.45
	12	10.9	24.6	37.193	24.6	37.190	0.96	0.071	2.63	1.44
10	1	251.2	16.4	36.328	16.4	36.324	0.96	0.066	0.00	1.43
	2	180.7	17.6	36.562	17.7	36.568	0.96	0.071	0.00	1.42
	3	151.1	18.6	36.739	18.6	36.736	0.96	0.076	0.00	1.40
	4	120.9	19.5	36.908	19.5	36.904	0.96	0.093	0.17	1.40
	5	101.2	20.1	37.016	20.1	37.013	0.96	0.113	0.59	1.41
	6	91.1	20.4	37.044	20.4	37.040	0.96	0.120	0.80	1.35
	7	91.1	20.4	37.048	20.4	37.045	0.96	0.118	0.80	1.32
	8	91.3	20.4	37.048	20.4	37.045	0.96	0.119	0.83	1.42
	9	76.6	21.0	37.098	21.1	37.097	0.96	0.121	1.20	1.41
	10	40.8	24.8	37.075	24.8	37.090	0.95	0.089	1.89	1.38
	11	21.8	24.9	36.909	24.9	36.907	0.95	0.084	2.39	1.41
	12	11.4	24.9	36.900	24.9	36.897	0.95	0.076	2.62	1.41
11	1	244.9	13.2	35.654	13.2	35.651	0.96	0.084	0.00	1.29
	2	162.0	14.0	35.712	14.0	35.709	0.96	0.087	0.00	1.42
	3	119.8	14.2	35.667	14.2	35.663	0.95	0.091	0.00	1.42
	4	61.2	16.0	35.878	16.0	35.875	0.95	0.123	0.41	1.42
	5	42.1	16.7	35.885	16.7	35.884	0.94	0.220	1.06	1.42
	6	42.3	16.7	35.895	16.7	35.891	0.94	0.214	1.04	1.42
	7	30.5	20.2	35.983	19.9	36.027	0.92	0.473	1.61	1.41
	8	30.5	22.6	36.173	22.5	36.164	0.91	0.358	1.62	1.41
	9	27.2	24.9	36.270	24.9	36.262	0.92	0.281	1.78	1.41
	10	22.4	25.1	36.275	25.1	36.273	0.91	0.315	1.99	1.41
	11	12.2	25.2	36.287	25.2	36.284	0.91	0.246	2.42	1.41
	12	3.5	25.3	36.291	25.3	36.289	0.91	0.144	2.82	1.41
12	1	250.2	11.1	35.082	11.1	35.077	0.96	0.082	0.00	1.41
	2	160.4	12.3	35.225	12.3	35.224	0.96	0.083	0.00	0.92

Table C2. (cont.) A summary of the CTD Bottle Log for AMT-5.

Cast	*Bottle*	*Depth*	T_1	S_1	T_2	S_2	T_r	F	PAR	PAR_S
12	3	100.4	14.1	35.443	14.1	35.441	0.96	0.111	0.00	1.04
	4	79.7	15.1	35.557	15.2	35.556	0.95	0.140	0.27	1.71
	5	60.1	16.4	35.642	16.5	35.645	0.95	0.181	0.85	1.71
	6	49.8	17.7	35.701	17.6	35.694	0.94	0.242	1.19	1.61
	7	43.5	19.2	35.807	19.2	35.804	0.92	0.366	1.35	1.14
	8	43.8	19.3	35.820	19.3	35.818	0.92	0.367	1.53	1.75
	9	30.5	21.8	35.884	22.1	35.810	0.93	0.161	2.08	1.72
	10	20.2	27.0	35.798	26.9	35.806	0.94	0.105	2.37	1.64
	11	10.7	28.4	35.708	28.4	35.708	0.94	0.094	2.62	1.61
	12	5.6	28.6	35.690	28.6	35.694	0.94	0.091	2.77	1.62
13	1	251.4	11.6	35.149	11.6	35.146	0.95	0.083	0.00	0.94
	2	161.2	12.9	35.278	12.9	35.277	0.95	0.081	0.00	1.02
	3	120.8	13.7	35.386	13.8	35.379	0.95	0.085	0.00	1.02
	4	101.2	14.7	35.490	14.6	35.482	0.95	0.099	0.00	1.01
	5	81.1	16.4	35.641	16.4	35.635	0.95	0.128	0.42	1.01
	6	66.0	18.1	35.756	18.4	35.782	0.95	0.148	0.80	1.00
	7	48.5	21.4	35.936	21.6	35.937	0.94	0.247	1.46	0.99
	8	48.2	21.7	35.941	21.8	35.942	0.93	0.272	1.44	1.00
	9	41.1	22.8	35.967	22.9	35.986	0.93	0.265	1.78	1.03
	10	31.1	26.4	35.690	26.2	35.717	0.94	0.106	2.15	1.09
	11	21.2	28.0	34.840	28.0	34.825	0.95	0.088	2.38	1.08
	12	3.5	28.1	34.306	28.1	34.308	0.95	0.077	2.89	1.05
14	1	248.8	12.8	35.249	12.8	35.245	0.95	0.079	0.00	0.87
	2	179.8	13.7	35.363	13.7	35.360	0.95	0.080	0.00	0.78
	3	151.0	13.9	35.396	13.9	35.393	0.95	0.081	0.00	0.72
	4	125.8	14.5	35.463	14.5	35.464	0.95	0.090	0.00	0.70
	5	100.7	17.1	35.668	17.3	35.676	0.95	0.124	0.22	0.68
	6	86.0	19.8	35.841	19.8	35.837	0.95	0.137	0.60	0.66
	7	75.8	25.4	35.899	25.4	35.889	0.94	0.193	0.89	0.64
	8	76.2	25.4	35.908	25.4	35.908	0.94	0.195	0.87	0.63
	9	60.4	26.9	35.838	27.1	35.825	0.95	0.117	1.21	0.64
	10	40.4	27.6	35.674	27.6	35.683	0.94	0.093	1.56	0.65
	11	21.0	27.6	35.561	27.6	35.559	0.94	0.088	1.94	0.66
	12	2.5	27.6	35.562	27.6	35.560	0.94	0.086	2.44	0.67
15	1	248.3	12.1	35.165	12.1	35.161	0.96	0.078	0.00	1.53
	2	177.1	13.9	35.392	13.9	35.389	0.96	0.075	0.00	1.15
	3	134.8	14.8	35.517	14.8	35.514	0.96	0.079	0.00	0.82
	4	91.6	16.9	35.818	16.9	35.814	0.96	0.095	0.70	1.53
	5	72.1	24.5	36.623	24.5	36.617	0.95	0.160	1.06	1.13
	6	62.0	25.0	36.266	25.0	36.252	0.95	0.225	1.41	1.47
	7	61.3	25.1	36.215	25.1	36.213	0.95	0.230	1.36	1.26
	8	62.1	25.1	36.246	25.1	36.243	0.95	0.230	1.05	1.24
	9	48.4	25.8	36.113	25.8	36.110	0.95	0.191	1.61	0.89
	10	38.5	25.9	36.099	25.9	36.096	0.95	0.147	2.04	1.56
	11	19.2	26.0	36.087	26.0	36.084	0.95	0.087	2.45	1.56
	12	1.1	26.1	36.088	26.1	36.085	0.95	0.073	2.69	0.94
16	1	250.5	10.1	34.915	10.1	34.909	0.96	0.078	0.00	1.41
	2	180.6	12.3	35.189	12.3	35.185	0.96	0.078	0.00	1.41
	3	140.2	16.2	35.664	16.2	35.660	0.96	0.096	0.00	0.46
	4	120.7	19.6	36.001	19.5	35.992	0.96	0.108	0.00	0.44
	5	100.7	23.6	35.888	23.4	35.919	0.95	0.161	0.40	0.44
	6	90.9	24.1	35.854	24.1	35.856	0.95	0.196	0.66	0.45
	7	83.9	24.8	35.901	24.8	35.899	0.95	0.238	0.86	0.44
	8	83.9	25.0	35.925	25.0	35.923	0.95	0.246	0.86	0.44

Table C2. (cont.) A summary of the CTD Bottle Log for AMT-5.

Cast	*Bottle*	*Depth*	T_1	S_1	T_2	S_2	T_r	F	PAR	PAR_S
16	9	66.1	25.1	35.912	25.1	35.910	0.95	0.224	1.34	0.44
	10	41.0	25.4	35.912	25.4	35.910	0.95	0.136	1.98	0.45
	11	21.1	25.4	35.922	25.4	35.918	0.95	0.104	2.41	0.45
	12	3.2	25.6	35.926	25.6	35.924	0.95	0.081	2.89	0.45
17	1	250.9	10.8	34.980	10.8	34.977	0.96	0.076	0.00	0.70
	2	200.7	13.3	35.273	13.3	35.274	0.96	0.076	0.00	0.59
	3	180.7	14.6	35.458	14.7	35.488	0.96	0.083	0.00	0.56
	4	160.5	16.5	35.772	16.5	35.762	0.96	0.098	0.02	0.56
	5	140.6	20.1	36.331	20.0	36.309	0.95	0.132	0.44	0.57
	6	131.4	20.5	36.387	20.5	36.387	0.95	0.141	0.65	0.56
	7	121.1	22.5	36.691	22.5	36.686	0.95	0.168	0.92	0.65
	8	121.3	22.5	36.695	22.5	36.693	0.95	0.165	0.92	1.40
	9	101.1	25.2	36.834	25.2	36.841	0.95	0.108	1.35	1.43
	10	60.7	25.9	36.589	25.9	36.590	0.95	0.090	1.95	1.45
	11	21.3	26.2	36.523	26.2	36.520	0.95	0.076	2.46	1.48
	12	2.8	26.2	36.523	26.2	36.520	0.95	0.073	2.85	1.43
18	1	251.0	13.5	35.303	13.4	35.281	0.96	0.074	0.00	1.12
	2	219.8	15.1	35.532	15.1	35.545	0.96	0.078	0.00	1.17
	3	201.5	16.7	35.786	16.7	35.788	0.96	0.083	0.00	0.96
	4	191.9	17.6	35.931	17.6	35.933	0.96	0.087	0.00	0.94
	5	179.0	19.6	36.254	19.6	36.254	0.96	0.097	0.00	1.00
	6	170.8	20.5	36.405	20.6	36.416	0.96	0.106	0.00	0.96
	7	156.0	22.0	36.665	22.0	36.663	0.96	0.135	0.15	0.92
	8	156.2	22.2	36.691	22.2	36.686	0.95	0.138	0.15	0.93
	9	140.7	23.0	36.838	23.0	36.833	0.95	0.138	0.54	0.92
	10	101.3	24.9	37.145	24.8	37.142	0.95	0.093	1.10	0.83
	11	41.1	26.4	36.845	26.3	36.845	0.90	0.078	1.81	0.88
	12	20.4	26.4	36.841	26.4	36.838	0.93	0.074	1.98	1.02
19	1	250.9	15.8	35.571	15.8	35.550	0.96	0.072	0.00	1.11
	2	200.8	19.4	36.193	19.4	36.181	0.96	0.083	0.00	1.12
	3	180.6	21.3	36.579	21.4	36.590	0.96	0.100	0.00	1.21
	4	161.5	23.4	37.073	23.5	37.082	0.95	0.118	0.29	1.33
	5	151.4	23.8	37.143	23.8	37.142	0.95	0.120	0.49	1.13
	6	141.7	23.9	37.153	23.9	37.151	0.95	0.128	0.61	1.26
	7	141.1	23.9	37.158	23.9	37.155	0.95	0.129	0.62	1.25
	8	130.9	23.9	37.181	23.9	37.177	0.95	0.124	0.81	1.36
	9	120.8	23.9	37.135	23.9	37.130	0.95	0.115	1.06	1.50
	10	101.0	24.1	37.155	24.1	37.153	0.95	0.093	1.27	1.33
	11	51.1	24.6	37.153	24.6	37.149	0.95	0.076	1.81	1.28
	12	2.3	25.5	37.168	25.5	37.165	0.95	0.068	2.56	1.26
20	1	251.0	15.7	35.526	15.7	35.524	0.96	0.072	0.00	1.38
	2	200.1	18.0	35.928	18.0	35.925	0.96	0.078	0.00	1.38
	3	180.0	18.8	36.065	18.7	36.050	0.96	0.082	0.00	1.38
	4	160.5	20.0	36.291	19.9	36.260	0.95	0.102	0.16	1.38
	5	145.6	20.6	36.413	20.5	36.406	0.95	0.115	0.44	1.38
	6	137.6	21.6	36.649	21.6	36.647	0.95	0.138	0.62	1.38
	7	137.6	21.6	36.647	21.6	36.641	0.95	0.138	0.62	1.38
	8	125.4	22.8	36.898	22.8	36.897	0.95	0.126	0.85	1.38
	9	110.6	23.4	37.055	23.4	37.052	0.95	0.102	1.11	1.38
	10	60.8	23.7	37.121	23.7	37.118	0.95	0.085	1.62	1.38
	11	20.4	23.9	37.126	23.9	37.122	0.95	0.078	1.70	1.38
	12	2.1	23.9	37.126	23.9	37.123	0.95	0.073	2.79	1.38
21	1	252.4	15.2	35.476	15.1	35.470	0.96	0.074	0.00	1.04
	2	201.7	16.3	35.635	16.3	35.631	0.96	0.074	0.00	1.03

Table C2. (cont.) A summary of the CTD Bottle Log for AMT-5.

Cast	*Bottle*	*Depth*	T_1	S_1	T_2	S_2	T_r	F	PAR	PAR_S
21	3	179.2	17.2	35.794	17.3	35.803	0.96	0.076	0.00	1.03
	4	141.7	18.7	36.058	18.6	36.046	0.95	0.092	0.00	1.04
	5	121.2	19.4	36.184	19.4	36.192	0.95	0.108	0.27	0.97
	6	108.6	20.3	36.345	20.3	36.342	0.95	0.132	0.51	0.95
	7	107.9	20.4	36.357	20.4	36.353	0.95	0.135	0.54	0.98
	8	102.0	20.6	36.401	20.6	36.399	0.95	0.138	0.69	0.98
	9	81.1	22.1	36.683	22.2	36.686	0.95	0.111	1.14	1.02
	10	51.7	22.8	36.805	22.8	36.802	0.95	0.092	1.62	1.08
	11	20.5	22.8	36.799	22.8	36.795	0.95	0.084	2.07	1.10
	12	3.2	22.8	36.797	22.8	36.793	0.95	0.076	2.52	1.08
22	1	252.3	13.8	35.305	13.8	35.302	0.96	0.075	0.00	0.39
	2	181.4	15.1	35.480	15.1	35.478	0.96	0.075	0.00	0.45
	3	161.8	15.8	35.581	15.7	35.566	0.96	0.076	0.00	0.47
	4	121.3	17.9	35.966	17.9	35.959	0.96	0.096	0.00	0.45
	5	96.9	20.3	36.445	20.2	36.440	0.95	0.107	0.06	0.40
	6	77.1	20.8	36.586	20.9	36.583	0.95	0.122	0.33	0.36
	7	61.6	20.9	36.591	20.9	36.588	0.95	0.124	0.57	0.33
	8	50.8	20.9	36.592	20.9	36.589	0.95	0.125	0.79	0.33
	9	37.3	20.9	36.592	20.9	36.589	0.95	0.123	1.26	0.43
	10	36.8	20.9	36.592	20.9	36.589	0.95	0.122	1.29	0.45
	11	21.2	20.9	36.592	20.9	36.589	0.95	0.126	1.63	0.48
	12	2.3	20.9	36.592	20.9	36.589	0.95	0.118	2.24	0.53
24	1	250.8	15.8	35.722	15.8	35.719	0.96	0.079	0.00	1.06
	2	202.2	16.0	35.734	16.0	35.733	0.96	0.080	0.00	1.06
	3	161.6	16.8	35.872	16.9	35.877	0.96	0.081	0.00	1.17
	4	121.8	17.9	36.062	17.9	36.054	0.96	0.082	0.00	1.20
	5	90.9	18.2	36.093	18.2	36.090	0.96	0.085	0.00	1.14
	6	70.8	19.3	36.263	19.3	36.259	0.96	0.103	0.15	1.11
	7	55.3	19.0	36.069	19.0	36.069	0.94	0.184	0.52	1.08
	8	45.4	19.0	36.077	19.0	36.073	0.93	0.227	0.83	1.08
	9	37.2	19.2	36.128	19.2	36.125	0.93	0.223	1.12	1.07
	10	36.9	19.2	36.134	19.2	36.130	0.93	0.218	1.14	1.07
	11	20.7	18.7	35.870	18.7	35.862	0.92	0.162	1.73	1.07
	12	2.6	18.7	35.868	18.7	35.866	0.93	0.136	2.49	1.10
25	1	252.7	14.3	35.616	14.3	35.613	0.96	0.095	0.00	1.43
	2	161.9	14.1	35.566	14.1	35.562	0.96	0.104	0.00	1.52
	3	102.1	14.1	35.547	14.1	35.546	0.96	0.107	0.00	0.46
	4	71.8	14.2	35.564	14.2	35.560	0.96	0.116	0.00	1.60
	5	51.7	14.3	35.566	14.3	35.563	0.94	0.177	0.00	0.44
	6	41.3	14.3	35.564	14.3	35.561	0.93	0.252	0.11	0.41
	7	31.6	14.3	35.556	14.3	35.552	0.91	0.308	0.51	0.42
	8	25.1	14.3	35.555	14.3	35.552	0.91	0.335	0.97	0.50
	9	25.5	14.3	35.557	14.3	35.554	0.91	0.323	1.30	0.75
	10	20.8	14.3	35.552	14.3	35.548	0.90	0.344	1.84	1.35
	11	11.2	14.3	35.549	14.3	35.546	0.90	0.292	2.31	1.57
	12	3.8	14.3	35.550	14.3	35.547	0.90	0.191	2.71	1.57
26	1	244.9	4.7	34.168	4.7	34.166	0.96	0.098	0.00	0.88
	2	157.9	6.1	34.272	6.1	34.271	0.96	0.102	0.00	0.87
	3	123.4	6.5	34.233	6.5	34.235	0.96	0.134	0.00	0.93
	4	89.2	8.1	34.385	8.1	34.383	0.96	0.104	0.00	0.92
	5	75.2	9.2	34.529	9.2	34.525	0.96	0.137	0.00	0.89
	6	65.2	9.7	34.622	9.7	34.620	0.95	0.154	0.15	0.87
	7	49.8	11.9	35.041	11.9	35.041	0.93	0.269	0.58	0.83
	8	35.4	12.6	35.214	12.6	35.214	0.93	0.267	1.04	0.85

Table C2. (cont.) A summary of the CTD Bottle Log for AMT-5.

Cast	*Bottle*	*Depth*	T_1	S_1	T_2	S_2	T_r	F	PAR	PAR_S
26	9	26.2	12.3	35.131	12.3	35.128	0.93	0.300	1.39	0.88
	10	26.2	12.3	35.131	12.3	35.128	0.93	0.301	1.39	0.90
	11	11.0	12.2	35.096	12.2	35.093	0.92	0.253	2.04	0.95
	12	3.0	12.3	35.104	12.3	35.101	0.92	0.179	2.49	1.00
27	1	301.4	5.3	34.229	5.3	34.227	0.96	0.090	0.00	1.52
	2	251.4	6.0	34.284	6.0	34.282	0.96	0.091	0.00	1.50
	3	202.9	6.6	34.298	6.6	34.296	0.96	0.091	0.00	1.49
	4	150.9	8.6	34.513	8.7	34.506	0.96	0.093	0.00	1.52
	5	122.0	11.7	35.062	11.8	35.065	0.96	0.105	0.00	1.51
	6	92.3	13.1	35.377	13.1	35.378	0.96	0.116	0.00	1.51
	7	72.3	13.4	35.442	13.4	35.432	0.96	0.140	0.00	1.51
	8	52.2	13.0	35.292	13.0	35.295	0.94	0.237	0.43	1.51
	9	37.1	12.7	35.209	12.7	35.206	0.91	0.348	1.05	1.51
	10	22.2	12.9	35.245	12.8	35.217	0.91	0.359	1.71	1.48
	11	12.2	13.1	35.301	13.0	35.274	0.91	0.235	2.19	1.26
	12	3.7	13.1	35.305	13.1	35.304	0.91	0.179	2.67	1.48
28	1	251.0	4.2	34.155	4.2	34.153	0.96	0.094	0.00	1.34
	2	161.3	4.9	34.172	4.9	34.169	0.96	0.095	0.00	1.32
	3	121.3	5.5	34.192	5.5	34.192	0.96	0.096	0.00	1.32
	4	101.5	5.7	34.177	5.7	34.170	0.96	0.096	0.00	1.34
	5	80.9	7.5	34.177	7.6	34.172	0.95	0.146	0.00	1.32
	6	61.1	7.8	34.185	7.7	34.183	0.94	0.208	0.17	1.33
	7	51.4	7.8	34.189	7.8	34.187	0.94	0.238	0.25	1.04
	8	36.2	7.8	34.157	7.8	34.155	0.91	0.339	0.80	1.33
	9	36.3	7.8	34.165	7.8	34.162	0.91	0.330	0.78	1.30
	10	21.5	7.8	34.149	7.8	34.147	0.91	0.333	1.01	1.33
	11	11.3	7.8	34.145	7.8	34.143	0.91	0.291	1.27	1.33
	12	3.2	7.8	34.143	7.8	34.141	0.91	0.206	1.67	1.35
29	1	252.5	3.7	34.127	3.7	34.125	0.96	0.099	0.00	1.37
	2	161.9	4.1	34.128	4.1	34.126	0.96	0.103	0.00	0.58
	3	109.4	4.4	34.119	4.4	34.116	0.96	0.125	0.00	0.60
	4	90.5	4.9	34.119	4.9	34.117	0.96	0.132	0.00	1.04
	5	65.7	5.4	34.104	5.5	34.100	0.95	0.186	0.39	1.05
	6	55.9	5.8	34.111	5.8	34.107	0.95	0.183	0.61	1.09
	7	45.3	6.7	34.119	6.7	34.116	0.92	0.300	1.10	1.67
	8	35.7	7.0	34.123	7.0	34.117	0.93	0.291	1.44	1.74
	9	28.9	7.5	34.127	7.5	34.125	0.91	0.290	1.57	1.44
	10	21.0	7.7	34.132	7.7	34.129	0.91	0.260	1.77	1.20
	11	11.1	7.8	34.133	7.8	34.130	0.92	0.163	1.99	0.88
	12	3.1	7.8	34.133	7.8	34.131	0.92	0.146	2.28	0.75
30	1	251.7	4.9	34.125	4.9	34.123	0.96	0.086	0.00	0.77
	2	181.7	4.9	34.075	4.9	34.073	0.96	0.092	0.00	0.70
	3	151.5	4.9	34.052	4.9	34.050	0.96	0.101	0.00	0.73
	4	121.2	5.0	34.033	5.0	34.031	0.96	0.130	0.00	0.73
	5	101.0	5.0	34.028	5.0	34.025	0.96	0.138	0.00	0.73
	6	81.1	5.1	34.018	5.1	34.015	0.96	0.148	0.00	0.76
	7	61.3	5.3	33.973	5.3	33.971	0.95	0.205	0.32	0.77
	8	41.2	5.6	33.954	5.5	33.952	0.92	0.249	0.88	0.79
	9	30.9	5.6	33.949	5.6	33.947	0.92	0.240	1.24	0.85
	10	21.2	5.6	33.948	5.6	33.946	0.92	0.214	1.57	0.88
	11	11.2	5.6	33.948	5.6	33.946	0.92	0.183	1.94	0.84
	12	2.8	5.6	33.948	5.6	33.945	0.92	0.145	2.41	0.88
31	1	252.6	5.0	34.111	5.0	34.109	0.96	0.106	0.00	1.44
	2	181.7	5.0	34.039	5.0	34.036	0.96	0.123	0.00	1.48

Table C2. (cont.) A summary of the CTD Bottle Log for AMT-5.

Cast	*Bottle*	*Depth*	T_1	S_1	T_2	S_2	T_r	F	PAR	PAR_S
31	3	151.3	5.1	34.024	5.1	34.018	0.96	0.127	0.00	1.51
	4	120.8	5.2	33.985	5.2	33.982	0.96	0.147	0.00	1.48
	5	100.7	5.3	33.966	5.3	33.964	0.95	0.167	0.00	1.21
	6	80.2	5.4	33.950	5.4	33.949	0.95	0.207	0.05	0.83
	7	60.7	5.6	33.949	5.6	33.947	0.93	0.239	0.57	0.85
	8	41.5	5.7	33.949	5.7	33.947	0.92	0.255	1.35	1.26
	9	31.3	5.7	33.949	5.7	33.947	0.92	0.222	1.73	1.49
	10	21.2	5.7	33.949	5.7	33.946	0.92	0.159	2.08	1.50
	11	11.4	5.7	33.949	5.7	33.947	0.92	0.147	2.41	1.46
	12	3.4	5.7	33.949	5.7	33.947	0.92	0.132	2.72	1.45

Table D1. A summary of the XBT casts for AMT-5. All times are in GMT.

Cast	*Type*	*Date*	*Time*	*Longitude*	*Latitude*	*File Name*
1	T–7	18 September	0700	−12.450	48.105	amt5001.dat
2	T–7	18 September	1055	−13.203	47.983	amt5002.dat
3	T–7	18 September	1614	−14.730	47.697	amt5003.dat
4	T–7	19 September	0146	−18.477	47.172	amt5004.dat
5	T–7	19 September	0738	−18.950	46.467	amt5005.dat
6	T–7	19 September	1242	−19.653	45.513	amt5006.dat
7	T–7	19 September	2202	−20.000	43.502	amt5007.dat
8	T–7	19 September	2210	−20.000	43.473	amt5008.dat
9	T–7	20 September	0142	−19.960	42.843	amt5009.dat
10	T–7	20 September	1732	−20.000	41.960	amt5010.dat
11	T–7	20 September	2213	−20.000	41.070	amt5011.dat
12	T–7	21 September	0651	−19.917	39.150	amt5012.dat
13	T–5	21 September	1203	−20.000	38.717	amt5013.dat
14	T–5	21 September	1405	−20.000	38.387	amt5014.dat
15	T–5	21 September	1558	−20.000	38.050	amt5015.dat
16	T–5	21 September	1755	−19.983	37.703	amt5016.dat
17	T–5	21 September	1804	−19.972	37.660	amt5017.dat
18	T–5	21 September	1946	−19.900	37.350	amt5018.dat
19	T–5	21 September	2202	−19.850	37.050	amt5019.dat
20	T–5	22 September	0052	−19.750	36.517	amt5020.dat
21	T–5	22 September	1204	−19.492	35.412	amt5021.dat
22	T–7	25 September	2142	−18.533	31.217	amt5022.dat
23	T–7	26 September	0832	−20.523	29.422	amt5023.dat
24	T–7	26 September	1300	−20.983	28.867	amt5024.dat
25	T–7	26 September	1841	−20.987	27.747	amt5025.dat
26	T–7	26 September	2351	−20.983	26.713	amt5026.dat
27	T–7	27 September	0900	−20.983	24.575	amt5027.dat
28	T–7	27 September	1318	−21.000	23.868	amt5028.dat
29	T–7	27 September	1850	−20.998	22.852	amt5029.dat
30	T–7	28 September	0047	−20.938	21.705	amt5030.dat
31	T–5	28 September	0534	−20.747	20.743	amt5031.dat
32	T–5	28 September	0544	−20.747	20.693	amt5032.dat
33	T–5	28 September	0918	−20.588	20.017	amt5033.dat
34	T–5	28 September	1211	−20.532	19.733	amt5034.dat
35	T–5	28 September	1723	−20.390	18.888	amt5035.dat
36	T–5	28 September	2055	−20.243	18.200	amt5036.dat
37	T–5	29 September	0117	−20.067	17.450	amt5037.dat
38	T–5	29 September	0516	−19.650	16.650	amt5038.dat
39	T–5	29 September	0710	−20.000	16.267	amt5039.dat
40	T–7	29 September	1254	−20.000	15.230	amt5040.dat

Table D1. A summary of the XBT casts for AMT-5. All times are in GMT.

Cast	*Type*	*Date*	*Time*	*Longitude*	*Latitude*	*File Name*
41	T–7	29 September	1854	−19.993	14.000	amt5041.dat
42	T–7	29 September	2356	−20.002	12.980	amt5042.dat
43	T–7	30 September	0915	−20.738	11.230	amt5043.dat
44	T–5	30 September	1701	−21.167	10.205	amt5044.dat
45	T–5	30 September	1855	−21.335	9.887	amt5045.dat
46	T–5	30 September	2109	−21.500	9.503	amt5046.dat
47	T–5	30 September	2310	−21.630	9.152	amt5047.dat
48	T–5	1 October	0053	−21.728	8.843	amt5048.dat
49	T–5	1 October	0302	−21.863	8.447	amt5049.dat
50	T–5	1 October	0508	−22.015	8.082	amt5050.dat
51	T–5	1 October	0707	−22.171	7.696	amt5051.dat
52	T–5	1 October	0848	−22.279	7.407	amt5052.dat
53	T–5	1 October	1155	−22.468	7.027	amt5053.dat
54	T–5	1 October	1420	−22.618	6.587	amt5054.dat
55	T–5	1 October	1617	−22.747	6.257	amt5055.dat
56	T–5	1 October	1818	−22.892	5.907	amt5056.dat
57	T–5	1 October	2035	−23.067	5.491	amt5057.dat
58	T–5	2 October	0001	−23.336	4.855	amt5058.dat
59	T–5	2 October	0202	−23.491	4.478	amt5059.dat
60	T–5	2 October	0405	−23.645	4.097	amt5060.dat
61	T–5	2 October	0611	−23.798	3.707	amt5061.dat
62	T–5	2 October	0803	−23.943	3.358	amt5062.dat
63	T–5	2 October	1009	−24.108	2.952	amt5063.dat
64	T–5	2 October	1752	−24.450	2.070	amt5064.dat
65	T–5	2 October	1840	−24.505	1.940	amt5065.dat
66	T–5	2 October	2153	−24.772	1.383	amt5066.dat
67	T–5	2 October	2325	−24.850	1.185	amt5067.dat
68	T–5	3 October	0054	−24.950	0.927	amt5068.dat
69	T–5	3 October	0522	−25.267	0.133	amt5069.dat
70	T–5	3 October	0719	−25.417	−0.200	amt5070.dat
71	T–5	3 October	1303	−25.692	−0.827	amt5071.dat
72	T–5	3 October	1541	−25.873	−1.297	amt5072.dat
73	T–5	3 October	1958	−26.067	−1.803	amt5073.dat
74	T–5	4 October	0020	−26.441	−2.616	amt5074.dat
75	T–7	4 October	0921	−27.190	−4.363	amt5075.dat
76	T–7	4 October	1659	−27.615	−5.350	amt5076.dat
77	T–7	4 October	2127	−27.990	−6.248	amt5077.dat
78	T–7	5 October	0957	−28.997	−8.683	amt5078.dat
79	T–7	5 October	1750	−29.390	−9.633	amt5079.dat
80	T–7	5 October	2103	−29.657	−10.240	amt5080.dat
81	T–7	6 October	0130	−29.967	−11.067	amt5081.dat
82	T–7	6 October	1326	−30.700	−12.887	amt5082.dat
83	T–7	6 October	1712	−30.945	−13.467	amt5083.dat
84	T–7	6 October	2011	−31.180	−13.970	amt5084.dat
85	T–7	6 October	2322	−31.425	−14.477	amt5085.dat
86	T–7	7 October	0333	−31.767	−15.245	amt5086.dat
87	T–7	7 October	0919	−32.204	−16.293	amt5087.dat
88	T–7	7 October	1714	−32.599	−17.337	amt5088.dat
89	T–7	7 October	1955	−32.798	−17.820	amt5089.dat
90	T–7	8 October	0034	−33.175	−18.665	amt5090.dat
91	T–7	8 October	0950	−34.038	−20.383	amt5091.dat
93	T–7	8 October	2211	−35.307	−21.887	amt5093.dat
94	T–7	9 October	0903	−36.900	−23.508	amt5094.dat
95	T–7	9 October	1227	−37.287	−23.902	amt5095.dat
96	T–7	9 October	1907	−38.346	−24.995	amt5096.dat

Table D1. A summary of the XBT casts for AMT-5. All times are in GMT.

Cast	*Type*	*Date*	*Time*	*Longitude*	*Latitude*	*File Name*
97	T–7	10 October	0033	−39.117	−25.823	amt5097.dat
98	T–7	10 October	0756	−40.393	−27.065	amt5098.dat
99	T–7	10 October	1422	−41.332	−28.030	amt5099.dat
100	T–7	10 October	2015	−42.287	−29.072	amt5100.dat
101	T–7	11 October	0157	−43.197	−29.920	amt5101.dat
102	T–7	11 October	0914	−44.395	−31.170	amt5102.dat
103	T–7	11 October	1355	−44.903	−31.633	amt5103.dat
104	T–7	11 October	1931	−45.877	−32.638	amt5104.dat
105	T–7	12 October	0200	−46.983	−33.717	amt5105.dat
106	T–7	12 October	1143	−48.732	−35.355	amt5106.dat
107	T–7	12 October	1527	−49.065	−35.723	amt5107.dat
108	T–7	12 October	1904	−49.482	−36.113	amt5108.dat
109	T–7	12 October	2252	−50.090	−36.702	amt5109.dat
110	T–7	13 October	0140	−50.460	−37.060	amt5110.dat
111	T–7	13 October	0345	−50.813	−37.443	amt5111.dat
112	T–5	13 October	0810	−51.420	−38.227	amt5112.dat
113	T–5	13 October	1051	−51.780	−38.668	amt5113.dat
114	T–5	13 October	1726	−52.105	−39.198	amt5114.dat
115	T–5	13 October	1911	−52.258	−39.450	amt5115.dat
116	T–5	13 October	2059	−52.468	−39.733	amt5116.dat
117	T–5	13 October	2314	−52.718	−40.110	amt5117.dat
118	T–5	14 October	0131	−52.983	−40.412	amt5118.dat
119	T–5	14 October	0312	−53.200	−40.678	amt5119.dat
120	T–5	14 October	0506	−53.424	−40.981	amt5120.dat
121	T–5	14 October	0732	−53.753	−41.369	amt5121.dat
122	T–5	14 October	0910	−53.964	−41.651	amt5122.dat
122	T–5	14 October	1111	−54.243	−42.017	amt5123.dat
124	T–5	14 October	1349	−54.505	−42.247	amt5124.dat
125	T–5	14 October	1856	−54.968	−42.940	amt5125.dat
126	T–5	14 October	2000	−55.105	−43.162	amt5126.dat
127	T–5	15 October	0006	−55.700	−43.933	amt5127.dat
128	T–5	15 October	0219	−55.953	−44.262	amt5128.dat
129	T–5	15 October	0408	−56.218	−44.579	amt5129.dat
130	T–5	15 October	0607	−56.515	−44.925	amt5130.dat
131	T–5	15 October	0812	−56.618	−45.318	amt5131.dat
132	T–5	15 October	1008	−56.667	−45.689	amt5132.dat
133	T–7	15 October	1503	−56.702	−46.148	amt5133.dat
134	T–7	15 October	1748	−56.753	−46.540	amt5134.dat
135	T–7	15 October	2346	−56.897	−47.703	amt5135.dat
136	T–7	16 October	0147	−56.960	−48.095	amt5136.dat

Table E1. A summary of the SeaOPS Station Log for AMT-5. All times are in GMT.

Cast		*Depth*	*Position*		*Darks*		*Assignments*				*Down Cast*		*CCD*	*Up Cast*	
No.	*SDY*	[m]	*Longitude*	*Latitude*	E_s	E_d/L_u	P_1	P_2	P_1	P_2	*Begin*	*End*	*Pic.*	*Begin*	*End*
0	258	15	−0.7067	50.5850	0654	0754	I29	R21	E_d	L_u	0811	0813		0815	0816
1	259	30	−1.6692	50.4278	1312	1312	I29	R21	E_d	L_u	1422	1425	1427	1428	1432
2	261	75	−13.2058	47.9836	0944	0958	I29	R21	E_d	L_u	1011	1017	1020	1023	1029
3	262	75	−18.4775	47.1710	0918	0918	I29	R21	E_d	L_u	1014	1021	1022	1023	1031
4	263	75	−19.9598	42.8446	1002	1002	I29	R21	E_d	L_u	1010	1016	1019	1021	1028
5	264	100	−20.0114	38.7162	0910	0910	I29	R21	E_d	L_u	1011	1019	1021	1022	1033
6	265	100	−19.5233	35.4452	0937	0937	I29	R21	E_d	L_u	1007	1016	1019	1020	1030
7	268	125	−17.2331	32.3105	1241	1241	I29	R21	E_d	L_u	1318	1329	1330	1331	1342
8	268	105	−17.2187	32.3118			I29	R21	E_d	L_u	1359	1408		1408	1418

Table E1. (cont.) A summary of the SeaOPS Station Log for AMT-5. All times are in GMT.

Cast		*Depth*	*Position*		*Darks*		*Assignments*				*Down Cast*		*CCD*	*Up Cast*	
No.	*SDY*	[m]	*Longitude*	*Latitude*	E_s	E_d/L_u	P_1	P_2	P_1	P_2	*Begin*	*End*	*Pic.*	*Begin*	*End*
9	269	125	−20.9705	29.0486	1025	1025	I29	R21	E_d	L_u	1111	1122	1130	1124	1137
10	270	125	−20.9991	24.1377	1030	1030	I29	R21	E_d	L_u	1107	1116		1116	1125
11	270	75	−20.9996	24.1396			I29	R21	E_d	L_u	1128	1136	1128	1137	1147
12	271	100	−20.5287	19.7219	1046	1046	I29	R21	E_d	L_u	1107	1116	1130	1117	1137
13	271	75	−20.5309	19.7290			I29	R21	E_d	L_u	1137	1144		1145	1152
14	272	75	−20.0112	15.4926	1035	1035	I29	R21	E_d	L_u	1106	1117		1117	1124
15	273	100	−20.8696	10.9225			I29	R21	E_d	L_u	1109	1118	1130	1120	1129
16	274	75	−22.4690	7.0265	1044	1044	I29	R21	E_d	L_u	1111	1117	1120	1123	1130
17	274	75	−22.4689	7.0272			I29	R21	E_d	L_u	1132	1138		1138	1146
18	275	35	−24.1642	2.8167	1048	1048	I29	I01	E_d	E_d	1106	1109	1115	1109	1112
19	275	35	−24.1642	2.8150		1117	I29	I40	E_d	E_d	1124	1127		1127	1131
20	275	35	−24.1636	2.8133		1137	R01	R21	L_u	L_u	1143	1146		1146	1149
21	275	35	−24.1629	2.8118		1154	R35	R21	L_u	L_u	1159	1202		1203	1206
22	275	125	−24.4572	2.0769	1642	1642	I29	R21	E_d	L_u	1652	1702	1706	1711	1728
23	276	110	−25.6631	−0.7728	1026	1026	I29	R21	E_d	L_u	1044	1056	1100	1103	1119
24	276	125	−25.6639	−0.7717			I29	R21	E_u	L_u	1129	1145	1212	1153	1209
25	277	125	−27.3701	−4.7853	1115	1115	I29	R21	E_d	L_u	1143	1154		1154	1206
26	277	100	−27.3744	−4.7853			I29	R21	E_u	L_u	1213	1224	1210	1226	1236
27	277	125	−27.3800	−4.7855			I29	R21	E_d	L_u	1242	1253		1253	1305
28	278	145	−29.1152	−8.9674	1116	1116	I29	R21	E_d	L_u	1139	1153	1156	1153	1213
29	279	35	−30.7054	−12.8766	1101	1101	I29	I40	E_d	E_d	1135	1138		1144	1148
30	279	35	−30.7047	−12.8770		1154	I29	I01	E_d	E_d	1200	1203		1203	1206
31	279	35	−30.7036	−12.8787		1212	R01	R21	L_u	L_u	1217	1220		1221	1224
32	279	35	−30.7022	−12.8804		1228	R35	R21	L_u	L_u	1234	1237		1238	1242
33	279	90	−30.7001	−12.8832		1246	I29	R21	E_d	L_u	1253	1303	1308	1305	1316
34	280	160	−32.3624	−16.6852	1054	1054	I29	R21	E_d	L_u	1137	1150	1155	1151	1205
35	280	150	−32.5454	−17.1483	1502	1502	I29	R21	E_d	L_u	1523	1536	1539	1537	1550
36	281	150	−34.2248	−20.6616	1106	1106	I29	R21	E_d	L_u	1143	1156	1200	1157	1210
37	281	50	−34.2243	−20.6632		1215	I29	I40	E_d	E_d	1221	1225		1225	1229
38	281	50	−34.2244	−20.6653		1234	I29	I01	E_d	E_d	1239	1244		1244	1248
39	281	50	−34.2245	−20.6679		1256	R01	R21	L_u	L_u	1301	1305		1305	1310
40	281	50	−34.2249	−20.6704		1314	R35	R21	L_u	L_u	1320	1324		1324	1329
41	282	100	−37.2864	−23.9030	1150	1150	I29	R21	E_d	L_u	1144	1153	1155	1153	1202
42	283	160	−40.9804	−27.6914	1104	1104	I29	R21	E_d	L_u	1137	1150	1153	1151	1205
43	284	100	−44.8700	−31.6209	1014	1014	I40	R35	E_d	L_u	1213	1221	1234	1221	1230
44	285	50	−48.8622	−35.4899	1227	1227	I40	R35	E_d	L_u	1244	1248	1250	1248	1252
45	286	100	−51.9132	−38.8361	1154	1154	I40	R35	E_d	L_u	1217	1226	1241	1226	1235
46	287	50	−54.4622	−42.2390	1146	1146	I40	R35	E_d	L_u	1241	1245		1247	1252
47	287	50	−54.4706	−42.2404			I40	R35	E_d	L_u	1253	1257		1257	1302
48	287	55	−54.4767	−42.2418			I40	R35	E_d	L_u	1302	1307		1307	1312
49	287	60	−54.4839	−42.2433			I40	R35	E_d	L_u	1313	1318		1319	1324
50	287	50	−54.4936	−42.2445			I40	R35	E_d	L_u	1325	1329	1339	1330	1334
51	287	50	−54.8680	−42.8034	1636	1636	I40	R35	E_d	L_u	1704	1708		1708	1713
52	287	50	−54.8693	−42.8126		1718	I40	I01	E_d	E_d	1724	1728	1730	1729	1734
53	287	50	−54.8735	−42.8192		1738	R01	R35	L_u	L_u	1743	1746		1747	1750
54	288	75	−56.6875	−46.0506	1136	1136	I40	R35	E_d	L_u	1305	1312		1313	1320
55	288	75	−56.6877	−46.0473			I40	R35	E_d	L_u	1336	1342	1330	1342	1350
56	288	75	−56.6873	−46.0444			I40	R35	E_u	L_u	1357	1404		1405	1416
57	289	75	−57.6614	−49.7933	1224	1224	I01	R35	E_d	L_u	1240	1247		1256	1302
58	289	65	−57.6643	−49.7936			I01	R35	E_d	L_u	1308	1314		1314	1320
59	289	75	−57.6614	−49.7933	1552	1558	I01	R35	E_d	L_u	1609	1615	1619	1623	1630
60	289	75	−57.6614	−49.7933			I01	R35	E_d	L_u	1630	1643		1643	1655
61	289	75	−57.6614	−49.7933			I01	R35	E_d	L_u	1655	1702		1702	1710
62	290	35	−57.6948	−51.6609	1108	1108	I40	R35	E_d	L_u	1133	1136		1137	1140

Table E1. (cont.) A summary of the SeaOPS Station Log for AMT-5. All times are in GMT.

Cast		*Depth*	*Position*		*Darks*		*Assignments*				*Down Cast*		*CCD*	*Up Cast*	
No.	*SDY*	[m]	*Longitude*	*Latitude*	E_s	E_d/L_u	P_1	P_2	P_1	P_2	*Begin*	*End*	*Pic.*	*Begin*	*End*
63	290	35	−57.6986	−51.6624			I40	R35	E_d	L_u	1144	1147		1147	1151
64	290	35	−57.7008	−51.6640			I40	R35	E_d	L_u	1152	1154	1159	1158	1201

Table E2. A summary of the SeaFALLS Station Log for AMT-5. All times are in GMT.

Cast		*Depth*	*Position*		*Darks*			*Down Cast*		*CCD*
No.	*SDY*	[m]	*Longitude*	*Latitude*	E_a	E_w	E_d/L_u	*Begin*	*End*	*Pic.*
1	263	100	−19.9607	42.4323	1342	1342	1342	1435	1437	
2	263	100	−19.9608	42.4314				1440	1442	
3	263	105	−19.9608	42.4304				1445	1447	1450
4	264	125	−20.0129	38.7200	0906	0906	0906	1056	1059	
5	264	75	−20.0133	38.7210				1103	1105	
6	264	125	−20.0130	38.7219				1107	1110	
7	264	125	−20.0123	38.7228				1113	1116	
8	265	125	−19.5281	35.4442	0939	1025	1025	1054	1057	
9	265	125	−19.5287	35.4473				1115	1117	
10	265	125	−19.1433	35.0352	1424	1424	1424	1432	1435	
11	265	125	−19.1411	35.0361				1438	1441	
12	268	150	−17.2250	32.3103	1240	1240	1240	1351	1354	
13	268	125	−17.2217	32.3111				1358	1401	
14	268	150	−17.2179	32.3118				1408	1411	
15	269	150	−20.9702	29.0484	1032	1032	1240	1117	1120	
16	269	150	−20.9712	29.0490				1126	1129	1130
17	269	75	−20.9718	29.0497				1133	1135	
18	269	150	−20.9723	29.0500				1138	1141	
19	269	50	−20.9730	29.0506				1146	1147	
20	269	150	−20.9735	29.0511				1148	1151	
21	269	150	−20.9929	28.6346	1401	1401	1401	1411	1414	
22	269	150	−20.9943	28.6364				1421	1424	
23	269	150	−20.9954	28.6376				1429	1432	1434
24	270	150	−20.9990	24.1374	1029	1029	1029	1111	1114	
25	270	150	−20.9995	24.1382				1118	1121	1128
26	270	150	−20.9994	24.1392				1129	1132	
27	270	100	−20.9996	24.1398				1137	1139	
28	270	150	−20.9996	24.1404				1143	1146	
29	270	150	−21.0087	23.7256	1359	1359	1359	1411	1414	
30	270	100	−21.0085	23.7262				1420	1422	1424
31	270	150	−21.0083	23.7261				1426	1429	
32	271	100	−20.5285	19.7214	1049	1049	1049	1112	1114	
33	271	100	−20.5290	19.7224				1117	1119	
34	271	100	−20.5294	19.7238				1122	1124	1130
35	271	100	−20.5306	19.7273				1136	1138	
36	271	150	−20.5309	19.7290				1141	1144	
37	271	150	−20.5315	19.7313				1149	1152	
38	271	100	−20.4177	19.0492	1559	1559	1559	1613	1615	
39	271	100	−20.4166	19.0485				1621	1623	1628
40	272	150	−20.0106	15.4926	1039	1039	1039	1109	1111	
41	272	100	−20.0129	15.4925				1124	1126	1130
42	273	150	−20.8696	10.9222	1035	1035	1035	1114	1117	
43	273	150	−20.8701	10.9233				1123	1126	1130
44	273	150	−21.1762	10.2121	1607	1607	1607	1636	1639	
45	273	150	−21.1752	10.2121				1643	1646	1650

Table E2. (cont.) A summary of the SeaFALLS Station Log for AMT-5. All times are in GMT.

Cast		*Depth*	*Position*		*Darks*			*Down Cast*		*CCD*
No.	*SDY*	[m]	*Longitude*	*Latitude*	E_a	E_w	E_d/L_u	*Begin*	*End*	*Pic.*
46	274	150	−22.4698	7.0269	1043	1043	1043	1111	1114	1120
47	274	150	−22.4690	7.0269				1123	1126	
48	274	150	−22.4690	7.0271				1132	1135	
49	275		−24.1579	2.8406	1048					
50	275	150	−24.4600	2.0770	1638	1638	1638	1652	1655	1120
51	275	150	−24.4555	2.0758				1711	1714	
52	275	150	−24.4530	2.0746				1721	1724	
53	275	150	−24.4505	2.0727				1731	1734	
54	276	150	−25.6628	−0.7728	1026	1026	1026	1050	1054	1100
55	276	145	−25.6633	−0.7726				1103	1106	
56	276	135	−25.6637	−0.7716				1115	1118	
57	276	150	−25.6630	−0.7713				1129	1132	
58	276	120	−25.6650	−0.7699				1140	1143	
59	276	130	−25.6656	−0.7699				1222	1225	
60	276	150	−25.8940	−1.3585	1607	1607	1607	1617	1620	
61	276	150	−25.8928	−1.3580				1629	1632	
62	276	150	−25.8900	−1.3588				1638	1641	
63	277	150	−27.3695	−4.7856	1115	1115	1115	1148	1151	
64	277	150	−27.3709	−4.7853				1157	1200	
65	277	150	−27.3717	−4.7851				1204	1207	
66	277	150	−27.3728	−4.7852				1213	1216	1210
67	277	165	−27.3746	−4.7854				1223	1226	
68	277	150	−27.3766	−4.7856				1234	1237	
69	277	150	−27.3786	−4.7857				1243	1246	
70	277	150	−27.3800	−4.7855				1250	1253	
71	277	150	−27.3814	−4.7854				1257	1301	
72	277	150	−27.3826	−4.7855				1305	1308	
73	277	150	−27.5987	−5.3100	1541	1541	1541	1608	1611	
74	277	125	−27.5994	−5.3117				1617	1620	
75	277	150	−27.6002	−5.3126				1624	1627	
76	277	175	−27.6011	−5.3139				1632	1635	1637
77	278	175	−29.1139	−8.9644	1116	1116	1116	1242	1246	
78	278	175	−29.1133	−8.9635				1254	1258	
79	278	175	−29.1127	−8.9625				1304	1307	
80	278	150	−29.3825	−9.6149	1645	1645	1645	1720	1723	1725
81	278	150	−29.3832	−9.6158				1728	1731	
82	279	175	−30.7007	−12.8821	1133	1133	1133	1250	1253	
83	279	175	−30.6700	−12.8833				1301	1305	1308
84	279	100	−30.6991	−12.8841				1311	1313	
85	279	100	−30.6986	−12.8847				1316	1318	
86	280	190	−32.5459	−17.1484	1502	1502	1502	1524	1528	
87	280	200	−32.5454	−17.1483				1533	1537	1539
88	280	200	−32.5449	−17.1488				1543	1547	
89	280	200	−32.5446	−17.1497				1553	1557	
90	281	185	−34.2248	−20.6616	1106	1106	1106	1152	1156	1200
91	281	165	−34.2246	−20.6619				1202	1205	
92	281	185	−34.2246	−20.6624				1211	1214	
93	281	190	−34.2245	−20.6629				1220	1223	
94	281	205	−34.2246	−20.6637				1229	1233	
95	281	200	−34.2244	−20.6652				1239	1243	
96	281	185	−34.2241	−20.6664				1248	1252	
97	281	215	−34.2242	−20.6676				1257	1301	
98	281	235	−34.2248	−20.6686				1308	1312	
99	281	180	−34.2250	−20.6702				1319	1323	

Table E2. (cont.) A summary of the SeaFALLS Station Log for AMT-5. All times are in GMT.

Cast *No.*	*SDY*	*Depth* [m]	*Position* *Longitude*	*Latitude*	*Darks* E_a	E_w	E_d/L_u	*Down Cast* *Begin*	*End*	*CCD* *Pic.*
100	281	220	−34.2259	−20.6715				1330	1334	
101	281	150	−34.5561	−21.0816	1630	1630	1630	1648	1651	
102	281	150	−34.5558	−21.0818				1655	1658	
103	285	100	−48.8612	−35.4852	1215		1215	1302	1304	
104	285	85	−48.8610	−35.4833				1310	1311	
105	285	100	−48.8606	−35.4813				1316	1318	
106	285	80	−48.8606	−35.4800				1322	1323	
107	285	90	−48.8611	−35.4783				1327	1329	
108	285	90	−49.4513	−36.0912	1800		1800	1806	1808	
109	285	90	−49.4553	−36.0930				1818	1820	
110	285	90	−49.4584	−36.0941				1829	1831	
111	285	90	−49.4619	−36.0951				1843	1845	
112	286	75	−51.9172	−38.8352	1151		1151	1300	1301	
113	286	105	−51.9184	−38.8359				1305	1307	
114	286	90	−51.9192	−38.8365				1309	1311	
115	286	100	−51.9200	−38.8375				1315	1317	
116	286	90	−51.9202	−38.8384				1320	1322	
117	286	100	−51.9206	−38.8391				1325	1327	
118	286	100	−51.9213	−38.8401				1333	1335	
119	286	100	−51.9215	−38.8408				1338	1340	
120	286	100	−52.1224	−39.1983	1613		1613	1652	1654	
121	286	90	−52.1174	−39.1989				1659	1701	
122	286	100	−52.1077	−39.1994				1713	1715	
123	287	90	−54.4631	−42.2391	1140		1140	1244	1246	
124	287	95	−54.4698	−42.2403				1254	1256	
125	287	95	−54.4767	−42.2418				1305	1307	
126	287	100	−54.4840	−42.2433				1316	1318	
127	287	95	−54.4874	−42.2438				1320	1322	
128	287	90	−54.4919	−42.2443				1325	1327	
129	287	85	−54.4969	−42.2449				1331	1333	
130	287	105	−54.5004	−42.2454				1335	1337	1339
131	287	65	−54.8776	−42.8228	1638		1638	1757	1759	
132	287	95	−54.8783	−42.8228				1801	1803	
133	288	50	−54.8776	−42.8228	1152		1152	1220	1221	
134	288	75	−56.6969	−46.0452				1223	1224	
135	288	75	−56.6965	−46.0454				1226	1227	
136	288	100	−56.6953	−46.0455				1231	1233	
137	288	100	−56.6935	−46.0475				1240	1242	
138	288	50	−56.6923	−46.0476				1245	1246	
139	288	115	−56.6912	−46.0489				1250	1252	
140	288	115	−56.6898	−46.0498				1255	1257	
141	288	110	−56.6884	−46.0499				1302	1304	
142	288	125	−56.6877	−46.0504				1308	1311	
143	288	115	−56.6869	−46.0509				1314	1316	
144	288	100	−56.6866	−46.0510				1319	1320	
145	288	95	−56.7496	−46.5431	1700		1700	1729	1731	
146	289	90	−57.6624	−49.7934	1218		1218	1300	1302	
147	289	90	−57.6638	−49.7936				1309	1311	
148	289	75	−57.6646	−49.7936				1313	1315	
149	289	75	−57.6655	−49.7937				1317	1319	
150	289	125	−58.2307	−49.8001	1549		1549	1624	1627	
151	289	100	−58.2307	−49.8001				1631	1633	
152	289	100	−58.2313	−49.8007				1642	1644	

Table E3. A summary of the LoCNESS Station Log for AMT-5. All times are in GMT.

Cast		*Depth*	*Position*		*Darks*		*Down Cast*		*CCD*
No.	*SDY*	[m]	*Longitude*	*Latitude*	E_s	E_d/L_u	*Begin*	*End*	*Pic.*
0	284	75	−44.8707	−31.6208	1014	1230	1224	1225	
1	285	100	−48.8612	−35.4852	1227	1217	1302	1304	
2	285	100	−48.8610	−35.4833			1310	1311	
3	285	135	−48.8606	−35.4813			1316	1318	
4	285	100	−48.8606	−35.4800			1322	1323	
5	285	100	−48.8611	−35.4783			1327	1329	
6	285	100	−49.4513	−36.0912	1756	1756	1806	1808	
7	285	100	−49.4553	−36.0930			1818	1820	
8	285	100	−49.4584	−36.0941			1829	1831	
9	285	100	−49.4619	−36.0951			1843	1845	
10	286	75	−51.9172	−38.8352	1154	1243	1300	1301	
11	286	105	−51.9192	−38.8365			1309	1311	
12	286	100	−51.9202	−38.8384			1320	1322	
13	286	100	−51.9213	−38.8401			1333	1335	
14	286	100	−51.9215	−38.8408			1338	1340	
15	286	100	−52.1344	−39.1970	1615	1615	1635	1637	
16	286	100	−52.1224	−39.1983			1652	1654	
17	286	100	−52.1174	−39.1989			1659	1701	
18	286	105	−52.1077	−39.1994			1713	1715	
19	287	100	−54.4631	−42.2391	1146	1146	1244	1246	
20	287	100	−54.4698	−42.2403			1254	1256	
21	287	100	−54.4767	−42.2418			1305	1307	
22	287	100	−54.4840	−42.2433			1316	1318	
23	287	100	−54.4874	−42.2438			1320	1322	
24	287	100	−54.4919	−42.2443			1325	1327	
25	287	75	−54.4969	−42.2449			1331	1333	
26	287	100	−54.5004	−42.2454			1335	1337	1339
27	287	85	−54.8776	−42.8228	1636	1639	1757	1759	
28	287	100	−54.8783	−42.8228			1801	1803	1339
29	288	50	−56.6980	−46.0447	1136	1144	1220	1221	
30	288	75	−56.6969	−46.0452			1223	1224	
31	288	75	−56.6965	−46.0454			1226	1227	
32	288	100	−56.6953	−46.0455			1231	1233	
33	288	100	−56.6935	−46.0475			1240	1242	
34	288	50	−56.6923	−46.0476			1245	1246	
35	288	115	−56.6912	−46.0489			1250	1252	
36	288	115	−56.6898	−46.0498			1255	1257	
37	288	110	−56.6884	−46.0499			1302	1304	
38	288	125	−56.6877	−46.0504			1308	1311	
39	288	115	−56.6869	−46.0509			1314	1316	
40	288	100	−56.6866	−46.0510			1319	1320	
41	288	100	−56.7496	−46.5431	1701	1701	1729	1731	
42	289	100	−57.6624	−49.7934	1224	1219	1300	1302	
43	289	100	−57.6638	−49.7936			1309	1311	
44	289	95	−57.6646	−49.7936			1313	1315	
45	289	95	−57.6655	−49.7937			1317	1319	
46	289	140	−58.2307	−49.8001	1549	1549	1624	1627	
47	289	110	−58.2307	−49.8001			1631	1633	
48	289	115	−58.2313	−49.8007			1642	1644	
49	289	100	−58.2314	−49.8015			1647	1649	
50	289	100	−58.2311	−49.8044			1658	1700	
51	289	100	−58.2312	−49.8044			1705	1707	
52	289	100	−58.2314	−49.8046			1710	1711	

Table F1. A summary of the Sun Photometer Log for AMT-5. All times are in GMT, P is the atmospheric pressure (mb), θ is the sun zenith angle (°), and A is the air mass. The activity codes are: `P` for port measurements (`G` is Grimsby, `M` is Madeira, and `S` is Stanley), `S` for on station (the number is the station number), `T` for optics trials, and `U` for underway.

Code	*SDY*	*Time*	*Lon.*	*Lat.*	P	θ [°]	A	*Code*	*SDY*	*Time*	*Lon.*	*Lat.*	P	θ	A
PG	256	0853	0.730	53.570		61.7	2.10	U	269	0950	−20.765	29.215	1020.7	57.1	1.83
PG	256	0931	0.730	53.570		57.5	1.85	U	269	0951	−20.768	29.212	1020.7	56.8	1.82
PG	256	1222	0.730	53.570		49.8	1.55	U	269	1018	−20.849	29.145	1020.8	51.6	1.61
PG	256	1244	0.730	53.570		50.5	1.57	U	269	1019	−20.855	29.140	1020.8	51.4	1.60
U	257	0727	1.240	53.172	1020.5	72.8	3.35	U	269	1021	−20.858	29.137	1020.8	51.1	1.59
U	257	0738	1.285	53.142	1020.5	71.2	3.08	U	269	1044	−20.932	29.074	1021.1	46.7	1.46
U	257	0755	1.354	53.094	1020.6	68.8	2.75	U	269	1045	−20.935	29.072	1021.1	46.5	1.45
U	257	0813	1.426	53.045	1021.0	66.4	2.48	U	269	1046	−20.938	29.069	1021.1	46.3	1.45
U	257	0838	1.529	52.980	1021.4	63.0	2.20	S11	269	1100	−20.968	29.047	1021.1	43.8	1.38
U	257	1000	1.842	52.775	1022.2	54.0	1.70	S11	269	1102	−20.968	29.047	1021.1	43.5	1.38
S3	261	0956	−13.205	47.983	1010.9	58.7	1.92	S11	269	1103	−20.968	29.047	1021.1	43.3	1.37
S3	261	0958	−13.206	47.983	1011.0	58.4	1.90	S11	269	1105	−20.968	29.047	1021.1	43.0	1.37
S3	261	1016	−13.205	47.984	1011.0	56.1	1.79	S11	269	1201	−20.975	29.052	1021.0	34.8	1.22
U	261	1319	−13.675	47.875	1010.7	46.2	1.44	U	269	1206	−20.978	29.049	1021.0	34.1	1.21
U	261	1326	−13.699	47.869	1010.6	46.5	1.45	U	269	1208	−20.978	29.049	1021.0	33.9	1.20
U	263	1344	−19.963	42.496	1021.9	41.8	1.34	U	269	1209	−20.978	29.049	1021.0	33.8	1.20
U	263	1347	−19.964	42.487	1021.9	41.9	1.34	U	269	1301	−20.984	28.853	1020.5	30.0	1.15
U	263	1353	−19.966	42.466	1021.9	42.1	1.35	U	269	1302	−20.984	28.850	1020.5	30.0	1.15
U	264	0949	−20.015	38.739	1021.8	59.9	1.99	U	269	1303	−20.985	28.840	1020.5	30.0	1.15
S7	264	1003	−20.011	38.716	1021.9	57.5	1.86	U	269	1327	−20.989	28.749	1020.2	29.9	1.15
S7	264	1023	−20.011	38.717	1021.9	54.2	1.70	U	269	1328	−20.989	28.746	1020.2	30.0	1.15
S7	264	1024	−20.011	38.717	1021.9	54.0	1.70	U	269	1330	−20.989	28.738	1020.2	30.0	1.15
S7	264	1026	−20.011	38.717	1021.9	53.7	1.69	S12	269	1406	−20.993	28.634	1019.8	32.2	1.18
S7	264	1034	−20.013	38.717	1021.9	52.4	1.64	S12	269	1411	−20.993	28.634	1019.8	32.7	1.19
S7	264	1042	−20.013	38.717	1021.9	51.2	1.59	S12	269	1412	−20.993	28.634	1019.8	32.8	1.19
S7	264	1101	−20.013	38.721	1022.0	48.3	1.50	S12	269	1414	−20.993	28.634	1019.8	33.0	1.19
S7	264	1103	−20.013	38.721	1022.0	48.1	1.49	S12	269	1420	−20.993	28.634	1019.8	33.6	1.20
S7	264	1104	−20.013	38.721	1022.0	47.9	1.49	S12	269	1421	−20.993	28.634	1019.8	33.8	1.20
U	265	1605	−18.962	34.819	1017.8	53.7	1.68	S12	269	1444	−20.994	28.631	1019.6	36.7	1.25
U	265	1607	−18.960	34.816	1017.8	54.1	1.70	S12	269	1445	−20.994	28.628	1019.6	36.8	1.25
U	265	1608	−18.955	34.819	1017.8	54.3	1.71	S12	269	1446	−20.994	28.624	1019.6	37.0	1.25
U	265	1613	−18.944	34.795	1017.8	55.2	1.75	U	269	1521	−21.001	28.492	1019.3	42.1	1.35
U	265	1615	−18.939	34.788	1017.7	55.5	1.76	U	269	1522	−21.001	28.488	1019.3	42.3	1.35
U	265	1616	−18.937	34.785	1017.7	55.8	1.77	U	269	1603	−21.003	28.327	1019.2	49.8	1.54
PM	267	1156	−17.065	32.250	1018.7	35.8	1.23	U	269	1637	−21.000	28.202	1019.1	56.4	1.80
PM	267	1157	−17.065	32.250	1018.7	35.7	1.23	U	269	1638	−21.000	28.198	1019.1	56.6	1.81
PM	267	1158	−17.065	32.250	1018.7	35.6	1.23	U	269	1639	−21.000	28.190	1019.1	56.9	1.82
PM	267	1200	−17.065	32.250	1018.7	35.5	1.19	U	269	1641	−21.000	28.183	1019.1	57.2	1.84
PM	267	1201	−17.065	32.250	1018.7	35.3	1.22	U	269	1710	−20.995	28.071	1019.1	63.6	2.23
PM	267	1609	−17.006	32.519	1017.3	55.3	1.75	U	269	1719	−20.995	28.038	1019.0	65.5	2.39
PM	267	1611	−17.006	32.519	1017.3	55.6	1.77	U	269	1730	−20.994	27.998	1019.0	67.8	2.63
PM	267	1613	−17.006	32.519	1017.3	55.9	1.78	U	269	1740	−20.993	27.963	1019.1	69.9	2.89
U	268	1208	−17.090	32.444	1019.8	35.2	1.22	U	269	1750	−20.992	27.927	1019.0	72.2	3.23
U	268	1210	−17.097	32.439	1019.8	35.1	1.22	U	269	1758	−20.991	27.898	1019.0	73.9	3.56
U	268	1211	−17.100	32.437	1019.8	35.0	1.22	U	270	0920	−20.992	24.489	1018.1	62.1	2.13
U	268	1314	−17.239	32.312	1019.8	33.1	1.19	U	270	0921	−20.992	24.485	1018.1	61.9	2.11
U	268	1315	−17.238	32.312	1019.8	33.1	1.19	U	270	0922	−20.993	24.481	1018.1	61.7	2.10
U	268	1316	−17.236	32.311	1019.8	33.1	1.19	U	270	0933	−20.993	24.435	1018.1	59.2	1.95
U	268	1630	−17.558	32.019	1019.3	59.1	1.94	U	270	0959	−20.995	24.341	1018.2	53.7	1.68
U	269	0920	−20.674	29.292	1020.5	63.2	2.21	U	270	1016	−20.995	24.274	1018.2	50.0	1.55
U	269	0921	−20.677	29.290	1020.5	63.0	2.19	U	270	1018	−20.995	24.270	1018.2	49.6	1.54
U	269	0922	−20.679	29.287	1020.5	62.8	2.18	U	270	1041	−20.996	24.183	1018.2	45.0	1.41
U	269	0949	−20.759	29.220	1020.7	57.3	1.85	U	270	1059	−20.998	24.135	1018.1	41.4	1.33

Table F1. (cont.) A summary of the Sun Photometer Log for AMT-5. All times are in GMT.

Code	*SDY*	*Time*	*Lon.*	*Lat.*	*P*	*θ*	*A*	*Code*	*SDY*	*Time*	*Lon.*	*Lat.*	*P*	*θ*	*A*
S13	270	1100	−20.998	24.135	1018.1	41.2	1.33	T	272	1059	−20.010	15.493	1015.0	36.9	1.25
S13	270	1102	−20.998	24.135	1018.1	40.9	1.32	T	272	1101	−20.010	15.493	1015.0	36.6	1.24
S13	270	1129	−20.999	24.139	1018.1	35.9	1.23	T	272	1104	−20.010	15.492	1015.0	35.9	1.23
S13	270	1149	−21.000	24.141	1018.1	33.0	1.19	U	272	1222	−20.014	15.346	1014.3	21.3	1.07
S13	270	1150	−21.000	24.141	1018.1	32.8	1.19	U	272	1224	−20.014	15.335	1014.2	21.0	1.07
S13	270	1152	−21.000	24.141	1018.1	32.5	1.19	U	272	1225	−20.014	15.325	1014.1	20.8	1.07
U	270	1221	−21.002	24.057	1017.8	28.6	1.14	S21	275	1721	−24.453	2.075	1010.5	58.9	1.93
U	270	1223	−21.002	24.054	1017.8	28.4	1.14	S21	275	1722	−24.453	2.075	1010.5	59.2	1.94
U	270	1225	−21.002	24.047	1017.8	28.2	1.13	S21	275	1723	−24.453	2.075	1010.5	59.4	1.96
U	270	1314	−21.007	23.873	1017.1	25.3	1.10	S21	275	1727	−24.452	2.074	1010.5	60.3	2.01
U	270	1315	−21.008	23.869	1017.1	25.3	1.10	S21	275	1728	−24.452	2.074	1010.5	60.6	2.03
U	270	1317	−21.008	23.862	1017.1	25.3	1.10	S21	275	1729	−24.451	2.073	1010.5	60.9	2.05
U	270	1338	−21.011	23.784	1016.8	25.8	1.11	S21	275	1732	−24.450	2.073	1010.5	61.7	2.10
U	270	1340	−21.011	23.780	1016.8	25.9	1.11	S21	275	1734	−24.451	2.072	1010.4	62.2	2.13
U	270	1341	−21.012	23.773	1016.8	26.0	1.11	S21	275	1741	−24.448	2.071	1010.4	63.8	2.25
S14	270	1413	−21.009	23.726	1016.4	28.8	1.14	S21	275	1748	−24.446	2.068	1010.4	65.6	2.41
S14	270	1426	−21.008	23.726	1016.3	30.5	1.16	U	276	0912	−25.575	−0.553	1011.2	64.6	2.32
S14	270	1431	−21.008	23.726	1016.3	31.2	1.17	U	276	0914	−25.576	−0.557	1011.4	64.1	2.28
U	270	1520	−21.006	23.583	1015.9	39.3	1.29	U	276	0915	−25.578	−0.563	1011.4	63.8	2.26
U	270	1521	−21.006	23.580	1015.9	39.5	1.29	U	276	0926	−25.592	−0.597	1011.4	61.1	2.06
U	270	1522	−21.006	23.576	1015.9	39.8	1.30	U	276	0937	−25.604	−0.628	1011.5	58.4	1.90
U	270	1548	−21.007	23.484	1015.7	44.7	1.40	U	276	1003	−25.636	−0.709	1011.8	52.0	1.62
U	270	1549	−21.007	23.477	1015.7	45.0	1.41	U	276	1004	−25.639	−0.715	1011.8	51.6	1.61
U	270	1551	−21.007	23.473	1015.7	45.3	1.42	U	276	1006	−25.640	−0.718	1011.8	51.2	1.59
U	270	1631	−21.005	23.332	1015.3	53.6	1.68	S22	276	1029	−25.664	−0.773	1012.0	45.4	1.42
U	270	1632	−21.005	23.328	1015.3	53.9	1.69	S22	276	1031	−25.665	−0.773	1012.0	45.0	1.41
U	270	1634	−21.004	23.322	1015.3	54.3	1.71	S22	276	1046	−25.663	−0.774	1012.4	41.2	1.33
U	270	1652	−21.005	23.259	1015.2	58.3	1.89	S22	276	1054	−25.662	−0.773	1012.4	39.2	1.29
U	270	1653	−21.005	23.255	1015.2	58.5	1.91	S22	276	1107	−25.663	−0.773	1012.6	36.0	1.23
U	270	1726	−21.003	23.138	1015.2	65.8	2.42	S22	276	1147	−25.666	−0.769	1012.8	26.0	1.11
U	271	0959	−20.563	19.890	1016.0	52.0	1.62	S22	276	1149	−25.666	−0.769	1012.8	25.6	1.11
U	271	1001	−20.562	19.886	1016.0	51.6	1.61	S22	276	1159	−25.664	−0.771	1012.8	23.1	1.09
U	271	1003	−20.561	19.880	1016.0	51.2	1.59	S22	276	1202	−25.664	−0.771	1012.8	22.4	1.08
U	271	1033	−20.541	19.779	1016.0	44.5	1.40	S22	276	1205	−25.664	−0.771	1012.8	21.6	1.07
U	271	1035	−20.541	19.775	1016.0	44.1	1.39	U	276	1224	−25.665	−0.770	1012.8	16.8	1.04
U	271	1037	−20.539	19.769	1016.0	43.7	1.38	U	276	1226	−25.665	−0.770	1012.8	16.3	1.04
S15	271	1112	−20.528	19.721	1016.2	36.4	1.24	U	276	1228	−25.666	−0.769	1012.8	16.0	1.04
S15	271	1117	−20.529	19.722	1016.2	35.5	1.23	S23	276	1618	−25.894	−1.359	1010.7	41.8	1.34
S15	271	1120	−20.529	19.723	1016.2	34.9	1.22	S23	276	1632	−25.893	−1.358	1010.7	45.2	1.42
S15	271	1135	−20.530	19.727	1016.0	32.1	1.18	S23	276	1639	−25.891	−1.359	1010.7	47.0	1.46
S15	271	1136	−20.530	19.727	1016.0	31.8	1.18	S23	276	1651	−25.887	−1.360	1010.7	50.0	1.55
S15	271	1138	−20.531	19.728	1016.0	31.5	1.17	U	276	1710	−25.908	−1.406	1010.5	54.7	1.72
S15	271	1147	−20.531	19.730	1015.9	30.0	1.15	U	276	1711	−25.909	−1.409	1010.5	55.0	1.74
S15	271	1158	−20.532	19.734	1015.9	28.1	1.13	U	276	1713	−25.911	−1.415	1010.4	55.4	1.75
U	271	1208	−20.531	19.736	1015.9	26.6	1.12	U	277	0932	−27.209	−4.408	1015.0	61.1	2.06
U	271	1221	−20.518	19.719	1015.9	24.9	1.10	U	277	0933	−27.212	−4.414	1015.0	60.8	2.05
U	271	1244	−20.509	19.655	1015.9	22.5	1.08	U	277	0934	−27.213	−4.418	1015.0	60.6	2.03
U	271	1259	−20.501	19.612	1015.9	21.6	1.08	U	277	0954	−27.240	−4.485	1015.3	55.6	1.76
U	271	1317	−20.493	19.560	1015.9	21.4	1.07	U	277	0956	−27.242	−4.488	1015.3	55.2	1.75
U	271	1353	−20.475	19.448	1015.9	23.6	1.09	U	277	0957	−27.243	−4.491	1015.3	54.9	1.74
U	271	1424	−20.460	19.352	1015.9	27.6	1.13	U	277	1056	−27.323	−4.691	1015.5	40.2	1.31
U	272	1043	−20.012	15.527	1015.0	40.5	1.31	U	277	1107	−27.336	−4.724	1015.6	37.5	1.26
U	272	1044	−20.012	15.524	1015.0	40.3	1.31	U	277	1108	−27.339	−4.731	1015.6	37.2	1.25
U	272	1046	−20.012	15.520	1014.9	39.9	1.30	U	277	1110	−27.340	−4.734	1015.6	36.8	1.25

Table F1. (cont.) A summary of the Sun Photometer Log for AMT-5. All times are in GMT.

Code	*SDY*	*Time*	*Lon.*	*Lat.*	*P*	*θ*	*A*	*Code*	*SDY*	*Time*	*Lon.*	*Lat.*	*P*	*θ*	*A*
S24	277	1130	−27.365	−4.784	1015.5	31.8	1.18	S28	279	1253 PM	−30.701	−12.882	1016.8	16.1	1.04
S24	277	1131	−27.366	−4.784	1015.5	31.5	1.17	S28	279	1306	−30.700	−12.883	1016.6	13.4	1.03
S24	277	1133	−27.367	−4.784	1015.5	31.0	1.17	S28	279	1308	−30.700	−12.884	1016.6	13.0	1.03
S24	277	1159	−27.371	−4.785	1015.5	24.6	1.10	S28	279	1315	−30.699	−12.884	1016.7	11.6	1.02
S24	277	1200	−27.371	−4.785	1015.5	24.3	1.10	U	279	1433	−30.758	−13.058	1015.6	13.4	1.03
S24	277	1201	−27.371	−4.785	1015.5	24.0	1.09	U	279	1434	−30.761	−13.064	1015.6	13.7	1.03
S24	277	1217	−27.373	−4.785	1015.4	20.1	1.06	U	279	1512	−30.811	−13.168	1015.1	21.9	1.08
S24	277	1218	−27.373	−4.785	1015.5	19.8	1.06	U	279	1514	−30.814	−13.173	1015.2	22.3	1.08
S24	277	1225	−27.375	−4.785	1015.5	18.1	1.05	U	279	1516	−30.816	−13.179	1015.1	22.7	1.08
S24	277	1252	−27.380	−4.785	1014.8	11.3	1.02	U	280	1244	−32.371	−16.729	1017.6	21.2	1.07
S24	277	1254	−27.380	−4.785	1014.8	10.9	1.02	U	280	1245	−32.374	−16.734	1017.6	20.9	1.07
S24	277	1255	−27.381	−4.785	1014.8	10.6	1.02	U	280	1252	−32.382	−16.752	1017.5	19.5	1.06
S24	277	1315	−27.384	−4.786	1014.6	5.7	1.00	U	280	1322	−32.421	−16.841	1017.7	14.3	1.03
S24	277	1317	−27.385	−4.786	1014.6	5.1	1.00	U	280	1324	−32.424	−16.847	1017.7	14.1	1.03
S24	277	1319	−27.385	−4.786	1014.6	4.7	1.00	U	280	1421	−32.495	−17.018	1017.4	13.1	1.03
U	277	1431	−27.480	−5.011	1013.6	13.4	1.03	U	280	1423	−32.497	−17.024	1017.5	13.3	1.03
U	277	1433	−27.482	−5.014	1013.6	13.8	1.03	U	280	1425	−32.500	−17.031	1017.5	13.5	1.03
U	277	1434	−27.485	−5.021	1013.6	14.1	1.03	S30	280	1506	−32.546	−17.144	1016.9	20.7	1.07
U	277	1506	−27.529	−5.131	1013.4	22.0	1.08	S30	280	1525	−32.546	−17.148	1016.8	24.6	1.10
U	277	1507	−27.530	−5.134	1013.4	22.3	1.08	S30	280	1527	−32.546	−17.148	1016.8	25.0	1.10
U	277	1511	−27.534	−5.144	1013.4	23.2	1.09	S30	280	1529	−32.546	−17.148	1016.7	25.4	1.11
U	277	1546	−27.581	−5.265	1012.9	31.9	1.18	S30	280	1536	−32.545	−17.148	1016.7	26.9	1.12
U	277	1554	−27.591	−5.289	1012.8	33.8	1.20	S30	280	1548	−32.545	−17.149	1016.6	29.6	1.15
S25	277	1632	−27.601	−5.314	1012.6	43.4	1.37	S30	280	1555	−32.544	−17.150	1016.5	31.3	1.17
S25	277	1634	−27.601	−5.314	1012.6	43.9	1.38	U	280	1634	−32.560	−17.226	1016.1	40.1	1.31
U	277	1652	−27.610	−5.337	1012.5	48.3	1.50	U	280	1649	−32.577	−17.276	1015.9	43.7	1.38
U	277	1654	−27.613	−5.343	1012.5	48.9	1.52	U	280	1722	−32.613	−17.371	1015.7	51.4	1.60
U	277	1727	−27.656	−5.446	1012.3	57.0	1.83	U	280	1739	−32.634	−17.422	1015.6	55.5	1.76
U	277	1728	−27.660	−5.456	1012.3	57.3	1.84	U	280	1741	−32.636	−17.428	1015.6	56.0	1.78
U	277	1750	−27.692	−5.530	1012.2	62.8	2.17	U	280	1751	−32.649	−17.458	1015.7	58.3	1.90
U	278	0932	−28.970	−8.606	1014.6	62.3	2.14	U	280	1753	−32.651	−17.464	1015.7	58.8	1.92
U	278	0934	−28.972	−8.613	1014.7	61.9	2.11	U	280	1803	−32.664	−17.494	1015.8	61.1	2.06
U	278	0935	−28.975	−8.618	1014.7	61.6	2.09	U	280	1809	−32.671	−17.512	1015.9	62.6	2.16
U	278	0946	−28.989	−8.650	1014.9	58.9	1.93	U	280	1818	−32.682	−17.534	1016.0	64.8	2.33
U	278	0959	−29.008	−8.694	1015.2	56.0	1.78	U	281	1054	−34.169	−20.580	1020.2	48.3	1.50
U	278	1109	−29.095	−8.913	1015.6	38.9	1.28	U	281	1111	−34.201	−20.628	1020.3	44.5	1.40
U	278	1112	−29.099	−8.922	1015.6	38.1	1.27	U	281	1115	−34.211	−20.643	1020.3	43.5	1.38
U	278	1117	−29.105	−8.938	1015.6	36.9	1.25	U	281	1117	−34.215	−20.649	1020.4	43.1	1.37
U	278	1118	−29.107	−8.945	1015.6	36.6	1.24	U	281	1119	−34.218	−20.655	1020.4	42.6	1.36
S26	278	1133	−29.115	−8.966	1015.8	32.9	1.19	S31	281	1130	−34.224	−20.663	1020.7	40.2	1.31
S26	278	1135	−29.116	−8.966	1015.7	32.4	1.18	S31	281	1132	−34.224	−20.663	1020.7	39.8	1.30
S26	278	1137	−29.116	−8.966	1015.7	32.0	1.18	S31	281	1133	−34.225	−20.663	1020.7	39.5	1.29
S26	278	1156	−29.116	−8.967	1015.5	27.4	1.13	S31	281	1143	−34.225	−20.662	1020.8	37.2	1.25
S26	278	1158	−29.116	−8.967	1015.5	26.7	1.12	S31	281	1153	−34.225	−20.661	1020.7	35.1	1.22
S26	278	1216	−29.114	−8.970	1015.4	22.4	1.08	S31	281	1204	−34.225	−20.662	1020.8	32.8	1.19
S26	278	1243	−29.114	−8.965	1015.1	15.9	1.04	S31	281	1213	−34.225	−20.662	1020.8	30.8	1.16
S26	278	1306	−29.113	−8.963	1015.0	10.5	1.02	S31	281	1224	−34.224	−20.663	1020.7	28.5	1.14
S26	278	1307	−29.113	−8.962	1014.9	10.3	1.02	S31	281	1235	−34.225	−20.664	1020.6	26.2	1.11
U	278	1557	−29.289	−9.421	1013.8	33.1	1.19	S31	281	1245	−34.224	−20.666	1020.6	24.3	1.10
U	278	1558	−29.292	−9.427	1013.7	33.4	1.20	S31	281	1256	−34.224	−20.667	1020.5	22.3	1.08
U	278	1600	−29.293	−9.430	1013.8	33.8	1.38	S31	281	1307	−34.225	−20.668	1020.5	20.3	1.07
S28	279	1246	−30.701	−12.881	1016.9	17.6	1.05	S31	281	1318	−34.225	−20.670	1020.4	18.6	1.05
S28	279	1251	−30.701	−12.882	1016.8	16.5	1.04	S31	281	1331	−34.225	−20.671	1020.3	17	1.04

Table F1. (cont.) A summary of the Sun Photometer Log for AMT-5. All times are in GMT.

Code	*SDY*	*Time*	*Lon.*	*Lat.*	*P*	θ	*A*	*Code*	*SDY*	*Time*	*Lon.*	*Lat.*	*P*	θ	*A*
S31	281	1341	−34.227	−20.672	1020.3	16.0	1.04	S41	287	1723	−54.869	−42.811	1015.0	43.5	1.38
U	281	1349	−34.228	−20.673	1020.2	15.4	1.04	S41	287	1728	−54.869	−42.813	1014.9	44.2	1.39
U	281	1624	−34.536	−21.058	1019.4	37.0	1.25	S41	287	1729	−54.870	−42.813	1014.9	44.3	1.40
U	281	1629	−34.549	−21.072	1019.4	38.2	1.27	S41	287	1730	−54.870	−42.814	1014.8	44.5	1.40
U	281	1631	−34.550	−21.074	1019.3	38.6	1.28	S41	287	1734	−54.871	−42.815	1014.6	45.0	1.41
U	281	1632	−34.552	−21.076	1019.3	38.8	1.28	S41	287	1736	−54.871	−42.816	1014.5	45.3	1.42
U	282	0934	−36.983	−23.594	1023.3	69.1	2.79	S41	287	1737	−54.872	−42.816	1014.5	45.5	1.42
U	282	1024	−37.109	−23.725	1023.9	58.2	1.89	U	288	1121	−56.690	−45.936	1013.4	65.0	2.36
U	282	1026	−37.114	−23.730	1024.0	57.7	1.87	U	288	1125	−56.692	−45.945	1013.4	64.4	2.30
U	282	1028	−37.119	−23.735	1024.0	57.3	1.85	U	288	1126	−56.692	−45.948	1013.4	64.2	2.29
U	282	1033	−37.129	−23.746	1024.0	56.2	1.79	U	288	1132	−56.693	−45.965	1013.4	63.2	2.21
U	283	1329	−41.184	−27.884	1018.2	26.0	1.11	S42	288	1209	−56.700	−46.044	1014.0	57.3	1.84
U	283	1331	−41.190	−27.890	1018.1	25.8	1.11	S42	288	1214	−56.699	−46.044	1014.0	56.5	1.81
U	283	1332	−41.193	−27.893	1018.0	25.6	1.11	S42	288	1222	−56.697	−46.045	1014.0	55.2	1.75
U	283	1338	−41.212	−27.910	1017.9	24.9	1.10	S42	288	1241	−56.693	−46.048	1014.0	52.4	1.64
U	283	1343	−41.230	−27.927	1017.9	24.3	1.10	S42	288	1243	−56.693	−46.048	1014.0	52.1	1.63
U	286	0952	−51.659	−38.510	1021.5	77.4	4.48	S42	288	1245	−56.692	−46.048	1014.0	51.8	1.61
U	286	0953	−51.661	−38.513	1021.5	77.2	4.42	S42	288	1253	−56.690	−46.049	1014.0	50.7	1.58
U	286	1011	−51.702	−38.564	1021.7	73.7	3.51	S42	288	1332	−56.689	−46.049	1014.2	45.6	1.43
U	286	1013	−51.702	−38.564	1021.7	73.3	3.44	S42	288	1333	−56.689	−46.048	1014.1	45.4	1.42
U	286	1018	−51.720	−38.587	1021.8	72.3	3.26	S42	288	1335	−56.689	−46.048	1014.1	45.2	1.42
U	286	1020	−51.723	−38.590	1021.8	72.0	3.20	S42	288	1351	−56.687	−46.046	1014.1	43.4	1.37
U	286	1021	−51.727	−38.595	1021.9	71.7	3.16	S42	288	1405	−56.687	−46.044	1014.2	42.0	1.34
U	286	1041	−51.766	−38.646	1022.3	67.9	2.64	S42	288	1411	−56.686	−46.045	1014.2	41.5	1.33
U	286	1042	−51.768	−38.649	1022.3	67.7	2.62	S42	288	1413	−56.686	−46.044	1014.2	41.3	1.33
U	286	1051	−51.787	−38.674	1022.5	66.0	2.45	S42	288	1414	−56.686	−46.043	1014.2	41.2	1.33
U	286	1053	−51.788	−38.676	1022.5	65.6	2.41	U	288	1425	−56.692	−46.044	1014.0	40.3	1.31
U	286	1054	−51.791	−38.679	1022.5	65.4	2.39	U	288	1514	−56.705	−46.196	1014.6	38.0	1.27
U	286	1104	−51.809	−38.703	1022.5	63.5	2.23	U	288	1525	−56.707	−46.228	1014.6	37.9	1.27
U	286	1106	−51.811	−38.706	1022.5	63.1	2.20	U	288	1600	−56.722	−46.343	1014.8	38.5	1.28
U	286	1126	−51.851	−38.760	1022.6	59.4	1.96	U	288	1601	−56.723	−46.350	1014.9	38.5	1.28
U	286	1128	−51.857	−38.769	1022.6	59.0	1.94	U	288	1603	−56.723	−46.353	1014.8	38.6	1.28
U	286	1147	−51.896	−38.823	1022.6	55.5	1.76	U	288	1647	−56.745	−46.500	1015.3	41.5	1.33
U	286	1149	−51.901	−38.828	1022.6	55.2	1.75	U	288	1654	−56.749	−46.520	1015.2	42.1	1.34
S38	286	1200	−51.910	−38.838	1023.1	53.2	1.45	U	288	1656	−56.751	−46.529	1015.3	42.3	1.35
S38	286	1202	−51.910	−38.838	1023.1	52.9	1.65	U	288	1658	−56.751	−46.531	1015.4	42.4	1.35
S38	286	1203	−51.911	−38.838	1023.2	52.6	1.64	U	288	1659	−56.752	−46.534	1015.3	42.5	1.36
S38	286	1212	−51.913	−38.836	1023.4	51.1	1.59	S43	288	1709	−56.753	−46.541	1015.5	43.5	1.38
S38	286	1214	−51.913	−38.836	1023.6	50.7	1.58	S43	288	1712	−56.753	−46.541	1015.5	43.8	1.38
S38	286	1225	−51.913	−38.836	1023.4	48.9	1.52	U	288	1840	−56.787	−46.726	1015.7	55.5	1.76
S38	286	1226	−51.913	−38.836	1023.4	48.6	1.51	U	288	1844	−56.790	−46.742	1015.7	56.1	1.79
S38	286	1228	−51.913	−38.836	1023.3	48.3	1.50	U	288	1856	−56.797	−46.782	1015.7	58.0	1.88
S38	286	1258	−51.917	−38.835	1023.5	43.4	1.37	U	288	1858	−56.798	−46.785	1015.7	58.2	1.89
S38	286	1300	−51.917	−38.835	1023.5	43.1	1.37	U	288	1908	−56.802	−46.818	1015.7	59.8	1.98
S38	286	1302	−51.918	−38.835	1023.6	42.8	1.36	U	288	1910	−56.803	−46.824	1015.7	60.1	2.00
S38	286	1319	−51.920	−38.838	1023.4	40.3	1.31	U	288	1919	−56.808	−46.855	1015.8	61.6	2.09
S38	286	1321	−51.920	−38.838	1023.4	40.0	1.30	U	288	1931	−56.812	−46.894	1015.7	63.5	2.23
S38	286	1322	−51.920	−38.839	1023.3	39.8	1.30	U	288	1941	−56.816	−46.927	1015.8	65.2	2.37
U	286	1345	−51.921	−38.842	1023.2	36.9	1.25	U	288	1955	−56.822	−46.974	1015.8	67.5	2.60
U	286	1347	−51.921	−38.843	1023.1	36.7	1.25	U	288	2008	−56.828	−47.016	1015.9	69.7	2.86
U	286	1348	−51.920	−38.845	1023.1	36.5	1.24	U	288	2020	−56.832	−47.056	1016.0	71.8	3.16
U	286	1438	−51.997	−38.969	1022.9	32.3	1.18	U	288	2032	−56.836	−47.095	1016.1	73.7	3.52
U	286	1440	−52.001	−38.974	1022.9	32.3	1.18	U	289	1404	−57.773	−49.794	1017.2	45.2	1.42
U	286	1535	−52.107	−39.120	1022.3	31.9	1.18	U	289	1406	−57.782	−49.794	1017.2	45.1	1.41
U	286	1537	−52.111	−39.126	1022.3	31.9	1.18	U	289	1407	−57.791	−49.794	1017.2	45.0	1.41

Table F1. (cont.) A summary of the Sun Photometer Log for AMT-5. All times are in GMT.

Code	*SDY*	*Time*	*Lon.*	*Lat.*	*P*	*θ*	*A*	*Code*	*SDY*	*Time*	*Lon.*	*Lat.*	*P*	*θ*	*A*
U	289	1524	−58.131	−49.795	1017.7	41.2	1.33	U	289	1849	−58.222	−49.957	1017.9	57.1	1.83
U	289	1525	−58.136	−49.795	1017.7	41.2	1.33	U	289	2005	−58.144	−50.145	1017.6	68.5	2.71
U	289	1534	−58.181	−49.795	1017.8	41.1	1.32	U	289	2025	−58.126	−50.193	1017.5	71.7	3.16
U	289	1536	−58.185	−49.795	1017.8	41.1	1.32	U	289	2037	−58.116	−50.222	1017.6	73.6	3.49
U	289	1538	−58.194	−49.795	1017.8	41.1	1.32	U	289	2106	−58.092	−50.293	1017.6	78.3	4.81
S45	289	1547	−58.230	−49.796	1018.0	41.1	1.33	S46	290	1134	−57.694	−51.661	1012.5	64.7	2.33
S45	289	1606	−58.233	−49.798	1017.9	41.5	1.33	S46	290	1135	−57.694	−51.661	1012.5	64.5	2.31
S45	289	1615	−58.232	−49.799	1018.0	41.8	1.34	S46	290	1137	−57.695	−51.661	1012.5	64.2	2.29
S45	289	1626	−58.231	−49.800	1017.9	42.3	1.35	S46	290	1145	−57.698	−51.662	1012.4	63.1	2.20
S45	289	1642	−58.231	−49.801	1018.1	43.2	1.37	S46	290	1146	−57.699	−51.662	1012.3	62.9	2.18
S45	289	1655	−58.231	−49.804	1018.2	44.1	1.39	S46	290	1148	−57.699	−51.663	1012.3	62.6	2.17
S45	289	1659	−58.231	−49.804	1018.2	44.4	1.40	S46	290	1156	−57.701	−51.664	1012.2	61.5	2.09
S45	289	1701	−58.231	−49.805	1018.2	44.6	1.40	S46	290	1203	−57.704	−51.665	1012.2	60.5	2.02
S45	289	1705	−58.231	−49.804	1018.2	44.9	1.41	PS	290	1312	−57.823	−51.691	1011.5	51.6	1.61
S45	289	1707	−58.231	−49.804	1018.2	45.1	1.41	PS	290	1313	−57.823	−51.691	1011.5	51.5	1.60
S45	289	1710	−58.231	−49.805	1018.1	45.3	1.42	PS	290	1457	−57.823	−51.691	1011.5	43.3	1.37
U	289	1729	−58.238	−49.807	1018.2	47.1	1.47	PS	290	1635	−57.823	−51.691	1011.5	44.3	1.40
U	289	1747	−58.254	−49.816	1018.3	49.0	1.52	PS	290	1707	−57.823	−51.691	1011.5	46.6	1.45
U	289	1802	−58.288	−49.844	1018.2	50.8	1.58	PS	290	1843	−57.823	−51.691	1011.5	57.2	1.84
U	289	1815	−58.263	−49.872	1018.0	52.4	1.64	PS	290	1946	−57.823	−51.691	1011.5	66.1	2.45
U	289	1835	−58.239	−49.919	1017.8	55.1	1.74								

Table G1. A summary of the XOTD Cast Log for AMT-5. All times are in GMT.

Cast	*S/N*	*SDY*	*Date*	*Time*	*Longitude*	*Latitude*	*Depth* [m]	*SST* [°C]
1	1015	262	19 September	1110	−18.475	47.170	754	17.3
2	1024	263	20 September	1145	−19.949	42.840	785	19.3
3	1014	264	21 September	1210	−20.000	38.693	523	22.3
4	1023	265	22 September	1150	−19.526	35.443	276	23.7
5	1016	269	26 September	1209	−20.983	29.044	361	24.7
6	1022	270	27 September	1153	−21.000	24.141		24.9
7	1019	270	27 September	1200	−21.002	24.135	298	24.9
8	1021	273	30 September	1200	−20.872	10.922	162	29.1
9	1020	274	1 October	1200	−22.471	7.022	129	28.1
10	1013	275	2 October	1212	−24.160	2.811	542	27.6
11	1017	276	3 October	1235	−25.668	−0.768	459	26.2
12	1018	277	4 October	1314	−27.393	−4.786	416	25.8
13	1064	278	5 October	1319	−29.111	−8.952	520	26.3
14	1061	279	6 October	1330	−30.698	−12.886	203	26.5
15	1065	280	7 October	1220	−32.363	−16.687	289	25.5
16	1062	281	8 October	1336	−34.226	−20.672	679	24.0
17	1063	282	9 October	1210	−37.287	−23.902	363	22.8
18	1067	283	10 October	1220	−40.984	−27.692	354	20.9
19	1068	285	12 October	1336	−48.862	−35.476	602	18.8
20	1069	286	13 October	1346	−51.921	−38.842	620	14.4
21	1070	287	14 October	1349	−54.514	−42.250	357	12.3
22	1064	287	14 October	1821	−54.893	−42.993	283	13.2
23		288	15 October	1420	−56.686	−46.046	690	7.9
24	1066	289	16 October	1330	−57.667	−49.794	300	5.6

Table H1. A summary of the FRRF Tow Log for AMT-5. All times are in GMT.

Tow	*SDY*	*Date*	*Begin*	*Lon.*	*Lat.*	*End*	*Lon.*	*Lat.*	*Time*	*Comment*
501	259	16 Sep.	1450	−1.6530	50.430	1600	−8.458	48.667		FRRF did not wake up.
502	261	18 Sep.	1047	−13.205	47.987	1419			3:32	FRRF not flashing on recovery.
505	271	28 Sep.	1000	−20.500	19.718	1430	−20.418	19.050	4:30	Pin failure (FRRF 182010 used).
506	273	30 Sep.	1155	−20.870	10.922	1604	−21.197	10.220	4:09	Data problems w/logger JA8.
507	274	1 Oct.	1200	−22.470	7.027	1600	−22.737	6.283	4:00	Data problems w/logger JA8.
508	275	2 Oct.	1215	−23.837	2.817	1635	−24.232	2.633	4:20	Data problems w/logger JA10.
509	278	5 Oct.	1318	−29.115	−8.967	1707	−29.382	−9.613	3:49	FRRF logs data for 30 min.
510	279	6 Oct.	1328	−30.705	−12.877	1639			3:11	FRRF logs OK; JA10 for 10 min.
511	280	7 Oct.	1226	−32.363	−16.683	1507	−32.547	−17.147	2:41	Successful tow.
512	281	8 Oct.	1350	−34.225	−20.662	1635	−34.557	−21.082	2:45	Successful tow.
513	285	12 Oct.	1342	−48.863	−35.492	1755	−49.450	−36.091	4:13	Successful tow.
514	286	13 Oct.	1350	−51.907	−39.832	1608	−52.133	−39.198	2:18	Successful tow.
515	287	14 Oct.	1346	−54.460	−42.238	1643	−54.867	−42.797	2:57	Successful tow.
516	288	15 Oct.	1346	−56.700	−46.043	1655	−56.753	−46.548	3:09	Successful tow.
517	289	16 Oct.	1340	−57.627	−49.793	1549	−58.185	−49.798	2:09	Successful tow.

Table I1. A summary of the Underway Filtration Log for AMT-5. All times are in GMT.

SDY	*Time*	*Sta.*	*Sample*	*Lon.*	*Lat.*	*S*	*C*	T_s	*SST*	*F*	HPLC	Chl.
257	0745		U1	13.0927	53.1248				15.85	3.0	5 reps 2l (each split)	
257	1101		U2	19.3079	52.6147		44.0286	17.45	17.14	1.0	5 reps 2l (each split)	
257	1300		U3	18.7558	52.2795		45.6183	18.51	18.23	1.0	4 reps 1l (each split)	
257	1500		U4	18.2358	51.9409		46.4170	18.67	18.33	1.0	5 reps 1l (each split)	
257	1659		U5	17.5983	51.5610		45.9428	18.08	17.77	1.0	5 reps 1l (each split)	
257	1900		U6	15.6966	51.1301		45.9561	18.12	17.81	1.0	5 reps 1l (each split)	
258	1029	0	U7 S0	9.9167	50.7218		45.8828	18.16	17.84	1.0	3 reps 1l (each split)	
259	1427	1 (1)	S1	−1.0701	50.4275		45.2950	18.02	17.67	1.0	*See Station Log*	
259	1700		U8	−2.4445	50.2537		43.2457	16.90	16.53	4.3	3 reps 1l (each split)	
259	1900		U9	−2.9950	50.1351		42.6221	16.94	16.60	4.4	3 reps 2l (each split)	
259	2100		U10	−3.5827	50.0098		44.3364	16.40	16.03	7.8	3 reps 2l (each split)	
259	2300		U11	−4.2084	49.8735		44.5440	16.82	16.51	4.6	3 reps 2l (each split)	
260	0100		U12	−4.9172	49.7180		43.6486	16.45	16.09	4.4	3 reps 2l (each split)	
260	0300		U13	−5.5164	49.6028		44.4624	16.87	16.55	3.1	3 reps 2l (each split)	
260	0500		U14	−6.0338	49.5065		44.4851	17.25	16.93	4.1	3 reps 2l (each split)	
260	0659		U15	−6.5800	49.4950		43.8964	16.96	16.65	4.2	3 reps 2l (each split)	
260	0958		U16	−7.4687	49.2851		44.7899	16.86	16.61	3.3	3 reps 2l (each split)	
260	1100		U17	−7.7587	49.0804		45.2754	17.06	16.80	2.3	3 reps 2l (each split)	
260	1300		U18	−8.2762	48.7159		45.5967	17.16	16.91	2.0	3 reps 2l (each split)	
260	1500		U19	−8.3735	48.6784		45.6887	17.21	16.90	2.2	3 reps 2l (each split)	
260	1625	2 (2)	S2	−8.4423	48.6735	35.55	45.6504	17.13	16.80	2.2	*See Station Log*	
260	1900		U20	−9.1369	48.5659		45.6556	17.16	16.90	2.4	2 reps 2l (each split)	
260	2059		U21	−9.7460	48.4659		45.3292	16.76	16.45	4.6	2 reps 2l (each split)	
260	2300		U22	−10.3236	48.3907		46.0968	17.48	17.23	2.9	2 reps 2l (each split)	
261	0100		U23	−10.8714	48.3186		45.6794	17.12	16.86	3.1	2 reps 2l (each split)	
261	0300		U24	−11.4245	48.2358		45.5223	16.98	16.70	3.9	2 reps 2l (each split)	
261	0500		U25	−11.9834	48.1640		46.0556	17.45	17.17	2.8	2 reps 2l (each split)	
261	0659		U26	−12.4994	48.0949		46.1391	17.55	17.24	2.6	2 reps 2l (each split)	
261	0900		U27	−12.9909	48.0165		46.3179	17.69	17.41	2.6	2 reps 2l (each split)	

Table I1. (cont.) A summary of the Underway Filtration Log for AMT-5. All times are in GMT.

SDY	*Time*	*Sta.*	*Sample*	*Lon.*	*Lat.*	*S*	*C*	T_s	*SST*	*F*	HPLC	Chl.
261	1025	3 (3)	S3	−13.2055	47.9834	35.63	46.3737	17.75	17.48	2.6	*See Station Log*	
261	1307		U28	−13.6502	47.8838		46.1980	17.64	17.36	2.3	2 reps 2l (each split)	
261	1500		U29	−14.0660	47.8042		46.2600	17.71	17.39	2.3	2 reps 2l (each split)	
261	1701		U30	−14.5438	47.7287		45.8189	17.22	16.94	3.0	2 reps 2l (each split)	
261	1900		U31	−14.9753	47.6592		46.4161	17.73	17.44	3.4	2 reps 2l (each split)	
261	2100		U32	−15.3908	47.6045		46.2011	17.57	17.26	3.7	3 reps 2l (each split)	
261	2300		U33	−15.7885	47.5476		46.1598	17.55	17.28	3.7	2 reps 2l (each split)	
262	0100		U34	−16.2183	47.4818		46.1171	17.51	17.22	3.8	2 reps 2l (each split)	
262	0300		U35	−16.6881	47.4278		46.1588	17.53	17.28	3.9	2 reps 2l (each split)	
262	0500		U36	−17.1742	47.3758		45.8354	17.22	16.94	3.5	2 reps 2l (each split)	
262	0659		U37	−17.6976	47.3037		45.9356	17.34	17.21	3.2	2 reps 2l (each split)	
262	0900		U38	−18.2395	47.2172		46.8811	18.08	17.78	3.1	2 reps 2l (each split)	
262	1025	4 (4)	S4	−18.4773	47.1707	35.76	46.8759	18.09	17.80	2.6	*See Station Log*	
262	1300		U39	−18.6347	46.9481		47.2324	18.23	18.01	2.9	2 reps 2l	1 rep 1l
262	1450		U40	−18.7656	46.7510		47.0671	18.38	18.19	3.3	2 reps 2l	1 rep 1l
262	1700		U41	−19.0244	46.3702	35.80	47.2366	18.40	18.17	2.4	2 reps 2l	1 rep 1l
262	1900		U42	−19.3123	45.9898	35.69	46.6124	17.93	17.72	3.2	2 reps 2l	1 rep 1l
262	2100		U43	−19.5830	45.6148	35.77	47.2221	18.40	18.17	2.6	3 reps 2l	1 rep 1l
262	2300		U44	−19.8487	45.2346	35.67	46.5556	17.88	17.63	3.1	2 reps 2l	1 rep 1l
263	0100		U45	−19.9945	44.8240	35.66	46.5070	17.85	17.64	2.8	2 reps 2l	1 rep 1l
263	0300		U46	−20.0097	44.3760	35.74	47.0226	18.21	17.97	2.3	2 reps 2l	1 rep 1l
263	0500		U47	−20.0127	43.9238	35.79	47.2841	18.46	18.19	2.5	2 reps 2l	1 rep 1l
263	0700		U48	−20.0019	43.4757	35.82	47.7885	18.91	18.69	1.9	2 reps 2l	1 rep 1l
263	0900		U49	−19.9776	43.0364	35.81	47.9146	19.04	18.84	2.0	2 reps 2l	1 rep 1l
263	1022	5 (5)	S5	−19.9595	42.8438	35.76	48.3425	19.41	19.17	2.6	*See Station Log*	
263	1259		U50	−19.9500	42.6307	35.88	48.3756	19.79	19.21	1.9	2 reps 2l	1 rep 1l
263	1405		U51	−19.9672	42.4500	35.83	48.6934	20.05	19.63	1.8	2 reps 2l	1 rep 1l
263	1501	6	U52	−19.9610	42.4170	35.92	49.0817	21.14	19.85	1.7	2 reps 2l	1 rep 1l
263	1700		U53	−19.9993	42.0343	36.14	50.4983	21.46	20.95	1.6	2 reps 2l	1 rep 1l
263	1900		U54	−20.0016	41.7245	36.18	50.6637	21.26	21.08	1.7	2 reps 2l	1 rep 1l
263	2100		U55	−20.0069	41.3224	35.98	50.0484	20.93	20.72	1.6	3 reps 2l	1 rep 1l
263	2300		U56	−20.0020	40.9291	36.15	50.9212	21.54	21.33	1.6	2 reps 2l	1 rep 1l
264	0100		U57	−19.9997	40.5311	36.10	50.5417	21.23	21.03	1.6	2 reps 2l	1 rep 1l
264	0300		U58	−20.0012	40.1297	36.03	50.4217	21.21	20.99	1.6	2 reps 2l	1 rep 1l
264	0500		U59	−19.9947	39.7265		51.2729	21.86	21.68	1.6	2 reps 2l	1 rep 1l
264	0700		U60	−20.0019	39.3207	36.08	51.4704	22.13	21.92	1.6	2 reps 2l	1 rep 1l
264	0903		U61	−20.0146	38.9000	35.83	51.9111	22.32	22.12	1.8	2 reps 2l	1 rep 1l
264	1023	7 (6)	S6	−20.0128	38.7223	36.24	51.9163	22.39	22.15	1.6	*See Station Log*	
264	1300		U63	−20.0020	38.5760	36.27	52.2163	22.61	22.41	1.6	2 reps 2l	1 rep 1l
264	1413		U64	−19.9978	38.3757	36.29	52.3042	22.63	22.48	1.6	2 reps 2l	1 rep 1l
264	1503		U65	−20.0004	38.2190	36.27	52.3425	22.74	22.54	1.6	2 reps 2l	1 rep 1l
264	1703		U66	−19.9965	37.8411	36.36	52.9001	23.12	22.92	1.6	2 reps 2l	1 rep 1l
264	2025		U67	−19.8872	37.2278		53.0129	23.19	22.96	1.6	2 reps 2l	1 rep 1l
264	2100		U68	−19.8676	37.1231		53.1029	23.34	23.14	1.6	3 reps 2l	none
264	2301		U69	−19.8187	36.8718	36.30	53.1929	23.50	23.30	1.6	2 reps 2l	1 rep 1l
265	0103		U70	−19.7506	36.4953	35.43	53.5530	23.67	23.50	1.5	2 reps 2l	1 rep 1l
265	0300		U71	−19.6746	36.1422	36.46	53.6710	23.74	23.65	1.5	2 reps 2l	1 rep 1l
265	0500		U72	−19.5985	35.7933	36.38	53.5209	23.68	23.51	1.6	2 reps 2l	1 rep 1l
265	0700	8	U73	−19.5324	35.4615	36.40	53.6027	23.77	23.59	1.6	2 reps 2l	1 rep 1l
265	1117	9 (7)	S8	−19.5297	35.4473	36.42	53.6275	23.82	23.67	1.6	*See Station Log*	
265	1300		U74	−19.3567	35.2623	36.45	54.0549	24.11	23.93	1.5	2 reps 2l	1 rep 1l
265	1430	10	U75	−19.1445	35.0346	36.39	54.2391	24.30	24.02	1.5	2 reps 2l	1 rep 1l
268	1347	T1 (8)	S9	−17.2281	32.3099	36.91	54.6376	24.14	24.02	1.4	*See Station Log*	

Table I1. (cont.) A summary of the Underway Filtration Log for AMT-5. All times are in GMT.

SDY	*Time*	*Sta.*	*Sample*	*Lon.*	*Lat.*	*S*	*C*	T_s	*SST*	*F*	HPLC	Chl.
268	1800		U76	−17.8372	31.7826	37.03	55.0785	24.35	24.15	1.5	2×2 bottles	1×1 bottle
268	2000		U77	−18.2116	31.4750	36.99	55.0030	24.33	24.15	1.5	2×2 bottles	1×1 bottle
268	2200		U78	−18.6060	31.1666		55.2007	24.45	24.27	1.5	3×2 bottles	1×1 bottle
269	0000		U79	−18.9853	30.8372		55.3953	24.76	24.57	1.5	2×2 bottles	1×1 bottle
269	0200		U80	−19.3523	30.5009	36.98	55.3611	24.67	24.49	1.5	2×2 bottles	1×1 bottle
269	0400		U81	−19.7100	30.1564	37.26	56.1603	25.08	24.89	1.5	2×2 bottles	1×1 bottle
269	0600		U82	−20.0680	29.8196	37.22	55.8735	24.85	24.69	1.4	2×2 bottles	1×1 bottle
269	0800		U83	−20.4341	29.5016	37.27	55.7441	24.69	24.52	1.5	2×2 bottles	1×1 bottle
269	1000		U84	−20.7931	29.1917	37.29	55.9574	24.84	24.62	1.5	2×2 bottles	1×1 bottle
269	1135	11 (9)	S10	−20.9718	29.0497	37.19	55.8342	24.84	24.62	1.5	*See Station Log*	
269	1407	12	U85	−20.9944	28.6341	37.24	56.1696	25.09	24.88	1.4	2×2 bottles	1×1 bottle
269	1700		U86	−20.9965	28.1127	37.27	56.2907	25.17	24.96	1.4	2×2 bottles	1×1 bottle
269	1855		U87	−20.9861	27.6849	37.26	56.3394	25.00	24.99	1.7	2×2 bottles	1×1 bottle
269	2100		U88	−20.9926	27.1222	37.16	56.3736	25.35	25.16	1.5	3×2 bottles	1×1 bottle
269	2300		U89	−20.9904	26.7727	37.13	56.0330	25.10	25.01	1.6	2×2 bottles	1×1 bottle
270	0100		U90	−20.9989	26.4383	37.14	56.0837	25.11	24.90	1.5	2×2 bottles	1×1 bottle
270	0300		U91	−21.0040	25.9671	37.04	55.9543	25.11	24.94	1.5	2×2 bottles	1×1 bottle
270	0500		U92	−20.9987	25.4952	36.97	55.8497	25.13	24.93	1.5	2×2 bottles	1×1 bottle
270	0700		U93	−20.9904	25.0299	37.10	56.1448	25.21	25.00	1.5	2×2 bottles	1×1 bottle
270	0900		U94	−20.9922	24.5694	37.02	56.0806	25.26	25.08	1.4	2×2 bottles	1×1 bottle
270	1125	13 (10)	S11	−20.9995	24.1386	36.89	55.7213	25.10	24.85	1.6	*See Station Log*	
270	1418	14	U95	−21.0084	23.7260	36.80	55.6333	25.14	24.96	1.6	2×2 bottles	1×1 bottle
270	1700		U96	−21.0042	23.2340	36.60	55.6737	25.42	25.27	1.6	2×2 bottles	1×1 bottle
270	1900		U97	−20.9978	22.8109	36.69	55.9708	25.58	25.41	1.6	2×2 bottles	1×1 bottle
270	2100		U98	−20.9902	22.3923	36.74	55.4843	25.07	24.88	1.6	2×4,000 ml	1×1 bottle
270	2300		U99	−20.9884	21.9895	36.74	55.5267	25.12	24.90	1.5	3×4,000 ml	1×1 bottle
271	0100		U100	−20.9308	21.6557	35.76	55.5484	25.11	24.90	1.6	2×2 bottles	1×1 bottle
271	0300		U101	−20.8511	21.2383	36.30	54.4772	24.54	24.29	2.2	2×2 bottles	1×1 bottle
271	0500		U102	−20.7646	20.8254	36.35	54.3105	24.46	24.29	2.0	2×3,840 ml	1×1 bottle
271	0700		U103	−20.6840	20.4489	36.31	54.9636	25.13	24.97	3.2	2×2,500 ml	1×1 bottle
271	0900		U104	−20.5997	20.0715	36.27	55.1726	25.37	25.18	3.5	2×1 bottle	1×1 bottle
271	1126	15 (11)	S12	−20.5295	19.7244	36.28	55.2040	25.89	25.22	3.7	*See Station Log*	
271	1500		U105	−20.4454	19.2381	36.19	54.9039	25.21	25.01	4.0	2×1 bottle	1×1 bottle
271	1608	16	U106	−20.4183	19.0501	36.21	55.0039	25.29	25.10	4.2	2×1 bottle	1×1 bottle
271	1900		U107	−20.3288	18.5598	36.22	55.2586	25.52	25.36	4.0	2×1 bottle	1×1 bottle
271	2100		U108	−20.2369	18.1705		55.8134	25.94	25.78	2.0	2×1 bottle	1×1 bottle
271	2300		U109	−20.1422	17.7976		56.1519	26.17	26.00	1.6	3×1 bottle	1×1 bottle
272	0100		U110	−20.0830	17.4816		56.9750	26.94	26.78	1.6	2×1 bottle	1×1 bottle
272	0300		U111	−20.0100	17.0903		56.9689	26.98	26.81	1.6	2×1 bottle	1×1 bottle
272	0500		U112	−19.9994	16.6999	36.29	57.2618	27.27	27.10	1.6	2×2 bottles	1×1 bottle
272	0700		U113	−20.0008	16.3010	36.23	57.6191	27.68	27.53	1.6	2×2 bottles	1×1 bottle
272	0900		U114	−20.0023	15.8953	36.15	57.9929	28.13	27.98	1.6	2×2 bottles	1×1 bottle
272	1113	T2	S13a	−20.0108	15.4926	36.25	58.0478	28.04	27.88	1.6	2×2 bottles	5×1 bottle
272	1345		U115	−20.0137	15.0502	35.19	58.1887	28.26	28.10	1.5	2×2 bottles	1×1 bottle
272	1500		U116	−19.9982	14.7930	36.02	58.1897	28.47	28.38	1.6	2×2 bottles	1×1 bottle
272	1700		U117	−19.9860	14.3880	35.72	57.7226	28.45	28.27	1.7	2×2 bottles	1×1 bottle
272	1850		U118	−19.9940	14.0192	35.83	58.2818	28.81	28.68	1.6	2×2 bottles	1×1 bottle
272	2100		U119	−20.0077	13.5784		58.0353	28.79	28.62	1.6	2×2 bottles	1×1 bottle
272	2300		U120	−20.0164	13.1658		57.5952	28.73	28.58	1.6	3×2 bottles	1×1 bottle
273	0100		U121	−20.0936	12.7765	35.31	57.6003	28.84	28.69	1.6	2×2 bottles	1×1 bottle
273	0300		U122	−20.2485	12.4043	34.92	56.8413	28.81	28.67	1.6	2×2 bottles	1×1 bottle
273	0500		U123	−20.4091	12.0251	35.43	57.7091	28.85	28.69	1.6	2×2 bottles	1×1 bottle
273	0700		U124	−20.5646	11.6401	35.51	58.0374	29.01	28.89	1.6	2×2 bottles	1×1 bottle

Table I1. (cont.) A summary of the Underway Filtration Log for AMT-5. All times are in GMT.

SDY	*Time*	*Sta.*	*Sample*	*Lon.*	*Lat.*	*S*	*C*	T_s	*SST*	*F*	HPLC	Chl.
273	0900		U125	−20.7204	11.2730	35.54	58.0415	28.99	28.85	1.6	2×2 bottles	1×1 bottle
273	1127	17 (12)	S13	−20.8702	10.9234	35.66	58.5397	29.25	28.97	1.6	*See Station Log*	
273	1500		U126	−21.1311	10.3914	35.53	58.8173	29.68	29.53	1.6	2×1 bottle	1×1 bottle
273	1612	18	U127	−21.1955	10.2193	35.59	58.5770	29.41	29.52	1.6	2×1 bottle	1×1 bottle
273	1900		U128	−21.3468	9.8698	35.51	58.1503	29.12	28.97	1.6	2×2 bottles	1×1 bottle
273	2100		U129	−21.4969	9.5160	35.07	56.9778	28.58	28.41	1.7	2×2 bottles	1×1 bottle
273	2300		U130	−21.6256	9.1695	35.49	57.6791	28.69	28.55	1.7	2×6450 ml	1×1 bottle
274	0100		U131	−21.7333	8.8233	35.57	57.9297	28.83	28.71	1.7	2×2 bottles	1×1 bottle
274	0300		U132	−21.8645	8.4502	35.24	57.4450	28.82	28.68	1.5	2×2 bottles	1×1 bottle
274	0500		U133	−22.0157	8.0807	34.31	55.9333	28.57	28.38	1.6	2×2 bottles	1×1 bottle
274	0700		U134	−22.1669	7.7067	34.41	55.8380	28.36	28.20	1.6	2×2 bottles	1×1 bottle
274	0900		U135	−22.2931	7.3654	34.66	56.1600	28.43	28.29	1.6	2×2 bottles	1×1 bottle
274	1129	19 (13)	S14	−22.4690	7.0269	34.26	55.3681	28.21	28.07	1.5	*See Station Log*	
274	1500		U136	−22.6631	6.4658	34.40	56.2314	28.83	28.58	1.5	2×2 bottles	1×1 bottle
274	1700		U137	−22.8000	6.1342	33.86	55.2376	28.62	28.43	1.5	2×2 bottles	1×1 bottle
274	1900		U138	−22.9456	5.7801	34.54	56.1589	28.84	28.70	1.5	2×2 bottles	1×1 bottle
274	2100		U139	−23.0996	5.4160	34.29	55.6734	28.49	28.35	1.5	2×2 bottles	1×1 bottle
274	2300		U140	−23.2611	5.0392	34.51	56.0202	28.49	28.36	1.4	3×2 bottles	1×1 bottle
275	0100		U141	−23.4117	4.6694	34.85	56.0482	28.05	27.89	1.5	2×2 bottles	1×1 bottle
275	0300		U142	−23.5630	4.2976	34.81	55.9623	28.01	27.86	1.5	2×2 bottles	1×1 bottle
275	0500		U143	−23.7167	3.9168	34.94	56.1901	28.04	27.90	1.6	2×2 bottles	1×1 bottle
275	0700		U144	−23.8630	3.5507	34.92	56.0876	27.93	27.76	1.6	2×2 bottles	1×1 bottle
275	0900		U145	−24.0213	3.1723	35.09	56.1932	27.81	27.69	1.6	2×2 bottles	1×1 bottle
275	1120	20 (14)	S15	−24.1643	2.8158	35.56	56.7351	27.74	27.62	1.6	*See Station Log*	
275	1500		U146	−24.3601	2.3302	35.91	56.8797	27.41	27.24	1.4	2×2 bottles	1×1 bottle
275	1641	21	U147	−24.4651	2.0774	35.90	56.8445	27.40	27.25	1.4	2×2 bottles	1×1 bottle
275	1900		U148	−24.5353	1.8881	35.89	56.8062	27.38	27.24	1.5	2×2 bottles	1×1 bottle
275	2100		U149	−24.7063	1.5335	35.85	56.6064	27.23	27.17	1.5	2×1 bottle	1×1 bottle
275	2300		U150	−24.8526	1.1910	35.86	56.0349	26.69	26.51	1.5	3×1 bottle	1×1 bottle
276	0100		U151	−24.9646	0.9123	36.05	56.7472	26.21	26.16	1.8	2×1 bottle	1×1 bottle
276	0300		U152	−25.1060	0.5418	35.11	55.7740	26.12	26.00	2.0	2×1 bottle	1×1 bottle
276	0500		U153	−25.2575	0.1867	36.13	55.8444	26.16	26.10	1.7	2×1 bottle	1×1 bottle
276	0700		U154	−25.4073	−0.1632	36.11	55.8092	26.17	26.02	1.8	2×1 bottle	1×1 bottle
276	0900		U155	−25.5595	−0.5136	36.09	55.7451	26.13	25.97	1.8	2×2 bottles	1×1 bottle
276	1100	22 (15)	S16	−25.6631	−0.7728	36.08	55.8196	26.19	26.02	1.5	*See Station Log*	
276	1512		U156	−25.8440	−1.2159	36.12	56.3527	26.66	26.51	1.5	2×2 bottles	1×1 bottle
276	1612	23	U157	−25.8970	−1.3585	36.12	56.1509	26.47	26.35	1.5	2×2 bottles	1×1 bottle
276	1904		U158	−26.0067	−1.6421	36.09	56.0639	26.42	26.27	1.6	2×2 bottles	1×1 bottle
276	2100		U159	−26.1636	−1.9960	36.12	56.0204	26.35	26.20	1.6	2×2 bottles	1×1 bottle
276	2300		U160	−26.3318	−2.3725	36.21	56.2109	26.41	26.26	1.6	3×2 bottles	1×1 bottle
277	0052		U161	−26.4831	−2.7139	36.22	56.0494	26.25	26.12	1.5	2×2 bottles	1×1 bottle
277	0300		U162	−26.6551	−3.1232	36.22	56.0505	26.25	26.11	1.5	2×2 bottles	1×1 bottle
277	0500		U163	−26.8218	−3.5120	36.22	55.9842	26.19	26.03	1.6	2×2 bottles	1×1 bottle
277	0700		U164	−26.9968	−3.9042	36.09	55.4976	25.89	25.72	1.8	2×2 bottles	1×1 bottle
277	0900		U165	−27.1659	−4.3004	35.96	55.0908	25.69	25.50	1.8	2×2 bottles	1×1 bottle
277	1210	24 (16)	S17	−27.3721	−4.7851	35.92	55.0877	25.74	25.57	1.6	*See Station Log*	
277	1500		U166	−27.5195	−5.1068	35.93	55.5711	26.17	26.02	1.5	2×2 bottles	1×1 bottle
277	1610	25	U167	−27.5987	−5.3090	35.94	55.8444	26.41	26.22	1.4	2×2 bottles	1×1 bottle
277	1800		U168	−27.7048	−5.5598	35.95	55.7223	26.32	26.17	1.6	2×2 bottles	1×1 bottle
277	2000		U169	−27.8751	−5.9603	35.94	55.5763	26.16	26.05	1.7	2×2 bottles	1×1 bottle
277	2200		U170	−28.0335	−6.3681	36.13	55.9397	26.27	26.07	1.6	3×2 bottles	1×1 bottle
278	0000		U171	−28.1796	−6.7787	36.21	55.9542	26.16	26.00	1.5	2×2 bottles	1×1 bottle
278	0200		U172	−28.3263	−7.1783	36.16	55.9418	26.23	26.15	1.6	2×2 bottles	1×1 bottle

Table I1. (cont.) A summary of the Underway Filtration Log for AMT-5. All times are in GMT.

SDY	*Time*	*Sta.*	*Sample*	*Lon.*	*Lat.*	*S*	*C*	T_s	*SST*	*F*	HPLC	Chl.
278	0400		U173	−28.4899	−7.5662	36.18	55.8869	26.16	25.98	1.6	2×2 bottles	1×1 bottle
278	0600		U174	−28.6641	−7.9446	36.21	55.8993	26.11	25.91	1.6	2×2 bottles	1×1 bottle
278	0800		U175	−28.8352	−8.3228	36.43	56.4180	26.35	26.17	1.4	2×2 bottles	1×1 bottle
278	1000		U176	−29.0078	−8.6941	36.64	56.7038	26.36	26.20	1.4	2×2 bottles	1×1 bottle
278	1205	26 (17)	S18	−29.1148	−8.9669	36.52	56.6675	26.44	26.29	1.4	*See Station Log*	
278	1500		U177	−29.2178	−9.2558	36.53	56.8166	26.56	26.37	1.4	2×2 bottles	1×1 bottle
278	1713	27	U178	−29.3813	−9.6136	36.68	56.6789	26.37	26.18	1.4	2×2 bottles	1×1 bottle
278	2000		U179	−29.5790	−10.0469	36.65	56.7649	26.36	26.15	1.3	2×2 bottles	1×1 bottle
278	2200		U180	−29.7301	−10.4280	36.69	56.8425	26.41	26.19	1.3	2×2 bottles	1×1 bottle
279	0000		U181	−29.8718	−10.8006	36.79	57.0641	26.46	26.30	1.4	3×2 bottles	1×1 bottle
279	0200		U182	−30.0405	−11.1604	36.64	56.9326	26.37	26.37	1.4	2×2 bottles	1×1 bottle
279	0400		U183	−30.1495	−11.5173	36.69	56.9896	26.35	26.35	1.4	2×2 bottles	1×1 bottle
279	0600		U184	−30.3075	−11.8875	36.78	56.9036	26.36	26.19	1.4	2×2 bottles	1×1 bottle
279	0800		U185	−30.4605	−12.2538	36.90	56.9948	26.27	26.09	1.4	2×2 bottles	1×1 bottle
279	1000		U186	−30.6067	−12.6201	36.89	56.9316	26.21	26.06	1.4	2×2 bottles	1×1 bottle
279	1148	28 (18)	S19	−30.7053	−12.8764	36.83	57.2205	26.55	26.43	1.4	*See Station Log*	
279	1500		U187	−30.7933	−13.1311	36.86	57.3768	26.66	26.53	1.4	2×2 bottles	1×1 bottle
279	1700		U188	−30.9343	−13.4360	36.76	57.2691	26.68	26.53	1.4	2×2 bottles	1×1 bottle
279	2000		U189	−31.1681	−13.9401	37.15	57.4421	26.35	26.18	1.4	2×2 bottles	1×1 bottle
279	2200		U190	−31.3331	−14.2806	37.14	57.1998	26.16	26.00	1.4	2×2 bottles	1×1 bottle
280	0000		U191	−31.5004	−14.6360	37.14	57.3158	26.25	26.06	1.4	2×2 bottles	1×1 bottle
280	0200		U192	−31.6542	−15.0012	37.20	57.1149	26.11	25.94	1.4	3×2 bottles	1×1 bottle
280	0400		U193	−31.8041	−15.3615	37.07	57.1553	26.20	26.02	1.4	2×2 bottles	1×1 bottle
280	0600		U194	−31.9471	−15.7163	37.27	57.5881	26.34	26.16	1.4	2×2 bottles	1×1 bottle
280	0800		U195	−32.1074	−16.0781	37.14	56.7028	25.70	25.55	1.4	2×2 bottles	1×1 bottle
280	1000		U196	−32.2588	−16.4238	37.17	56.7007	25.66	25.51	1.4	2×2 bottles	1×1 bottle
280	1209	29 (19)	S20	−32.3624	−16.6864	37.16	56.6469	25.62	25.47	1.4	*See Station Log*	
280	1518	30	U197	−32.5471	−17.1478	37.30	56.9254	25.69	25.51	1.4	2×2 bottles	1×1 bottle
280	1540		U198	−32.5453	−17.1484	37.31	56.9078	25.68	25.52	1.4	2×2 bottles	1×1 bottle
280	1755		U199	−32.6525	−17.4666	37.30	56.9482	25.72	25.54	1.4	2×2 bottles	1×1 bottle
280	2000		U200	−32.8071	−17.8401	37.30	56.6086	25.41	25.25	1.5	2×2 bottles	1×1 bottle
280	2200		U201	−32.9618	−18.2018	37.23	56.2007	25.13	24.94	1.5	2×1 bottle	1×1 bottle
281	0000		U202	−33.1318	−18.5673	37.27	56.1489	25.05	24.92	1.5	2×1 bottle	1×1 bottle
281	0200		U203	−33.3057	−18.9443	37.28	56.0195	24.91	24.74	1.4	3×2 bottles	1×1 bottle
281	0400		U204	−33.4837	−19.3274	37.28	56.0661	24.95	24.74	1.4	2×2 bottles	1×1 bottle
281	0600		U205	−33.6301	−19.7061	37.25	55.9398	24.90	24.74	1.5	2×2 bottles	1×1 bottle
281	0800		U206	−33.8317	−20.0661	37.22	55.9243	24.85	24.65	1.4	2×2 bottles	1×1 bottle
281	1000		U207	−34.0616	−20.4182	37.12	54.9647	24.14	23.94	1.5	2×2 bottles	1×1 bottle
281	1212	31 (20)	S21	−34.2246	−20.6623	37.11	54.9109	24.10	23.89	1.5	*See Station Log*	
281	1530		U208	−34.4123	−20.9159	37.12	54.9947	24.16	23.99	1.5	2×2 bottles	1×1 bottle
281	1645	32	U209	−34.5563	−21.0817	37.18	55.1562	24.25	24.05	1.5	2×2 bottles	1×1 bottle
281	1709		U210	−34.5538	−21.0834	37.17	55.1231	24.23	24.05	1.5	2×2 bottles	1×1 bottle
281	2000		U211	−34.9845	−21.5336	37.05	54.6345	23.92	23.71	1.7	2×2 bottles	1×1 bottle
281	2200		U212	−35.2803	−21.8544	36.86	53.8966	23.48	23.29	1.6	2×2 bottles	1×1 bottle
282	0000		U213	−35.5947	−22.1657	36.93	54.0974	23.56	23.35	1.6	3×2 bottles	1×1 bottle
282	0200		U214	−35.8807	−22.4634	37.08	54.5942	23.85	23.66	1.6	2×2 bottles	1×1 bottle
282	0400		U215	−36.1698	−22.7547	37.08	54.5993	23.85	23.66	1.6	2×2 bottles	1×1 bottle
282	0600		U216	−36.4546	−23.0483	36.92	53.9380	23.43	23.24	1.6	2×2 bottles	1×1 bottle
282	0800		U217	−36.7453	−23.3490	36.95	53.8863	23.36	23.16	1.6	2×2 bottles	1×1 bottle
282	1000		U218	−37.0455	−23.6592	36.87	53.5965	23.18	22.98	1.6	2×2 bottles	1×1 bottle
282	1159	33 (21)	S22	−37.2869	−23.9024	36.79	53.2509	22.96	22.74	1.6	*See Station Log*	
282	1409		U219	−37.7538	−24.1565	36.86	53.4910	23.10	22.90	1.5	2×2 bottles	1×1 bottle
282	1600		U220	−37.8374	−24.4640	36.81	53.3089	22.98	22.74	1.5	2×2 bottles	1×1 bottle

Table I1. (cont.) A summary of the Underway Filtration Log for AMT-5. All times are in GMT.

SDY	*Time*	*Sta.*	*Sample*	*Lon.*	*Lat.*	*S*	*C*	T_s	*SST*	*F*	HPLC	Chl.
282	1742		U221	−38.1160	−24.7558	36.83	53.1568	22.82	22.61	1.6	2×2 bottles	1×1 bottle
282	1951		U222	−38.4696	−25.1227	36.82	53.1195	22.80	22.61	1.5	2×2 bottles	1×1 bottle
282	2200		U223	−38.7928	−25.4868	36.47	51.3650	21.57	21.41	1.6	2×2 bottles	1×1 bottle
283	0000		U224	−39.1074	−25.8142	26.34	50.8116	21.20	21.07	1.6	3×2 bottles	1×1 bottle
283	0200		U225	−39.3668	−26.0654	36.31	50.4093	20.86	20.67	1.7	2×2 bottles	1×1 bottle
283	0400		U226	−39.7221	−26.3987	36.16	49.8468	20.50	20.32	1.7	2×2 bottles	1×1 bottle
283	0600		U227	−40.0711	−26.7370	36.60	50.9296	21.06	20.96	2.0	2×2 bottles	1×1 bottle
283	0800		U228	−40.4099	−27.0777	36.61	51.0837	21.15	20.97	2.1	2×2 bottles	1×1 bottle
283	1000		U229	−40.7422	−27.4302	36.72	51.9039	21.78	21.60	2.1	2×2 bottles	1×1 bottle
283	1212	34 (22)	S23	−40.9842	−27.6920	36.58	50.9730	21.08	20.86	2.5	*See Station Log*	
283	1402		U230	−41.2803	−27.9752	36.60	51.0113	21.09	20.95	2.3	2×2 bottles	1×1 bottle
283	1600		U231	−41.6077	−28.3178	36.53	50.4807	20.67	20.48	2.4	2×2 bottles	1×1 bottle
283	1754		U232	−41.9180	−28.6592	36.61	51.1478	21.20	20.99	2.3	2×2 bottles	1×1 bottle
283	2000		U233	−42.2487	−29.0333	36.16	48.3291	19.04	18.85	2.9	2×2 bottles	1×1 bottle
283	2200		U234	−42.5926	−29.3666	35.90	46.8242	17.87	17.67	2.5	2×1 bottle	1×1 bottle
284	0000		U235	−42.9322	−29.6716	36.17	48.0056	18.71	18.52	3.3	2×1 bottle	1×1 bottle
284	0200		U236	−43.2105	−29.9305	36.14	47.9673	18.72	18.51	3.2	2×1 bottle	1×1 bottle
284	0400		U237	−43.5340	−30.2771	36.06	47.2201	18.09	17.88	3.6	2×1 bottle	1×1 bottle
284	0600		U238	−43.8666	−30.6140	36.11	47.4805	18.28	18.07	4.1	2×1 bottle	1×1 bottle
284	0800		U239	−44.1977	−30.9586	36.10	47.3710	18.19	17.99	4.6	2×1 bottle	1×1 bottle
284	1000		U240	−44.5309	−31.3052	36.11	47.4092	18.22	17.99	6.1	2×1 bottle	1×1 bottle
284	1223	35 (23)	S24a	−44.8707	−31.6208	36.11	47.5291	18.34	18.11	5.2	3×1 bottle	1×1 bottle
284	1410		U241	−44.9504	−31.6765	36.12	47.8071	18.58	18.36	5.4	2×1 bottle	1×1 bottle
284	1550		U242	−45.2575	−31.9665	26.22	48.2878	18.93	18.81	6.3	2×1 bottle	1×1 bottle
284	1700		U243	−45.4629	−32.1796	36.28	48.5441	19.12	18.89	6.9	2×1 bottle	1×1 bottle
284	1800		U244	−45.6311	−32.3654	36.13	48.3735	19.12	18.91	5.4	2×1 bottle	1×1 bottle
284	2000		U245	−45.9628	−32.7261	36.12	48.5472	19.33	19.13	4.4	2×1 bottle	1×1 bottle
284	2200		U246	−46.3061	−33.0600	36.20	48.7984	19.41	19.29	4.9	2×1 bottle	1×1 bottle
285	0000		U247	−46.6407	−33.3885	35.86	47.9177	18.73	18.45	4.3	3×1 bottle	1×1 bottle
285	0200		U248	−46.9884	−33.7177	35.88	47.5290	18.81	18.60	3.4	2×1 bottle	1×1 bottle
285	0400		U249	−47.3602	−34.0535	35.81	46.4016	17.50	17.25	6.2	2×1 bottle	1×1 bottle
285	0600		U250	−47.7459	−34.4067	35.86	46.1991	17.34	17.14	7.9	2×1 bottle	1×1 bottle
285	0800		U251	−48.1015	−34.7771	35.08	43.3553	15.36	15.21	9.4	2×1 bottle	1×1 bottle
285	1000		U252	−48.4584	−35.0975	36.20	48.4676	19.13	18.91	6.7	2×1 bottle	1×1 bottle
285	1124		U253	−48.6874	−35.3100	36.11	48.1616	18.85	18.62	4.3	2×1 bottle	1×1 bottle
285	1301	36 (24)	S24	−48.8611	−35.4860	35.83	47.8805	19.00	18.76	4.6	*See Station Log*	
285	1513		U254	−49.0364	−35.6901	35.16	45.4820	17.06	16.93	5.1	2×1 bottle	1×1 bottle
285	1655		U255	−49.2923	−35.9447	35.50	46.8945	18.41	18.19	4.7	2×1 bottle	1×1 bottle
285	1803	37	U256	−49.4495	−36.0907	36.16	48.5379	19.27	19.12	4.2	2×1 bottle	1×1 bottle
285	1927		U257	−49.5476	−36.1742	36.24	48.5638	19.18	18.96	5.1	2×1 bottle	1×1 bottle
285	2100		U258	−49.8002	−36.4161	36.23	48.3446	18.98	18.75	4.6	2×1 bottle	1×1 bottle
285	2300		U259	−50.1161	−36.7288	34.39	45.2350	17.88	17.46	4.3	2×1 bottle	1×1 bottle
286	0100		U260	−50.4439	−37.0381	34.76	45.4602	17.86	17.65	4.6	3×1 bottle	1×1 bottle
286	0300		U261	−50.6871	−37.3012	35.57	47.1063	18.54	18.33	4.1	2×1 bottle	1×1 bottle
286	0500		U262	−50.9962	−37.6798	35.50	40.5731	14.18	13.89	18.3	2×1 bottle	1×1 bottle
286	0700		U263	−51.2929	−38.0307	34.73	43.2530	16.20	16.12	13.9	2×2 bottles	1×1 bottle
286	0900		U264	−51.5355	−38.3600	35.48	42.7513	14.35	14.10	16.6	2×1 bottle	1×1 bottle
286	1052		U265	−51.7868	−38.6744	35.57	43.1179	14.58	14.31	14.3	2×1 bottle	1×1 bottle
286	1231	38 (25)	S25	−51.9135	−38.8360	35.54	43.0807	14.58	14.32	14.3	*See Station Log*	
286	1516		U266	−52.0715	−39.0677	35.30	44.5214	16.28	15.95	13.0	2×1 bottle	1×1 bottle
286	1623	39	U267	−52.1431	−39.1970	35.27	43.6011	15.39	15.15	17.8	2×1 bottle	1×1 bottle
286	1652	39	U268	−52.1240	−39.1981	35.29	43.5320	15.30	15.01	19.2	2×1 bottle	1×1 bottle
286	1813		U269	−52.1903	−39.3093	35.27	43.5361	15.32	15.08	20.8	2×1 bottle	1×1 bottle

Table I1. (cont.) A summary of the Underway Filtration Log for AMT-5. All times are in GMT.

SDY	*Time*	*Sta.*	*Sample*	*Lon.*	*Lat.*	*S*	*C*	T_s	*SST*	*F*	HPLC	Chl.
286	1900		U270	−52.2345	−39.4231	35.58	44.4325	16.11	15.87	19.1	2×1 bottle	1×1 bottle
286	2000		U271	−52.3612	−37.5754	35.70	44.8860	16.21	15.98	19.6	2×1 bottle	1×1 bottle
286	2100		U272	−52.4721	−39.7374	35.61	44.6650	16.08	15.85	18.9	2×1 bottle	1×1 bottle
286	2200		U273	−52.5732	−39.8961	35.66	44.7476	16.11	15.87	18.6	2×1 bottle	1×1 bottle
286	2300		U274	−52.6905	−40.0700	35.25	44.3623	16.18	15.83	16.8	2×1 bottle	1×1 bottle
287	0000		U275	−52.8298	−40.2430	35.01	42.0451	14.10	13.25	22.5	2×1 bottle	1×1 bottle
287	0100		U276	−52.9735	−40.3937	34.28	38.8450	11.56	11.28	25.4	2×1 litre	1×1 litre
287	0200		U277	−53.0412	−40.4898	34.41	39.2793	11.90	11.16	24.8	2×1 litre	1×1 litre
287	0300		U278	−53.1829	−40.6563	34.22	39.4743	12.14	12.07	27.7	3×1 bottle	1×1 bottle
287	0400		U279	−53.3034	−40.8075	34.11	38.0765	10.89	10.58	25.3	2×1 bottle	1×1 bottle
287	0500		U280	−53.4207	−40.9770	33.91	35.7358	8.59	8.57	27.4	2×1 bottle	1×1 bottle
287	0600		U281	−53.5424	−41.1219	34.04	34.8823	7.53	7.29	27.6	2×1,195 ml	1,324 ml
287	0700		U282	−53.6919	−41.2899	34.71	38.7542	11.01	10.77	28.1	2×1 litre	1×1 litre
287	0800		U283	−53.8176	−41.4542	34.70	38.7078	10.97	10.65	29.9	2×1 bottle	1×1 bottle
287	0900		U284	−53.9522	−41.6341	34.69	38.4386	10.69	10.41	27.3	2×1 bottle	1×1 bottle
287	1000		U285	−54.0729	−41.8050	34.25	36.6595	9.24	8.89	25.3	2×1 bottle	1×1 bottle
287	1100		U286	−54.2228	−41.9878	34.10	36.3131	9.02	8.74	25.1	2×1 bottle	1×1 bottle
287	1255	40 (26)	S26	−54.4690	−42.2401	35.09	40.5434	12.48	12.20	22.4	*See Station Log*	
287	1500		U287	−54.6649	−42.4623	35.27	41.4661	13.23	12.93	16.9	2×1 bottle	1×1 bottle
287	1600		U288	−54.7872	−42.6564	35.27	41.5734	13.34	13.05	16.6	2×1 bottle	1×1 bottle
287	1705	41 (27)	S27	−54.8676	−42.8016	35.30	41.1714	13.45	13.19	18.3	*See Station Log*	
287	1900		U289	−54.9786	−42.9540	35.29	41.7293	13.47	13.17	17.6	2×1 bottle	1×1 bottle
287	2000		U290	−55.1108	−43.1684	34.11	36.5791	9.29	8.95	19.6	2×1 bottle	1×1 bottle
287	2100		U291	−55.2454	−43.3691	34.29	36.2575	8.77	8.39	24.7	2×1 bottle	1×1 bottle
287	2200		U292	−55.4006	−43.6580	34.90	38.2519	10.19	9.27	21.6	2×1 bottle	1×1 bottle
287	2300		U293	−55.5396	−43.7464	34.56	38.2209	10.47	9.91	22.1	2×1 bottle	1×1 bottle
288	0000		U294	−55.6900	−43.9238	34.66	38.0260	10.38	10.13	20.0	3×1 bottle	1×1 bottle
288	0100		U295	−55.8264	−44.0764	34.84	39.2195	11.36	11.19	19.3	2×1 bottle	1×1 bottle
288	0200		U296	−55.9166	−44.2046	34.79	39.0730	11.26	10.95	18.8	2×1 bottle	1×1 bottle
288	0300		U302	−55.0530	−44.3871	34.07	35.3080	7.96	7.63	16.8	2×1 bottle	1×1 bottle
288	0400		U303	−56.2076	−44.5678	34.11	35.6121	8.25	7.92	20.9	2×1 bottle	1×1 bottle
288	0500		U304	−56.3466	−44.7303	34.05	35.0596	7.71	7.42	25.7	2×1 bottle	1×1 bottle
288	0600		U305	−56.5039	−44.9129	34.10	35.5327	8.17	7.90	26.2	2×1 bottle	1×1 bottle
288	0700		U297	−56.5931	−45.0886	34.15	35.6204	8.22	7.92	22.7	2×1 bottle	1×1 bottle
288	0800		U298	−56.6151	−45.2959	34.14	35.4719	8.07	7.76	21.5	2×1 bottle	1×1 bottle
288	0900		U299	−56.6402	−45.4737	34.20	35.7100	8.28	7.98	18.7	2×1 bottle	1×1 bottle
288	1000		U300	−56.6654	−45.6781	34.21	35.7533	8.31	8.02	19.4	2×1 bottle	1×1 bottle
288	1100		U301	−56.6840	−45.8629	34.19	35.6946	8.26	7.95	16.2	2×1 bottle	1×1 bottle
288	1231	42 (28)	S28	−56.6956	−46.0459	34.13	35.5162	8.13	7.83	16.8	*See Station Log*	
288	1526		U306	−56.7074	−46.2284	34.11	35.5266	8.16	7.83	14.7	2×1 bottle	1×1 bottle
288	1610		U307	−56.7253	−46.3722	34.13	35.4678	8.07	7.71	14.2	2×1 bottle	1×1 bottle
288	1727	43 (29)	S29	−56.7502	−46.5426	34.11	35.4771	8.10	7.79	14.6	*See Station Log*	
288	1910		U308	−56.8023	−46.2212	34.13	35.2029	7.78	7.47	14.1	2×1 bottle	1×1 bottle
288	2045		U309	−56.8413	−47.1330	34.13	34.7206	7.26	6.96	14.6	2×1 bottle	1×1 bottle
288	2300		U310	−56.8793	−47.5631	34.09	32.6856	5.02	4.69	16.1	2×1 bottle	1×1 bottle
289	0100		U311	−56.9319	−47.9482	34.11	32.7660	5.08	4.75	17.5	2×1 bottle	1×1 bottle
289	0300		U312	−57.0169	−48.3270	34.09	32.4251	4.78	4.49	16.2	2×1 bottle	1×1 bottle
289	0500		U313	−57.0715	−48.6837	34.08	33.0431	5.43	5.74	14.5	3×1 bottle	1×1 bottle
289	0700		U314	−57.1283	−49.0482	34.07	33.2419	5.67	5.38	13.8	2×1 bottle	1×1 bottle
289	0900		U315	−57.2015	−44.4125	33.97	33.3274	5.85	5.58	12.6	2×1 bottle	1×1 bottle
289	1100		U316	−57.2422	−49.7760	33.88	33.3016	5.92	5.60	12.6	2×1 bottle	1×1 bottle
289	1252	44 (30)	S30	−57.6615	−49.7933	33.93	33.3181	5.89	5.57	11.6	*See Station Log*	
289	1519		U317	−58.1041	−49.7949	33.93	33.4490	6.04	5.70	10.1	2×1 bottle	1×1 bottle

Table I1. (cont.) A summary of the Underway Filtration Log for AMT-5. All times are in GMT.

SDY	*Time*	*Sta.*	*Sample*	*Lon.*	*Lat.*	*S*	*C*	T_s	*SST*	*F*	HPLC	Chl.
289	1629	45 (31)	S31	−58.2306	−49.8000	33.94	33.5572	6.11	5.75	9.5	*See Station Log*	
289	1918		U318	−58.1921	−50.0277	33.87	33.7241	6.41	6.02	9.8	2×1 bottle	1×1 bottle
289	2100		U319	−58.0977	−50.2755	33.83	33.4562	6.14	5.81	12.7	2×1 bottle	1×1 bottle
289	2300		U320	−57.9870	−50.5822	33.90	33.4707	6.06	5.72	14.0	2×1 bottle	1×1 bottle
290	0100		U321	−57.8369	−50.9018	33.88	33.3707	5.99	5.64	12.2	2×1 bottle	1×1 bottle
290	0300		U322	−57.6651	−51.2284	33.83	33.0698	5.71	5.39	11.0	2×1 bottle	1×1 bottle
290	0500		U323	−57.5114	−51.5127	33.83	33.2141	5.90	5.59	14.5	2×1 bottle	1×1 bottle
290	0700		U324	−57.3608	−51.6730	33.84	33.1523	5.80	5.47	11.5	2×1 bottle	1×1 bottle
290	0900		U325	−57.4552	−51.6733	33.80	33.1636	5.85	5.49	10.3	2×1 bottle	1×1 bottle
290	1105	46	U326	−57.6923	−51.6589	33.73	33.1358	5.88	5.56	18.6	2×1 bottle	1×1 bottle
290	1146	46	U327	−57.6982	−51.6623	33.75	33.1141	5.84	5.53	18.6	2×1 litre	1×1 litre

Table I2. A summary of the Station Filtration Log for AMT-5. All times are in GMT.

SDY	*Time*	*CTD*	*Sta.*	*Lon.*	*Lat.*	*S*	*T*	*F*	*Depths*	HPLC	Chl.	*Notes*
259	1427	1	S1	−1.0701	50.4275		17.67	1.0	2	4 reps 1l; 4 reps 0.5l (split)		
									5	3 reps 1l		
									10	3 reps 1l		
									15	3 reps 1l		
									25	3 reps 1l		
260	1625	2	S2	−8.4423	48.6735	35.55	16.80	2.2	5	3 reps 2l (each split)		
									10	2 reps 2l (each split)		
									15	2 reps 2l (each split)		
									25	2 reps 2l (each split)		
									35	3 reps 2l (each split)		
									45	2 reps 2l (each split)		
									60	3 reps 2l (each split)		
									80	2 reps 2l (each split)		
									100	2 reps 2l (each split)		
									120	2 reps 2l (each split)		
261	1025	3	S3	−13.2055	47.9834	35.63	17.48	2.6	5	3 reps 2l (each split)		
									10	2 reps 2l (each split)		
									15	2 reps 2l (each split)		
									30	*No Sample Available*		
									40	3 reps 2l (each split)		
									60	2 reps 2l (each split)		
									80	3 reps 2l (each split)		
									100	2 reps 2l (each split)		
									160	2 reps 2l (each split)		
									250	2 reps 2l (each split)		
262	1025	4	S4	−18.4773	47.1707	35.76	17.80	2.6	5	3 reps 2l	1 rep 1l	
									10	2 reps 2l	1 rep 1l	
									20	1 rep 2l	1 rep 1l	
									40	2 reps 2l	1 rep 1l	
									50	3 reps 2l	1 rep 1l	
									65	*Did Not Fire*		
									80	3 reps 2l	1 rep 1l	
									100	*Did Not Fire*		
									160	2 reps 2l	1 rep 1l	
									250	2 reps 2l	1 rep 1l	

Table I2. (cont.) A summary of the Station Filtration Log for AMT-5. All times are in GMT.

SDY	*Time*	*CTD*	*Sta.*	*Lon.*	*Lat.*	*S*	*T*	*F*	*Depths*	HPLC	Chl.	*Notes*
263	1021	5	S5	−19.9595	42.8438	35.86	19.17	1.8	5	3 reps 2l	1 rep 1l	
									10	2 reps 2l	1 rep 1l	
									20	2 reps 2l	1 rep 1l	
									30	2 reps 2l	1 rep 1l	
									40	3 reps 2l	1 rep 1l	
									50	2 reps 2l	1 rep 1l	From 2nd CTD cast.
									60	3 reps 2l	1 rep 1l	From 2nd CTD cast.
									100	2 reps 2l	1 rep 1l	From 2nd CTD cast.
									160	2 reps 2l	1 rep 1l	From 2nd CTD cast.
									250	2 reps 2l	1 rep 1l	
264	1023	6	S6	−20.0128	38.7223	36.24	22.15	1.6	5	3 reps 2l	1 rep 1l	
									10	2 reps 2l	1 rep 1l	
									20	2 reps 2l	1 rep 1l	
									40	2 reps 2l	1 rep 1l	From 2nd CTD cast.
									65	2 reps 2l	1 rep 1l	
									80	3 reps 2l	1 rep 1l	
									90	3 reps 2l	1 rep 1l	From 2nd CTD cast.
									120	2 reps 2l	1 rep 1l	
									160	2 reps 2l	1 rep 1l	From 2nd CTD cast.
									250	2 reps 2l	1 rep 1l	
265	1017	7	S8	−19.5297	35.4473	36.42	23.67	1.6	5	2 reps 2l	1 rep 1l	
									10	2 reps 2l	1 rep 1l	
									20	2 reps 2l	1 rep 1l	
									40	2 reps 2l	1 rep 1l	
									60	2 reps 2l	1 rep 1l	
									75	2 reps 2l	1 rep 1l	
									85	2 reps 2l	1 rep 1l	
									100	2 reps 2l	1 rep 1l	
									120	2 reps 2l	1 rep 1l	
									160	2 reps 2l	1 rep 1l	
									250	2 reps 2l	1 rep 1l	
268	1347	8	S9	−17.2281	32.3099	36.91	24.02	1.4	7	2×2 bottles	1×1 bottle	From nontoxic.
									10	2×2 bottles	1×1 bottle	
									20	2×2 bottles	1×1 bottle	
									40	2×2 bottles	1×1 bottle	
									60	2×1 bottles	1×1 bottle	
									75	2×2 bottles	1×1 bottle	
									100	2×2 bottles	620 ml	
									120	2×2 bottles	860 ml	
									160		*Did Not Fire*	
									250	2×2 bottles	1×1 bottle	
269	1135	9	S10	−20.9718	29.0497	37.19	24.62	1.5	7	2×2 bottles	1×1 bottle	From nontoxic.
									10	2×2 bottles	640 ml	
									20	2×2 bottles	1×1 bottle	
									40	2×2 bottles	1×1 bottle	
									80	2×2 bottles	1×1 bottle	
									120	2×2 bottles	1×1 bottle	
									140	2×2 bottles	945 ml	
									160	2×2 bottles	960 ml	
									180		*Did Not Fire*	
									250	2×2 bottles	1×1 bottle	

Table I2. (cont.) A summary of the Station Filtration Log for AMT-5. All times are in GMT.

SDY	*Time*	*CTD*	*Sta.*	*Lon.*	*Lat.*	*S*	*T*	*F*	*Depths*	HPLC	Chl.	*Notes*
270	1125	10	S11	−20.9995	24.1386	36.89	24.85	1.6	7	3×2 bottles	1×1 bottle	From nontoxic.
									10	2×2 bottles	725 ml	
									20	2×2 bottles	1×1 bottle	
									40	2×2 bottles	1×1 bottle	
									75	2×2 bottles	1×1 bottle	
									90	3×2 bottles	1×1 bottle	
									100	2×2 bottles	1×1 bottle	100 and 120 m
									120	2×2 bottles	790 ml	pooled.
									150	2×2 bottles	1,020 ml	
									250	2×2 bottles	1×1 bottle	
271	1126	11	S12	−20.5295	19.7244	36.28	25.22	3.7	2	2×1 bottles	1×1 bottle	
									7	2×1 bottles	1×1 bottle	From nontoxic.
									10	2×1 bottles	1×1 bottle	
									20	2×1 bottles	1×1 bottle	
									25	2×1 bottles	1×1 bottle	
									30	2×1 bottles	1×1 bottle	
									40	2×1 bottles	1×1 bottle	
									60	2×1 bottles	1×1 bottle	
									160	2×1 bottles	1×1 bottle	
									250	2×1 bottles	1×1 bottle	
273	1127	12	S13	−20.8702	10.9234	35.66	28.97	1.6	5	2×1 bottles	1×1 bottle	
									7	3×3,135 ml	1×1 bottle	From nontoxic.
									10	2×1 bottles	1×1 bottle	
									20	2×1 bottles	1×1 bottle	
									30	2×1 bottles	1×1 bottle	
									43	3×1 bottles	1×1 bottle	
									60	2×1 bottles	1×1 bottle	
									100	3×1 bottles	1×1 bottle	
									160	2×2 bottles	980 ml	
									250	2×2 bottles	1×1 bottle	
274	1129	13	S14	−22.4690	7.0269	34.26	28.07	1.5	2	2×2 bottles	670 ml	
									7	3×2 bottles	1×1 bottle	From nontoxic.
									20	2×2 bottles	1×1 bottle	
									30	2×2 bottles	1×1 bottle	
									47	3×1 bottles	1×1 bottle	
									65	2×2 bottles	1×1 bottle	
									80	2×2 bottles	1×1 bottle	
									120	2×2 bottles	1,020 ml	
									160	2×2 bottles	975 ml	
									250	2×2 bottles	1×1 bottle	
275	1120	14	S15	−24.1643	2.8158	35.56	27.62	1.6	2	2×2 bottles	665 ml	
									7	3×2 bottles	1×1 bottle	From nontoxic.
									20	2×2 bottles	1×1 bottle	
									40	2×2 bottles	1×1 bottle	
									60	2×2 bottles	1×1 bottle	
									75	3×1 bottles	1×1 bottle	
									100	2×2 bottles	1×1 bottle	
									125	2×2 bottles	865 ml	
									180	2×2 bottles	910 ml	
									250	2×2 bottles	1×1 bottle	

Table I2. (cont.) A summary of the Station Filtration Log for AMT-5. All times are in GMT.

SDY	*Time*	*CTD*	*Sta.*	*Lon.*	*Lat.*	*S*	*T*	*F*	*Depths*	HPLC	Chl.	*Notes*
276	1100	15	S16	−25.6631	−0.7728	36.08	26.02	1.5	2	2×2 bottles	660 ml	
									7	3×2 bottles	1×1 bottle	From nontoxic.
									20	2×2 bottles	1×1 bottle	
									40	2×2 bottles	1×1 bottle	
									50	2×2 bottles	1×1 bottle	
									60	3×1 bottles	1×1 bottle	
									80	2×2 bottles	1×1 bottle	
									100	2×2 bottles	955 ml	
									140	2×2 bottles	1,075 ml	
									250	2×2 bottles	1×1 bottle	
277	1210	16	S17	−27.3721	−4.7851	35.92	25.57	1.6	2	2×2 bottles	665 ml	
									7	3×2 bottles	1×1 bottle	From nontoxic.
									20	2×2 bottles	1×1 bottle	
									40	2×2 bottles	1×1 bottle	
									65	2×2 bottles	1×1 bottle	
									83	3×1 bottles	1×1 bottle	
									90	2×2 bottles	1×1 bottle	
									120	2×2 bottles	995 ml	
									180	2×2 bottles	910 ml	
									250	2×2 bottles	1×1 bottle	
278	1205	17	S18	−29.1148	−8.9669	36.52	26.29	1.4	2	2×2 bottles	660 ml	
									7	3×2 bottles	1×1 bottle	From nontoxic.
									20	2×2 bottles	1×1 bottle	
									60	2×2 bottles	1×1 bottle	
									100	2×2 bottles	1×1 bottle	
									120	3×1 bottles	1×1 bottle	
									140	2×2 bottles	1×1 bottle	
									160	2×2 bottles	940 ml	
									200	2×2 bottles	1,090 ml	
									250	2×2 bottles	1×1 bottle	
279	1148	18	S19	−30.7053	−12.8764	36.83	26.43	1.4	7	3×2 bottles	1×1 bottle	From nontoxic.
									20	2×2 bottles	860 ml	
									40	2×2 bottles	1×1 bottle	
									100	2×2 bottles	1×1 bottle	
									140	2×2 bottles	1×1 bottle	
									156	3×1 bottles	1×1 bottle	
									180	2×2 bottles	1×1 bottle	
									200	2×2 bottles	920 ml	
									220	2×2 bottles	670 ml	
									250	2×2 bottles	1×1 bottle	
280	1209	19	S20	−32.3624	−16.6864	37.16	25.47	1.4	2	2×2 bottles	700 ml	
									7	3×2 bottles	1×1 bottle	From nontoxic.
									50	2×1 bottles	1×1 bottle	
									100	2×2 bottles	1×1 bottle	
									120	2×2 bottles	1×1 bottle	
									141	3×1 bottles	1×1 bottle	
									160	2×2 bottles	1,070 ml	
									180	2×2 bottles	945 ml	
									200	2×2 bottles	1×1 bottle	
									250	2×2 bottles	1×1 bottle	

Table I2. (cont.) A summary of the Station Filtration Log for AMT-5. All times are in GMT.

SDY	*Time*	*CTD*	*Sta.*	*Lon.*	*Lat.*	*S*	*T*	*F*	*Depths*	HPLC	Chl.	*Notes*
281	1212	20	S21	−34.2246	−20.6623	37.11	23.89	1.5	2	2×2 bottles	410 ml	
									7	3×2 bottles	1×1 bottle	From nontoxic.
									50	2×2 bottles	1×1 bottle	
									100	2×1 bottles	1×1 bottle	
									110	2×2 bottles	1×1 bottle	
									125	2×2 bottles	1×1 bottle	
									137	3×1 bottles	1×1 bottle	
									145	2×2 bottles	1,920 ml	
									160	2×2 bottles	1,080 ml	
									180	2×2 bottles	705 ml	
									200	2×2 bottles	1×1 bottle	
									250	2×2 bottles	2,000 ml	
282	1159	21	S22	−37.2869	−23.9024	36.79	23.66	1.6	2	2×2 bottles	600 ml	
									7	3×2 bottles	1×1 bottle	From nontoxic.
									20	2×2 bottles	1×1 bottle	
									50	2×2 bottles	1×1 bottle	
									80	2×2 bottles	1×1 bottle	
									100	2×2 bottles	1×1 bottle	
									107	3×1 bottles	1×1 bottle	
									120	2×2 bottles	2,000 ml	
									140	2×2 bottles	1,065 ml	
									180	2×2 bottles	820 ml	
									200	2×2 bottles	1×1 bottle	
									250	2×2 bottles	2,000 ml	
283	1151	22	S23	−40.9842	−27.6920	36.58	20.86	2.5	2	2×2 bottles	700 ml	
									7	3×2 bottles	1×1 bottle	From nontoxic.
									20	2×2 bottles	1×1 bottle	
									35	3×1 bottles	1×1 bottle	
									50	2×1 bottles	1×1 bottle	
									60	2×2 bottles	1×1 bottle	
									75	2×2 bottles	1×1 bottle	
									95	2×2 bottles	2,000 ml	
									120	2×2 bottles	970 ml	
									160	2×2 bottles	660 ml	
									180	2×2 bottles	1×1 bottle	
									250	2×2 bottles	1,995 ml	
285	1301	24	S24	−48.8611	−35.4860	35.83	18.76	4.6	2	2×1 bottles	1×1 bottle	
									7	3×1 bottles	1×1 bottle	From nontoxic.
									20	2×1 bottles	1×1 bottle	
									35	3×1 bottles	1×1 bottle	
									45	2×1 bottles	1×1 bottle	
									55	2×1 bottles	1×1 bottle	
									70	2×1 bottles	1×1 bottle	
									90	3×1 bottles	1×1 bottle	
									120	2×1 bottles	1×1 bottle	
									160	2×1 bottles	1×1 bottle	All cryovials for
									200	2×1 bottles	1×1 bottle	S24 are wrongly
									250	2×1 bottles	1×1 bottle	marked JD 284.

Table I2. (cont.) A summary of the Station Filtration Log for AMT-5. All times are in GMT.

SDY	*Time*	*CTD*	*Sta.*	*Lon.*	*Lat.*	*S*	*T*	*F*	*Depths*	HPLC	Chl.	*Notes*
286	1231	25	S25	−51.9135	−38.8360	35.54	14.32	14.3	2	2×1 bottles	1×1 bottle	
									7	3×1 bottles	1×1 bottle	From nontoxic.
									10	2×1 bottles	1×1 bottle	
									20	2×1 bottles	1×1 bottle	
									24	3×1 bottles	1×1 bottle	
									30	2×1 bottles	1×1 bottle	
									40	2×1 bottles	1×1 bottle	
									50	2×1 bottles	1×1 bottle	
									70	3×1 bottles	1×1 bottle	
									100	2×1 bottles	1×1 bottle	
									160	2×1 bottles	1×1 bottle	
									250	2×1 bottles	1×1 bottle	
287	1255	26	S26	−54.4690	−42.2401	35.09	12.20	22.4	2	2×1 bottles	1×1 bottle	
									7	3×1 bottles	1×1 bottle	From nontoxic.
									10	2×1 bottles	1×1 bottle	
									25	3×1 bottles	1×1 bottle	
									35	2×1 bottles	1×1 bottle	
									50	3×1 bottles	1×1 bottle	
									65	2×1 bottles	1×1 bottle	
									75	2×1 bottles	1×1 bottle	
									90	2×1 bottles	1×1 bottle	
									125	2×1 bottles	1×1 bottle	
									160	2×1 bottles	1×1 bottle	
									250	2×1 bottles	1×1 bottle	
287	1705	27	S27	−54.8676	−42.8016	35.30	13.19	18.3	2	2×1 bottles	1×1 bottle	
									7	3×1 bottles	1×1 bottle	From nontoxic.
									10	2×1 bottles	1×1 bottle	
									20	2×1 bottles	1×1 bottle	
									35	2×1 bottles	1×1 bottle	
									50	2×1 bottles	1×1 bottle	
									70	2×1 bottles	1×1 bottle	
									90	2×1 bottles	1×1 bottle	
									120	2×1 bottles	1×1 bottle	
									150	2×1 bottles	1×1 bottle	
									200	2×1 bottles	1×1 bottle	
									300	2×1 bottles	1×1 bottle	Validation CDT.
288	1231	28	S28	−56.6956	−46.0459	34.13	7.83	14.9	2	2×1 bottles	1×1 bottle	
									7	3×1 bottles	1×1 bottle	From nontoxic
									10	2×1 bottles	1×1 bottle	
									20	2×1 bottles	1×1 bottle	
									35	2×1 bottles	1×1 bottle	
									50	2×1 bottles	1×1 bottle	
									60	2×1 bottles	1×1 bottle	
									80	2×1 bottles	1×1 bottle	
									100	2×1 bottles	1×1 bottle	
									120	2×1 bottles	1×1 bottle	
									160	2×1 bottles	1×1 bottle	
									250	2×1 bottles	1×1 bottle	

Table I2. (cont.) A summary of the Station Filtration Log for AMT-5. All times are in GMT.

SDY	*Time*	*CTD*	*Sta.*	*Lon.*	*Lat.*	*S*	*T*	*F*	*Depths*	HPLC	Chl.	*Notes*
288	1727	29	S29	−56.7502	−46.5426	34.11	7.79	14.6	2	2×1 bottles	1×1 bottle	
									7	3×1 bottles	1×1 bottle	From nontoxic.
									10	2×1 bottles	1×1 bottle	
									20	2×1 bottles	1×1 bottle	
									28	2×1 bottles	1×1 bottle	
									35	2×1 bottles	1×1 bottle	
									45	2×1 bottles	1×1 bottle	
									55	2×1 bottles	1×1 bottle	
									65	2×1 bottles	1×1 bottle	
									90	2×1 bottles	1×1 bottle	
									110	2×1 bottles	1×1 bottle	
									160	2×1 bottles	1×1 bottle	
									250	2×1 bottles	1×1 bottle	
289	1252	30	S30	−57.6615	−49.7933	33.93	5.57	11.6	2	2×1 bottles	1×1 bottle	
									7	3×1 bottles	1×1 bottle	From nontoxic.
									10	2×1 bottles	1×1 bottle	
									20	2×1 bottles	1×1 bottle	
									30	2×1 bottles	1×1 bottle	
									40	2×1 bottles	1×1 bottle	
									60	2×1 bottles	1×1 bottle	
									80	2×1 bottles	1×1 bottle	
									100	2×1 bottles	1×1 bottle	
									120	2×1 bottles	1×1 bottle	
									150	2×1 bottles	1×1 bottle	
									180	2×1 bottles	1×1 bottle	
									250	2×1 bottles	1×1 bottle	
289	1629	31	S31	−58.2306	−49.8000	33.94	5.75	9.5	2	2×1 bottles	1×1 bottle	
									7	3×1 bottles	1×1 bottle	From nontoxic.
									10	2×1 bottles	1×1 bottle	
									20	2×1 bottles	1×1 bottle	
									30	2×1 bottles	1×1 bottle	
									40	2×1 bottles	1×1 bottle	
									60	2×1 bottles	1×1 bottle	
									80	2×1 bottles	1×1 bottle	
									100	2×1 bottles	1×1 bottle	
									120	2×1 bottles	1×1 bottle	
									150	2×1 bottles	1×1 bottle	
									180	2×1 bottles	1×1 bottle	
									250	2×1 bottles	1×1 bottle	

Table J1. A summary of the Nutrients Sample Log for AMT-5. All times are in GMT. CTD cast 23 was aborted, so no samples were collected from this cast.

Date	*SDY*	*CTD*	*Depths*	*Lon.*	*Lat.*	*Date*	*SDY*	*CTD*	*Depths*	*Lon.*	*Lat.*
16 Sep.	259	1	3	−1.39	50.28	2 Oct.	275	14	11	−24.10	2.49
17 Sep.	260	2	7	−8.27	48.40	3 Oct.	276	15	10	−25.40	−0.47
18 Sep.	261	3	10	−13.12	47.59	4 Oct.	277	16	11	−27.22	−4.47
19 Sep.	262	4	9	−18.29	47.11	5 Oct.	278	17	11	−29.07	−8.58
20 Sep.	263	5/5a	11	−19.58	42.51	6 Oct.	279	18	11	−30.42	12.53
21 Sep.	264	6	11	−20.00	38.43	7 Oct.	280	19	11	−32.22	16.41
22 Sep.	265	7	4	−19.32	35.27	8 Oct.	281	20	11	−34.14	20.40
22 Sep.	265	7	11	−19.32	35.27	9 Oct.	282	21	10	−37.17	23.54
25 Sep.	268	8	8	−17.14	32.19	10 Oct.	283	22	11	−40.59	27.42
26 Sep.	269	9	8	−20.58	20.03	11 Oct.	284	23	0	−44.52	31.37
27 Sep.	270	10	10	−20.60	24.08	12 Oct.	285	24	11	−48.52	35.29
28 Sep.	271	11	10	−20.32	19.43	13 Oct.	286	25	11	−51.55	38.50
30 Sep.	273	12	11	−20.52	10.55	14 Oct.	287	26	11	−54.27	42.14
1 Oct.	274	13	11	−22.29	7.02						

Table K1. A summary of the Nitrate Sample Log for AMT-5. All times are in GMT. CTD cast 23 was aborted, so no samples were collected from this cast.

Date	*SDY*	*CTD*	*Depth* [m]	*Lon.*	*Lat.*	*Date*	*SDY*	*CTD*	*Depth* [m]	*Lon.*	*Lat.*
18 Sep.	261	3	15	−13.12	47.59	4 Oct.	277	16	20	−27.22	−4.47
19 Sep.	262	4	20	−18.29	47.11	5 Oct.	278	17	20	−29.07	−8.58
20 Sep.	263	5/5a	20	−19.58	42.51	6 Oct.	279	18	40	−30.42	−12.53
21 Sep.	264	6	20	−20.00	38.43	7 Oct.	280	19	50	−32.22	−16.41
22 Sep.	265	7	20	−19.32	35.27	8 Oct.	281	20	60	−34.14	−20.40
26 Sep.	269	9	20	−20.58	20.03	9 Oct.	282	21	50	−37.17	−23.54
27 Sep.	270	10	20	−20.60	24.08	10 Oct.	283	22	20	−40.59	−27.42
28 Sep.	271	11	10	−20.32	19.43	11 Oct.	284	23		−44.52	−31.37
30 Sep.	273	12	10	−20.52	10.55	12 Oct.	285	24	20	−48.52	−35.29
1 Oct.	274	13	20	−22.29	7.02	13 Oct.	286	25	10	−51.55	−38.50
2 Oct.	275	14	20	−24.10	2.49	14 Oct.	287	26	10	−54.27	−42.14
3 Oct.	276	15	20	−25.40	−0.47	15 Oct.	288	27	10		

Table L1. A summary of the OPC Sample Log for AMT-5. All times are in GMT. The Biomass, >2,000 μm, and OPC column entries are from 200 m samples.

Date	*SDY*	*Time*	*Biomass*	*> 2,000 μm*	*OPC*	*20 m*	*Extras*	*No.*	*Underway*	*Time*	*Duration*
16 Sep.	259	1400				1	Not thru OPC.		1	1843	1.88
17 Sep.	260	1600	1	1		1	100 m only.				
18 Sep.	261	1000	1	1	1				1	0730	1.50
18 Sep.	261								1	1430	2.00
18 Sep.	261								1	1850	1.67
19 Sep.	262	1000	1		1	1			1	0730	1.86
19 Sep.	262								1	1230	2.17
20 Sep.	263	1000	1	1	1	1			1	0100	2.17
20 Sep.	263								1	1500	3.00
20 Sep.	263								1	1941	2.00

Table L1. (cont.) A summary of the OPC Sample Log for AMT-5. All times are in GMT.

Date	*SDY*	*Time*	*Biomass*	*>2,000 μm*	*OPC*	*20 m*	*Extras*	*No.*	*Underway*	*Time*	*Duration*
21 Sep.	264	1000	1	1	1	1			1	1440	3.67
21 Sep.	264	2200	1	1	1						
22 Sep.	265	0700	1	1	1		200 m	2	1	1240	5.42
22 Sep.	265	1000	1	1	1	1					
25 Sep.	268	1330	1	1	1						
26 Sep.	269	1100	1	1	1	1			1	0815	2.00
26 Sep.	269	2300	1	1	1				1	1400	2.00
27 Sep.	270	1100	1	1	1	1			1	0640	4.25
27 Sep.	270	2300	1	1	1				1	1355	4.75
28 Sep.	271	1100	1	1	1	1			1	0915	1.50
28 Sep.	271	2300	1	1	1				1	1525	1.77
29 Sep.	272	1100	1	1	1				1	1400	2.17
30 Sep.	273	1100	1	1	1	1			1	0810	2.35
30 Sep.	273								1	1331	1.83
30 Sep.	273								1	2034	3.12
1 Oct.	274	1100	1	1	1	1			1	0900	1.75
1 Oct.	274								1	1650	2.50
1 Oct.	274								1	2142	1.92
2 Oct.	275	1100	1	1	1	1			1	0854	1.70
2 Oct.	275	2300	1	1	1				1	1645	2.33
3 Oct.	276	1030	1	1	1	1			1	1520	3.00
4 Oct.	277	1130	1	1	1	1			1	0955	1.67
4 Oct.	277								1	1700	0.80
4 Oct.	277								1	2130	2.67
5 Oct.	278	1130	1	1	1	1			1	1500	2.50
5 Oct.	278								1	2145	4.75
6 Oct.	279	1130	1	1	1	1			1	1700	2.67
6 Oct.	279								1	2140	1.50
7 Oct.	280	1130	1	1	1	1			1	0930	1.75
7 Oct.	280								1	1530	3.67
8 Oct.	281	1130	1	1	1	1	200 m thru OPC	1	1	0920	0.47
8 Oct.	281								1	1545	3.92
8 Oct.	281								1	2115	12.67
9 Oct.	282	1130	1	1	1	1			1	1555	4.33
9 Oct.	282	2359	1	1	1				1	2130	2.17
10 Oct.	283	1130	1	1	1	1			1	1810	1.55
10 Oct.	283	2359	1	1	1						
11 Oct.	284	1130	1	1	1	1	200 m 1/2 thru OPC	1	1	0945	2.00
11 Oct.	284	1130					20 m not thru OPC	1	1	1555	3.17
12 Oct.	285	1230	1	1	1	1			1	1000	3.00
12 Oct.	285	0100	1	1	1				1	1655	
13 Oct.	286	1200	1	1	1	1			1	1040	1.00
13 Oct.	286	0100	1	1	1				1	1542	2.75
13 Oct.	286								1	2142	1.00
13 Oct.	286								1	0215	0.58
14 Oct.	287	1230	1	1	1	1			1	1530	2.17
14 Oct.	287	0100							1	2210	0.50
14 Oct.	287								1	2340	0.50
15 Oct.	288	1200	1	1	1	1			1	0950	0.50
15 Oct.	288								1	1635	4.42
16 Oct.	289	1230	1	1	1	1			1	1115	1.42
16 Oct.	289								1	1435	4.42
		Total	38	37	37	26		5	57		

Table M1. A summary of the CHN Sample Log for AMT-5. All times are in GMT and all volumes are in liters. For the zooplankton samples, all portions were 50. The S_1, S_2, and S_3, zooplankton entries correspond to the 1,000–2,000 μm, 500–1,000 μm, and 200–500 μm size fractions, respectively. For the particulate samples, the V_1, V_2, V_3, and V_4 entries correspond to $< 200\,\mu$m (surface), $< 5\,\mu$m (surface), $< 200\,\mu$m (chlorophyll maximum), and $< 5\,\mu$m (chlorophyll maximum), respectively. The fractional numbers in front of the particulate sample numbers are the filtered volumes in liters. The blanks on SDY 277 and 281 are GF/F blanks, and the blank on SDY 273 is an in-line total.

Zooplankton									*Particulates*				
SDY	*Sta.*	*Net*	*Vol.*	*Tray*	S_1	S_2	S_3	*Blanks*	*Tray*	V_1	V_2	V_3	V_4
260	1600	52	1.00	1	B1-3	B4-6	B7-9		1	0.50 A1-3	0.25 A4-6	0.25 A7-9	0.25 A10-12
261	1000	26	0.50	1	D1-3	D4-6	D7-9		1	0.50 C1-3	0.50 C4-6	0.50 C7-9	0.50 C10-12
262	1000	26	0.50	2	A1-3	A4-6	A7-9		2	0.50 B1-3	0.50 B4-6	0.50 B7-9	0.50 B10-12
263	1000	26	0.50	3	A1-3	A4-6	A7-9	A10-12	2	0.50 D1-3	0.50 D4-6	0.50 D7-9	0.50 D10-12
264	1000	26	0.50	3	C1-3	C4-6	C7-9		3	0.50 D1-3	0.50 D4-6	0.50 D7-9	0.50 D10-12
264	2200	26	0.50	3	E1-3	E4-6	E7-9						
265	1000	26	0.50	3	F1-3	F4-6	F7-9		3	0.50 G1-3	0.50 G4-6	0.50 G7-9	0.50 G10-12
265	0700	26	0.50	3	H1-3	H4-6	H7-9	H10-12					
268	1330	26	0.50	4	B1-3	B4-6	B7-9		4	0.50 A1-3	0.50 A4-6	0.50 A7-9	0.50 A10-12
269	1100	26	0.50	4	C1-3	C4-6	C7-9	C10-12	4	0.50 D1-3	0.50 D4-6	0.50 D7-9	0.50 D10-12
270	1100	26	0.50	5	B1-3	B4-6	B7-9		5	0.50 A1-3	0.50 A4-6	0.50 A7-9	0.50 A10-12
270	2300	26	1.00	5	C1-3	C4-6	C7-9						
271	1100	26	1.00	6	A1-3	A4-6	A7-9		5	0.50 D1-3	0.50 D4-6	0.50 D7-9	0.50 D10-12
271	2300	26	1.00	6	B1-3	B4-6	B7-9						
272	1100	26	0.50	6	C1-3	C4-6	C7-9	C10-12					
273	1100	26	1.00	7	B1-3	B4-6	B7-9	B10-12	7	0.50 A1-3	0.50 A4-6	0.50 A7-9	0.50 A10-12
274	1100	26	0.50	7	D1-3	D4-6	D7-9		7	0.50 C1-3	0.50 C4-6	0.50 C7-9	0.50 C10-12
275	1100	26	0.50	8	B1-3	B4-6	B7-9		8	0.50 A1-3	0.50 A4-6	0.50 A7-9	0.50 A10-12
275	2300	26	1.00	8	C1-3	C4-6	C7-9						
276	1030	26	0.50	8	E1-3	E4-6	E7-9	E10-12	8	0.50 D1-3	0.50 D4-6	0.50 D7-9	0.50 D10-12
277	1130	26	1.00	9	B1-3	B4-6	B7-9	B10-12	9	0.50 A1-3	0.50 A4-6	0.50 A7-9	0.50 A10-12
278	1130	26	0.50	9	D1-3	D4-6	D7-9		9	0.50 C1-3	0.50 C4-6	0.50 C7-9	0.50 C10-12
279	1130	26	0.50	10	B1-3	B4-6	B7-9	B10-12	10	0.50 A1-3	0.50 A4-6	0.50 A7-9	0.50 A10-12
280	1130	26	0.50	10	D1-3	D4-6	D7-9		10	1.00 C1-3	1.00 C4-6	0.50 C7-9	0.50 C10-12
281	1130	26	0.50	10	F1-3	F4-6	F7-9	F10-12	10	1.00 E1-3	1.00 E4-6	0.50 E7-9	0.50 E10-12
282	1130	26	0.50	11	B1-3	B4-6	B7-9		11	1.00 A1-3	1.00 A4-6	0.50 A7-9	0.50 A10-12
282	2400	26	1.00	11	C1-3	C4-6	C7-9						
283	1130	26	0.50	12	B1-3	B4-6	B7-9	B10-12	12	0.50 A1-3	0.50 A4-6	0.50 A7-9	0.50 A10-12
283	2400	26	1.00	12	C1-3	C4-6	C7-9						
284	1130	26	0.50	12	E1-3	E4-6	E7-9		12	0.50 D1-3	0.50 D4-6		
285	1230	26	0.50	13	B1-3	B4-6	B7-9		13	0.50 A1-3	0.50 A4-6	0.50 A7-9	0.50 A10-12
285	0100	26	1.00	13	C1-3	C4-6	C7-9						
286	1200	26	1.00	13	E1-3	E4-6	E7-9		13	0.50 D1-2	0.50 D3-5	0.50 D6-8	0.50 D9-11
286	0100	26	1.00	13	F1-3	F4-6	F7-9						
287	1230	26	1.00	14	B1-3	B4-6	B7-9		14	0.50 A1-3	0.50 A4-6	0.50 A7-9	0.50 A10-12
287	0100	26	1.00	14	C1-3	C4-6	C7-9						
288	1200	26	0.50	14	E1-3	E4-6	E7-9		14	0.50 D1-3	0.50 D4-6	0.50 D7-9	0.50 D10-12
289	1230	26	0.50	14	G1-3	G4-6	G7-9		14	0.50 F1-3	0.50 F4-6	0.50 F7-9	0.50 F10-12

Table N1. A summary of the Microzooplankton Sample Log for AMT-5. All times are in GMT.

Date	*SDY*	*Longitude*	*Latitude*	*CTD*	*Depths* [m]
18 September	261	−13.2058	47.9833	3	5, 10, 40, 100
19 September	262	−18.4803	47.1727	4	5, 20, 50, 80
20 September	263	−19.9615	42.8430	5	5, 20, 40, 80
21 September	264	−20.0117	38.7167	6	5, 20, 40, 65, 80, 100
22 September	265	−19.5238	35.4460	7	5, 20, 40, 60, 85, 100
26 September	269	−20.9677	29.0473	9	7, 20, 40, 80, 120, 130
27 September	270	−20.9987	24.1360	10	7, 20, 40, 75, 90, 100
28 September	271	−20.5270	19.7193	11	2, 10, 20, 30, 40, 100
30 September	273	−20.8697	10.9212	12	5, 20, 30, 42, 80, 100
1 October	274	−22.4690	7.0265	13	2, 20, 40, 48, 60, 100
2 October	275	−24.1642	2.8173	14	2, 20, 40, 60, 75, 100
3 October	276	−25.6630	−0.7745	15	2, 20, 40, 60, 80, 100
4 October	277	−27.3678	−4.7857	16	2, 20, 40, 65, 80, 100
5 October	278	−29.1157	−8.9663	17	2, 20, 60, 100, 120, 130
6 October	279	−30.7057	−12.8765	18	7, 20, 40, 100, 160, 180
7 October	280	−32.3630	−16.6843	19	2, 50, 100, 120, 140, 160
8 October	281	−34.2227	−20.6633	20	2, 20, 110, 137, 160
9 October	282	−37.2868	−23.9025	21	2, 20, 50, 80, 110, 140
10 October	283	−40.6905	−27.6905	22	2, 20, 35, 50, 75, 95
12 October	285	−48.8618	−35.4890	24	2, 20, 35, 55, 70, 90
13 October	286	−51.9128	−38.8367	25	2, 10, 20, 24, 40, 70
14 October	287	−54.4580	−42.2392	26	2, 10, 25, 35, 50, 90

Table O1. A summary of the DNA Extractions in DOC Buffer Log for AMT-5. All times are in GMT.

CTD No.	*DNA No.*	*Genus and Species*	*No.*	*SDY*	*Date*
2	1	*Neogloboquadrina pachyderma*	1	260	17 September
	2	*Globorotalia inflata*	1	260	17 September
	3	*Globigerina bulloides*	1	260	17 September
	4	*Globigerina bulloides*	1	260	17 September
	5	*Globigerinella siphonifera*	1	260	17 September
	14	*Neogloboquadrina pachyderma*	1	261	18 September
	100	*Globigerina bulloides*	3	266	23 September
3	6	*Globorotalia scitula*	1	261	18 September
	7	*Globigerinoides sacculifer*	1	261	18 September
	8	*Globigerinoides sacculifer*	1	261	18 September
	9	*Globigerinoides sacculifer*	1	261	18 September
	10	*Globigerinella siphonifera*	1	261	18 September
	11	*Globorotalia inflata*	1	261	18 September
	12	*Globorotalia inflata*	1	261	18 September
	13	*Neogloboquadrina dutertrei* (incompta)	1	261	18 September
4	15	*Globorotalia scitula*	1	262	19 September
	16	*Globorotalia scitula*	1	262	19 September
	17	*Globorotalia scitula*	5	262	19 September
	18	*Neogloboquadrina pachyderma*	1	262	19 September
	19	*Neogloboquadrina pachyderma*	1	262	19 September
	20	*Neogloboquadrina pachyderma*	1	262	19 September
	21	*Neogloboquadrina pachyderma*	1	262	19 September
	22	*Neogloboquadrina pachyderma*	1	262	19 September
	23	*Globigerina incompta*	1	262	19 September
	24	*Orbulina universa*	1	262	19 September
	25	*Orbulina universa*	1	262	19 September
	26	*Orbulina universa*	1	262	19 September

Table O1. (cont.) A summary of the DNA Extractions in DOC Buffer Log for AMT-5. All times are in GMT.

CTD No.	*DNA No.*	*Genus and Species*	*No.*	*SDY*	*Date*
4	27	*Globigerinoides ruber* (pink variety)	1	262	19 September
	28	*Globigerinoides ruber* (white variety)	1	262	19 September
	101	*Globigerinoides ruber* (white variety)	6	266	23 September
5	29	*Orbulina universa*	1	263	20 September
	30	*Orbulina universa*	1	263	20 September
	31	*Orbulina universa*	1	263	20 September
	32	*Globorotalia scitula*	1	263	20 September
	33	*Globorotalia scitula*	3	263	20 September
	34	*Globigerinoides ruber* (white variety)	1	263	20 September
	35	*Globigerinoides ruber* (white variety)	1	263	20 September
	36	*Globigerinoides sacculifer*	1	263	20 September
	37	*Globigerinoides sacculifer*	1	263	20 September
	38	*Globigerinoides sacculifer*	1	263	20 September
	39	*Globigerinella siphonifera*	1	263	20 September
	40	*Globigerinella siphonifera*	1	263	20 September
	41	*Globigerinella siphonifera*	1	263	20 September
	42	*Globigerinita minuta*	1	263	20 September
6	43	*Orbulina universa*	1	264	21 September
	44	*Orbulina universa*	1	264	21 September
	45	*Orbulina universa*	1	264	21 September
	46	*Orbulina universa*	1	264	21 September
	47	*Orbulina universa*	1	264	21 September
	48	*Globigerinoides ruber* (pink variety)	1	264	21 September
	49	*Globigerinoides ruber* (pink variety)	1	264	21 September
	50	*Globigerinoides ruber* (pink variety)	1	264	21 September
	51	*Globigerinoides ruber* (pink variety)	5	264	21 September
	52	*Globigerinoides sacculifer*	1	264	21 September
	53	*Globigerinoides sacculifer*	1	264	21 September
	54	*Globigerinoides sacculifer*	1	264	21 September
	55	*Hastigerina pelagica*	1	264	21 September
	56	*Hastigerina pelagica*	1	264	21 September
	57	*Hastigerina pelagica*	1	264	21 September
	58	*Hastigerina pelagica*	7	264	21 September
	59	*Globigerinoides conglobatus*	1	264	21 September
	60	*Globigerinoides conglobatus*	1	264	21 September
	61	*Globigerinoides conglobatus*	1	264	21 September
	62	*Globigerinoides conglobatus*	1	264	21 September
	63	*Globigerinoides conglobatus*	6	264	21 September
	64	*Globorotalia scitula*	1	264	21 September
	65	*Globigerinita glutinata*	1	264	21 September
	66	*Globigerinita glutinata*	1	264	21 September
	67	*Globigerinita glutinata*	3	264	21 September
	68	*Globigerinita glutinata*	2	264	21 September
7	69	*Orbulina universa*	1	265	22 September
	70	*Orbulina universa*	1	265	22 September
	71	*Orbulina universa*	1	265	22 September
	72	*Orbulina universa*	1	265	22 September
	73	*Orbulina universa*	1	265	22 September
	74	*Orbulina universa*	1	265	22 September
	75	*Orbulina universa*	1	265	22 September
	76	*Orbulina universa*	1	265	22 September
	77	*Orbulina universa*	1	265	22 September
	78	*Orbulina universa*	1	265	22 September
	79	*Globigerinita glutinata*	1	265	22 September
	80	*Globigerinita glutinata*	1	265	22 September

Table O1. (cont.) A summary of the DNA Extractions in DOC Buffer Log for AMT-5. All times are in GMT.

CTD No.	*DNA No.*	*Genus and Species*	*No.*	*SDY*	*Date*
7	81	*Globigerinita glutinata*	5	265	22 September
	82	*Hastigerina pelagica*	1	265	22 September
	83	*Hastigerina pelagica*	1	265	22 September
	84	*Hastigerina pelagica*	5	265	22 September
	85	*Globigerinella siphonifera*	1	265	22 September
	86	*Globigerinella siphonifera*	1	265	22 September
	87	*Globigerinella siphonifera*	2	265	22 September
	88	*Globigerinoides ruber* (pink variety)	1	265	22 September
	89	*Globigerinoides ruber* (pink variety)	1	265	22 September
	90	*Globigerinoides ruber* (pink variety)	5	265	22 September
	91	*Globigerinoides conglobatus*	1	265	22 September
	92	*Globigerinoides conglobatus*	1	265	22 September
	93	*Globigerinoides conglobatus*	5	265	22 September
	94	*Globigerinoides ruber*	1	265	22 September
	95	*Globigerinoides sacculifer*	1	265	22 September
	96	*Globigerinoides sacculifer*	1	265	22 September
	97	*Globigerinoides sacculifer*	7	265	22 September
	98	*Globorotalia scitula*	3	265	22 September
	99	*Globorotalia hirsuta* (juveniles)	1	265	22 September
8	102	*Orbulina universa*	1	268	25 September
	103	*Orbulina universa*	1	268	25 September
	104	*Orbulina universa*	1	268	25 September
	105	*Globigerinella siphonifera*	1	268	25 September
	106	*Globigerinella siphonifera*	1	268	25 September
	107	*Globigerinella siphonifera*	1	268	25 September
	108	*Globigerinella siphonifera*	1	268	25 September
	109	*Globigerinella siphonifera*	1	268	25 September
	110	*Globigerinella siphonifera*	1	268	25 September
	111	*Globigerinoides sacculifer*	1	268	25 September
	112	*Globorotalia truncatulinoides*	4	268	25 September
	113	*Tenuitella fleisheri* (?)	3	268	25 September
	114	*Tenuitella fleisheri* (?)	1	268	25 September
	115	*Globigerinita glutinata*	1	268	25 September
	116	*Globigerinita glutinata*	1	268	25 September
	117	*Globigerinita glutinata*	1	268	25 September
	118	*Hastigerina pelagica*	1	268	25 September
	119	*Hastigerina pelagica*	1	268	25 September
	120	*Globigerinoides ruber*	4	268	25 September
9	121	*Globigerinella siphonifera*	1	269	26 September
	122	*Globigerinella siphonifera*	1	269	26 September
	123	*Globigerinella siphonifera*	1	269	26 September
	124	*Globigerinoides ruber* (pink variety)	1	269	26 September
	125	*Globigerinoides ruber* (pink variety)	2	269	26 September
	126	*Globorotalia scitula* (juveniles?)	1	269	26 September
	127	*Globorotalia scitula* (juveniles?)	2	269	26 September
	128	*Globigerinita glutinata*	1	269	26 September
	129	*Globigerinita glutinata*	1	269	26 September
	130	*Globorotalia truncatulinoides*	1	269	26 September
	131	*Globigerina incompta*	1	269	26 September
	132	*Globigerinoides sacculifer*	1	269	26 September
	133	*Globigerinoides sacculifer*	1	269	26 September
	134	*Hastigerina pelagica*	1	269	26 September
	135	*Acantharea sp.*	30	269	26 September
10	136	*Orbulina universa*	1	270	27 September
	137	*Orbulina universa*	1	270	27 September

Table O1. (cont.) A summary of the DNA Extractions in DOC Buffer Log for AMT-5. All times are in GMT.

CTD No.	*DNA No.*	*Genus and Species*	*No.*	*SDY*	*Date*
10	138	*Orbulina universa*	1	270	27 September
	139	*Orbulina universa*	10	270	27 September
	140	*Globigerinoides ruber* (pink variety?)	1	270	27 September
	141	*Globigerinoides ruber* (pink variety?)	1	270	27 September
	142	*Globigerinoides ruber* (pink variety?)	1	270	27 September
	143	*Globigerinoides ruber* (pink variety?)	1	270	27 September
	144	*Globigerinoides ruber* (pink variety?)	1	270	27 September
	145	*Globigerinoides ruber* (pink variety?)	10	270	27 September
	146	*Globorotalia menardii*	1	270	27 September
	147	*Globorotalia menardii*	1	270	27 September
	148	*Globorotalia menardii*	5	270	27 September
	149	*Globorotalia hirsuta*	1	270	27 September
	150	*Globigerinita glutinata*	1	270	27 September
	151	*Globigerinita glutinata*	1	270	27 September
	152	*Globigerinita glutinata*	1	270	27 September
	153	*Globigerinita glutinata*	1	270	27 September
	154	*Globigerinita glutinata*	1	270	27 September
	155	*Globigerinita glutinata*	13	270	27 September
	156	*Tenuitella fleisheri/parkerae* (?)	1	270	27 September
	157	*Tenuitella fleisheri/parkerae* (?)	1	270	27 September
	158	*Tenuitella fleisheri/parkerae* (?)	2	270	27 September
	159	*Globigerinoides sacculifer*	14	270	27 September
	160	*Globigerinoides sacculifer*	1	270	27 September
	161	*Globigerinoides conglobatus*	7	270	27 September
	162	*Globigerinoides conglobatus*	1	270	27 September
	163	*Globigerina bulloides*	1	270	27 September
	164	*Neogloboquadrina dutertrei*	1	270	27 September
	165	*Neogloboquadrina dutertrei*	1	270	27 September
	166	*Pulleniatina obliquiloculata*	1	270	27 September
	167	*Globorotalia scitula*	1	270	27 September
11	168	*Globorotalia scitula*	1	271	28 September
	169	*Globorotalia scitula*	1	271	28 September
	170	*Globorotalia scitula*	1	271	28 September
	171	*Globorotalia scitula*	5	271	28 September
	172	*Globorotalia scitula*	10	271	28 September
	173	*Globorotalia scitula*	30	271	28 September
	174	*Orbulina universa*	1	271	28 September
	175	*Orbulina universa*	1	271	28 September
	176	*Orbulina universa*	1	271	28 September
	177	*Orbulina universa*	1	271	28 September
	178	*Orbulina universa*	1	271	28 September
	179	*Orbulina universa*	1	271	28 September
	180	*Orbulina universa*	1	271	28 September
	181	*Orbulina universa*	1	271	28 September
	182	*Globorotalia crassaformis*	1	271	28 September
	183	*Globorotalia inflata*	1	271	28 September
	184	*Globorotalia inflata*	1	271	28 September
	185	*Globorotalia inflata*	1	271	28 September
	186	*Globorotalia inflata*	5	271	28 September
	187	*Globorotalia inflata*	20	271	28 September
	188	*Turborotalita quinqueloba* (?)	1	271	28 September
	189	*Turborotalita quinqueloba* (?)	1	271	28 September
	190	*Turborotalita quinqueloba* (?)	1	271	28 September
	191	*Turborotalita quinqueloba* (?)	1	271	28 September
	192	*Turborotalita quinqueloba* (?)	6	271	28 September

Table O1. (cont.) A summary of the DNA Extractions in DOC Buffer Log for AMT-5. All times are in GMT.

CTD No.	*DNA No.*	*Genus and Species*	*No.*	*SDY*	*Date*
11	193	*Turborotalita quinqueloba* (?)	25	271	28 September
	194	*Neogloboquadrina pachyderma*	1	271	28 September
	195	*Neogloboquadrina pachyderma*	1	271	28 September
	196	*Turborotalita humilis*	1	271	28 September
	197	*Neogloboquadrina pachyderma*	1	271	28 September
	198	*Neogloboquadrina pachyderma*	1	271	28 September
	199	*Neogloboquadrina pachyderma*	6	271	28 September
	200	*Neogloboquadrina pachyderma*	25	271	28 September
	201	*Globigerinita uvula*	1	271	28 September
	221	*Globigerinita glutinata*	1	272	29 September
	222	*Globigerinita glutinata*	3	272	29 September
	223	*Tenuitella fleisheri/quinqueloba* (?)	9	272	29 September
	224	*Globigerinoides sacculifer*	1	272	29 September
	225	*Globigerinoides sacculifer*	7	272	29 September
	226	*Globigerinoides ruber*	1	272	29 September
	227	*Globigerinoides ruber*	8	272	29 September
	228	*Globorotalia scitula*	7	272	29 September
None	202	*Orbulina universa*	1	272	29 September
	203	*Orbulina universa*	1	272	29 September
	204	*Orbulina universa*	1	272	29 September
	205	*Orbulina universa*	1	272	29 September
	206	*Orbulina universa*	1	272	29 September
	207	*Globorotalia menardii*	1	272	29 September
	208	*Globorotalia menardii*	1	272	29 September
	209	*Neogloboquadrina dutertrei*	1	272	29 September
	210	*Neogloboquadrina dutertrei*	1	272	29 September
	211	*Neogloboquadrina dutertrei*	3	272	29 September
	212	*Neogloboquadrina dutertrei*	1	272	29 September
	213	*Hastigerina pelagica*	1	272	29 September
	214	*Hastigerina pelagica*	1	272	29 September
	215	*Globigerinoides sacculifer*	1	272	29 September
	216	*Globigerinoides sacculifer*	1	272	29 September
	217	*Globigerinoides sacculifer*	5	272	29 September
	218	*Globigerinoides ruber* (pink variety)	1	272	29 September
	219	*Globigerinoides ruber* (pink variety)	1	272	29 September
	220	*Globigerinoides ruber* (pink variety)	16	272	29 September
	242	*Pulleniatina obliquiloculata*	1	273	30 September
	243	*Beella digitata*	1	273	30 September
	244	*Globorotalia menardii*	1	273	30 September
	253	*Globigerinita glutinata*	3	273	30 September
12	229	*Orbulina universa*	1	273	30 September
	230	*Orbulina universa*	1	273	30 September
	231	*Orbulina universa*	1	273	30 September
	232	*Orbulina universa*	1	273	30 September
	233	*Orbulina universa*	1	273	30 September
	234	*Orbulina universa*	1	273	30 September
	235	*Globorotalia crassaformis*	1	273	30 September
	236	*Globorotalia crassaformis*	1	273	30 September
	237	*Globorotalia crassaformis*	2	273	30 September
	238	*Globorotalia menardii*	1	273	30 September
	239	*Globorotalia menardii*	1	273	30 September
	240	*Globorotalia menardii*	1	273	30 September
	241	*Neogloboquadrina dutertrei*	1	273	30 September
	245	*Globigerinita glutinata*	1	273	30 September
	247	*Globigerinita glutinata*	3	273	30 September

Table O1. (cont.) A summary of the DNA Extractions in DOC Buffer Log for AMT-5. All times are in GMT.

CTD No.	*DNA No.*	*Genus and Species*	*No.*	*SDY*	*Date*
12	248	*Globigerinoides sacculifer*	1	273	30 September
	249	*Globigerinoides sacculifer*	12	273	30 September
	250	*Globigerinoides ruber* (pink variety)	1	273	30 September
	251	*Globigerinoides ruber* (white variety)	1	273	30 September
	252	*Globigerinoides ruber* (pink variety)	6	273	30 September
	254	*Globigerinella siphonifera*	1	273	30 September
	255	*Globigerina flaconensis*	1	273	30 September
	256	*Globorotalia scitula*	1	273	30 September
	257	*Globorotalia scitula*	21	273	30 September
	258	*Globorotalia crassaformis*	1	273	30 September
	259	*Globorotalia menardii* (?)	4	273	30 September
13	260	*Orbulina universa*	1	274	1 October
	261	*Orbulina universa*	1	274	1 October
	262	*Orbulina universa*	1	274	1 October
	263	*Orbulina universa*	1	274	1 October
	264	*Orbulina universa*	1	274	1 October
	265	*Orbulina universa*	1	274	1 October
	266	*Globorotalia menardii*	1	274	1 October
	267	*Globorotalia crassaformis*	1	274	1 October
	268	*Neogloboquadrina dutertrei*	1	274	1 October
	269	*Globorotalia scitula*	1	274	1 October
	270	*Globorotalia scitula*	1	274	1 October
	271	*Globorotalia scitula*	1	274	1 October
	272	*Globorotalia scitula*	17	274	1 October
	273	*Globorotalia menardii* (juveniles?)	1	274	1 October
	274	*Globorotalia menardii* (juveniles?)	3	274	1 October
	275	*Globorotalia crassaformis* (juveniles)	1	274	1 October
	276	*Globigerinita glutinata*	1	274	1 October
	277	*Globigerinita glutinata*	1	274	1 October
	278	*Globigerinita glutinata*	1	274	1 October
	279	*Globigerinita glutinata*	14	274	1 October
	280	*Globigerinoides sacculifer*	1	274	1 October
	281	*Globigerinoides sacculifer*	20	274	1 October
	282	*Hastigerina pelagica*	1	274	1 October
	283	*Hastigerina pelagica*	2	274	1 October
	284	*Globigerinoides ruber* (pink variety?)	1	274	1 October
	285	*Globigerinoides ruber* (white variety)	8	274	1 October
	286	*Globigerinella siphonifera*	1	274	1 October
	287	*Globigerinella siphonifera*	1	274	1 October
	288	*Globigerinella siphonifera*	1	274	1 October
	289	*Globigerinita uvula*	1	274	1 October
14	290	*Orbulina universa*	1	275	2 October
	291	*Orbulina universa*	1	275	2 October
	292	*Orbulina universa*	1	275	2 October
	293	*Orbulina universa*	1	275	2 October
	294	*Orbulina universa*	1	275	2 October
	295	*Orbulina universa*	1	275	2 October
	296	*Pulleniatina obliquiloculata*	1	275	2 October
	297	*Pulleniatina obliquiloculata*	1	275	2 October
	298	*Pulleniatina obliquiloculata*	1	275	2 October
	299	*Candeina nitida*	1	275	2 October
	300	*Globorotalia menardii*	1	275	2 October
	301	*Globorotalia menardii*	1	275	2 October
	302	*Globorotalia menardii*	3	275	2 October
	303	*Globorotalia menardii*	1	275	2 October

Table O1. (cont.) A summary of the DNA Extractions in DOC Buffer Log for AMT-5. All times are in GMT.

CTD No.	*DNA No.*	*Genus and Species*	*No.*	*SDY*	*Date*
14	304	*Globorotalia menardii*	6	275	2 October
	305	*Globorotalia scitula*	1	275	2 October
	306	*Globorotalia scitula*	6	275	2 October
	307	*Neogloboquadrina dutertrei*	1	275	2 October
	308	*Neogloboquadrina dutertrei*	1	275	2 October
	309	*Neogloboquadrina dutertrei*	1	275	2 October
	310	*Neogloboquadrina dutertrei*	8	275	2 October
	311	*Globigerinoides sacculifer*	1	275	2 October
	312	*Globigerinoides sacculifer*	1	275	2 October
	313	*Globigerinoides sacculifer*	5	275	2 October
	314	*Globigerinoides ruber* (white variety)	2	275	2 October
	315	*Globigerinoides ruber* (pink variety)	1	275	2 October
	316	*Globigerinoides ruber* (pink variety)	8	275	2 October
	317	*Globigerinita glutinata*	1	275	2 October
	318	*Globigerinita glutinata*	1	275	2 October
	319	*Globigerinita glutinata*	13	275	2 October
	320	*Candeina nitida*	1	275	2 October
	321	*Globigerinella siphonifera*	1	275	2 October
	322	*Globigerinella siphonifera*	8	275	2 October
	323	*Globigerinella siphonifera*	1	275	2 October
	324	*Globigerinella calida* (?)	1	275	2 October
15	325	*Orbulina universa*	1	276	3 October
	326	*Orbulina universa*	1	276	3 October
	327	*Orbulina universa*	1	276	3 October
	328	*Orbulina universa*	1	276	3 October
	329	*Orbulina universa*	1	276	3 October
	330	*Orbulina universa*	1	276	3 October
	331	*Pulleniatina obliquiloculata*	2	276	3 October
	338	*Globorotalia menardii*	1	277	4 October
	339	*Globorotalia menardii*	1	277	4 October
	340	*Globorotalia menardii*	1	277	4 October
	341	*Globorotalia menardii*	16	277	4 October
16	332	*Orbulina universa*	1	277	4 October
	333	*Orbulina universa*	1	277	4 October
	334	*Orbulina universa*	1	277	4 October
	335	*Orbulina universa*	1	277	4 October
	336	*Orbulina universa*	1	277	4 October
	337	*Orbulina universa*	1	277	4 October
	337	*Orbulina universa*	31	277	4 October
	342	*Pulleniatina obliquiloculata*	1	277	4 October
	343	*Pulleniatina obliquiloculata*	1	277	4 October
	344	*Pulleniatina obliquiloculata*	1	277	4 October
	345	*Pulleniatina obliquiloculata*	1	277	4 October
	346	*Pulleniatina obliquiloculata*	6	277	4 October
	347	*Globigerinella siphonifera*	1	277	4 October
	348	*Globigerinella siphonifera*	1	277	4 October
	349	*Globigerinella siphonifera*	1	277	4 October
	350	*Globigerinella siphonifera*	20	277	4 October
	351	*Globigerinoides sacculifer*	1	277	4 October
	352	*Globigerinoides sacculifer*	1	277	4 October
	353	*Globigerinoides sacculifer*	1	277	4 October
	354	*Globigerinoides sacculifer*	20	277	4 October
	355	*Globigerinoides conglobatus*	1	277	4 October
	356	*Globigerinoides ruber* (white variety)	1	277	4 October
	357	*Globigerinoides ruber* (white variety)	6	277	4 October

Table O1. (cont.) A summary of the DNA Extractions in DOC Buffer Log for AMT-5. All times are in GMT.

CTD No.	*DNA No.*	*Genus and Species*	*No.*	*SDY*	*Date*
16	358	*Globigerinoides ruber* (pink variety)	1	277	4 October
	359	*Globigerinoides ruber* (pink variety)	10	277	4 October
	360	*Globorotalia tumida* (?)	1	277	4 October
	361	*Globorotalia tumida/menardii* (?)	1	277	4 October
	362	*Globorotalia menardii* (some tumida?)	12	277	4 October
	397	*Globigerinita glutinata*	3	279	6 October
	398	*Pulleniatina obliquiloculata*	3	279	6 October
17	363	*Orbulina universa*	1	278	5 October
	364	*Globigerinella siphonifera*	1	278	5 October
	365	*Globigerinella siphonifera*	6	278	5 October
	366	*Globigerinella siphonifera*	1	278	5 October
	367	*Globigerinella siphonifera*	11	278	5 October
	368	*Globigerinella calida* (?)	1	278	5 October
	369	*Globigerinoides sacculifer*	1	278	5 October
	370	*Globigerinoides sacculifer*	1	278	5 October
	371	*Globigerinoides sacculifer*	16	278	5 October
	372	*Globigerinoides ruber* (white variety)	1	278	5 October
	373	*Globigerinoides ruber* (white variety)	9	278	5 October
	374	*Globigerinoides ruber* (pink variety)	2	278	5 October
	375	*Neogloboquadrina dutertrei*	1	278	5 October
	376	*Globorotalia menardii*	1	278	5 October
	377	*Globorotalia menardii*	7	278	5 October
18	378	*Orbulina universa*	1	279	6 October
	379	*Orbulina universa*	1	279	6 October
	380	*Orbulina universa*	1	279	6 October
	381	*Orbulina universa*	1	279	6 October
	382	*Orbulina universa*	1	279	6 October
	383	*Hastigerina pelagica*	1	279	6 October
	384	*Hastigerina pelagica*	1	279	6 October
	385	*Hastigerina pelagica*	3	279	6 October
	386	*Globigerinoides sacculifer*	1	279	6 October
	387	*Globigerinoides sacculifer*	1	279	6 October
	388	*Globigerinoides sacculifer*	10	279	6 October
	389	*Globigerinella siphonifera*	1	279	6 October
	390	*Globigerinella siphonifera*	1	279	6 October
	391	*Globigerinella siphonifera*	12	279	6 October
	392	*Globigerinoides ruber* (white variety)	7	279	6 October
	393	*Globigerinoides ruber* (pink variety)	1	279	6 October
	394	*Globigerinoides ruber* (pink variety)	2	279	6 October
	395	*Globigerinita glutinata*	1	279	6 October
	396	*Globorotalia menardii*	5	279	6 October
19	399	*Orbulina universa*	1	279	6 October
	400	*Hastigerina pelagica*	1	280	7 October
	401	*Hastigerina pelagica*	1	280	7 October
	402	*Globigerinoides sacculifer*	1	280	7 October
	403	*Globigerinoides sacculifer*	1	280	7 October
	404	*Globigerinoides sacculifer*	20	280	7 October
	405	*Globigerinita glutinata*	2	280	7 October
	406	*Globigerinita glutinata*	6	280	7 October
	407	*Globigerinita glutinata* (?)	1	280	7 October
	408	*Globorotalia menardii*	3	280	7 October
	409	*Globorotalia truncatulinoides*	1	280	7 October
	410	*Globigerinoides ruber* (white variety)	1	280	7 October
	411	*Globigerinoides ruber* (white variety)	21	280	7 October
	412	*Globigerinoides ruber* (pink variety)	1	280	7 October

Table O1. (cont.) A summary of the DNA Extractions in DOC Buffer Log for AMT-5. All times are in GMT.

CTD No.	*DNA No.*	*Genus and Species*	*No.*	*SDY*	*Date*
19	413	*Globigerinoides ruber* (pink variety)	11	280	7 October
	414	*Globigerinella siphonifera*	1	280	7 October
	415	*Globigerinella siphonifera*	6	280	7 October
	416	*Neogloboquadrina dutertrei*	1	280	7 October
	417	*Pulleniatina obliquiloculata/dutertrei* (?)	1	280	7 October
20	418	*Orbulina universa*	1	281	8 October
	419	*Orbulina universa*	1	281	8 October
	420	*Orbulina universa*	1	281	8 October
	421	*Orbulina universa*	1	281	8 October
	422	*Orbulina universa*	1	281	8 October
	423	*Globorotalia truncatulinoides*	1	281	8 October
	424	*Globorotalia truncatulinoides*	1	281	8 October
	425	*Globorotalia truncatulinoides*	5	281	8 October
	426	*Globorotalia truncatulinoides*	1	281	8 October
	427	*Globigerinoides ruber* (pink variety)	1	281	8 October
	428	*Globigerinoides ruber* (pink variety)	10	281	8 October
	429	*Globigerinoides ruber* (white variety)	1	281	8 October
	430	*Globigerinoides ruber* (white variety)	11	281	8 October
	431	*Globigerinoides sacculifer*	1	281	8 October
	432	*Globigerinoides sacculifer*	6	281	8 October
	433	*Hastigerina pelagica*	3	281	8 October
	434	*Globigerinella calida* (?)	1	281	8 October
	435	*Globigerinella calida* (?)	3	281	8 October
	436	*Globigerinita glutinata*	1	281	8 October
	437	*Globigerinita glutinata*	9	281	8 October
21	438	*Orbulina universa*	1	282	9 October
	439	*Orbulina universa*	1	282	9 October
	440	*Orbulina universa*	1	282	9 October
	441	*Orbulina universa*	1	282	9 October
	442	*Orbulina universa*	1	282	9 October
	443	*Globorotalia truncatulinoides*	1	282	9 October
	444	*Globorotalia truncatulinoides*	1	282	9 October
	445	*Globorotalia truncatulinoides*	4	282	9 October
	446	*Globigerinella siphonifera*	1	282	9 October
	447	*Globigerinella calida* (?)	1	282	9 October
	448	*Globigerinella calida* (?)	1	282	9 October
	449	*Globigerinella calida* (?)	6	282	9 October
	450	*Hastigerina pelagica*	1	282	9 October
	451	*Globigerinoides sacculifer*	1	282	9 October
	452	*Globigerinoides sacculifer*	11	282	9 October
	453	*Globigerinoides ruber* (pink variety)	5	282	9 October
	454	*Globigerinoides ruber* (white variety)	1	282	9 October
	455	*Globigerinoides ruber* (white variety)	12	282	9 October
	456	*Globigerinita glutinata*	3	282	9 October
	457	*Globorotalia hirsuta*	1	282	9 October
	458	*Globorotalia ungulata*	1	282	9 October
	459	*Globorotalia tumida* (?)	1	282	9 October
	460	*Globorotalia menardii*	1	282	9 October
	461	*Globorotalia tumida/menardii* (?)	1	282	9 October
	462	*Globorotalia tumida* (?)	5	282	9 October
	525	*Globorotalia menardii*	6	285	12 October
22	463	*Orbulina universa*	1	283	10 October
	464	*Orbulina universa*	1	283	10 October
	465	*Orbulina universa*	1	283	10 October
	466	*Neogloboquadrina dutertrei*	1	283	10 October

Table O1. (cont.) A summary of the DNA Extractions in DOC Buffer Log for AMT-5. All times are in GMT.

CTD No.	*DNA No.*	*Genus and Species*	*No.*	*SDY*	*Date*
22	467	*Neogloboquadrina dutertrei*	1	283	10 October
	468	*Neogloboquadrina dutertrei*	7	283	10 October
	469	*Globigerinita glutinata*	1	283	10 October
	470	*Globigerinita glutinata*	1	283	10 October
	471	*Globigerinita glutinata*	1	283	10 October
	472	*Globigerinita glutinata*	10	283	10 October
	473	*Globigerinita glutinata*	30	283	10 October
	474	*Pulleniatina obliquiloculata*	1	283	10 October
	475	*Globorotalia crassaformis*	1	283	10 October
	476	*Globorotalia crassaformis* (?)	1	283	10 October
	477	*Globorotalia hirsuta*	1	283	10 October
	478	*Globorotalia hirsuta*	4	283	10 October
	479	*Globorotalia truncatulinoides*	1	283	10 October
	480	*Globorotalia truncatulinoides*	3	283	10 October
	481	*Globorotalia hirsuta*	1	283	10 October
	482	*Globorotalia truncatulinoides*	1	283	10 October
	483	*Globorotalia truncatulinoides*	3	283	10 October
	484	*Turborotalita humilis* (?)	1	283	10 October
	485	*Turborotalita humilis* (?)	1	283	10 October
	486	*Turborotalita humilis* (?)	10	283	10 October
	487	*Tenuitella fleisheri*	15	283	10 October
	488	*Globigerinoides sacculifer*	8	283	10 October
	489	*Globigerinoides ruber* (white variety)	10	283	10 October
	490	*Globigerinella siphonifera*	4	283	10 October
	491	*Globorotalia menardii*	1	283	10 October
	526	*Neogloboquadrina dutertrei*	10	285	12 October
	527	*Globorotalia ungulata*	1	285	12 October
	528	*Globorotalia tumida* (?)	1	285	12 October
	529	*Globorotalia menardii*	1	285	12 October
23	492	*Orbulina universa*	1	284	11 October
	493	*Orbulina universa*	1	284	11 October
	494	*Orbulina universa*	1	284	11 October
	495	*Orbulina universa*	1	284	11 October
	496	*Globorotalia inflata*	1	284	11 October
	497	*Globorotalia inflata*	1	284	11 October
	498	*Globorotalia inflata*	5	284	11 October
	499	*Globorotalia truncatulinoides*	1	284	11 October
	500	*Globorotalia truncatulinoides*	6	284	11 October
	501	*Globorotalia truncatulinoides*	1	284	11 October
	502	*Globorotalia truncatulinoides*	15	284	11 October
	503	*Globorotalia hirsuta*	1	284	11 October
	504	*Globorotalia hirsuta*	1	284	11 October
	505	*Globorotalia hirsuta*	3	284	11 October
	506	*Globorotalia hirsuta*	10	284	11 October
	507	*Globigerinella siphonifera*	1	284	11 October
	508	*Globigerinella siphonifera*	1	284	11 October
	509	*Globigerinella siphonifera*	3	284	11 October
	510	*Globigerinella siphonifera*	10	284	11 October
	511	*Neogloboquadrina dutertrei*	1	284	11 October
	512	*Neogloboquadrina dutertrei*	4	284	11 October
	513	*Globorotalia menardii*	1	284	11 October
	514	*Globorotalia tumida* (?)	1	284	11 October
	515	*Globigerinoides sacculifer*	1	284	11 October
	516	*Globigerinoides sacculifer*	10	284	11 October
	517	*Globigerinoides ruber* (white variety)	9	284	11 October

Table O1. (cont.) A summary of the DNA Extractions in DOC Buffer Log for AMT-5. All times are in GMT.

CTD No.	*DNA No.*	*Genus and Species*	*No.*	*SDY*	*Date*
23	518	*Hastigerina pelagica*	1	284	11 October
	519	*Globigerina bulloides*	1	284	11 October
	520	*Globigerina bulloides*	9	284	11 October
	521	*Globorotalia scitula*	8	284	11 October
	522	*Globigerinita glutinata*	8	285	12 October
	523	*Globigerina bulloides* (?)	2	285	12 October
	524	*Neogloboquadrina pachyderma*	2	285	12 October
24	530	*Globigerina bulloides*	1	285	12 October
	531	*Globigerina bulloides*	10	285	12 October
	532	*Globigerina bulloides*	1	285	12 October
	533	*Globigerinoides sacculifer*	1	285	12 October
	534	*Globigerinoides sacculifer*	6	285	12 October
	535	*Globigerinoides ruber* (white variety)	1	285	12 October
	536	*Globigerinoides ruber* (white variety)	3	285	12 October
	537	*Globigerinoides ruber* (white variety)	14	285	12 October
	538	*Globorotalia truncatulinoides*	2	285	12 October
	539	*Globorotalia truncatulinoides*	4	285	12 October
	540	*Neogloboquadrina dutertrei*	1	285	12 October
	541	*Neogloboquadrina dutertrei*	1	285	12 October
	542	*Neogloboquadrina dutertrei*	5	285	12 October
	543	*Globorotalia inflata*	1	286	13 October
	544	*Globorotalia inflata*	2	286	13 October
	545	*Globorotalia inflata*	1	286	13 October
	546	*Globorotalia inflata*	5	286	13 October
	547	*Globorotalia menardii*	2	286	13 October
	548	*Globorotalia hirsuta*	1	286	13 October
	549	*Globorotalia hirsuta*	5	286	13 October
	550	*Globigerinita uvula*	1	286	13 October
25	551	*Globorotalia hirsuta*	1	286	13 October
	552	*Globorotalia hirsuta*	5	286	13 October
	553	*Globorotalia hirsuta*	25	286	13 October
	554	*Globorotalia hirsuta*	1	286	13 October
	555	*Globorotalia hirsuta*	2	286	13 October
	556	*Globigerina bulloides*	1	286	13 October
	557	*Globigerina bulloides*	5	286	13 October
	558	*Globigerina bulloides*	20	286	13 October
	559	*Globigerina bulloides*	1	286	13 October
	560	*Globigerina bulloides*	1	286	13 October
	561	*Globigerina bulloides*	10	286	13 October
	562	*Globigerinella siphonifera*	1	286	13 October
	563	*Globigerinella siphonifera*	1	286	13 October
	564	*Globigerinella siphonifera*	6	286	13 October
	565	*Globorotalia inflata*	1	286	13 October
	566	*Globorotalia inflata*	1	286	13 October
	567	*Globorotalia inflata*	5	286	13 October
	568	*Globigerinita glutinata*	9	287	14 October
	569	*Turborotalita quinqueloba*	1	287	14 October
	570	*Turborotalita quinqueloba*	11	287	14 October
26	571	*Globorotalia hirsuta*	1	287	14 October
	572	*Globorotalia hirsuta*	2	287	14 October
	573	*Globigerina bulloides*	1	287	14 October
	574	*Globigerina bulloides*	1	287	14 October
	575	*Globigerina bulloides*	1	287	14 October
	576	*Globigerina bulloides*	13	287	14 October
	577	*Globigerina bulloides*	1	287	14 October

Table O1. (cont.) A summary of the DNA Extractions in DOC Buffer Log for AMT-5. All times are in GMT.

CTD No.	*DNA No.*	*Genus and Species*	*No.*	*SDY*	*Date*
26	578	*Globigerina bulloides*	1	287	14 October
	579	*Globigerina bulloides*	1	287	14 October
	580	*Globigerina bulloides*	10	287	14 October
	581	*Globorotalia inflata*	1	287	14 October
	582	*Globorotalia inflata*	1	287	14 October
	583	*Globorotalia inflata*	1	287	14 October
	584	*Globorotalia inflata*	1	287	14 October
	585	*Globorotalia inflata*	13	287	14 October
	586	*Globorotalia truncatulinoides*	1	287	14 October
	587	*Globorotalia truncatulinoides*	1	287	14 October
	588	*Globorotalia truncatulinoides*	1	287	14 October
	589	*Globorotalia truncatulinoides*	13	287	14 October
	590	*Turborotalita quinqueloba*	1	287	14 October
	591	*Turborotalita quinqueloba*	1	287	14 October
	592	*Turborotalita quinqueloba*	1	287	14 October
	593	*Turborotalita quinqueloba*	3	287	14 October
	594	*Turborotalita quinqueloba*	25	287	14 October
28	595	*Globorotalia inflata*	1	288	15 October
	596	*Globorotalia truncatulinoides*	1	288	15 October
	597	*Globorotalia truncatulinoides*	1	288	15 October
	598	*Globorotalia truncatulinoides*	1	288	15 October
	599	*Globorotalia truncatulinoides*	12	288	15 October
	600	*Globigerina bulloides*	1	288	15 October
	601	*Globigerina bulloides*	1	288	15 October
	602	*Globigerina bulloides*	1	288	15 October
	603	*Globigerina bulloides*	3	288	15 October
	604	*Globigerina bulloides*	12	288	15 October
	605	*Globorotalia inflata*	1	288	15 October
	606	*Globorotalia inflata*	1	288	15 October
	607	*Globorotalia inflata*	1	288	15 October
	608	*Globorotalia inflata*	3	288	15 October
	609	*Globorotalia inflata*	18	288	15 October
	610	*Neogloboquadrina dutertrei* (?)	1	288	15 October
	611	*Neogloboquadrina dutertrei* (?)	8	288	15 October
	612	*Turborotalita quinqueloba*	1	289	16 October
	613	*Turborotalita quinqueloba*	1	289	16 October
	614	*Turborotalita quinqueloba*	1	289	16 October
	615	*Turborotalita quinqueloba*	1	289	16 October
	616	*Turborotalita quinqueloba*	1	289	16 October
	617	*Turborotalita quinqueloba*	1	289	16 October
	618	*Turborotalita quinqueloba*	5	289	16 October
	619	*Turborotalita quinqueloba*	15	289	16 October
	620	*Turborotalita quinqueloba*	17	289	16 October
	632	*Globigerinita glutinata* (?)	2	289	16 October
	633	*Turborotalita quinqueloba*	1	289	16 October
	634	*Turborotalita quinqueloba*	1	289	16 October
	635	*Turborotalita quinqueloba*	30	289	16 October
30	621	*Globorotalia truncatulinoides*	1	289	16 October
	622	*Globorotalia truncatulinoides*	1	289	16 October
	623	*Globorotalia truncatulinoides*	1	289	16 October
	624	*Globorotalia truncatulinoides*	11	289	16 October
	625	*Globorotalia hirsuta*	1	289	16 October
	626	*Globorotalia inflata*	1	289	16 October
	627	*Globorotalia inflata*	1	289	16 October

Table O1. (cont.) A summary of the DNA Extractions in DOC Buffer Log for AMT-5. All times are in GMT.

CTD No.	*DNA No.*	*Genus and Species*	*No.*	*SDY*	*Date*
30	628	*Globorotalia inflata*	10	289	16 October
	629	*Globigerina bulloides*	1	289	16 October
	630	*Globigerina bulloides*	1	289	16 October
	631	*Globigerina bulloides*	8	289	16 October

Table O2. A summary of the DNA Extractions in Guanidinium Buffer Log for AMT-5. All times are in GMT.

CTD No.	*DNA No.*	*Genus and Species*	*SDY*	*Date*
2	1– 8	*Orbulina universa*	260	17 September
3	9– 17	*Orbulina universa*	261	18 September
	18– 22	*Orbulina universa*	261	18 September
4	23– 44	*Orbulina universa*	262	19 September
	45– 64	*Globigerinoides sacculifer*		
5	65– 67	*Orbulina universa*	263	20 September
6	68– 85	*Orbulina universa*	264	21 September
	86–100	*Globigerinoides sacculifer*		
7	101–112	*Orbulina universa*	265	22 September
8	113–116	*Orbulina universa*	268	25 September
	117–131	*Globigerinella siphonifera*		
10	132–149	*Orbulina universa*	270	27 September
	150–164	*Globigerinoides ruber*		
None	165–168	*Orbulina universa*	272	29 September
12	169–184	*Orbulina universa*	273	30 September
13	185–199	*Orbulina universa*	274	1 October
14	200–214	*Orbulina universa*	275	2 October
15	215–228	*Orbulina universa*	276	3 October
16	229–250	*Orbulina universa*	277	4 October
18	251	*Orbulina universa*	279	6 October
20	252–267	*Orbulina universa*	281	8 October
21	268–276	*Orbulina universa*	282	9 October
	299	*Orbulina universa*	282	9 October
22	277–287	*Orbulina universa*	283	10 October
	288–290	*Globigerinoides sacculifer*		
	291–298	*Globigerinoides ruber*		
23	301–315	*Orbulina universa*	284	11 October
24	316–318	*Orbulina universa*	285	12 October
25	319	*Orbulina universa*	286	13 October
	320	*Globorotalia truncatulinoides*		
26	340–360	*Globorotalia truncatulinoides*	289	16 October

Appendix P

AMT-5 Cruise Participants

The AMT-5 science team are presented alphabetically.

James Aiken
Plymouth Marine Laboratory
Prospect Place, West Hoe
Plymouth PL1 3DH
UNITED KINGDOM
Voice: 44–1–752–633–429
Fax: 44–1–752–633–101
Net: `j.aiken@pml.ac.uk`

Jean-François Berthon
Space Applications Institute
Marine Environmental Unit T.P. 272
Joint Research Center
Ispra, I–21020 (VA)
ITALY
Voice: 39–332–789–934
Fax: 39–332–789–034
Net: `jean-francois.berthon@jrc.it`

Denise Cummings
Plymouth Marine Laboratory
Prospect Place, West Hoe
Plymouth PL1 3DH
UNITED KINGDOM
Voice: 44–1–752–633–470
Fax: 44–1–752–633–101
Net: `d.cummings@pml.ac.uk`

Cyril Dempsey
Satlantic, Inc.
Richmond Terminal, Pier 9
3295 Barrington Street
Halifax, Nova Scotia B3K 5X8
CANADA
Voice: (902) 492–4780
Fax: (902) 492–4781
Net: `cyril@satlantic.com`

Columban de Vargas
Universite de Geneve
154 route de Malagnou
Chene-Boorgeries
SWITZERLAND
Voice: 41–22–349–8644
Fax: 41–22–349–2647
Net: `devargas@sc2a.unige.ch`

Craig Donlan
UC/CCAR/Aero Engineering
Campus Box 431
Boulder, Colorado 80309
USA
Voice: (303) 492–0955
Fax: (303) 492–2825
Net: `cjdn@colorado.edu`

Rosa Barciela-Fernandez
Universidad de Vigo
Depto. de Ecologia y Biologia Animal
Campus Lagoas-Marcosende
36200 Vigo
SPAIN
Voice: 34–86–812–591
Fax: 34–86–812–556
Net: `barciela@uvigo.es`

Stuart Gibb
Plymouth Marine Laboratory
Prospect Place, West Hoe
Plymouth PL1 3DH
UNITED KINGDOM
Voice: 44–1–752–633–486
Fax: 44–1–752–633–101
Net: `s.gibb@pml.ac.uk`

Natalia González-Benítez
Universidad de Oviedo
Depto. de Biologia de Organismos y Sistemas
Catedratico Rodrigo Uria S/N
E-33071 Oviedo
SPAIN
Voice: 34–85–104–830
Fax: 34–85–104–866
Net: `nataliag@sci.cpd.uniovi.es`

Stanford Hooker
NASA/GSFC/Code 970.2
Bldg. 28, Room W121
Greenbelt, MD 20771–5000
USA
Voice: 301–286–9503
Fax: 301–286–1775
Net: `stan@ardbeg.gsfc.nasa.gov`

Ignacio Huskin
Universidad de Oviedo
Depto. de Biologia de Organismos y Sistemas
Catedratico Rodrigo Uria S/N
E-33071 Oviedo
SPAIN
Voice: 34–85–104–830
Fax: 34–85–104–866
Net: `ihuskin@sci.cpd.uniovi.es`

Cliff Law†
Plymouth Marine Laboratory
Prospect Place, West Hoe
Plymouth PL1 3DH
UNITED KINGDOM
Voice: 44–1–752–633–438
Fax: 44–1–752–633–101
Net: `c.law@pml.ac.uk`

Conor McKee
School of Environmental Sciences
University of East Anglia
Norwich NR4 7TJ
UNITED KINGDOM
Voice: 44–1–603–592–545
Net: `c.mckee@uea.ac.uk`

Mario Quevedo
Universidad de Oviedo
Depto. de Biologia de Organismos y Sistemas
Catedratico Rodrigo Uria S/N
E-33071 Oviedo
SPAIN
Voice: 34–85–104–831
Fax: 34–85–104–866
Net: `mquevedo@sci.cpd.uniovi.es`

† Left the cruise early at Madeira.

Nigel Rees
Plymouth Marine Laboratory
Prospect Place, West Hoe
Plymouth PL1 3DH
UNITED KINGDOM
Voice: 44–1–752–633–406
Fax: 44–1–752–633–101
Net: nwr@pml.ac.uk

David Suggett
Southampton Oceanography Centre
Empress Dock
European Way
Southampton SO14 3ZH
UNITED KINGDOM
Voice: 44–1–703–596–666
Net: djs3@soton.ac.uk

Peter Wood
Dept. of Physics and App. Sciences
John Anderson Building
University of Strathclyde
Glasgow G4 0NG
UNITED KINGDOM
Voice: 44–1–415–483–068
Fax: 44–1–415–522–891
Net: cabs26@pop-hub.strath.ac.uk

Rachel Woodd-Walker
Plymouth Marine Laboratory
Prospect Place, West Hoe
Plymouth PL1 3DH
UNITED KINGDOM
Voice: 44–1–752–633–414
Fax: 44–1–752–633–101
Net: rsww@wpo.nerc.ac.uk

Malcolm Woodward
Plymouth Marine Laboratory
Prospect Place, West Hoe
Plymouth PL1 3DH
UNITED KINGDOM
Voice: 44–1–752–633–459
Fax: 44–1–752–633–101
Net: emsw@wpo.nerc.ac.uk

James Woolfenden
Plymouth Marine Laboratory
Prospect Place, West Hoe
Plymouth PL1 3DH
UNITED KINGDOM
Voice: 44–1–752–633–406
Fax: 44–1–752–633–101
Net: jgw1@ub.npm.ac.uk

Glossary

A/D Analog-to-Digital
ADCP Acoustic Doppler Current Profiler
AMT Atlantic Meridional Transect
AMT-5 The Fifth AMT Cruise
AOT Aerosol Optical Thickness
ASCII American Standard Code for Information Interchange
ATSR Along-Track Scanning Radiometer
AVHRR Advanced Very High Resolution Radiometer

BAS British Antarctic Survey
BSST Bulk Sea Surface Temperature

C-FALLS Software package for logging SeaFALLS data.
C-OPS Combined Operations
CANIGO Canary Islands, Azores, Gibraltar Observations
CCAR Colorado Center for Astrodynamics Research
CCD Charge-Coupled Device
CCMS Centre for Coastal and Marine Studies
CCN Cloud Condensation Nucleii
CHN Carbon-Hydrogen-Nitrogen
COTS Commercial Off-The-Shelf
CT Conductivity and Temperature
CTD Conductivity, Temperature, and Depth

DC Direct Current
DCM Deep Chlorophyll Maximum
DMA Dimethylamine
DMS Dimethylsulfide
DMSP Dimethylsulphoniopropionate
DMSPd Dissolved DMSP
DMSPp DMSP within phytoplankton cells
DNA Deoxyribonucleic Acid
DOC Dissolved Organic Carbon
DUT Device Under Test
DVM Digital Voltmeter

EDTA Ethylenediaminetetraacetic Acid
EEZ Exclusive Economic Zone
e-mail Electronic Mail
ERS-2 The Second Earth Resources Satellite
EU European Union
EUC Equatorial Under Current

FIGD-IC Flow Injection Gas-Diffusion Coupled to Ion Chromatography
FRRF Fast Repetition Rate Fluorometer
GF/F Not an acronym, but a specific type of glass fiber filter manufactured by Whatman.

GMT Greenwich Mean Time
GOES-8 The Eighth Geostationary Operational Environmental Satellite
GPIB General Purpose Interface Bus
GSFC Goddard Space Flight Center

HPLC High Performance Liquid Chromatography
HTCO High Temperature Catalytic Oxidation

IDL Interactive Data Language
IOS (SOC) Institute of Oceanographic Sciences

JCR (RRS) *James Clark Ross*

LoCNESS Low-Cost NASA Environmental Sampling System

MA Methylamine
METEOSAT Meteorological Satellite
MMA Monomethylamine
MODIS Moderate Resolution Imaging Spectroradiometer
MVDS Multichannel Visible Detector System

NASA National Aeronautics and Space Administration
NEC North Equatorial Current
NECC North Equatorial Counter Current
NEUC North Equatorial Undercurrent
NIST National Institute of Standards and Technology
NOAA National Oceanic and Atmospheric Administration

OCI Ocean Color Irradiance
OCR Ocean Color Radiance
OPC Optical Plankton Counter

P-I Photosynthesis-Irradiance
PAR Photosynthetically Available Radiation
PC Personal Computer
PCR Polymerase Chain Reaction
PML Plymouth Marine Laboratory
POC Particulate Organic Carbon
PRIME Plankton Reactivity in the Marine Environment
PRT Platinum Resistance Temperature (sensor)
PSU Practical Salinity Units
PTFE Polyfluorotetraethylene
PVC Polyvinylchloride

RAM Random Access Memory
ROSSA Radiometric Observations of the Sea Surface and Atmosphere
RRS Royal Research Ship
RSG (PML) Remote Sensing Group
RSMAS Rosenstiel School for Marine and Atmospheric Science
RVS (BAS) Research Vessel Services

S/N Serial Number
SACZ Sub-Antarctic Convergence Zone
SBE Sea-Bird Electronics
SDY Sequential Day of the Year
SeaACE SeaWiFS Atlantic Characterization Experiment
SeaBOSS SeaWiFS Buoyant Optical Surface Sensor
SeaFALLS SeaWiFS Free-Falling Advanced Light Level Sensors
SeaOPS SeaWiFS Optical Profiling System
SeaSURF SeaWiFS Square Underwater Reference Frame
SeaWiFS Sea-viewing Wide Field-of-view Sensor
SEC South Equatorial Current
SEM Scanning Electronic Microscopy
SEUC South Equatorial Undercurrent
SMSR SeaWiFS Multichannel Surface Reference
SOC Southampton Oceanography Centre
SOMARE Sampling, Observations and Modelling of Atlantic Regional Ecosystems
SOSSTR Ship of Opportunity Sea Surface Temperature Radiometer
SPMR SeaWiFS Profiling Multichannel Radiometer
SQM SeaWiFS Quality Monitor
SSH Sea Surface Height
SSM/I Special Sensor for Microwave/Imaging
SSST Sea Surface Skin Temperature

TMA Trimethylamine
TOC Total Organic Carbon
TOPEX Topography Experiment
TSG Thermosalinograph

UIC Underway Instrumentation and Control
UK United Kingdom
UOR Undulating Oceanographic Recorder

WOCE World Ocean Circulation Experiment

XBT Expendable Bathythermograph
XOTD Expendable Optical, Temperature, and Depth

Symbols

A Air mass.
a_O^* The spectral absorption coefficient for ozone.

$\hat{C}$ The retrieved (remote sensing) chlorophyll concentration.
$\tilde{C}$ The measured (*in situ*) chlorophyll concentration.
C_O The atmospheric ozone concentration.
C_0, C_1, C_2, C_3 Polynomial coefficients.

$E(\lambda)$ The solar irradiance.
$E_0(\lambda)$ The extraterrestrial solar irradiance.
$E_d(z,\lambda)$ The spectral downwelling irradiance as a function of depth.
$E_d(0^-,\lambda)$ The spectral downwelling irradiance measured just below the sea surface.
$E_s(0^+,\lambda)$ The solar irradiance measured just above the sea surface.
$E_u(z,\lambda)$ The spectral upwelling irradiance as a function of depth.

F Chlorophyll fluorescence.

H Altitude.

$L_u(z,\lambda)$ The spectral upwelling irradiance as a function of depth.
$L_W(\lambda)$ The spectral water-leaving radiance.

$K(\lambda)$ The diffuse attenuation coefficient.
$K_d(\lambda)$ The spectral diffuse attenuation coefficient calculated from E_d data.
$\hat{K}_d$ The modeled diffuse attenuation coefficient.
$\tilde{K}_d$ The measured diffuse attenuation coefficient.
$K_{L_u}(\lambda)$ The spectral diffuse attenuation coefficient calculated from L_u data.

m The relative air mass.

P Atmospheric pressure.
P_0 The standard atmospheric pressure at sea level.

R^2 The square of the linear correlation coefficient.
R_{rs} Remote sensing reflectance.

S Salinity.

T Temperature.
T_r Transmittance in percent of light transmitted.

y The ordinate, meridional coordinate, or an empirical factor (depending on usage).

z The vertical coordinate (frequently water depth).

α The Ångström exponent.
β The Ångström coefficient.
θ The sun zenith angle.
λ Wavelength.
λ_i A particular wavelength.
$\tau(\lambda)$ The spectral atmospheric total optical thickness.
$\hat{\tau}_A(783)$ The estimated atmospheric optical thickness at 783 nm using the Ångström law parameters computed for the pair ($\tau_A(671)$,$\tau_A(868)$).
$\tilde{\tau}_A(783)$ The measured atmospheric optical thickness at 783 nm.
τ_A The aerosols component (molecules of the air) of the atmospheric optical thickness.
τ_O The ozone component (molecules of the air) of the atmospheric optical thickness.
τ_R The Rayleigh component (molecules of the air) of the atmospheric optical thickness.

References

Aiken, J., G.F. Moore, and P.M. Holligan, 1992: Remote-sensing of oceanic biology in relation to global climate change. *J. Phycol.,* **28,** 579–590.

Ångström , A., 1961: Techniques of determining the turbidity of the atmosphere. *Tellus,* **13,** 214–223.

Barlow, R.G., R.F.C. Mantoura, M.A. Gough, and T.W. Fileman, 1993: Pigment signatures of the phytoplankton composition in the northeastern Atlantic during the 1990 spring bloom. *Deep-Sea Res. II,* **40,** 459–477.

——, D.G. Cummings, and S.W. Gibb, 1998: Improved resolution of mono- and divinyl chlorophylls *a* and *b* and zeaxanthin and lutein in phytoplankton extracts using reverse phase C-8 HPLC. *Mar. Ecol. Prog. Ser.,* **161,** 303–307.

Bjornland, T., and S. Liaaen-Jensen, 1989: Distribution patterns of carotenoids in relation to chromophyte phylogeny and systematics. In: *The Chromophyte Algae: Problems and Perspectives.* J.C. Green, B.S.C. Leadbeater, and W.L. Diver, Eds. Clarendon Press, Oxford, 37–61.

Brewer, P.G., and J.P. Riley, 1965: The automatic determination of nitrate in sea water. *Deep-Sea Res.,* **12,** 765–772.

Charlson, R.J., J.E. Lovelock, M.O. Andreae, and S.G. Warren, 1987: Oceanic phytoplankton, atmospheric sulphur, cloud albedo, and climate. *Nature,* **326,** 655–661.

Chisholm, S.W., R.J. Olson, E.R. Zettler, R. Goericke, J.B. Waterbury, and N.A. Welschmeyer, 1988: A novel free-living prochlorophyte abundant in the oceanic euphotic zone. *Nature,* **334,** 340–343.

Emery, W.J., and J.S. Dewar, 1982: Mean temperature and salinity-depth and temperature-depth curves for the North Atlantic and the North Pacific. *Prog. Oceanog.,* **11,** 219–305.

Fröhlich, C., and G.E. Shaw, 1980: New determination of Rayleigh scattering in the terrestrial atmosphere. *Appl. Opt.,* **19,** 1,773–1,775.

Furnas, M.J., 1990: *In situ* growth rates of marine phytoplankton: approaches to measurement, community and species growth rates. *J. Plank. Res.,* **12,** 1,117–1,151.

Garside, C., 1982: Chemiluminescent technique for the determination of nanomolar concentrations of nitrate and nitrite in seawater. *Mar. Chem.,* **11,** 159–167.

Gibb, S.W., J.W. Wood, and R.F.C. Mantoura, 1995: Automation of flow injection gas diffusion-ion chromatography for the nanomolar determination of methylamines and ammonia in seawater and atmospheric samples. *J. Autom. Chem.,* **17,** 205–212.

——, R.F.C. Mantoura, P.S. Liss, and R.G. Barlow, 1998: Distribution and biogeochemistry of methylamines and ammonia in the Arabian Sea. *Deep-Sea Res.,* (in press).

Grasshoff, K., 1976: *Methods of Seawater Analysis.* Verlag Chemie, Weiheim, 317 pp.

Holm-Hansen, O., C.J. Lorenzen, R.W. Holmes, and J.D.H. Strickland, 1965: Fluorometric determination of chlorophyll. *J. du Cons. Int'l. pour l'Explor. de la Mer,* **30,** 3–15.

Hooker, S.B., and J. Aiken, 1998: Calibration evaluation and radiometric testing of field radiometers with the SeaWiFS Quality Monitor (SQM). *J. Atmos. Oceanic Tech.,* 995–1,007.

——, and C.R. McClain, 1998: A Comprehensive Plan for the Calibration and Validation of SeaWiFS Data. *Prog. Oceanogr.,* (submitted).

Iqbal, M., 1983: *An Introduction to Solar Radiation.* Academic, New York, 390 pp.

Jeffrey S.W., R.F.C. Mantoura, and S.W. Wright, Eds., 1997: Phytoplankton Pigments in Oceanography: Guidelines to Modern Methods. UNESCO Monograph in Oceanographic Methods. *SCOR-UNESCO Monographs on Oceanographic Methodology. Report for SCOR WH 78.* Paris, France.

Johnson, B.C., P-S. Shaw, S.B. Hooker, and D. Lynch, 1998: Radiometric and engineering performance of the SeaWiFS Quality Monitor (SQM): A portable light source for field radiometers. *J. Atmos. Oceanic Tech.,* 1,008–1,022.

Jones, R.D., 1991: An improved fluorescence method for the determination of nanomolar concentrations of ammonium in natural waters. *Limnol. Oceanogr.,* **36,** 814–819.

Karsten, F., 1966: A new table and approximate formula for relative optical air mass. *Arch. Meteorol. Geophys. Bioklimatol. Ser. B,* **14,** 206–223.

Keller, M.D., W.K. Bellows, and R.R.L. Guillard, 1989: Dimethylsulphide production in marine phytoplankton. In: *Biogenic Sulphur in the Environment.* E.S. Saltzman and W.J. Cooper, Eds., Am. Chem. Soc., Washington, DC, 167–182.

King, G.M., 1988: Distribution and metabolism of quaternary amines in marine sediments. In: *Nitrogen Cycling in Coastal Marine Environments.* T.H. Blackburn and J. Sorenson, Eds., John Wiley and Sons, Chichester, United Kingdom, 143–173.

Kiorbe, T., 1993: Turbulence, phytoplankton cell size, and the structure of pelagic food webs. *Adv. Mar. Biol.,* **29,** 1–72.

Kirkwood, D.S., 1989: Simultaneous determination of selected nutrients in seawater. *ICES CM1989,* **29,** 12 pp.

Landry, M.R., 1993: Estimating rates of growth and grazing mortality of phytoplankton by the dilution method. In: *Handbook of Methods in Aquatic Microbial Ecology,* P.F. Kemp, B.F. Sherr, E.B. Sherr, and J.J. Cole, Eds., Lewis Publishers, Boca Raton, Florida, 714–722.

Leckner, B., 1978: The spectral distribution of solar radiation at the Earth's surface—Elements of a model. *Solar Energy,* **20,** 143–150.

Liu, B.Y.H., and K.W. Lee, 1976: Efficiency of membrane Nucleopore filters for submicrometer aerosols. *Env. Sci. Tech.,* **10,** 345–50.

Mantoura, R.F.C., and E.M.S. Woodward, 1983: Optimization of the indophenol blue method for the automated determination of ammonia in estuarine waters. *Estuar. Coastal Shelf Sci.,* **17,** 219–224.

——, S.W. Wright, S.W. Jeffrey, R.G. Barlow, and D.G. Cummings, 1997: "Phytoplankton pigments in oceanography: Guidelines to modern methods." In: S.W. Jeffrey, R.F.C. Mantour, and S.W. Wright, Eds., UNESCO Monograph in Oceanographic Methods. *Report for SCOR WH 78. SCOR-UNESCO Monographs on Oceanographic Methodology.* Paris, France, 662 pp.

Marggraf, W.A., and M. Griggs, 1969: Aircraft measurements and calculations of the total downward flux of solar radiation as a function of altitude. *J. Atmos. Sci.,* **26,** 469–477.

McClain, C.R., W.E. Esaias, W. Barnes, B. Guenther, D. Endres, S.B. Hooker, G. Mitchell, and R. Barnes, 1992: Calibration and Validation Plan for SeaWiFS, *NASA Tech. Memo. 104566, Vol. 3,* S.B. Hooker and E.R. Firestone, Eds., NASA Goddard Space Flight Center, Greenbelt, Maryland, 41 pp.

——, M.L. Cleave, G.C. Feldman, W.W. Gregg, S.B. Hooker, and N. Kuring, 1998: Science quality SeaWiFS data for global biosphere research. *Sea Technol.,* **39,**(9), 10–16.

Moore, G., J. Aiken, N. Rees, and S. Hooker, 1997: Remote Sensing of Bio-Optical Provinces. Abstract. *Proc. 23rd Annual Conf. Exhib. Remote Sens. Soc.,* 545–550.

Morris, A.W., R.J.M. Howland, and A.J. Bale, 1978: A filtration unit for use with continuous autoanalytical systems applied to highly turbid waters. *Estuar. Coastal Mar. Sci.,* **6,** 105–109.

Mueller, J.L., and R.W. Austin, 1995: Ocean Optics Protocols for SeaWiFS Validation, Revision 1. *NASA Tech. Memo. 104566, Vol. 25,* S.B. Hooker, E.R. Firestone, and J.G. Acker, Eds., NASA Goddard Space Flight Center, Greenbelt, Maryland, 66 pp.

Muller-Karger, F., C.R. McClain, and P. Richardson, 1988: The dispersal of the Amazon water. *Nature,* **333,** 56–59.

Owens, N.J.P., and A.P. Rees, 1989: Determination of Nitrogen-15 at submicrogram levels of nitrogen using automated continuous-flow isotope ratio mass spectrometry. *Analyst,* **114,** 1,655–1,657.

Partensky, F., N. Hoepffner, W.K.W. Li, O. Ulloa, and D. Vaulot, 1993: Photoacclimation of Prochlorococcus sp. (Prochlorophyta) strains isolated from the North Atlantic and the Mediterranean Sea. *Plant Physiol.,* **101,** 285–296.

Quinn, P.K., 1988: Simultaneous observations of ammonia in the ocean and atmosphere in the remote marine environment. Ph.D. Thesis, University of Washington, 138 pp.

——, R.J. Charlson, and T.S. Bates, 1988: Simultaneous observations of ammonia in the atmosphere and ocean. *Nature,* **335,** 336–338.

——, T.S. Bates, J.E. Johnson, J.E. Covert, and R.J. Charlson, 1990: Interactions between the sulfur and reduced nitrogen cycles over the central Pacific Ocean. *J. Geophys. Res.,* **95,** 16,405–16,416.

Robins, D.B., A.J. Bale, G.F. Moore, N.W. Rees, S.B. Hooker, C.P. Gallienne, A.G. Westbrook, E. Marañón, W.H. Spooner, and S.R. Laney, 1996: AMT-1 Cruise Report and Preliminary Results. *NASA Tech. Memo. 104566, Vol. 35,* S.B. Hooker and E.R. Firestone, Eds., NASA Goddard Space Flight Center, Greenbelt, Maryland, 87 pp.

Robinson, N., 1966: *Solar Radiation.* American Elsevier, New York, 347 pp.

Tanré, D., C. Deroo, P. Duhaut, M. Herman, J.J. Morcrette, J. Perbos, and P.Y. Deschamps, 1990: Description of a computer code to simulate the satellite signal in the solar spectrum: The 5S code. *Int. J. Remote Sens.,* **11,** 656–668.

Van Neste, A., R.A. Duce, and C. Lee, 1987: Methylamines in the marine atmosphere. *Geophys. Res. Lett.,* **14,** 711–714.

Verity, P.G., D.K. Stoecker, M.E. Sieracki, and J.R. Nelson, 1996: Microzooplankton grazing of primary production at 140°W in the equatorial Pacific. *Deep-Sea Res. II,* **43,** 1,227–1,255.

Vigroux, E., 1953: *Contribution à l'étude expérimentale de l'absorption de l'ozone. Ann. Phys.,* **8,** 709–762.

Waters, K.J., R.C. Smith, and M.R. Lewis, 1990: Avoiding ship-induced light-field perturbation in the determination of oceanic optical properties, *Oceanogr.,* **3,** 18–21.

Welschmeyer, N.A., 1994: Fluorometric analysis of chlorophyll-*a* in the presence of chlorophyll-*b* and pheopigments. *Limnol. Oceanogr.,* **39,** 1,985–1,992.

Wright, S.W., S.W. Jeffrey, R.F.C. Mantoura, C.A. Llewellyn, T. Bjornland, D. Repeta, and N. Welschmeyer, 1991: Improved HPLC method for the analysis of chlorophylls and carotenoids from marine phytoplankton. *Mar. Ecol. Prog. Ser.,* **77,** 183–196.

Young, A.T., 1980: Revised depolarization corrections for atmospheric extinction. *Appl. Opt.,* **19,** 3,427–3,428.

The SeaWiFS Postlaunch Technical Report Series

Vol. 1

Johnson, B.C., J.B. Fowler, and C.L. Cromer, 1998: The SeaWiFS Transfer Radiometer (SXR). *NASA Tech. Memo. 1998–206892, Vol. 1,* S.B. Hooker and E.R. Firestone, Eds., NASA Goddard Space Flight Center, Greenbelt, Maryland, 58 pp.

<u>*Vol. 2*</u>

Aiken, J., D.G. Cummings, S.W. Gibb, N.W. Rees, R. Woodd-Walker, E.M.S. Woodward, J. Woolfenden, S.B. Hooker, J-F. Berthon, C.D. Dempsey, D.J. Suggett, P. Wood, C. Donlon, N. González-Benítez, I. Huskin, M. Quevedo, R. Barciela-Fernandez, C. de Vargas, and C. McKee, 1998: AMT-5 Cruise Report. *NASA Tech. Memo. 1998–206892, Vol. 2,* S.B. Hooker and E.R. Firestone, Eds., NASA Goddard Space Flight Center, Greenbelt, Maryland, 113 pp.